Titre: Title:	Understanding the Impact of Climate change on a Series of Climate indices Related to Food Security, Infrastructure Resilience, and Human Health in Canada Using the State-of-the-Art CMIP6 Simulations
Auteur: Author:	Sarah-Claude Bourdeau-Goulet
Date:	2021
Type:	Mémoire ou thèse / Dissertation or Thesis
Référence: Citation:	Bourdeau-Goulet, S.-C. (2021). Understanding the Impact of Climate change on a Series of Climate indices Related to Food Security, Infrastructure Resilience, and Human Health in Canada Using the State-of-the-Art CMIP6 Simulations [Master's thesis, Polytechnique Montréal]. PolyPublie. https://publications.polymtl.ca/9126/

POLYTECHNIQUE MONTRÉAL

affiliée à l'Université de Montréal

Understanding the impact of climate change on a series of climate indices related to food security, infrastructure resilience, and human health in Canada using the state-of-the-art CMIP6 simulations

SARAH-CLAUDE BOURDEAU-GOULET

Département de génie civil, géologique et des mines

Mémoire présenté en vue de l'obtention du diplôme de *Maîtrise ès sciences appliquées*

Génie civil

Août 2021

POLYTECHNIQUE MONTRÉAL

affiliée à l'Université de Montréal

Ce mémoire intitulé:

Understanding the impact of climate change on a series of climatic indices related to food security, infrastructure resilience, and human health in Canada using the state-of-the-art CMIP6 simulations

présenté par **Sarah-Claude BOURDEAU-GOULET**

en vue de l'obtention du diplôme de *Maîtrise ès sciences appliquées*

a été dûment accepté par le jury d'examen constitué de :

Françoise BICHAI, présidente

Elmira HASSANZADEH, membre et directrice de recherche

Ahmad SHAKIBAEINIA, membre

DEDICATION

Je dédie ce mémoire à toutes les personnes m'ayant offert du support lors de ma maîtrise; ma famille, mes ami(e)s ainsi que mes collègues de Polytechnique.

Et surtout, à ma directrice, Dr. Elmira Hassanzadeh, pour son savoir, sa disponibilité, son dévouement, ses idées et sa confiance.

ACKNOWLEDGEMENTS

I would like to thank my supervisor, Dr. Elmira Hassanzadeh, without whom the presentation of this work would not have been possible. Throughout my research, she was a source of knowledge, support, encouragement, and guidance with an admirable upmost involvement. The trust she gave me for my research and many other projects helped me surpass myself academically.

I would like to acknowledge the financial support provided for this project from the Natural Sciences and Engineering Research Council of Canada (NSERC) and the programme PIED of Polytechnique Montréal.

I would like to express my gratitude to my jury examiners, Dr. Bichai and Dr. Shakibaeinia, for their feedback, as well as to Dr. Ali Nazemi whom offered innovative ideas for my research.

Thank you to my colleagues, Khalil, Henrique, Ali, Andrea, Faezeh, Alexandra, and others, with whom I exchanged ideas as well as the challenges of being a graduate student during the COVID19 pandemic.

Finally, I would like to thank all my friends and family who gave me so much support during this journey into academic research.

RÉSUMÉ

Les conditions climatiques jouent un rôle important pour les communautés, l'économie et l'environnement d'un pays. Les effets des changements climatiques, causés par l'activité humaine, sont déjà fortement ressentis au Canada altérant les normales climatiques du pays. En effet, la température annuelle moyenne du pays a augmenté de 1.7°C en soixante ans ce qui est le double de l'accroissement moyen planétaire. Cette augmentation de température est encore plus évidente dans le nord du pays. Le Canada fait aussi face à une accélération de la fréquence et un accroissement de l'intensité des évènements extrêmes tels que les inondations et les vagues de chaleurs. Au même moment que le pays se réchauffe, le Canada devient davantage vulnérable aux changements de températures et précipitations. En particulier, l'agriculture, la résilience des infrastructures ainsi que la santé humaine et environnementale sont à très forts risques de dégradation.

Les modèles climatiques sont les outils les plus crédibles pour prédire le climat futur. Ainsi, le comportement de ces modèles est critique pour quantifier l'impact des changements climatiques. Les avancées en calculs numériques ont permis à ces modèles d'être continuellement mis à jour en améliorant leurs processus physiques et leur résolution spatiale. Les simulations de pointe provenant des modèles participant au «*Climate Model Intercomparison Project Phase 6*» (CMIP6) ont récemment été rendues disponibles au grand public. L'importance des mises à jour de ces nouveaux modèles en comparaison avec leurs prédécesseurs participant à CMIP5 rend primordiale l'analyse de leurs comportements pour divers indices climatiques, surtout en ce qui a trait aux scénarios futurs. L'évapotranspiration potentielle (PET) est essentielle pour les modélisations hydrologiques et de productivité agricole dû à sa représentation de l'évapotranspiration maximale pour une herbe verte de petite taille. Conséquemment, il est capital d'avoir une meilleure connaissance des changements futurs de PET à travers le Canada à l'aide des modèles de CMIP6. Toutefois, des analyses de ce genre, utilisant les modèles de CMIP6, n'ont pas encore été réalisées pour le Canada et très peu d'études considèrent plusieurs simulations par modèle même à l'échelle mondiale.

Tout d'abord, dans la présente étude, les simulations provenant de 7 modèles climatiques de CMIP6 et 7 modèles climatiques de CMIP5 sont comparées à travers les régions canadiennes. Au total,

389 simulations sont utilisées pour estimer un ensemble d'indices climatiques. Ces indices incluent; les degrés-jours de croissance et la pluie saisonnière moyenne (influençant l'agriculture), les cycles de gel et dégel ainsi que la précipitation maximale annuelle (affectant la résilience des infrastructures) et finalement, le nombre maximum de jours chauds ainsi que le nombre maximal de jours secs consécutifs (ayant des impacts sur la santé humaine et environnementale). Deux réanalyses créées par les groupes «*National Oceanic and Atmospheric Administration*» (NOAA) et «*National Centers for Envrionmental Prediction*» (NCEP), sont utilisées à titre de référence pour la comparaison des modèles climatiques durant la période historique de 1961-1990. Les résultats révèlent l'absence de supériorité évidente entre les modèles de CMIP6 et CMIP5 en respect aux valeurs estimés par NOAA et NCEP. Bien que la différence entre la moyenne des ensembles multimodèles des phases de CMIP soit petite, leurs valeurs ne concordent pas nécessairement avec celles de NOAA et NCEP selon la région étudiée. Par ailleurs, les sorties des modèles climatiques ne se chevauchent pas et présentent des projections divergentes pour la même phase de CMIP. L'écart entre les projections des modèles de CMIP6 et CMIP5 est plus perceptible dans le futur sous le forçage radiatif 8.5 W/m^2. Généralement, la distribution spatiale, le signe et l'ordre de grandeur du changement des indices dans le futur dépendent du modèle et du scénario utilisé. Toutefois, bien que les simulations de CMIP6 et de CMIP5 projettent différentes valeurs, les modèles climatiques montrent tous une modification majeure de la température, de la précipitation et des indices étudiés pour le futur, ce qui est alarmant pour l'impact des changements climatiques pour le Canada. De plus amples analyses, utilisant la correction de biais et diverses modélisations, sont requises pour évaluer l'étendue de ces impacts sur l'agriculture, les infrastructures et la santé au Canada.

Par la suite, la PET est estimée durant la période historique avec 7 modèles climatiques de CMIP6 ainsi que NOAA et la combinaison du «*Climatic Research Unit gridded Time Series*» (CRU-TS) avec le «*Japanse 55 years Reanalysis*» (JRA-55), CRU/JRA, pour trois modèles empiriques de PET (Penman-Monteith, Priestley-Taylor et Hargreaves). Les PET estimées avec les modèles climatiques et les données de références sont comparées pour évaluer les erreurs potentielles des estimations basées sur les simulations de CMIP6. Les moyennes des PET estimées avec des ensembles multimodèles présentent des distributions spatiales similaires à NOAA et CRU/JRA. Cependant, leur ordre de grandeur diverge, surtout dans le sud du Canada. De ce fait, le «*Quantile*

Delta Mapping» (QDM) est utilisé pour corriger le biais des simulations de CMIP6, une fois avec NOAA et une autre avec CRU/JRA. Les mesures de performance ont montré que QDM est hautement efficace pour corriger les simulations de modèles climatiques en réduisant l'erreur à moins de 10%. Les projections corrigées par biais sont ensuite utilisées pour calculer les trois équations empiriques de PET dans le futur sous deux scénarios durant les périodes 2021-2050 et 2071-2100. Les résultats démontrent une augmentation majeure de PET dans le futur, particulièrement pour le scénario projetant le plus d'émissions de gaz à effet de serre pendant la période 2071-2100. Le nord du Nunavut et le Nunavik sont particulièrement affectés par cet accroissement dépassant les 50% en comparant les projections corrigées passées et futures de PET. L'équation Priestley-Taylor affiche les valeurs les plus élevées de PET dans plusieurs régions canadiennes. Il a été démontré que l'ordre de grandeur des valeurs estimées de PET est hautement dépendant, par ordre d'importance, de la localisation, le mois de l'année, l'équation utilisée, les données de référence utilisées pour la correction de biais et les simulations de modèle climatique.

Pour conclure, ces résultats témoignent du besoin urgent d'étude d'impacts des changements climatiques pour divers secteurs canadiens utilisant les sorties des modèles climatiques de CMIP6. Par exemple, les simulations de CMIP6 peuvent être utilisées pour estimer les débits de pointe ou d'étiage à l'aide de modèles hydrologiques ainsi que le rendement de récoltes avec une modélisation agricole. Ces études sont essentielles pour déterminer le risque lié aux catastrophes climatiques futures, comme des crues éclairs et les périodes de sécheresse. Ainsi, ces analyses seront essentielles pour la formulation de mesures d'adaptations adéquates permettant de diminuer l'exposition ainsi que la vulnérabilité des communautés canadiennes aux évènements extrêmes et aux changements climatiques.

ABSTRACT

Climatic conditions play an important role in shaping countries' society, economy, and environment. Canada has already been affected by the human-induced changes in climate, therefore altering normal climatic conditions in the country. Canada's annual average temperature has increased by 1.7℃ in sixty years, which is double the world average increase. This rise of temperature is even more evident in the Canadian North. The country is also facing more frequent and intense extreme events. As Canada gets warmer, the country becomes vulnerable to changes in temperature and precipitation. Particularly, agricultural production, infrastructure stability, and human and environmental health are at great risks of degradation.

Climate models are the most credible tools to project future climate; therefore, their behaviour is critical to quantify climate change impacts. The advancements in computation allowed these models to continuously get updated with a greater goal of better representing physical processes and increasing models' spatial resolution. The simulations of the state-of-the-art Climate Model Intercomparison Project Phase 6 (CMIP6) have become recently available to the public. Due to important updates in these new models in comparison to their precedent CMIP5 ones, especially in terms of future scenarios, it is crucial to first analyze the behaviour of CMIP6 models over Canada in representing pertinent climate indices during the historical and future period. Second, due to the importance of potential evapotranspiration (PET) for hydrological and agricultural production modelling, it is essential to have a better understanding of changes in PET across Canadian regions in the future using the CMIP6 models. Such analyses considering a large set of CMIP6 simulations are not yet provided in the literature for Canadian regions.

In this study first, the simulations of 7 CMIP6 and 7 CMIP5 climate models are compared across Canadian regions. In total, 389 climate simulations are used to estimate a set of pertinent climate indices. These indices include growing degree days and mean seasonal rainfall (influencing agriculture productivity), freeze-and-thaw cycle and annual maximum precipitation (affecting infrastructure resilience) as well as the maximum number of hot days and maximum number of consecutive dry days (impacting human and ecosystem health). Two reanalyses made by the National Oceanic and Atmospheric Administration (NOAA) and the National Centers for Environmental Prediction (NCEP), are also used as benchmarks to compare climate model

simulations in the historical period. Results reveal that there is no clear superiority of CMIP6 models over CMIP5 in representing the estimated values by NOAA and NCEP. Although there is a small difference between the multi-model ensemble mean values of both CMIP phases, they do not necessarily match the reanalyses across Canadian zones. Moreover, the outputs of climate models do not overlap and the models even for the same CMIP phase might present diverging projections. The difference between projections of CMIP6 and CMIP5 models is more noticeable under the radiative forcing 8.5 W/m^2. Generally, the spatial pattern, sign, and magnitude of changes in climate indices in the future depend on the utilized climate model and future scenario. Nevertheless, although the projections of CMIP5 and CMIP6 models are not necessarily similar, they all show significant alterations in temperature, precipitation and the considered climate indices in the future, which can be alarming for Canada. Further analyses using bias-corrected simulations are needed to assess the extent of climate change impacts on Canada's agriculture, infrastructure as well as environmental health.

Secondly, PET is estimated in the historical period using the simulations of 7 CMIP6 models, as well as NOAA and the combination of the Climatic Research Unit gridded Time Series (CRU-TS) with the Japanese 55 years Reanalysis (JRA-55), CRU/JRA, for three PET empirical equations (Penman-Monteith, Priestley-Taylor and Hargreaves). The estimated PET values based on the climate models and benchmark datasets are then compared to evaluate the potential errors in CMIP6 models-based estimates across Canada. PET estimated with CMIP6 multi-model ensemble presents similar spatial patterns to the two benchmarks. However, their magnitudes are diverging especially in Southern Canada. Accordingly, Quantile Delta Mapping (QDM) is applied to correct climate models-based simulations once with NOAA and once with CRU/JRA. The performance measures show that QDM is highly efficient in correcting the climate models' simulations, reducing the error in PET estimates to less than 10%. The bias-corrected projections are then fed to the noted empirical models to estimate PET in the future under two scenarios during 2021-2050 and 2071-2100. Results portray a major increase of PET in the future, particularly under the worst-case scenario and for the end of the century. Northern Nunavut and Nunavik are particularly affected by this augmentation which exceeds 50% when comparing the past and future bias-corrected values. Priestley-Taylor estimates often display higher PET values than the other equations for most Canadian regions. It is also found that the PET estimated magnitudes highly

depend on the location, the month of the year, applied PET equation, benchmark for bias-correction and climate model values.

These results highlight the urgent need for assessments of climate change impacts on different Canadian sectors using the outputs of CMIP6 climate models. For example, CMIP6 simulations can be used to estimate low and high flows in hydrological models or crop yield in agricultural models. Such studies are crucial to determine the risks linked to future hazards, like droughts and flash floods, to propose appropriate adaptation policies with a greater goal of protecting Canadian communities and supporting sustainable development in the future.

TABLE OF CONTENTS

LIST OF TABLES

LIST OF FIGURES

LIST OF SYMBOLS AND ABBREVIATIONS

AMP	Annual maximum precipitation
CMIP5	Coupled Model Intercomparison Project Phase 5
CMIP6	Coupled Model Intercomparison Project Phase 6
CV	Coefficient of variation
e_a	actual vapor pressure
e_s	saturated vapor pressure
ET	Evapotranspiration
FAT	Freeze and thaw cycle
G	Soil heat flux
GCM	General circulation model
GDD	Growing degree days
IPCC	Intergovernmental Panel on Climate Change
MAMD	Mean absolute monthly difference
MCD	Maximum consecutive number of dry days
MNH	Maximum number of hot days
MSR	Mean seasonal rainfall
P	Precipitation
PET	Potential evapotranspiration

Pr	Pressure
QDM	Quantile Delta Mapping
R_a	Extraterrestrial radiation
RATV	Ratio of temporal variance
RCP	Representative concentration pathway
Rh	Relative humidity
rlds	surface downwelling longwave flux in air
rlus	surface upwelling longwave flux in air
R_n	Net radiation
ROYA	Ratio of yearly amplitudes
rsds	surface downwelling shortwave flux in air
rsus	surface upwelling shortwave flux in air
SSP	Shared socioeconomic pathway
T	Mean air temperature
TD	Temperature difference
Tmax	Maximum air temperature
Tmin	Minimum air temperature
U	Wind speed
α	coefficient equals to 1.26

γ	psychrometric constant
λ	latent heat of vaporisation
Δ	slope vapor pressure

LIST OF APPENDICES

CHAPTER 1 INTRODUCTION

1.1 Background

Weather fluctuations can be easily observed in our everyday life. For instance, the temperature might go above 20˚C in one day and drop below 10˚C the day after. By statistically analyzing these weather data over a longer period (e.g., 30 years), one can study the climate of a point of interest. Throughout history, the Earth's climate has changed naturally. For example, glacial and interglacial cycles have occurred in the last millions of years, which caused a diminution in snow and sea ice as well as warming of water vapor. Theses cycles were caused by variations in the Earth's orbit geometry around the sun (Herring and Lindsey, 2020). However, since the last century the Earth's climate has exceptionally changed mainly due to increasing concentrations of greenhouse gases in the atmosphere, generated by human activities. These activities include fossil fuels usage, industrialization, urbanization, extensive agricultural production, advancement in technologies, among others. For instance, between 1850 and 2018, 440 ± 20 gigatons of carbon dioxide were emitted around the world due to the combustion of fossil fuels (Lindsey, 2020). Such increase in the concentration of heat-trapping gases has increased the Earth's temperature by around 0.07℃ per decade since 1880. Even, the oceans' first 75m temperature has warmed by 0.11℃ per decade between 1971 and 2010 (IPCC, 2014). Observations also showed an average increase of 1.09 mm per decade in precipitation between 1901 and 2005 across the globe (IPCC, 2007).

The impacts of climate change around the world can be significant. Changes in temperature can affect growing season and potentially impact agricultural productivity and therefore affect countries food security. It can also cause longer and more frequent droughts, heatwaves and wildfires directly, which impact on local communities as well as fauna and flora health. Other alterations in the climate, such as changes in the characteristics of rainfall can affect the magnitude, duration and frequency of floods but also the timing of these events in snow dominant zones due to earlier snow/glacier melt. Northern latitudes are also affected by a diminution in permafrost. The continuous rise in sea level due to warming climate can also cause coastal erosion, aquifer and agriculture soil contamination as well as coastal flooding due to increases in extreme events such as hurricanes and typhoons (IPCC, 2014).

Recent extreme events have exposed the vulnerability of communities around the world as well as ecosystems to climate conditions. Common impacts, for instance, infrastructure losses, disruption

of food production, human mortality, mental health issues including post-traumatic stress and depression, are observed in many countries. Considering these emerging threats, it has become essential for policy makers around the world to consider the changes in climate and understand their impacts among top priorities to propose proper mitigation and adaptation plans to reduce communities' vulnerabilities.

1.1 Case study and problem definition

Canada is a vast country with a variety of climate conditions. Figure 1.1 shows ten Canadian climate zones, namely, East Arctic, North East Forest, Great Lakes, Canadian Maritimes, Northern Plains, Mackenzie Valley, North West Forest, West Coast, Western Cordillera and Yukon (Plummer et al.,2006). The demarcation of these zones was defined by similitudes in topography and climatic variations, which are briefly summarized in Table 1.1 below.

Figure 1.1 Canadian climatic zones adopted from Plummer et al., (2006)

Across these Canadian zones, significant impacts of climate change are already observed. Between 1948 and 2016, the country's mean annual temperature has increased by 1.7°C, which is more than double the globe average. Northern Canada is particularly affected due to its sensitive climate with an augmentation of temperature by 2.3°C. The number of hot days (temperature higher than 30°C) is also on the rise, from 1 up to 3 days per year depending on the region. The increase in temperature has already affected the depth and duration of snow cover causing earlier snowmelt, particularly in the Rocky Mountains.

Table 1.1 Climatic zones and their respective characteristics (Bernhardt, 2010)

Climatic zones	**Characteristics**
East Arctic	Colder and driest zone; Annual average temperature under 0°C; Low precipitation (less than 200 mm/year); Covered by permafrost; Arctic desert
Mackenzie Valley	Short summers and long winters; Annual average temperature under 0°C; Widespread of permafrost; Ice over free surface water lasts up to eight months; Low precipitation
Yukon	Northern part of the Rocky Mountains; Less than 300 mm/year in precipitation and 2/3 in solid form; Short and cool summers; Snow covers for more than half the year
West Coast	Wet weather; Cool summers and mild winters; Less extreme between seasons temperature; Areas receive up to 4000 mm/year
Western Cordillera	Contains two mountain ranges; Important difference in temperature between North and South; Orographic precipitation; West receives more precipitation than East
North West Forest	Annual average temperature close to 0°C; Short and warm summers with cold winters; Less precipitation in the West than East (300 vs 600 mm)
Northern Plains	Very dry zone; Low precipitation; High winds; Extreme temperatures due to the distance from oceans
North East Forest	Mild winter; Summers around 10°C; Maritime influence in the East gives high precipitation (up to 1600 mm/year)
Canadian Maritimes	Cooler summers and warmer winters; High moisture; Precipitation ranging from 900 to 1500 mm/year; Important number of storms
Great Lakes	Highly changeable weather; Cool winters and warm summers; Home to half the population of Canada

In addition to temperature, Canadian precipitation has also changed. However, no consistent positive or negative trends in precipitation are observed over Canadian zones. Nevertheless, analyses of recorded data between 1948 and 2012 show around 20% increase in normalized precipitation and up to 30% increase in the Canadian North. There is also a decline in solid precipitation in the South and an increase in highest one-day rainfall in various regions. Changes in climate have also affected the Evapotranspiration (ET) in Canadian regions. Analyses of over 101 local Canadian stations between 1960 and 2000 show significant positive trends in ET in 35% of the locations (Bush and Lemmen, 2019; Fernandes et al., 2007; Lemmen et al., 2008). More precisely, 80% of the stations present increases in ET with a rate of up to 0.73% per year while a decrease in ET with a maximum rate of 0.25% per year is shown over the Prairies and in Arctic (Fernandes et al., 2007). In addition, it was found that for 1˚C increase in temperature, ET can augment by up to 8% in the Great Lakes region (Fernandes et al., 2007; Lemmen et al., 2008).

Such observed changes in climate conditions in Canada can potentially affect the characteristics of normal and extreme events and lead to alterations in socioeconomic activities as well as environmental conditions. As Canada is the 5th agricultural exporter in the world (Faith, 2017), changes in climate may affect the country's food security e.g., by altering heat accumulation available for plants' development, and water availability for irrigation (Smith et al., 2013). This can be even more problematic given the growing world population and the need to feed them. Another potential climate change impact is the augmentation of the number of freeze-and-thaw cycles, which can affect soil stability and erosion. Therefore, these cycles damage infrastructure and their foundations (Council of Canadian Academies, 2019; Guest et al., 2020; Mohammed et al., 2020; Palko, 2017). Additionally, ice roads, which are commonly used for travel up north by the local indigenous communities for food supplies (hunting and fishing) or accessing traditional sites and other communities, can be greatly affected by freeze and thaw cycles (Bush and Lemmen, 2019; Lemmen et al., 2008). Flash floods caused by extreme precipitation also create huge damages on infrastructure and often total loss of their value which is extremely costly for communities and governments (Sills et al., 2016). Finally, the increase in extreme events of hot temperature such as heatwaves presents an important risk for densely urban areas, such as Montreal, Toronto, Vancouver, and Calgary, where heat islands are already common due to the lack of vegetation and high presence of pavements. Thus, global warming puts citizens at higher risk of heat stroke and

even mortality. Furthermore, these extreme events can also cause wildfires which are devastating for local communities requiring to be evacuated and are also disastrous for the environment as ecosystems are destroyed. Changes in ET, with considerable increases in both East and West coasts, can not only affect power production and agricultural activities but also add pressure on water supplies for municipalities, and tourism (Lemmen et al., 2008). It is therefore crucial to evaluate the changes in future ET across Canadian regions to propose appropriate adaptation policies. Having an improved understanding of possible changes in climate and their impact on a series of vulnerability assessment indicators allows communities as well as provincial and federal governments to be more prepared for the future.

Therefore, the aim of this study is to investigate the performance of available climate models and use them to estimate the impact of climate change in Canada. The characteristics of these climate models, observation benchmarks, as well as utilized bias-correction method in this study are explained in Chapter 2. The specific objectives of this research as well as the organization of the thesis remaining chapters are elaborated in Chapter 3.

CHAPTER 2 LITERATURE REVIEW

The present section offers a review of the scientific literature around climate models, reanalysis, bias-correction technique, and potential evapotranspiration.

2.1 General Circulation Models

General Circulation Models' (GCMs) first aim was to represent the Earth's climate conditions by employing primitives' equations, including Newton's laws of motion, mass conservation, hydrodynamic state, and thermodynamic energy equations. The represented processes, calculation speed, and spatial resolution of these models have evolved over the years. While earlier models could only simulate the atmosphere processes, recent models are capable of projecting land surface, clouds, oceans, etc. (Edwards, 2011). The Coupled Model Intercomparison Project (CMIP) first phase started in 1990, which focused on comparing GCMs coupling dynamic interactions between the atmosphere, oceans, and cryosphere. These models were considered as more comprehensive than the ones only using atmospheric interactions, as oceans play a key role in the Earth's climate. These coupled models, considering the atmosphere, oceans and cryosphere interactions, had only been created 10 years prior to the first phase of CMIP (in the 80s) due to their high requirements in calculations, in comparison to models using only atmospheric processes.

In addition, different climate modelling centers provide the outputs of GCMs. The performance of these models may diverge, and they might provide contradictory future projections (Fu et al., 2013; Sheffield et al., 2013; Yu et al., 2019). This may be caused by usage of different physical processes, initialization, feedback mechanisms, parameterization, etc. (IPCC-TGICA, 2007). Therefore, it is often recommended to consider the simulations of multiple climate models for analyses. Climate models also often provide a range of simulations for future climate. Theses simulations (members) are distinguished by having different initialization for the model run. Therefore, multiple model simulations better represent the model's forced response and its answer to external radiative forcing (Lehner et al., 2020; Maher et al., 2019; Martel et al., 2018). As a result, the usage of numerous simulations per model is recommended in the literature. Since the past decade, GCMs' projections have been widely used in many scientific domains for impact assessments (Dibike et al., 2018; Hao et al., 2018). Most importantly, the Intergovernmental Panel on Climate Change (IPCC) uses CMIPs analyses in their reports. Over the past couple of decades, the outputs of CMIP phase 3

(CMIP3) models which consider different emission scenarios (radiative forcing) in the future are commonly used for impact assessment in Canada and elsewhere (Touzé-Peiffer et al., 2020). The CMIP5 models are available since 2011 and scientists across the globe still use these models for impact assessment. CMIP6 models have very recently become available to the public. The following sections present a brief review of these two CMIP phases, which are also used in this thesis.

2.1.1 Climate Models - CMIP5

The design of the CMIP5 project started in 2007 with 20 modelling groups participating and its first outputs were made available at the beginning of 2011 (PCDMI, 2013). CMIP5 used a new set of future scenarios for greenhouse gas concentration through the 21st century considering different economic activities, energy sources, population growth and other socioeconomic factors. These scenarios are called the Representative Concentration Pathways (RCPs). RCPs represent four different end of the century radiative forcing (2.6, 4.5, 6.0 and 8.5 W/m^2) with the highest forcing (8.5) being the worst-case scenario in terms of climate change (Taylor et al., 2012; Van Vuuren, 2011). Radiative forcing measures the Earth's surface heating in function of greenhouse gas concentration, aerosols, clouds, and changes in land surface. As previously noted, CMIP5 outputs have been largely used in the literature for different purposes. An analysis of 280 published articles in six well-known scientific journals showed that 40% of these studies used CMIP5 models to address future climate change and their uncertainties, 28% of them compared model results to observations and 32% of them interpreted models' outputs (Touzé-Peiffer et al., 2020).

CMIP5 models are also used in Canada for different purposes, ranging from assessing their performance in the historical period to using them for impact assessment on Canadian sectors over various regions. Examples of such studies for agriculture are Bock et al. (2018), who analyzed the land sustainability rating system for Canadian crops. Grenier et al. (2019), studied the uncertainties linked to spatial analogs (association between projected future climate change for a given location and similar recent past climates at a remote location) for five farms in Quebec. Quian et al. (2020) evaluated the uncertainties linked to climate variability in Canadian crops production. Hassanzadeh et al. (2019), used CMIP5 models to explore the impacts of climate change for extreme precipitation in Montreal. Jaramillo and Nazemi (2018) used an ensemble of models to evaluate

the climate change impacts on water security in Montréal. For the whole country, Tam et al. (2019), assessed future drought projections using the Standardized Precipitation Evapotranspiration Index while Gaur et al. (2018), specifically studied future flood hazards.

2.1.2 Climate Models - CMIP6

The design of CMIP6 models started in 2013 while its outputs have become available to the public since 2019. The 49 climate modelling groups participating in this project keep on updating the simulations and some groups still add new simulations even up to this day (PCDMI, 2019). CMIP6 models present new climate scenarios called the Shared Socioeconomic Pathways (SSPs). The SSPs are a parallel approach to the RCPs to better represent policies, political issues, share and access of resources, usage of fossil fuels, durability, etc. More precisely, the SSPs rank future possibilities from one to five in terms of mitigation and adaptation to challenges. SSP 1 represents sustainability (low challenges) and SSP2 shows the middle of the road (intermediate challenges). SSP3 presents a regional rivalry (high challenges), SSP4 displays inequality in which adaptation challenges dominate, and SSP5 considers fossil-fuelled developments in which mitigation challenges dominate. This way, different RCPs and SSPs can be combined together, offering different possibilities of end of the century forcing and socioeconomic policies such as SSP 5-8.5 and SSP 5-3.4 or SSP 1-2.6 and SSP 1-2.9.

Due to the recent availability of CMIP6 outputs, a limited number of studies used its datasets until today especially when it comes to future impact assessments. So far, many studies used only one simulation per model to understand the behaviors at the global scale (Na et al., 2020) and over regions (Akinsanola et al., 2020; Almazroui et al., 2020; Wang J. et al., 2020; H. Zhu et al., 2020; Z. Chen et al., 2020). These studies highlight the advantages of using multi-model ensembles over individual models and that GCMs still presented biases such as a high number of wet days. Also, analyses of future CMIP6 projections displayed similar values for most SSPs until half of the century, but after 2050 a great increase in temperature values is observed under SSP 5-8.5 (Cook et al., 2020). However limited studies use all available simulations per climate model (Papalexiou et al., 2020; Schurer et al., 2020; Shrestha et al., 2020; Yazdandoost et al., 2020). Regarding the Canadian regions, there is one local study that analyzed the CMIP6 models' precipitation and temperature behaviour in the historical period with one simulation per model in Alberta, Canada

(Masud et al., 2021). They found that simulations of temperature showed a good representation of reality while precipitation values presented biases as they were missing local processes like convective rainfall.

2.1.3 Comparison of CMIP5 and CMIP6 Models

It is considered a good practice to compare the performance and/or projections of precedent and new generations of climate models due to their importance for impact assessment. For instance, how much do temperature values estimated by CMIP6 and CMIP5 models differ? This is a legitimate question because first, their considered future scenarios are different from one another. For example, SSP 5-8.5 (combination of SSP 5 and RCP 8.5) presents around 20% higher carbon dioxide concentrations for the whole 21st century in comparison to CMIP5's RCP 8.5. In contrast, RCP 4.5 of CMIP5 shows lower emission values than SSP 2-4.5 until 2050 but projects larger values after the mid-century (Hausfather, 2019). Furthermore, CMIP6 now offers a wider range of end of the century forcing (more than four) which allows research teams to better assess the impacts of climate change with a wider range of possibilities (Eyring et al., 2016; Hausfather, 2019; Riahi et al., 2017; Stouffer et al., 2017). CMIP6 models also aim to better simulate the physical process, have smaller spatial resolutions, and a higher number of members per model (Eyring et al., 2016; O'neil et al., 2016; Stouffer et al., 2017). Recent studies have compared CMIP5 and CMIP6 models' behaviour using only one simulation per model over the world (Chen H. et al., 2020; Di Luca et al., 2020; Fan et al., 2020; Kim et al., 2020; Seneviratne and Hauser, 2020). These studies highlighted the resemblance between CMIP5 and CMIP6 multi-model projections during the historical period, but generally observed slight improvements in the performance of CMIP6 simulations and a reduction in the spread of values. Apart from Cook et al. (2020) and E. Zhu et al. (2020), studies rarely used multiple simulations per model. However, to our best knowledge, no comparison of CMIP5 and CMIP6 GCMs was made specifically for Canada and key climate indices influencing the country's main hazards.

2.1.4 Bias Correction

Literature previous analyses showed that systematic biases exist in GCMs' simulations in respect to observed records, which can stem from various factors such as the limitations of physical

phenomenon knowledge, coarse spatial resolution, and the difficulties to represent climate natural variability (Prudhomme, 2006; Cannon, 2020). For example, climate models present errors for both cold and hot temperatures in Northern latitude as well as wetter days in cooler regions (Sheffield et al., 2013; Sillmann et al., 2013). One commonly used technique to reduce these errors is called bias correction (Casanueva et al., 2020). Various bias-correction methods exist in the literature. These methods first measure the differences between the observed and GCMs simulations statistics for the same baseline period. Accordingly, future GCMs' simulations are corrected by incorporating these differences. Linear scaling, delta change, and quantile mapping are some of the commonly used bias-correction methods (Teutschbein and Seibert, 2012). Cannon et al., (2015) evaluated the performance of three bias correction methods for Canada in improving the precipitation estimates of CMIP5 models. Among the methods, Quantile Delta Mapping (QDM) showed a good performance and also has the advantage of preserving the relative change signal of future simulation, meaning that the quantiles ratio between raw future and historical projections of GCMs is preserved without consideration of benchmarks data. QDM has two main steps:

1) Detrending (removing trend) of future climate projections and bias-correcting them using the commonly known quantile mapping method with respect to reference data.

2) The GCMs quantiles projected relative change is superimposed on the outputs of step 1.

In terms of mathematical formulation, first, the calculation of the non exceedance probability for time (t), $\tau_{m,p}(t)$, from the time-dependant cumulative distribution function (CDF) of the model projected series $x_{m,p}(t)$.

$$\tau_{m,p}(t) = F_{m,p}^{(t)}\left[x_{m,p}(t)\right], \qquad \tau_{m,p}(t) \in \{0,1\} \tag{2.1}$$

The given relative change in quantiles between historical period and time t, $\Delta_m(t)$, is then estimated.

$$\Delta_m(t) = \frac{F_{m,p}^{(t)-1}\left[\tau_{m,p}(t)\right]}{F_{m,h}^{-1}\left[\tau_{m,p}(t)\right]} = \frac{x_{m,p}(t)}{F_{m,h}^{-1}\left[\tau_{m,p}(t)\right]} \tag{2.2}$$

The inverse CDF of the benchmark historical period values, $x_{b,h}(t)$, is used to bias correct the GCMs projections quantiles, $\tau_{m,p}(t)$, similarly to quantile mapping.

$$\hat{x}_{b:m,h:p}(t) = F_{b,h}^{-1}\left[\tau_{m,p}(t)\right] \quad 2.3$$

At last, the GCMs future projections is bias-corrected with a multiplication of the last step and $\Delta_m(t)$.

$$\hat{x}_{m,p}(t) = \hat{x}_{b:m,h:p}(t)\Delta_m(t) \quad 2.4$$

In this study this approach is used to bias-correct GCMs' outputs to estimate future evapotranspiration values in Chapter 5.

2.2 Reanalyses

Reanalyses provide a wide range of grid-based climatic observations over the globe with significant time coverage (Touzé-Peiffer et al., 2020). In brief, a reanalysis uses historical observations assimilated in a past short-range weather forecast. Therefore, they are similar to day-to-day weather forecasts but are based on the past analysis. Observed data are also pre-processed to have better results (ECMWF, 2020). The outputs of various reanalyses such as the National Oceanic and Atmosphere Administration reanalysis (NOAA), the National Centers for Environmental Prediction reanalysis (NCEP), 40-years European Centre for Medium-Range Weather Forecasts Reanalysis (ERA-40) and the Japanese 55 years Reanalysis (JRA-55) are freely available to the public. They have a wide application ranging from estimating flow in ungauged basins to evaluating the performance of GCMs in the baseline period.

However, reanalyses present their own biases and therefore may not perfectly represent the past climate which should be taken into consideration. For example, inhomogeneities, limitations and noises in observed datasets as well as errors in the assimilation schemes and models uncertainty (Donat et al., 2014; Fujiwara et al., 2017) can cause too large diurnal cycles during the warm season and biased precipitation (Beck et al., 2018; Kalnay et al., 1996). Thus, in this thesis, different reanalyses are used to assess the performance of CMIP models in the historical period.

2.3 Evapotranspiration

In this section, some information about Potential Evapotranspiration (PET) is provided since it is one of the most important variables considered in this research. ET is one of the key water cycle components as it represents the water going into the atmosphere from evaporation and from plants transpiration. While transpiration is responsible for 10% of the moisture found in the atmosphere, surface water evaporation like oceans, seas, and lakes are responsible for the last 90% of atmospheric moisture. ET also allows two third of continental rainfall to return to the atmosphere (Anctil et al., 2012). As previously noted, estimation of ET has a high importance in Canada. However, understanding the evolution of actual ET is highly challenging especially at the large country scale, due to the need for field measurements and usage of advanced tools such as lysimeters and Eddy-covariance systems (Djaman et al., 2019; Hargreaves et al., 2003; Kumar et al., 2012; Xing et al., 2008). Therefore, empirical models to estimate potential ET (PET) are often employed to model changes in maximum ET and assuming that enough water would be available for evapotranspiration (Kumar et al., 2012; NOAA, 2020). PET has become an essential gauge of ET in various domains such as in hydrology e.g., for assessments of wetland restoration, for hydraulic infrastructure design, and to estimate irrigation water demand (Atmaya et al., 2014; Prudhomme and Williamson, 2013). Various methods ranging from temperature-based, radiation-based, combinatory-based as well as water balance and mass transfer, exist to estimate PET (Xu and Singh, 2002). The performance of PET estimation methods has been assessed in the literature at the local and regional scales (e.g., Hassanzadeh et al., 2014; Maulé et al., 2006; Seiller et al., 2016), and globally (Weiß and Menzel, 2008). Overall, it is found that the estimated PET values by the methods can vary considerably, depending on the location, as well as availability and quality of climatic data (Barnett et al., 1998; Djaman et al., 2019). PET's future estimates over North America have shown that the magnitude of estimates varies depending on the applied equation and considered location. This indicates that analyses based on using only one PET formula might lead to incomplete knowledge of future changes (Dallaire et al., 2021).

One common approach to estimate future PET is based on using the outputs of GCMs. The CMIP5 models are often used to estimate future PET over the globe (Berg and Sheffield, 2019; Dong and Dai, 2017; Scheff and Frierson, 2015). Most of the existing studies in Canada estimate the PET with CMIP5 outputs (Dallaire et al., 2021; Qian et al., 2013; Tam et al., 2019; Yan and

Mohammadian, 2020). For instance, Tam et al., (2019) used 29 CMIP5 GCMs and estimated PET using three equations. Comparison of PET estimates based on one simulation of CMIP5 and CMIP6 models with one empirical equation showed that the estimations of the two GCMs generations can be different and that future projections over the Northern Hemisphere present higher anomalies for CMIP6 than CMIP5 (Liu et al., 2020). CMIP6 models are also used to evaluate PET across various regions and have projected an increase in estimates over the upcoming decade (Ajjur & Al-Ghamdi, 2021; Shrestha et al., 2020; Su et al., 2021; Zhai et al., 2020). No study has yet used more than one PET equation and bias-corrected CMIP6 outputs to evaluate PET specifically for Canada.

CHAPTER 3 ORGANISATION OF THE WORK

As previously noted, Canada may face an increasing number of risks affecting agricultural production, infrastructure resilience, and human as well as environmental health in particular in the north. Successful policies for adaptation and mitigation to climate change require profound knowledge of future climate hazards in the country. GCMs are currently the most reliable tools available to estimate future climatic variables and therefore are advantageous means to evaluate future climate change impacts. CMIP6's climate model outputs have very recently become available, in 2019. Due to important updates in these models, especially in terms of future scenarios, it is crucial to analyze their behaviour over Canada in representing pertinent climate indices as well as key components of hydrological and agriculture models. Moreover, it is also important to use these climate models to understand the changes in variables across Canadian regions. It has even greater significance to do so, considering there is currently a gap in the literature for such studies using CMIP6 simulations over Canada.

Therefore, the specific objectives of this study are:

1) Comparing the historical and future projections of six climate indices influencing food security, infrastructure resilience and human as well as environmental health using CMIP6 GCMs and their precedent CMIP5 simulations. The advantage of using one simulation versus multi-simulations per GCM over Canada is also analyzed.

2) Estimating the potential evapotranspiration (PET) in the future using CMIP6 models and three different PET empirical equations. The importance of using different climate models, bias correction using different benchmarks, and PET equations is also analyzed.

Addressing these objectives will improve our knowledge of future climate over Canada as well as the behaviors of the new-state-of-the-art GCMs participating in CMIP6 considering three experiments: historical as well as two end of the centuries radiative forcing 4.5 and 8.5 W/m2. As none of the future scenarios, and therefore end of the century radiative forcing, are more likely to occur than another, the most catastrophic scenario forcing 8.5 W/m2 is used to highlight the most disastrous impacts of climate change over Canada. The forcing 4.5 is also employed to represent the lower intermediate pathway as it considers implementation of policies protecting the

environment in the future (IPCC, 2014).Chapter 4 and Chapter 5 correspond to each of these objectives.

In **Chapter 4,** 389 daily simulations of precipitation (Pr), maximum temperature (Tmax) and minimum temperature (Tmin), provided by seven CMIP6 and seven CMIP5 GCMs are used to estimate the values of six climate indices over Canada. These indices are growing degree days and mean seasonal rainfall (both relevant to Canadian agriculture); freeze-and-thaw cycles and annual maximum precipitation (influencing infrastructure resilience); and maximum number of hot days and maximum number of consecutive dry days (pertinent for human as well as environmental health). All six indices are estimated for the historical period, 1961-1990, and future periods, 2021-2050 and 2071-2100 under two scenarios, RCP 4.5 & RCP8.5 for CMIP5 and SSP 2-4.5 & SSP 5-8.5 for CMIP6. The long-term annual average and coefficient of variation (CV) of the indices, estimated by ensembles of CMIP5 and CMIP6 models are compared to two reanalyses, NOAA and NCEP in the historical period. Then, the relative difference between the values of individual CMIP6 and CMIP5 models during both historical and future periods are analyzed. Finally, the added value of using multi-simulations per model is investigated by presenting the range of indices for each GCM in ten Canadian climatic zones. These analyses were performed for all periods and climate scenarios.

The article presented in Chapter 4 was published in the *Earth's Future* journal (Impact Factor: 7.5) on April 13, 2021.

Chapter 5 presents a series of analyses for quantification of PET during the historical and future periods over Canada. First, the outputs of CMIP6 models, as well as two benchmark, NOAA (reanalysis) and CRU/JRA (combined data) were obtained. During the historical period of 1961-1990, these datasets were used to estimate PET over Canada using temperature-, radiation-based and combined PET empirical equations. The estimated PET values based on climate models and reanalyses were compared to observe potential errors in GCM-based estimates across Canada. Accordingly, QDM was used to bias correct the GCM simulations once with NOAA and once with CRU/JRA during historical and future periods. Then, using a set of performance measures, the impact of QDM bias correction on improving GCM-based simulations was explored. Finally, using the bias-corrected GCMs and the three empirical evapotranspiration equations, PET values in the future across Canada were estimated. Further analyses are provided to understand the relative

difference in PET values between future and past projections. Finally, the monthly ranges for future PET over each Canadian climatic zone using PET equation, individual GCM as well as each future scenarios and periods are provided. Such visualizations allowed us to investigate the importance of each of these factors in estimation of PET in the future.

Finally, Chapter 6 describes the contributions of this work, limitations, and recommendations for future research.

CHAPTER 4 ARTICLE 1: COMPARISONS BETWEEN CMIP5 AND CMIP6 MODELS: SIMULATIONS OF CLIMATE INDICES INFLUENCING FOOD SECURITY, INFRASTRUCTURE RESILIENCE, AND HUMAN HEALTH IN CANADA

Sarah-Claude Bourdeau-Goulet[1] and Elmira Hassanzadeh[1]

[1] *Department of Civil, Geological, and Mining Engineering, Polytechnique Montréal, Montréal, QC, Canada*

Published in **Earth's Future** Journal

Contribution of the Master Student

The master student obtained the data and did its curation, formal analysis and visualization as well as writing the original draft. Dr. Elmira Hassanzadeh in partnership with the master student did the investigation, research methodology, validation, reviewing and editing. Dr. Hassanzadeh acquired the funding as well as administrated the project.

Abstract

The warming climate can considerably affect socioeconomic activities and environmental health conditions in Canada. Climate models play a key role in evaluating the impact of climate change and developing adaptation and mitigation strategies corresponding to Canadian regions. This study compares the behaviour of climate models participating in the Climate Model Intercomparison Project Phase 6 (CMIP6) with their CMIP5 predecessors in representing a set of climate indices relevant to Canada's agricultural productivity, infrastructure resilience, and environmental health. Our results show that although CMIP5 and CMIP6 multi-model ensemble mean values for the considered indices are almost similar, the behaviour of individual CMIP5 and CMIP6 models or even the model pairs of the same modelling center can be different across Canada. Moreover, the CMIP6 models do not necessarily outperform CMIP5 in comparison to NOAA and NCEP reanalysis datasets in simulating the annual mean and coefficient of variation values for the indices during the historical period. The comparisons between models' simulations also reveal that the envelope of estimated values based on individual CMIP6 models does not cover or overlap with their CMIP5 counterparts or even with other CMIP6 models. Therefore, the CMIP6 models with

higher number of simulations do not necessarily provide a larger range of projections over Canadian regions. The divergence between CMIP5 and CMIP6 models' behaviour is more obvious under the 8.5 W/m^2 forcing in the long-term horizon. Overall, the estimated sign, magnitude, and spatial pattern of changes in the climate indices depend on the considered climate model and forcing scenario.

4.1 Introduction

Human activities have influenced the climate conditions worldwide since the last century. Notably, Canada's mean annual temperature has increased by around 1.7 °C over the past few decades, which is more than twice the global rate, causing alterations in the characteristics of hydroclimatic variables locally and regionally (Council of Canadian Academies, 2019). These changes have raised serious concerns about the extent of climate change impacts on Canada's society, economy, and environment (Bush and Lemmen., 2019; Lemmen et al., 2008). For instance, Canada's agriculture and food security, infrastructure sustainability, and human health, particularly in northern regions are identified as key areas at high risks in the upcoming future (Council of Canadian Academies, 2019). Therefore, an improved understanding of climate change impacts over these sensitive areas is essential to propose reliable adaptation strategies.

General Circulation Models (GCMs), from the Coupled Model Intercomparison Project (CMIP), are the most advanced tools to project climate conditions (Randall et al., 2007). The CMIP5 provides GCMs' outputs under different Representative Concentration Pathways (RCPs) (Stouffer et al., 2017; Taylor et al., 2012). Individual and ensemble of CMIP5 models have been used to assess the impact of climate change for example, on a series of indices related to agriculture (Bock et al., 2018; Grenier et al., 2019), infrastructure design (Hassanzadeh et al., 2019; Jaramillo & Nazemi, 2018), and natural hazards (Gaur et al., 2018; Tam et al., 2019) in Canada. These studies find that the sign and magnitude of changes depend on the considered climate models, and overall large uncertainties exist in the projections. More specifically, the models show warm as well as cold biases over northern latitude, and wet biases in cooler regions (Sheffield et al., 2013; Sillmann et al., 2013; Wazneh et al., 2020).

The new state-of-the-art CMIP6 models' simulations have recently become available and aim to fill the gaps in CMIP5, most importantly, to better represent physical processes at smaller scales

(Eyring et al., 2016; O'neil et al., 2016; Stouffer et al., 2017). Moreover, CMIP6 offer a wider range of forcing than CMIP5 due to inclusion of the Shared Socio-Economic Pathway (SSP) scenario matrix, which considers broader socio-economic conditions for the future (Eyring et al., 2016; Riahi et al., 2017; Stouffer et al., 2017). In brief, the SSPs are parallel approaches to RCPs accounting for mitigation and adaptation to the diverse challenges in our societies and offer a possibility for research groups to specifically assess the impacts of these challenges' responses (Hausfather, 2019). In addition, CMIP6 provides a higher number of simulations for the same forcing to better represent internal variabilities (Eyring et al., 2016; Merrifield et al., 2020; Pascoe et al., 2019; Stouffer et al., 2017). The performance of multiple CMIP6 models in representing precipitation and temperature conditions are assessed in different regions (Akinsanola et al., 2020; Almazroui et al., 2020; Z. Chen et al., 2020; Ha et al., 2020; Jiang et al., 2020; Masud et al., 2021; Wang et al., 2020) and at the global scale (Fan et al., 2020; Na et al., 2020) by considering one simulation per model.

Understanding the differences between behavior of CMIP5 and CMIP6 models is essential due to their critical role in evaluating the impact of climate change. Various studies show that CMIP5 and CMIP6 multi-model ensemble temperature (and precipitation) values tend to be roughly similar at the global scale (see H. Chen et al., 2020; Kim et al., 2020; Seneviratne & Hauser, 2020). In addition, CMIP6 models have globally improved their historical representations of climate extremes indices compared to CMIP5 models (H. Chen et al., 2020; Di Luca et al., 2020). Studies at the smaller scale for example, in China (H. Zhu et al., 2020), India (Gusain et al., 2020), and Australia (Grose et al., 2020) also show a better representation of spatial pattern and seasonality of climate variables by CMIP6 in comparison to CMIP5 models during the historical period. Although using an ensemble of simulations per climate models are recommended to represent GCMs' "forced response" (Lehner et al., 2020; Maher et al., 2019; Martel et al., 2018), most recent studies use only one or a limited number of simulations per GCM for their CMIP5 and CMIP6 comparison (H. Chen et al., 2020; Di Luca et al., 2020; Grose et al., 2020; Kim et al., 2020; H. Zhu et al., 2020). Only a few studies analyze CMIP6 simulations (Papalexiou et al., 2020; Schurer et al., 2020; Shrestha et al., 2020; Yazdandoost et al., 2020) or even compare multi-simulation ensembles of CMIP5 and CMIP6 models (Cook et al., 2020; E. Zhu et al., 2020). Nevertheless, to the best

knowledge of authors, no specific study on comprehensive assessment of CMIP5 and CMIP6 simulations over Canada has been done yet.

This study aims to compare the CMIP5 and CMIP6 simulations in estimating a set of climate indices related to agriculture security, infrastructure sustainability, and environmental health in Canada during the historical and future periods. In particular, the specific objectives of this study are to understand whether the considered CMIP5 models can be replaced by CMIP6 models and if an individual CMIP6 model, containing a large number of simulations, can be solely used for impact assessment in Canada. Section 4.2 introduces the CMIP5 and CMIP6 models, two reanalysis datasets that are used to benchmark GCMs' performances, as well as six climate indices analyzed in this study. Section 4.3 presents the results of inter-comparisons during the historical and future periods. Discussions about uncertainties in projected changes in the climate indices and further directions for impact assessments are provided in Section 4.4.

4.2 Materials and Methods

4.2.1 CMIP5 and CMIP6 Models

The daily precipitation (P), maximum temperature (Tmax), and minimum temperature (Tmin) datasets for seven CMIP5 and seven CMIP6 models, a total of 389 simulations, are obtained from the Earth System Grid Federation (https://esgf-data.dkrz.de/projects/esgf-dkrz/) in fall 2020. Table 4.1 shows the name of climate modelling centers, GCMs and their spatial resolutions as well as number of simulations and future scenarios. These climate models are selected due to their large number of simulations available for the studied variables. For more information on these CMIP models, please refer to the Program for Climate Model Diagnosis & Intercomparison (https://pcmdi.llnl.gov/). Moreover, RCPs 4.5 and 8.5 for CMIP5 and SSPs 2–4.5 and 5–8.5 for CMIP6 models are considered as future scenarios. Both SSPs and RCPs used in this study present the same end of the century forcing (4.5 and 8.5 W/m^2), which are measures of the Earth's heating surface as a function of greenhouse gases concentration, aerosols, clouds, and changes in land surface (Van Vuuren, 2011). In brief, CMIP6 SSP 5–8.5 presents higher values (around 20%) of CO_2 emission than RCP 8.5 for the whole 21st century, while SSP 2–4.5 starts with higher CO_2 emissions than RCP 4.5 and ends up with less emissions, with a slower and more continuous

decline by the end of century (Hausfather, 2019). This study considers a historical period of 1961–1990 as well as short-term (2021–2050) and long-term (2071–2100) future horizons.

Table 4.1 Considered climate models and their grid resolution as well as number of simulations during the historical and future periods, along with the future scenarios.

Climate modelling centers	CMIPs	Spatial resolution	Number of simulations			Future scenarios
			Historical period	Future periods		
CanESM	CanESM2	2.8° × 2.8°	5	5	5	RCPs 4.5 and 8.5
	CanESM5	2.8° × 2.8°	50	50	50	SSPs 2-4.5 and 5-8.5
CNRM	CNRM-CM5	1.4° × 1.4°	10	1	1	RCPs 4.5 and 8.5
	CNRM-CM6-1	1.4° × 1.5°	30	1	1	SSPs 2-4.5 and 5-8.5
Had/UK	HadGEM2-ES	1.9° × 1.2°	5	4	4	RCPs 4.5 and 8.5
	UKESM1.0-LL	1.9° × 1.3°	19	5	4	SSPs 2-4.5 and 5-8.5
IPSL	IPSL-CM5A-LR	3.8° × 1.9°	6	4	4	RCPs 4.5 and 8.5
	IPSL-CM6A-LR	2.5° × 1.3°	32	6	6	SSPs 2-4.5 and 5-8.5
Miroc	MIROC5	1.4° × 1.5°	5	3	3	RCPs 4.5 and 8.5
	MIROC6	1.4° × 1.4°	10	3	3	SSPs 2-4.5 and 5-8.5
MPI	MPI-ESM-LR	1.9° × 1.9°	3	3	3	RCPs 4.5 and 8.5
	MPI-ESM1-2-LR	1.9° × 1.9°	10	10	10	SSPs 2-4.5 and 5-8.5
MRI	MRI-CGCM3	1.1° × 1.1°	5	1	1	RCPs 4.5 and 8.5
	MRI-ESM2.0	1.1° × 1.1°	6	1	1	SSPs 2-4.5 and 5-8.5

Note. The information for CMIP5 and CMIP6 is respectively shown in light and dark gray rows.

Moreover, the daily P, Tmax, and Tmin from two different reanalysis datasets, namely NCEP (Kalnay et al., 1996) and NOAA (Compo et al., 2011; Slivinski et al., 2019, 2020) are considered here to represent the historical climate conditions (Sillman et al., 2013) over Canada, and to benchmark the performance of CMIPs during this period. Both reanalyses were chosen due to their

temporal coverage of the considered historical period. NOAA has a 1° spatial resolution and is one of the most recently updated reanalyses which assimilates observed synoptic pressure, prescribe sea surface temperature and sea ice distribution (Slivinski et al., 2019). On the other hand, NCEP is one of the oldest reanalyses and therefore its performance and uncertainties are well assessed in the literature (Decker et al., 2012; Donat et al., 2014). NCEP has a spatial resolution of 2.5º (Kalnay et al., 1996). Due to the mismatch among the spatial scale of climate models and reanalyses, the Nearest Neighbor algorithm (Schulzweida et al., 2006) from the Climate Data Operator (https://code.zmaw.de/projects/cdo) is considered to regrid the model outputs to a common resolution of 1.5°.

4.2.2 Climate Indices and Their Significations

Canada is a large country with diverse topographic features and climatic conditions (Jeong et al., 2016). Changes in Canada's climate can potentially affect the length of growing season, presence of frozen soil, cycles of dry and wet years, heatwaves, forest fires, drought, and flood events, among others, with great impacts on socioeconomic growth and environmental conditions. This study evaluates the behaviour of CMIP5 and CMIP6 models using a set of climate indices, namely Growing Degree Day (GDD), Mean Seasonal Rainfall (MSR), Freeze and Thaw Cycles (FTC), Annual Maximum Precipitation (AMP), Maximum Number of Hot days (MNH), and Maximum Consecutive number of Dry days (MCD). Table 4.2 presents these indices, which are estimated similarly to the Climate Atlas of Canada (Prairie Climate Centre, 2019).

Canada is among the top 10 agricultural exporters in the world (Turcotte, 2013). Therefore, assuring Canada's crop production in the future is essential not only to feed the ever-increasing global population but also to support the country's economic growth (Qian et al., 2013, 2020). GDD and MSR, calculated for the months of May to October, are one of the important factors affecting the soil moisture and crop conditions over the growing season (Smith et al., 2013). The GDD is commonly used to estimate the length of growing season for various crops. Here, the GDD with a base temperature of 5° is considered, which is relevant for the forage and canola production, two of the main crops in the country (Prairie Climate Centre, 2019; Qian et al., 2020). The MSR, rainfall during the growing season, is also critical for crop growth and yield (Grenier et al., 2019; Huber & Gillespie, 1992). Changes in the characteristics of GDD and MSR can potentially

influence the food security at local, regional, and global scales (Lemmen et al., 2008; NRTEE, 2010).

Table 4.2 Climate indices and their specifications.

No	Indices	Specifications/calculations	Unit
(1)	Growing Degree days (GDD)	$GDD_{day} = \begin{cases} \frac{(Tmax + Tmin)}{2} - tb, & \frac{(Tmax + Tmin)}{2} > tb \\ 0, & \frac{(Tmax + Tmin)}{2} \leq tb \end{cases}$ $GDD_{annual\ growing\ season} = \sum_{1}^{214} GDD_{day}$ $Base\ temperature\ (tb) = 5℃$	°C/ year
(2)	Mean Seasonal Rainfall (MSR)	Mean precipitation between May to October in each year are estimated.	mm/day
(3)	Freeze and Thaw Cycle (FTC)	Number of days with $T_{max} > 0^{\circ}C$ and $T_{min} < -1^{\circ}C$ are found for each year.	Number of days/year
(4)	Annual Maximum Precipitation (AMP)	Daily maximum precipitation values are found for each year.	mm/day
(5)	Maximum Number of Hot days (MNH)	Number of days with $T_{max} > 30^{\circ}C$ are counted for each year.	Number of days/year
(6)	Maximum Consecutive number of Dry days (MCD)	Maximum number of consecutive days with $T_{max} > 20^{\circ}C$ and Pr $< 0.5\ mm/day$ are found for each year.	Number of days/year

FTC and AMP are critical for design and maintenance of Canadian infrastructures. An FTC occurs when Tmax is higher than 0 °C and Tmin is lower than −1 °C during the same day (Prairie Climate Centre, 2019). Changes in the historical characteristics of FTCs can potentially affect the land conditions such as soil stability and erosion, and cause damages to existing roads, buildings, power

lines, and mining sites (Council of Canadian Academies, 2019; Guest et al., 2020; Mohammed et al., 2020; Palko, 2017). Thawing permafrost has already affected the existing infrastructure in Canadian North, where mostly indigenous communities reside and whose culture and livelihood revolve partly around the existing FTCs (Bush and Lemmen, 2019; NRTEE, 2010). In addition to FTCs, the characteristics of AMPs are important for design, maintenance, and upgrade of various infrastructure including reservoirs and urban drainage systems (Mailhot et al., 2010; Yigzaw et al., 2013). Floods are the most catastrophic natural hazards in Canada and the federal government spends a large portion of disaster assistance budget for flood management (IBC, 2015). Therefore, an increase of AMPs can potentially augment the chance of flooding at urban and regional scales (Hassanzadeh et al., 2014; Henstra & Thistlethwaite, 2017).

Canada also has a long history of heatwaves, which have caused death and hospitalization of several hundreds of people, especially in major cities (Bustinza, 2013; Direction régionale de santé publique du CIUSSS, 2019). MNH and MCD provide an understanding of individual and continuous hot and dry days, which are critical to the health of not only older adults or people with chronic medical conditions, but also young and even physically active individuals (Government of Canada, 2020a). Moreover, increases in the number of hot and dry days can affect the ecosystems and cause forest fires with major environmental consequences. Therefore, it is important to assess the evolution of MNH and MCD to develop efficient adaptation strategies, specifically in the areas, where the risk of heatwaves is higher (Council of Canadian Academies, 2019).

4.2.3 Intercomparison Procedure

For our analyses, the long-term annual average as well as Coefficient of Variation (CV) values for the six climate indices are calculated at 1.5° grids for NOAA and NCEP, as well as each simulation of CMIP5 and CMIP6 models over the historical and future periods. The “multi-simulation ensemble mean” for a given climate model in each grid represents the averaged long-term annual mean (and CV) values over all simulations, that is, one value per model. The “multi-model ensemble mean” values are then calculated by taking the average of multi-simulation ensemble mean (and CV) values over all seven climate models for CMIP5 (and CMIP6), that is, one value per project. The behaviour of models based on multi-simulation ensemble mean values (and CVs) as well as multi-model ensemble mean values (and CVs) are compared at the grid scale across

Canada. Moreover, the difference between the simulations of the climate models over 10 Canadian climatic zones is evaluated. These climatic zones, shown in Figure 1.1, are the East Artic, Great Lakes, Mackenzie Valley, Canadian Maritimes, Northern Plains, Northeast Forest, Northwest Forest, West Coast, Western Cordillera, and Yukon Territory. For more information on these zones, please refer to Plummer et al. (2006) and Mladjic et al. (2011).

4.3 Results

In the following sections, the behaviour of CMIP5 and CMIP6 models is compared during the historical and future periods over Canada. In brief, Sections 4.3.1 to 4.3.3 answer the following questions during the historical period: Do CMIP5 and CMIP6 multi-model ensemble mean values (and CVs) for the six indices have similar magnitude and pattern of variations as reanalyses over Canada? Is there any difference between the behaviour of individual CMIP5 and their corresponding CMIP6 model pairs? Are the envelopes of CMIP6 and CMIP simulations comparable? Sections 4.3.4 to 4.3.6 address similar questions but for the future period.

4.3.1 CMIPs' Multi-Model Ensemble Mean Versus Reanalyses During the Historical Period

Little difference exists between CMIP5 and CMIP6 multi-model ensemble mean GDD, MSR, FTC, AMP, MNH, and MCD indices over Canada during the historical period – see Figure 4.1. CMIP6 precipitation-based estimates are slightly higher in Northern Canada while temperature-based values are smaller in Southern Canada compared to CMIP5 (except for GDD). Although the spatial pattern of variation for reanalyses and CMIPs' multi-model ensemble mean values is almost similar, their estimated values are significantly different in some regions. For instance, in southern parts of Canada, where the agricultural activities are important, the GCMs underestimate the GDD values by more than 300% in comparison to reanalyses. Further investigations reveal that CMIPs underestimate the GDD and FTC and overestimate the AMP, MCD and MNH in comparisons to reanalyses values. This observation agrees with former studies noting that CMIP6 models present a higher number of wet days (Akinsola et al., 2020). Similarly, the multi-model ensemble mean CVs for the six climate indices based on CMIP5 and CMIP6 are compared in Figure A1. Same as average values, the difference between estimated multi-model ensemble mean CVs of for CMIP5

and CMIP6 is almost negligible. Moreover, the two reanalyses present almost similar patterns and magnitudes of CVs, except for MSR and FTC. The largest divergence between CVs of reanalyses and CMIPs is observed for the MNH index.

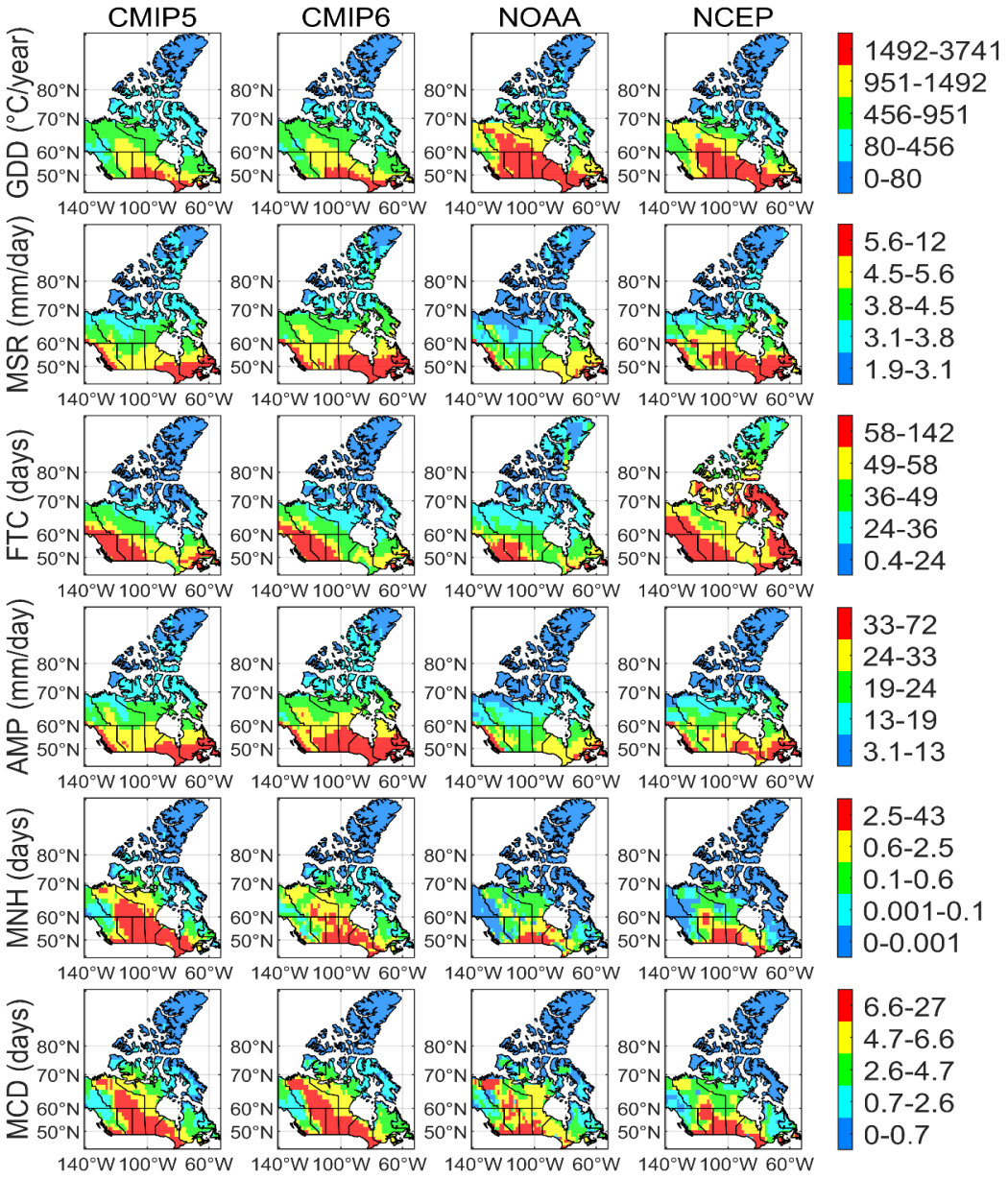

Figure 4.1 GDD, MSR, FTC, AMP, MNH, and MCD multi-model ensemble mean values, based on CMIP5 and CMIP6 in comparison to NOAA and NCEP estimates during the historical period.

4.3.2 CMIP5 Versus CMIP6 Individual Models During the Historical Period

Here, the multi-simulation ensemble mean and CV values, estimated by individual CMIP5 models are compared with their CMIP6 counterparts from the same modelling center over Canada during the historical period. Figure 4.2 displays the percentage of relative difference between the values of six climate indices, estimated by CMIP5 and CMIP6 model pairs for each modelling center in each column. The black areas in this figure display the grids, where the CMIP6 model values are more than 100% larger than their corresponding CMIP5 ones. On the opposite, gray zones present grids where CMIP5 values are 100% or larger than CMIP6 projections.

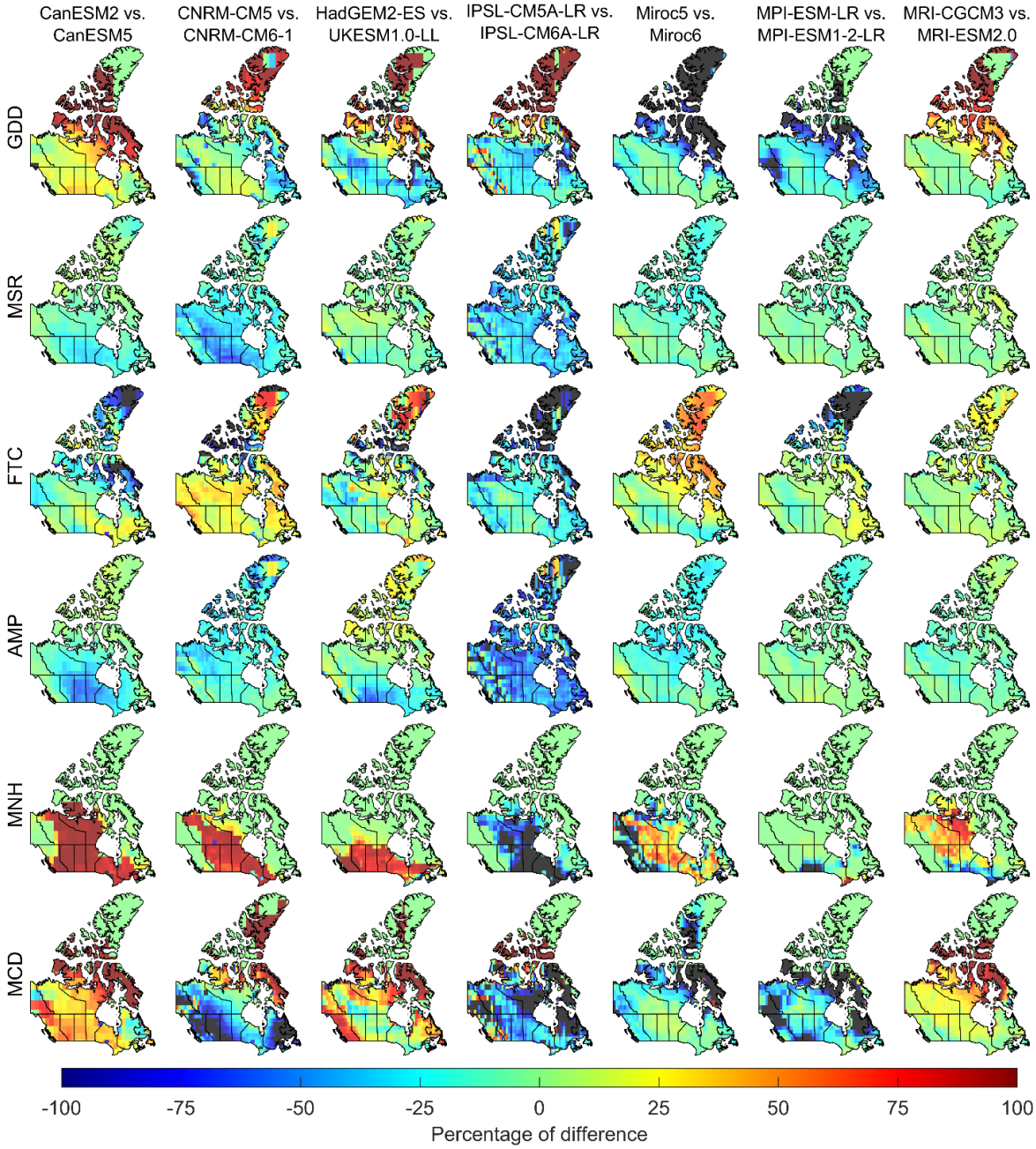

Figure 4.2 Relative difference between the multi-simulation ensemble mean values, estimated by CMIP5 models and their CMIP6 counterparts during the historical period.

The figure displays that CMIP6 and CMIP5 estimated values for the same modelling center are different. Moreover, the magnitude and pattern of differences between CMIP6 models and their predecessors among the considered modelling centers are not necessarily similar, for example, compare the two left columns. Considering the GDD, the largest divergence between most of the

CMIP5/6 model pairs is observed over the northern regions, see the dark areas in the top row. Same as GDD, there is a high difference between FTC estimations of model pairs over northern regions. Regarding the precipitation-based in- dices, while CMIP6 models of CanESM, CNRM, Had/UK, and IPSL show higher values than their predecessors over Central and Southern regions, the difference between model pairs by Miroc, MPI, and MRI is very small in most regions. Overall, the largest divergence between the estimated values by CMIP5 and CMIP6 models is observed for MCD. This is logical as both precipitation and temperature values are required to estimate this index. Therefore, the difference between estimated values by CMIP5 and CMIP6 models for these two variables propagates to the results. These analyses reveal that even though the multi-model ensemble mean values of CMIPs are almost alike (Figure 4.1), the estimations by individual CMIP5 and CMIP6 models can be considerably different.

The divergence between multi-simulation ensemble mean CVs, estimated by CMIP5 and CMIP6 models from the same modelling center can be significant in various cases – see Figure A2. These differences within and among modelling centers are not spatially consistent. It is interesting to note that even though the multi-model ensemble CVs, shown in Figure A1, display null values in Northern Canada, there is an important difference between CVs of some model pairs over this area – see the columns CNRM and Miroc in Figure A2.

4.3.3 CMIP5 and CMIP6 Simulations During the Historical Period Compared to Reanalyses

Here, the objective is to understand whether the observed differences between CMIP5 and CMIP6 model pairs signify an improvement in the CMIP6 outputs over Canada or not. For this purpose, the estimated long-term annual average values of climate indices by climate models' simulations are compared with NOAA and NCEP over Canada's 10 climate zones. Therefore, for each simulation, the grid-based values are averaged over the given zones. Figure 4.3 illustrates the boxplots for simulations of CMIP5 (black) and CMIP6 (red) models as well as expected values based on NOAA (dotted line) and NCEP (dashed line) for the six indices over the East Arctic, North East Forest, and Great Lakes. Figure A3 and Figure A4 display similar plots for the rest of climate zones. Each boxplot shows the values corresponding to the ensemble of simulations per

CMIP model at the zone scale. As an example, the boxplots for CanESM5 and CanESM2 contain 50 and five values, respectively.

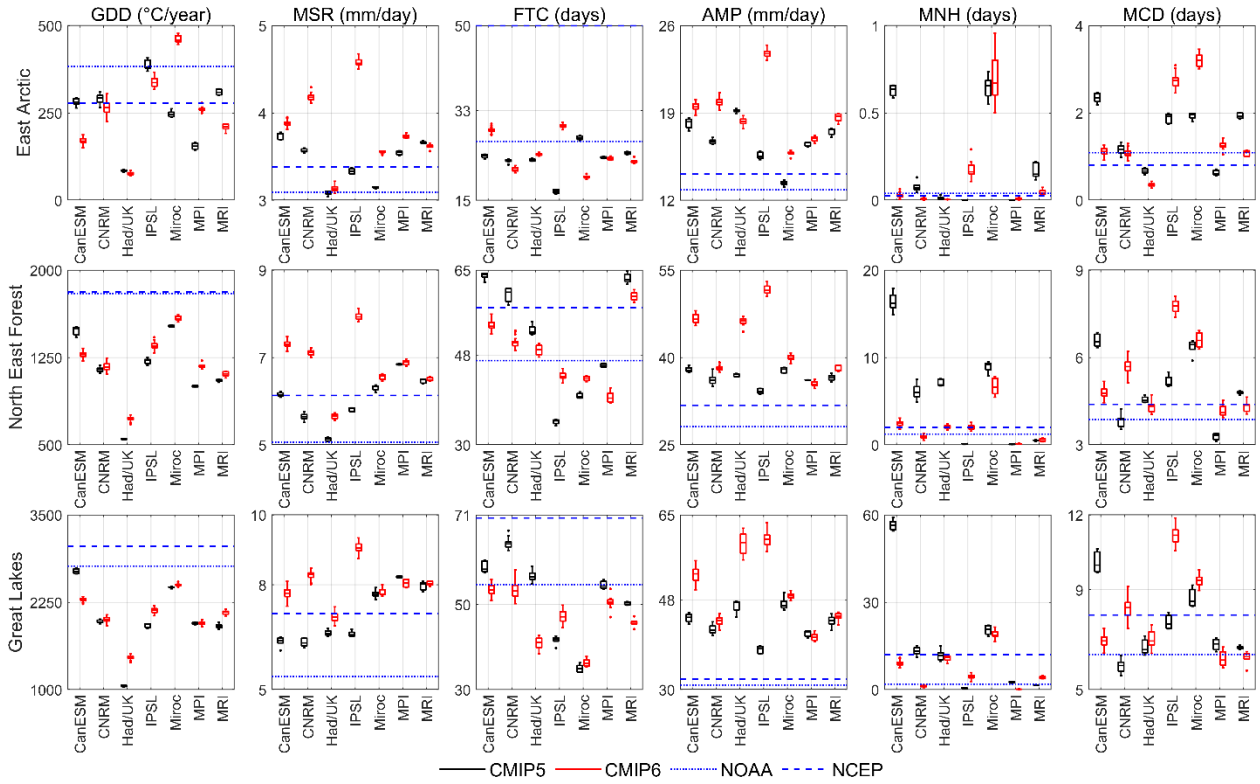

Figure 4.3 Long-term annual average values for six climate indices, estimated by simulations of CMIP5 (black boxplots) and CMIP6 (red boxplots), as well as NOAA (dotted line), and NCEP (dashed line) in the East Arctic, North East Forest and Great Lakes.

Comparisons among all zones reveal that CMIP6 and CMIP5 simulations do not necessarily overlap. Among CMIP6 models, the CanESM5, which includes the largest number of simulations, neither covers the estimated values by CMIP5 nor other CMIP6 models. Even the largest CMIP6 model ensembles, that is, based on CanESM5, CNRM-CM6-1, and IPSL-CM6A-LR models do not cover the spread of other CMIP6 models. Interestingly, MRI-ESM2.0, which has a smaller number of simulations, occasionally presents a large spread in comparison to other models – see FTC in the North East Forest (middle row and third column from the top). Therefore, the number of simulations for an individual model do not necessarily imply that the model covers a large or small variability in respect to the mean. The results also show that the performance of climate models varies among indices and zones. Both CMIP5 and CMIP6 models in most cases

underestimate the GDD values by the reanalysis datasets. Moreover, most of CMIP6 models considerably overestimate the MSR of reanalyses in comparison to CMIP5 models. Estimated FTCs by CMIP6 models are much closer to the range of reanalyses than CMIP5, except in the Great Lakes and Canadian Maritimes (see Figure 4.3, Figure A3 and Figure A4). Although CMIP6 models do not outperform the CMIP5 models in representing the AMPs, they perform better in estimating the MNH values. CMIP5 and CMIP6 models overestimate the MCD values of reanalyses in northern regions.

Likewise, Figure A5 to Figure A7 display the CVs of the six indices based on all simulations of CMIPs as well as reanalyses. The ensemble of CVs based on CMIP6 simulations do not necessarily cover or overlap with the CMIP5. However, the spread and values of CVs are usually similar for both CMIPs and are close to the reanalyses, except for the MNH index for which some models present important span and estimates–see fifth left column in Figure A5. Had/UK pair tends to overestimate the CVs for GDD in all zones. In addition, both CMIPs often overestimate the CVs for MSR in comparison to reanalyses.

4.3.4 CMIP5 Versus CMIP6 Multi-Model Ensemble Mean During the Future Period

The CMIP5 and CMIP6 multi-model ensemble mean values for the six climate indices are compared under different future scenarios over short- and long-term horizons in Figure A8 and Figure 4.4, respectively. Despite relative similarities between CMIP5 and CMIP6 multi-model ensemble mean values during the historical period, there are some differences between their future magnitudes. For instance, although the values under RCP 4.5 and SSP 2–4.5 for the short-term horizon look almost identical at first glance, CMIP6 presents a slight increase in GDD, MSR, AMP, and MCD indices over the Central Canada (Figure A8). The same observation can also be made under RCP 8.5 and SSP 5–8.5. Higher numbers of FTCs are projected in Northern Canada under SSP 5–8.5 than under RCP 8.5. Interestingly, under forcing 4.5 W/m^2, MNH values by CMIP6 are lower than CMIP5. The opposite can be seen under the 8.5 W/m^2 forcing, where MNH projections by CMIP6 are larger for the whole country.

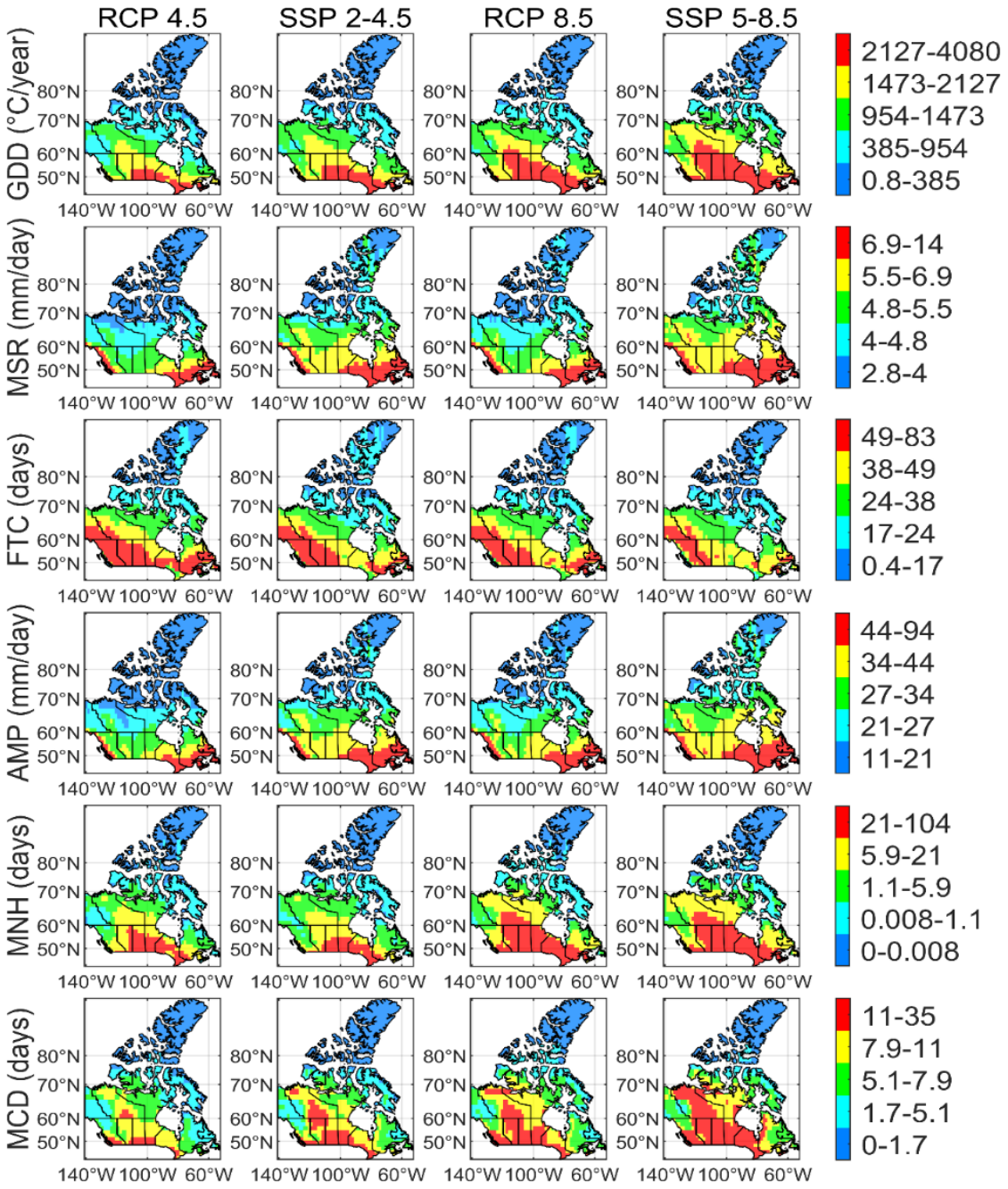

Figure 4.4 GDD, MSR, FAT, AMP, MNH, and MCD multi-model ensemble mean values, estimated by CMIP5 (RCPs 4.5 and 8.5) and CMIP6 (SSPs 2–4.5 and 5–8.5) scenarios during 2071–2100.

For the end of the century under forcing 4.5 W/m2, both multi-model ensemble mean values again present resembling patterns and values, however there is an increase in CMIP6 values over Northern and Central Canada except for FTC and MNH – see Figure 4.4 two left columns. Under

the 8.5 W/m^2 forcing in the long-term horizon, CMIP6 projects an increase in all indices except for FTC. Similarly, Figure A9 and Figure A10 exhibit the CMIP5 and CMIP6 multi-model ensemble mean CVs over the short- and long-term horizons under different scenarios, respectively. It is interesting to note that MNH has a significant increase in mean values projected by the end of century under forcing 8.5 W/m^2 over Central Canada as seen in Figure A10 fourth column.

4.3.5 CMIP5 Versus CMIP6 Individual Models in the Future Period

The relative difference between projections of CMIP5 and CMIP6 models from the same modelling center is shown for two sets of forcing during 2021–2050 (Figure A11 and Figure A12) and 2071–2100 (Figure 4.5 and Figure 4.6), respectively. The black areas in these figures display grids where CMIP6 values increased by over 100% in comparison to their CMIP5 predecessors' values. Gray areas present the opposite incident. Considering each index, it is obvious that there is a divergence between projections of CMIP5 and CMIP6 individual models. In fact, for most of these indices the relative difference between the estimates of the pairs can be close or more than 100 percent, as an example see the dark areas for GDD, MNH, and MCD indices. Thus, using an individual climate model may lead to over or underestimation of future changes in the climate indices across Canada. Moreover, same as the historical period, the relative difference among CMIP5 and CMIP6 models is not resembling among modelling centers, regions, and indices. Another observation is that for the same index, the sign and pattern of relative difference between the estimates of most model pairs for the same modelling center are almost similar between the historical and future periods. Moreover, the magnitudes of differences between CMIP5 and CMIP6 models' averages are often larger under 8.5 W/m^2 than 4.5 W/m^2 forcing during the 2071–2100 period.

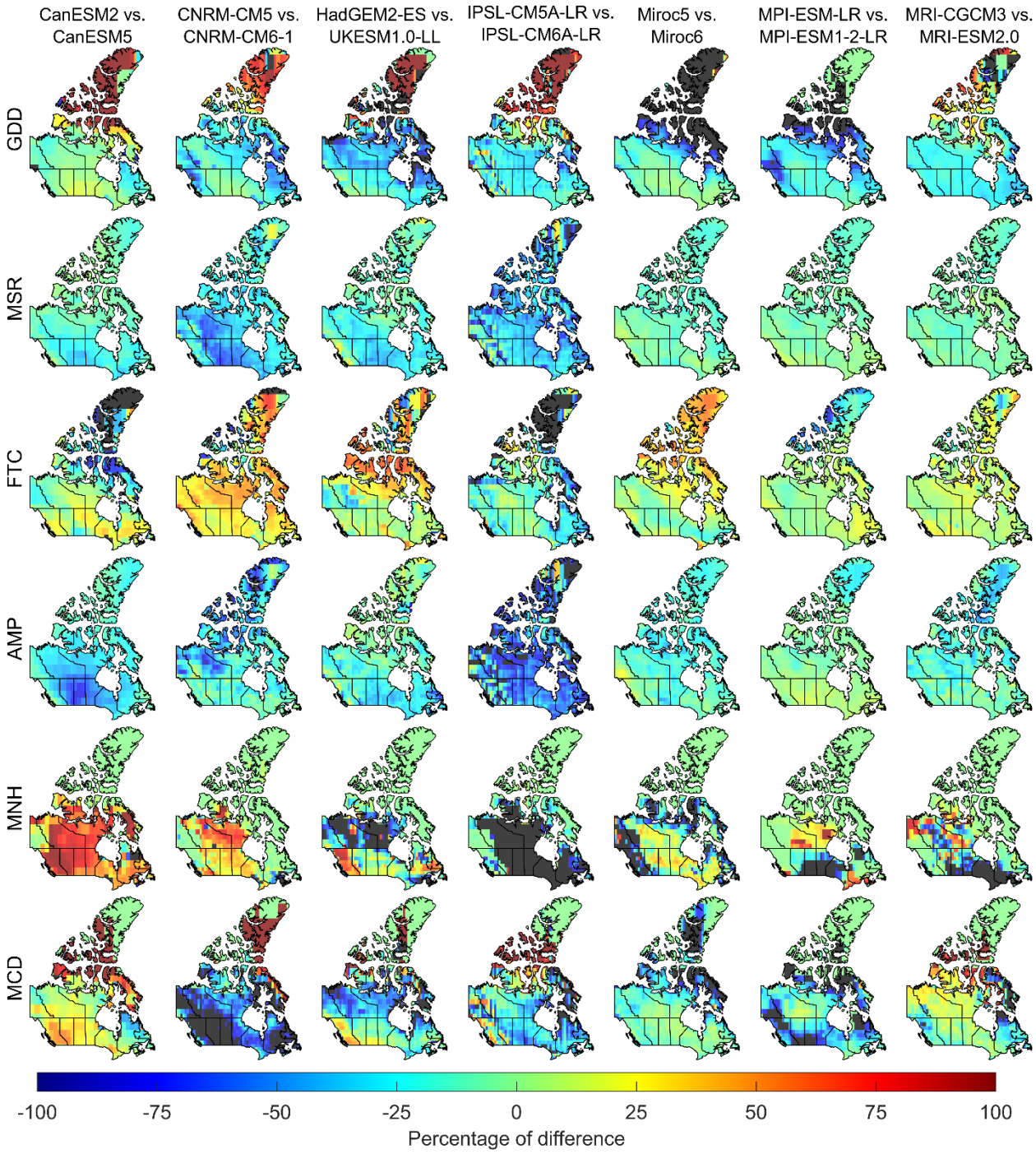

Figure 4.5 Relative difference between the multi-simulation ensemble mean values, estimated by CMIP5 models and their CMIP6 counterparts under 4.5 W/m^2 forcing during 2071–2100.

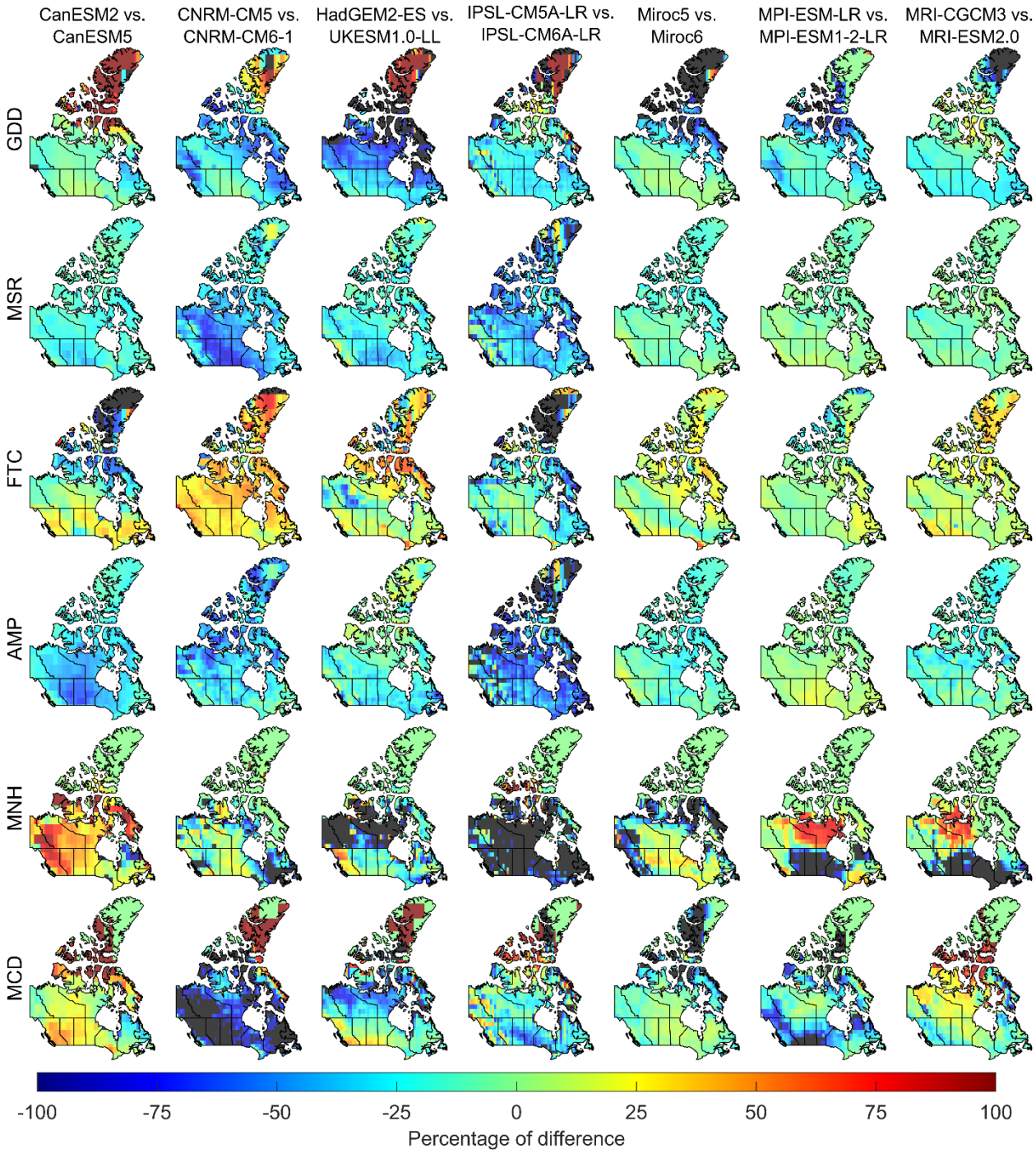

Figure 4.6 Relative difference between the multi-simulation ensemble mean values, estimated by CMIP5 models and their CMIP6 counterparts under 8.5 W/m^2 forcing during 2071–2100.

Likewise, Figure A13 to Figure A16 present the relative difference between CVs of CMIP5 and CMIP6 models for the four future experiments during the short and long-term horizons, respectively. Contrary to the multi-model ensemble mean CVs (Figure A9 and Figure A10), the relative difference between multi-simulation mean CVs of CMIP5 and CMIP6 models is considerably large. For all projections and forcing scenarios, the spatial pattern of CVs for precipitation related indices tends to be random while for temperature related indices the CVs often present a consistent spatial pattern, especially for the GDD index. Like mean values, the relative difference for CVs is comparable for the same index and modelling center during short- and long-term periods as well as future scenarios, except for GDD and MNH. These observations again highlight the existing divergence between projections of individual CMIP5 and CMIP6 models, which cannot be observed by analyzing the multi-model ensemble mean values.

4.3.6 CMIP5 Versus CMIP6 Models' Simulations During the Future Period

In this section, we compare the simulations of CMIP5 and CMIP6 models over the Canadian climatic zones under two forcing scenarios in the future horizons. For this purpose, the projected long-term annual mean of indices for each simulation at the grid scale are averaged over the climate zones under the considered scenarios. Projected values for climate indices by CMIP5 (red) and CMIP6 (black) models over the East Arctic, North East Forest, and Great Lakes under 4.5 W/m^2 and 8.5 W/m^2 forcing during 2071–2100 are shown in Figure 4.7 and Figure 4.8, respectively. Results for the rest of climatic zones under future horizons and scenarios are presented in Figure A17 to Figure A22. Akin to the historical period, the models with a larger number of simulations do not necessary provide a wider envelop of projections. For instance, the envelope of AMPs by CanESM2 with five realization is larger than its corresponding CMIP6 model (CanESM5) with 50 simulations–see the fourth left column in Figure 4.8. In addition, CMIP6 projections tend to have higher values than CMIP5 under 4.5 and 8.5 W/m^2 scenarios for most of the indices (except FTC) and zones. Interestingly, projected values by CMIP6 SSP 2–4.5 are larger than CMIP5 RCP 8.5 in some cases. This implies that using CMIP5 models solely, even under the pessimistic future conditions, may lead to underestimation of changes in the indices (e.g., see the projections by CanESM for MSR over Mackenzie Valley in Figure A21). Some of CMIP5 and CMIP6 models provide contradictory future projections for the same index in the same region. For instance, while

CanESM2 simulations project lower AMPs than its historical values over the East Arctic zone, CanESM5 projects an increase in this index during the 2071–2100 period. UKESM1.0-LL presents abnormally large values for temperature-based indices over all zones under the forcing 8.5 W/m^2 for the short-term horizon (Figure A18 to Figure A20).

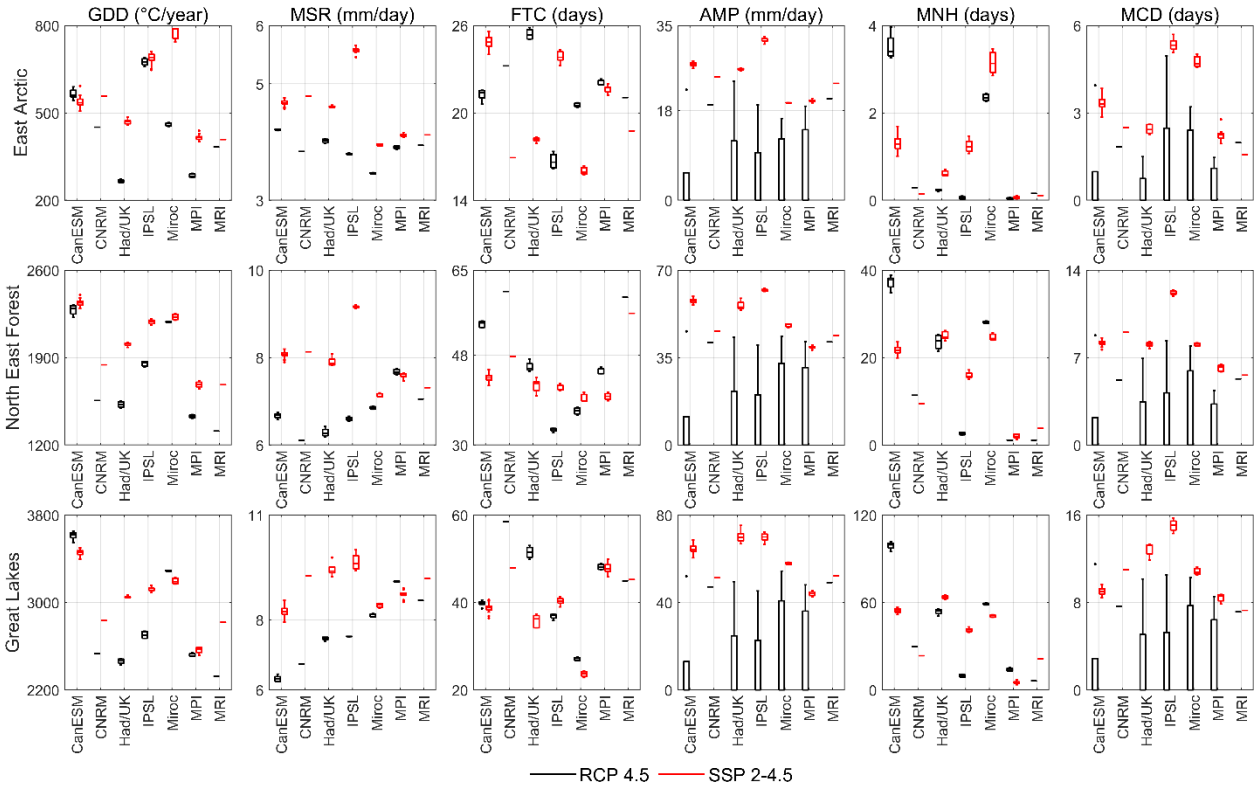

Figure 4.7 Long-term annual average values of six climate indices, estimated by simulations of CMIP5 under RCP 4.5 (black boxplots), and CMIP6 under SSP 2–4.5 (red boxplots), in the East Arctic, North East Forest and Great Lakes during 2071–2100.

In addition, Figure A23 to Figure A30 exhibit the CV values for the six indices over the 10 Canadian climatic zones in the future. In general, the estimated CVs for all scenarios and projections tend to be similar for the same climate index in the future. Moreover, the sign and magnitude of changes in CV values between the historical and future periods depend on the considered index, climate model, and climatic zone.

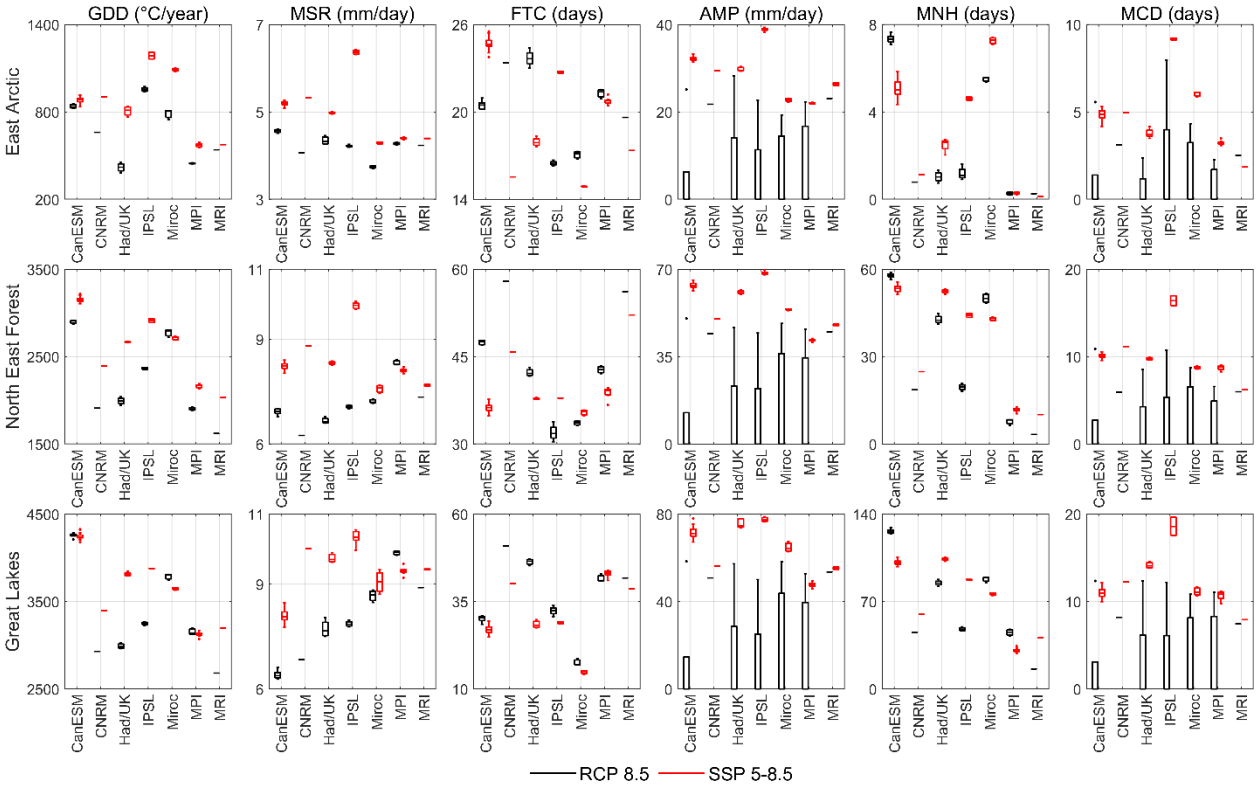

Figure 4.8 Long-term annual average values of six climate indices, estimated by simulations of CMIP5 under RCP 8.5 (black boxplots), and CMIP6 under SSP 5–8.5 (red boxplots), in the East Arctic, North East Forest and Great Lakes during 2071–2100.

4.4 Discussion and Conclusions

As Canada loses its cool, an improved understanding of climate change impacts over the country's society, economy and environment is required. The outputs of the state-of-the-art CMIP6 models have become recently available, therefore, their performance over CMIP5 models for climate change impact assessment have been questioned. Therefore, in this study, the behaviors of 389 simulations from seven CMIP6 and seven CMIP5 models in representing six important climate indices are compared across Canada during the historical and future periods. Our analyses show that there is no clear superiority of CMIP6 over CMIP5 models based on their performance in representing the mean and CV characteristics of climate indices in comparison to NOAA and/or NCEP during the historical period. Moreover, none of the estimated values by individual CMIP5/CMIP6 models necessarily match with reanalysis datasets. In fact, the simulations generally tend to underestimate the GDD and overestimate the MSR. There are also models that

present more considerable biases for some indices and zones, such as IPSL-CM6A-LR for MSR and AMP or Miroc6 for MNH. Moreover, comparisons between climate models' simulations during the historical and future period reveal a considerable change in the climate indices by the end of the century. These changes include an increase in GDD in Southern regions, an increment in MNH over the Great Lakes and Northern Plains zones, as well as changes in FTCs and precipitation-based indices across Canada. These changes can potentially cause challenges, for example, for agriculture, infrastructure, as well as human and environmental health depending on the considered Canadian region. However, further analyses are needed to develop adaptation and mitigation strategies to protect Canadian communities and ecosystems and support the country's economy. In the future studies, bias correcting both CMIP5 and CMIP6 models' simulations is required before using them for impact assessments (Masud et al., 2021; Prairie Climate Centre, 2019). Due to the existence of various bias-correction methods (Maraun & Widmann, 2018), the uncertainties associated with their implementation should be also addressed (Cannon et al., 2015; Teutschbein & Seibert, 2012). In addition, although considered reanalyses can be employed for bias correction, usage of combined datasets such as MSWEP (Beck, Wood, et al., 2019) or diverse sources such as satellite and gauge observations is also recommended (Beck et al., 2017; Beck, Pan, et al., 2019; Donat et al., 2014; Faramarzi et al., 2015; Schurer et al., 2020; Sillmann et al., 2013) as reanalysis datasets often present numerous biases (Beck, et al, 2017; Beck, Pan, et al., 2019; Donat et al., 2014). Furthermore, even though regridding is commonly used to compare different climate datasets in the same resolution, this process adds uncertainty to the comparison procedure. This is because regridding can alter the statistical characteristics of model outputs, thus modify models' performance scores (Accadia et al., 2003). In addition, the nearest neighbor method is used in this study for regridding. It would be interesting to investigate the differences between the simulations caused by using other regridding approaches, such as bilinear interpolation or first and second order conservative remapping (P. W. Jones, 1999; Shea, 2014).

It should also be noted that the intercomparisons done in this study are based on the long-term annual mean and CVs. Hence, further analyses for example, at monthly and seasonal scales can be performed to better explore the inter-annual variability of climate variables/indices. Moreover, usage of larger sets of climate indices and/or more specific models is recommended for proper assessment of climate change impact on different sectors. For example, advanced models such as

the Decision Support System for Agrotechnology Transfer module (J. W. Jones et al., 2003) can be used to evaluate crop growth and yield by taking into accounts economic and environmental factors in the future (Qian et al., 2020). Hydrological and water resources system models can be also utilized to project streamflow and assess flood risk (Seiller & Anctil, 2016). In addition, more profound investigations of impacts on the environment such as analyses of the Canadian Forest Weather Index System indices are needed to better assess climate change impacts on forest fires (Bush and Lemmen, 2019; Stocks et al., 2002).

Data Availability Statement

The datasets for this research are available online in https://esgf-data.dkrz.de/projects/esgf-dkrz/ for the CMIP5 and CMIP6 model simulations, as well as https://psl.noaa.gov/data/gridded/reanalysis/ for NOAA and NCEP reanalysis datasets.

CHAPTER 5 ESTIMATION OF FUTURE POTENTIAL EVAPOTRANSPIRATION IN CANADA USING THE BIAS-CORRECTED CMIP6 SIMULATIONS

In the previous chapter, we evaluated the performance of CMIP6 models in representing a series of climate indices in Canada and compared them to their CMIP5 predecessors. In this chapter, CMIP6 outputs are used to estimate potential evapotranspiration in the country. Specific questions to be addressed in this chapter are how much PET would change in the future under different scenarios and horizons? Are the projected changes in PET sensitive to the choice of climate models? Also how much the estimated change in PET is sensitive to the selection of PET equation? Finally, would bias correcting GCMs' outputs using different benchmarks affect the estimated changes in PET in the future? Section 5.1 presents the materials and methods used for PET estimations and QDM performance assessment. Section 5.2 shows the PET values estimated using the raw and bias-corrected GCMs as well as the benchmarks in the historical period. In addition, future change in PET in the short- and long-term horizon under different scenarios are also analyzed across Canadian zones.

5.1 Materials and Methods

Figure 5.1 shows the flowchart for addressing above-noted questions with a greater goal of understanding the impact of climate change on PET in Canada. For this purpose, first, the PET values are estimated during the historical period using three PET equations with the simulations of seven CMIP6 models, and two benchmarks. Accordingly, the GCM-based and benchmarks-based PETs are inter-compared during the historical period (1961-1990). If biases exist in the GCM-based estimates, the QDM will be used to bias correct the simulations of climate models once with NOAA and once with CRU/JRA. Performance measures are used to assess the quality of bias-corrected simulations during the historical period. Afterwards, PET values are estimated during two future horizons (2021-2050 and 2071-2100) and under scenarios SSP 2-4.5 and SSP 5-8.5 using the bias-corrected GCMs simulations and three PET equations. Accordingly, the relative difference between the future and historical values of PET are found. Finally, the monthly range

of PET estimates for all simulations and models under the future SSPs and horizons are presented in each climatic zone (Figure 1.1).

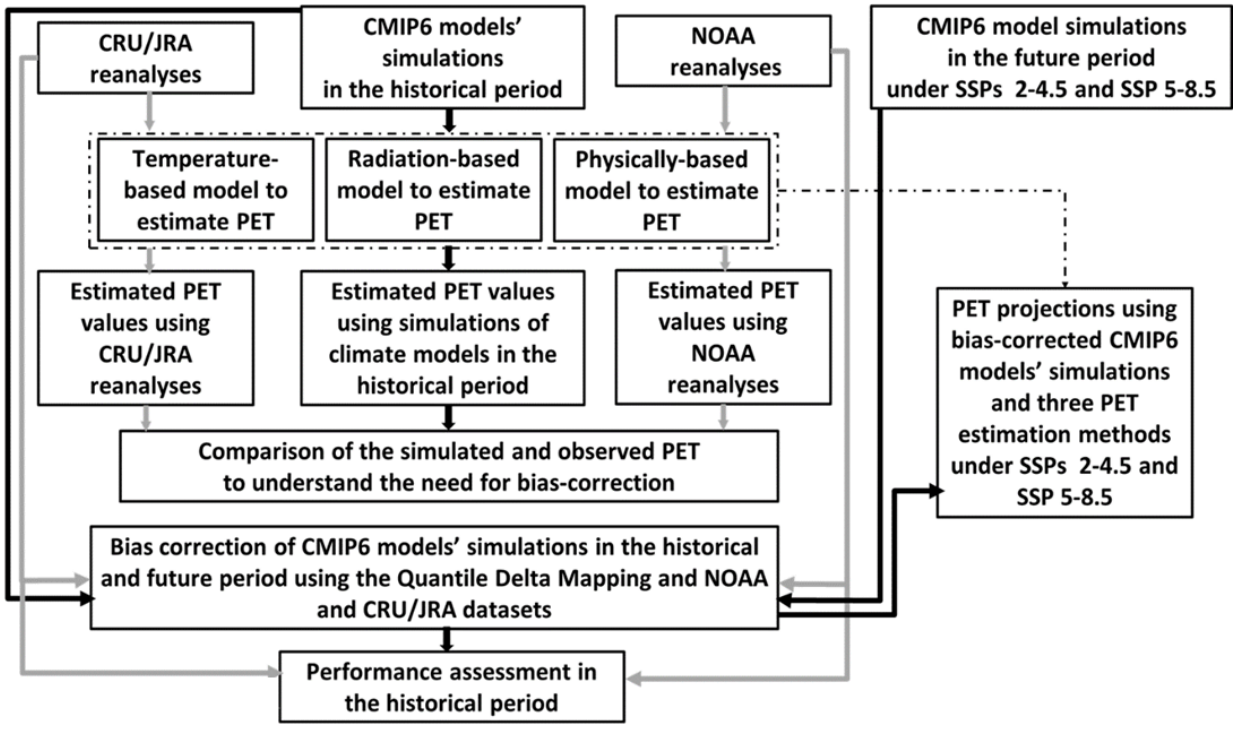

Figure 5.1 Flowchart showing the approach used to estimate potential evapotranspiration.

5.1.1 PET equations

Three commonly used equations, namely, combination-based Penman-Monteith FAO56 (Allen et al., 1998), radiation-based Priestley-Tailor (Priestley and Taylor, 1972) and temperature-based Hargreaves (Droogers and Allen, 2002) are used to estimate PET in Canada. These equations often performed well in comparison to other models in their respective categories, e.g., in Switzerland (Xu and Singh 1998, 2002) and in Canada (Sentelhas et al., 2010).

The FAO56 Penman-Monteith (Allen et al., 1998) equation requires much more input of climatic variables as it represents a combination of the energy balance with the mass transfer method (Anctil et al., 2012). It has been shown that estimations based on this model match lysimeter ET values; and is therefore often used as a benchmark (Oudin et al., 2005).

$$PET = \frac{0.408(R_n - G) + \gamma \frac{900}{T + 273} u_2 (e_s - e_a)}{\Delta + \gamma (1 + 0.34 u_2)} \quad 5.1$$

In this formula, R_n is the net radiation at the crop surface (MJ m^{-2} day^{-1}) determined with the longwave and shortwave radiation. G is the soil heat flux density (MJ m^{-2} day^{-1}) considered null due to its value being negligible in comparison to R_n (Sentelhas et al., 2010). T is the mean air temperature at 2m height (◦C), determined with maximum and minimum temperature (Tmax and Tmin). U_2 is the wind speed at 2 m height (m s^{-1}), which is directly taken from the GCMs outputs or converted to the correct height calculated from zonal and meridional wind for the benchmarks data (Allen, 1998). While e_s presents the saturation vapour pressure (kPa) estimated with Tmax and Tmin, e_a is the actual vapour pressure (kPa) calculated with Tmax, Tmin as well as relative humidity. The slope vapour pressure curve (kPa ◦C^{-1}), Δ, is estimated with T. Finally, γ represents the psychrometric constant (kPa ◦C^{-1}), which is estimated with atmospheric pressure.

The Radiation-based Priestley (Priestley and Taylor, 1972) also uses the energy conservation but requires fewer variables than Penman-Monteith (wind speed and relative humidity are not needed).

$$PET = \alpha \frac{\Delta}{\Delta + \gamma} \frac{R_n}{\lambda} \quad 5.2$$

This formula also considers, the α coefficient equal to 1.26 and λ is the latent heat of vaporization, considered to be equal to 2.45, MJ kg^{-1}. Once again, R_n is the net radiation, Δ the slope vapour pressure curve and γ the psychrometric constant (kPa ◦C^{-1}).

Finally, Hargreaves equation (Droogers and Allen, 2002) only requires data of Tmax and Tmin, which are often the only climatic variables available in most areas (Kumar et al., 2012; Xu and Singh, 2002). Due to its simplicity, Hargreaves equation is commonly used in the literature.

$$PET = \ 0.0023 * 0.408 R_a (T + 17.8) TD^{0.5} \quad 5.3$$

In this equation, T is the mean air temperature and TD is the difference between minimum and maximum temperature (◦C). R_a is the extraterrestrial radiation (MJ m^{-2} day^{-1}), function of the latitude and day of the year.

5.1.2 Climate Data

The monthly maximum and minimum temperature (Tmax and Tmin), longwave upward and downward radiation (rlus and rlds), shortwave upward and downward radiation (rsus and rsds), relative humidity (Rh), 2 m wind speed (U) and sea level pressure (Pr) datasets for seven CMIP6 climate models, cumulating 426 simulations, to estimate PET are acquired in spring 2021 from https://esgf-data.dkrz.de/projects/esgf-dkrz/. The name of these models, their spatial resolution as well as their number of simulations during the historical period of 1961 to 1990 and future period of 2021-2050 and 2071-2100 for each scenario of SSP 2-4.5 and SSP 5-8.5 are presented in Table 5.1.

Table 5.1 The name, spatial resolution, as well as number of simulations for CMIP6 climate models during the historical and future periods.

Model	**Spatial Resolution**	**Number of historical simulations**	**Number of SSP 2-4.5 simulations**	**Number of SSP 5-8.5 simulations**
CanESM5	2.8° × 2.8°	65	50	50
CNRM-CM6-1	1.4° × 1.5°	30	6	6
IPSL-CM6A-LR	2.5° × 1.3°	32	11	6
MIROC6	1.4° × 1.4°	50	3	50
MPI-ESM1-2-LR	1.9° × 1.9°	10	9	10
MRI-ESM2.0	1.1° × 1.1°	7	1	2
UKESM1.0-LL	1.9° × 1.3°	18	5	5

As previously noted, SSP 5-8.5 represents the worst-case scenario, with the highest end of the century radiative forcing, 8.5 W/m^2, which is a measure of the Earth's surface heating (Van

Vuuren, 2011) and the worst SSP5, which represents a fossil-fuel based development with the domination of mitigation challenges (Eyring et al., 2016; Riahi et al., 2017; Stouffer et al., 2017). On the other hand, SSP 2-4.5 presents the middle of the road for both SSP2 (intermediate challenges) and end of the century forcing 4.5 W/m^2. Further information on these models can be found at https://pcmdi.llnl.gov/.

Data from multiple sources are used to evaluate the performance of raw and bias-corrected GCMs. NOAA reanalysis data were obtained for the same variables noted for GCMs, except wind speed at 10 m (Compo et al., 2011; Slivinski et al., 2019, 2020). NOAA has a 1° spatial resolution and is the first reanalysis offering coverage over a full century, which was possible due to the assimilation of observed synoptic pressure as well as prescribe sea surface temperature and sea ice distribution (Slivinski et al., 2019). Apart from NOAA, the values for the same variables are obtained from a combination of observed and reanalysis datasets of Climatic Research Unit gridded Time Series version 4.04 (CRU-TS 4.04), Japanese 55 years Reanalysis (JRA55), and CRU-JRA. This way other types of datasets than reanalyses are used as benchmarks. In brief, CRU TS 4.04 provides interpolated angular-distance weighting observed monthly datasets for Tmax, Tmin and vapor pressure (to estimate relative humidity) with a resolution of 0.5˚ (Harris et al., 2020). The JRA55 provides data of rlus and rsus at the 1.5˚ resolution (Kobayashi et al., 2015). The CRU-JRA, which combines the JRA55 reanalysis and CRU-TS dataset made by the Climatic Research Unit, and provides daily Pr, rlds, rsds, as well as U at 10 m with a resolution of 0.5˚ (Harris et al., 2020; Kobayashi et al., 2015). The CRU, CRU-JRA and JRA55 datasets were combined to provide the values for all considered variables in CMIP6 GCMs to estimate PET in the same way (Iizumi et al., 2020; Zang et al., 2020). It should be noted that the monthly values for the variables are found based on the means of their daily (or hourly) data to be comparable to the GCM monthly outputs. In addition, since the climate models, reanalyses, observed, and mix data do not have similar resolution, all datasets are regridded to a common 1.5° using the nearest neighbor algorithm (Shea, 2014) from the xESMF python module (https://doi.org/10.5281/zenodo.1134365).

5.1.3 QDM Performance Assessment

QDM bias correction is used to improve the GCMs' simulations considering both NOAA and CRU/JRA datasets separately as benchmarks. For this purpose, the available Python codes of

Xclim module, which is prepared by Travis Logan et al. (https://xclim.readthedocs.io) are used. Accordingly, different measures are used to assess the performance of QDM. For this purpose, Percentage of Relative Difference (PRED) is used to evaluate the relative difference between the expected (average) estimations of all GCMs' simulations with respected to benchmark (NOAA and CRU/JRA) values for climate variables. Moreover, three other measures namely the Mean Absolute Monthly Difference (MAMD), Ratio of Yearly Amplitude (ROYA) as well as Ratio of Temporal Variances (RATV) (Keuler et al., 2006; Schoetter et al., 2012) are used to analyze the behaviour of bias-corrected simulations per individual GCMs at the monthly scale. Equations 5.4 to 5.7 show these measures. The bias-corrected simulations are compared with the benchmarks, NOAA and CRU/JRA in the baseline period.

$$\%diff = \frac{\bar{M} - \bar{B}}{\bar{B}} * 100 \qquad 5.4$$

$$MAMD = \frac{1}{12}\sum_{m=1}^{12} |\overline{M_m} - \overline{B_m}| \qquad 5.5$$

$$ROYA = \frac{\max(\overline{M_m}) - \min(\overline{M_m})}{\max(\overline{B_m}) - \min(\overline{B_m})} \qquad 5.6$$

$$RATV = \frac{\sigma_M^2}{\sigma_B^2} \qquad 5.7$$

where M and B respectively present GCMs simulations and benchmarks values. σ and m are respectively standard deviation and the month of the year.

MAMD allows to measure the absolute average bias (error) of GCMs in comparison to the reference dataset at the monthly scale. ROYA notifies us about the ratio of the simulated and benchmark climatic variable annual cycle by evaluating the monthly amplitude of values. However, ROYA tends to the optimal value (1.0) for climatic variables with strong dominant annual cycle such as temperature (Schoetter et al., 2012). Finally, RATV gives the ratio of variance between the GCMs and benchmark monthly values for the studied period, which indicates the resemblance in the spread of values around the mean of the two datasets.

5.2 Results

Here the PET values for the benchmarks, NOAA and CRU/JRA, as well as raw and bias-corrected CMIP6 simulations during the historical and future periods are presented.

5.2.1 Estimated PET using Raw CMIP6 Simulations versus Reanalyses during the Historical Period

The monthly PET in each grid is estimated using the raw GCM simulations fed into the Penman-Monteith, Priestley-Taylor and Hargreaves equations. These values are then averaged over all simulations and seven climate models to represent monthly GCM-based (or multi-model ensemble mean) PET. The same three equations are also used to estimate the monthly average using the reanalyses datasets. Figure 5.2 presents the long-term average daily PET values (mm/day) using GCMs (left column), CRU/JRA (middle column), and NOAA (right column).

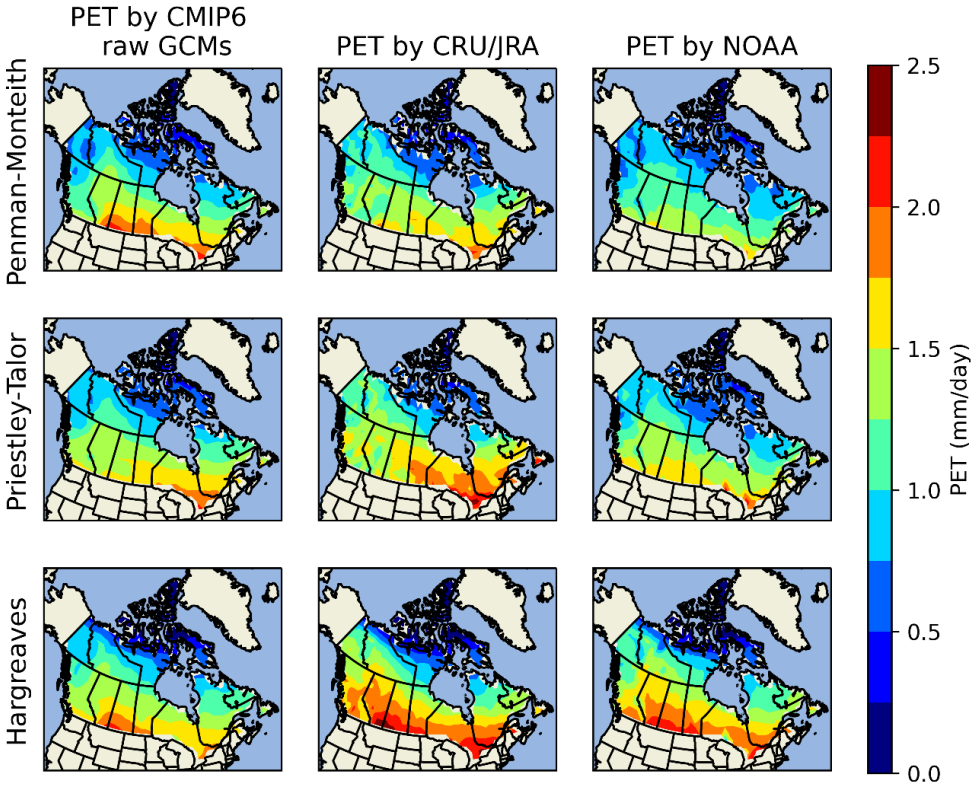

Figure 5.2 Long-term annual PET values, estimated based on combination-based Penman-Monteith, radiation-based Priestley-Taylor and temperature-based Hargreaves, using the raw simulations of raw GCMs, CRU/JRA and NOAA during the historical period.

The impact of using different PET estimation method can be seen in each row. The spatial distribution of GCM-based estimates by these equations is almost similar. Furthermore, observing the reanalyses, there is a visible difference between their estimates by Priestley-Taylor particularly in the South compared to the other two formulas. Since the same equation is employed in each row, the divergence between PET values is only associated with using different datasets. As it can be seen there is a difference between the PET spatial distribution and estimates by GCMs and reanalyses particularly in Southern Canada. Also, the reanalyses of NOAA and CRU/JRA themselves do not necessarily present similar PET values for the same equation, especially for Priestley-Taylor estimates. The divergence between PET values of CMIP6 and benchmarks is more noticeable using the temperature-based equation, which can be caused by the differences between applied models' temperature values specifically in the Prairies, where PET estimations are critical for irrigation planning.

5.2.2 Performance of QDM Bias-Correction

Due to the difference between CMIP6 simulations and both reference datasets, shown by Figure 5.2, QDM is used to correct the biases in the GCMs for both historical and future simulations. In this section, first the performance of bias-corrected and raw simulations per climate models, 7 in total, and in each grid is compared with the benchmarks using MAMD, ROYA, and RATV. Accordingly, the result of this comparison is shown for ten Canadian climatic zones, as seen in Figure 1.1 and utilized in Bourdeau-Goulet and Hassanzadeh (2021), to better accentuate and visualize the results across the country. As an example, the performance of bias-corrected and raw simulations per seven GCM models for Tmax and Tmin in Yukon climatic zone is presented in Figure 5.3 and Figure 5.4. Tmax and Tmin are used to show the results here due to their importance in PET equations. In fact, there is a strong rank correlation between PET estimates and these variables, see Kendall-tau values in Figure B1 to Figure B3. Figure B4 to Figure B21 also present the results of these variables in the remaining Canadians climatic zones. The efficiency of QDM is blatant for both benchmarks, ten zones, two climatic variables as well as for the three measures. Indeed, MAMD, ROYA, and RATV values are all close to their optimum, 0 for MAMD as well as 1.0 for ROYA and RATV when considering the bias-corrected simulations versus benchmark values. On the other hand, these measures are much larger when comparing raw simulations with

benchmarks, up to 10 times higher values for MAMD in Yukon (Figure 5.4). Thereby, this visualization also confirms the important divergence between raw GCMs simulations and the two benchmarks as they perform poorly in comparison to bias-corrected data for all measures, zones, and models. The GCMs raw simulations tend to present large biases in Northern zones such as East Arctic, Yukon and Mackenzie Valley (Figure B14, Figure 5.3 and Figure B16). Generally, ROYA is the measure where raw simulation values are closer to the optimal value (1.0) compared to MAMD (0) and RATV (1.0). This might be due to the dominant annual cycle in temperature which improves the performance of raw GCMs for this measure. However, for both ROYA and RATV, most raw GCMS simulations present higher (>1.0) or lower (<1.0) annual cycle amplitude and variation around the mean.

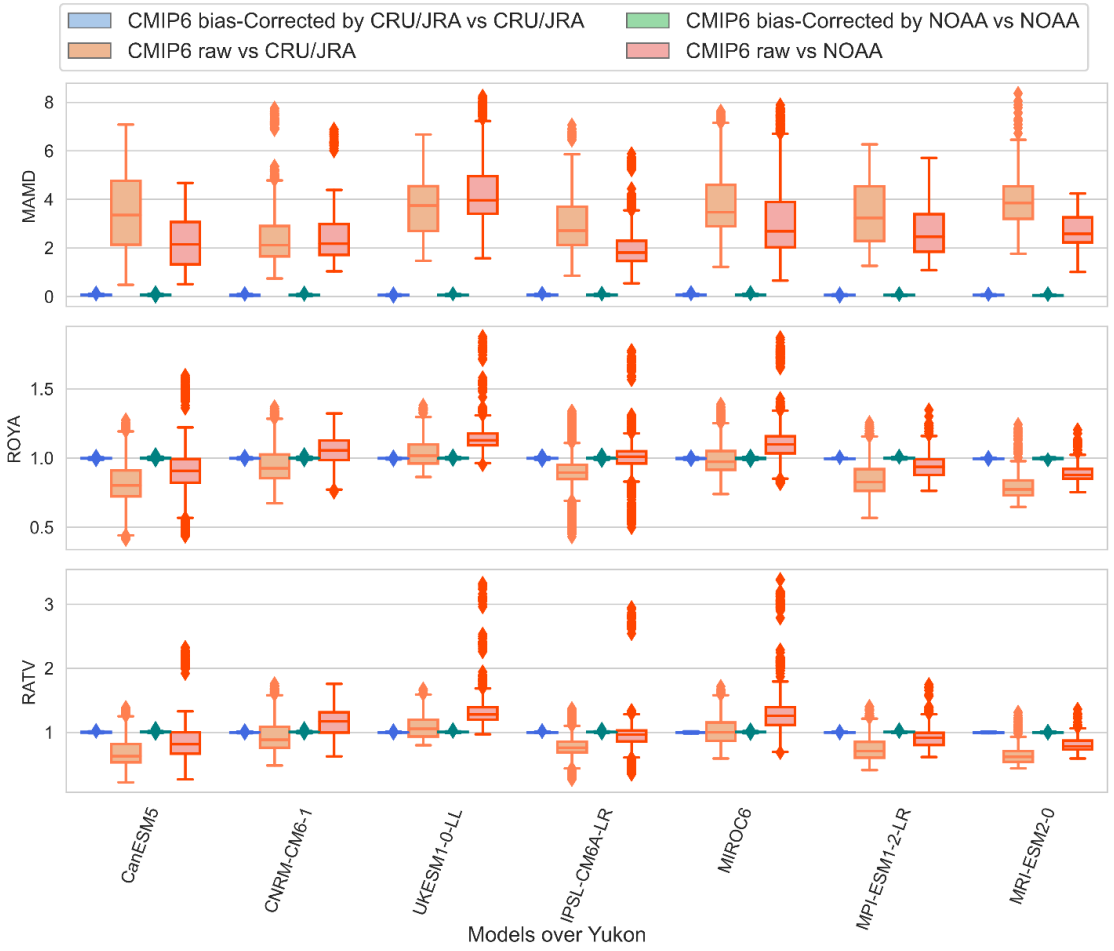

Figure 5.3 Monthly performance measures of Tmax bias-corrected and raw CMIP6 simulations compared to their respective benchmark (CRU/JRA and NOAA) over Yukon during 1961-1990.

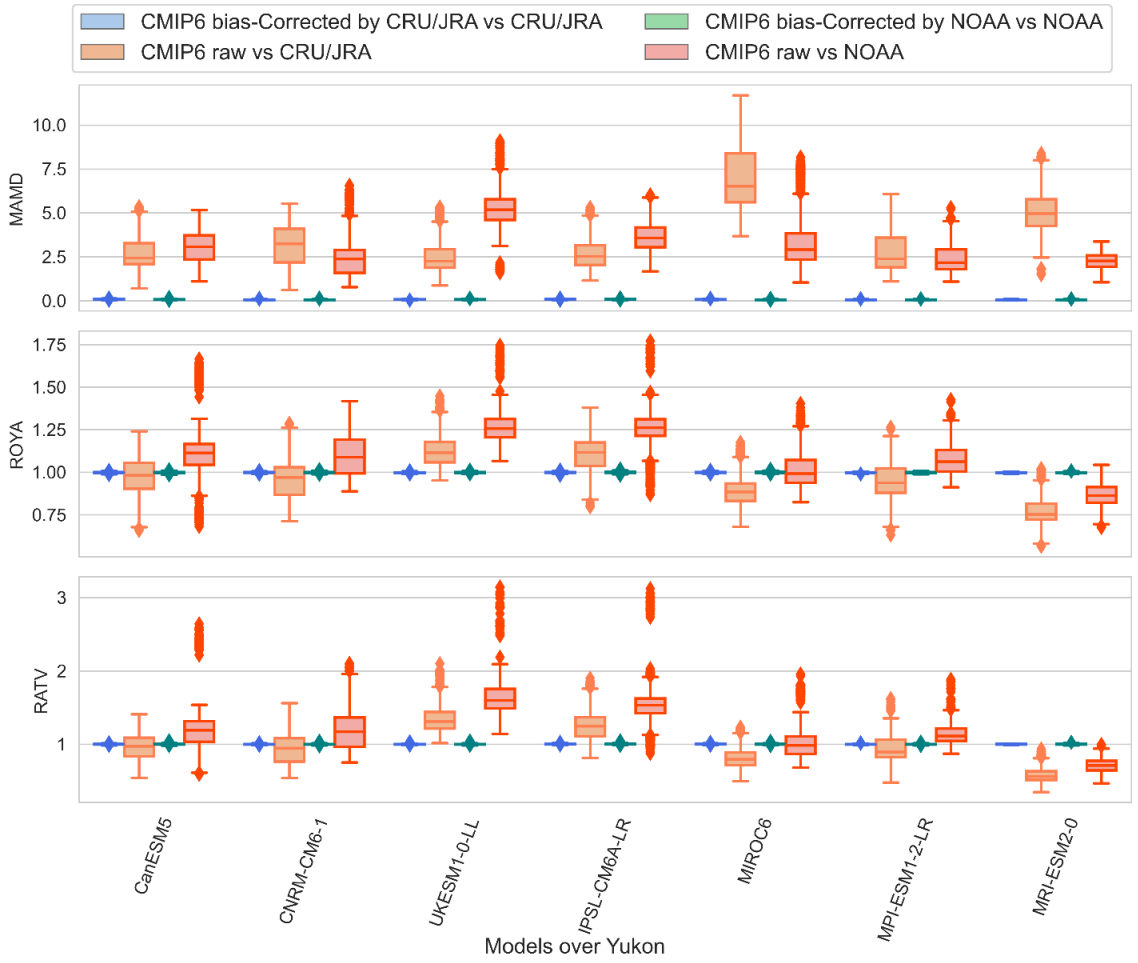

Figure 5.4 Monthly performance measures of Tmin bias-corrected and raw CMIP6 simulations compared to their respective benchmark (CRU/JRA and NOAA) over Yukon during 1961-1990.

Since the difference between the performance of bias-corrected values by CRU/JRA and NOAA is not completely visible in the former Figure 5.3 and Figure 5.4, here Figure 5.5 presents the same results but only for the bias-corrected values of Tmax and Tmin over Yukon for better comparison purposes. Figure B22 to Figure B30 present the same visualizations for the remaining climatic zones. As it can be seen, there is a difference between the error values per climate models depending on their benchmarks, NOAA or CRU/JRA. It also depends on the type of studied variable and/or climatic zone. Again, despite these differences, considering the ranges for these performance measures, the applied bias correction method is highly efficient in reducing errors, bringing closer the mean annual cycle amplitude of the GCMs to the one of the benchmarks and give similar results for the spread around the mean.

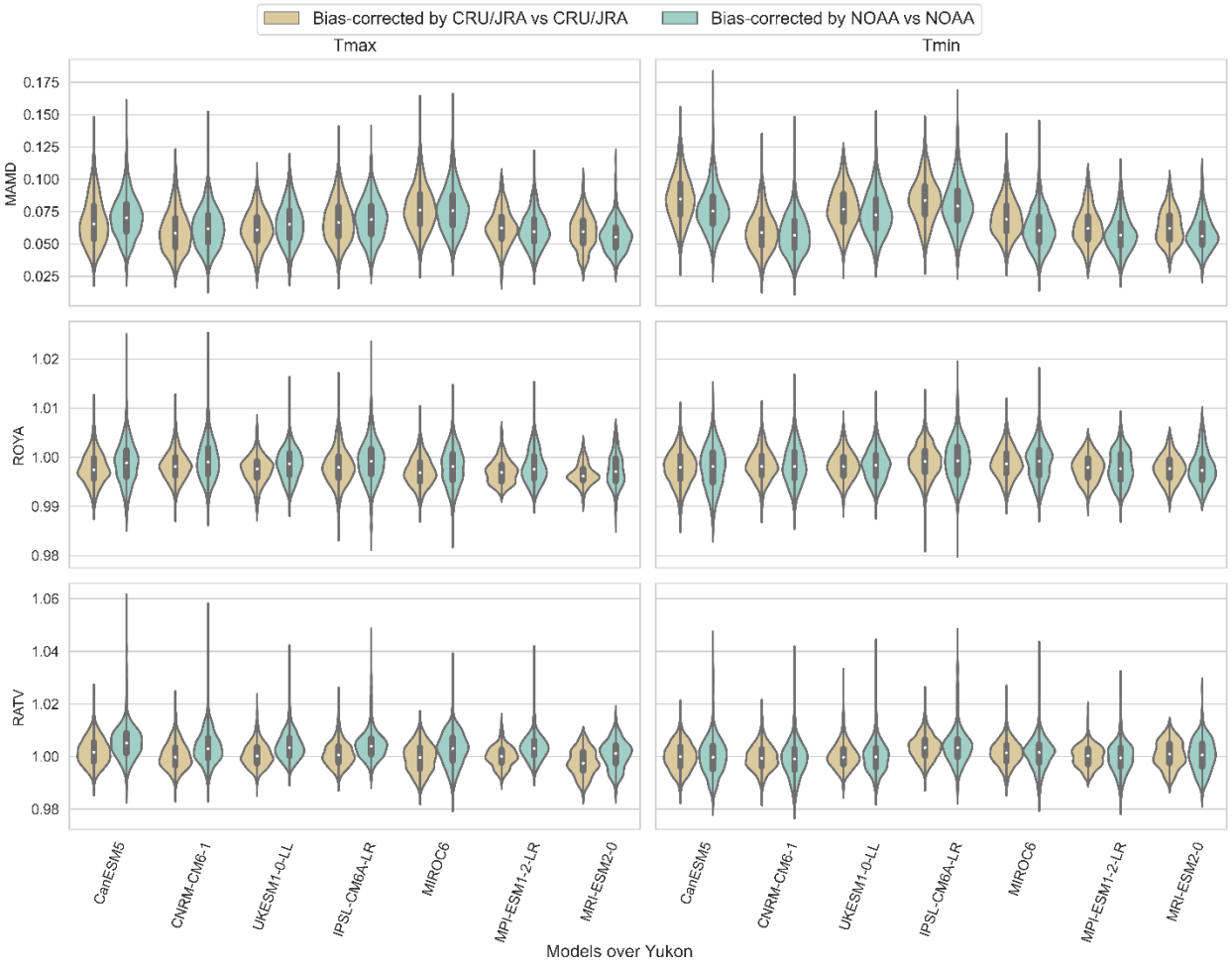

Figure 5.5 Monthly performance measures of Tmax and Tmin bias-corrected CMIP6 simulations compared to their respective benchmark (CRU/JRA and NOAA) over Yukon during 1961-1990.

Using the bias-corrected GCMs' simulations with NOAA and CRU/JRA, the monthly PET values are estimated for three evapotranspiration equations during the historical period. Figure 5.6 displays the relative error in percentages between multi-model ensemble mean PET based on bias-corrected simulations and their corresponding benchmarks CRU/JRA (left column) and NOAA (third left column) as well as the PET difference between raw GCMs simulations and reference datasets (second and fourth columns). The results for Penman-Monteith, Priestley-Taylor, and Hargreaves are shown from top to bottom rows respectively. Focusing on each row reveals that the differences between PET values by bias-corrected simulations with NOAA are smaller than with CRU/JRA, similar to the relative difference with raw simulations. In addition, the spatial distribution of the error with respect to NOAA (third column) is almost similar using different PET

equations. The CMIP6 bias-corrected PET values still underestimate NOAA values, although the divergence is very small (less than 5%). Considering the left column, it can be seen that the PET values by bias-corrected CMIP6 are also underestimating the CRU/JRA PET values in most regions and overestimate them up north. This divergence is more visible using radiation-based PET equation over Central Canada and temperature-based in Northern Canada. The difference between PETs by benchmarks and raw simulations is around ±30%. Since the relative differences between bias-corrected and benchmark PET values have become very small i.e., less than ±10%, the performance of Quantile Delta Mapping method is acceptable.

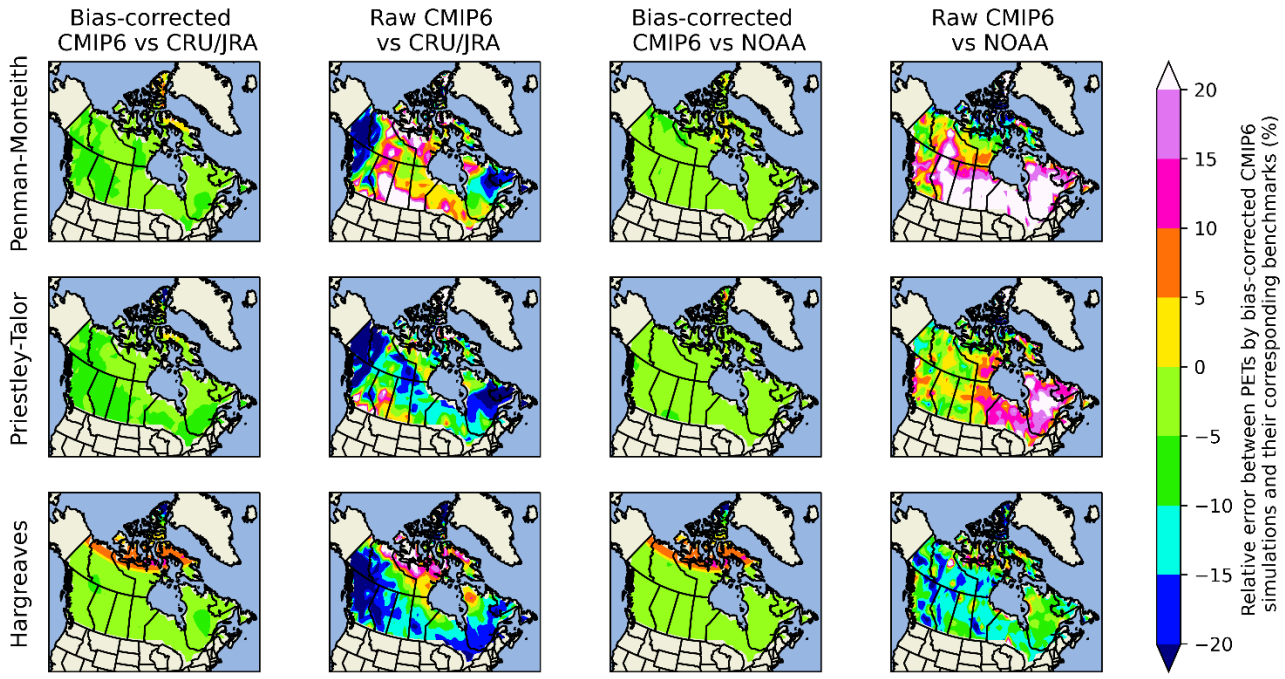

Figure 5.6 Percentage of relative error between the long-term annual average PET values estimated by bias-corrected as well as raw CMIP6 models and their respective benchmark CRU/JRA (left) and NOAA (right) using the Penman-Monteith (top row), Priestly-Taylor (middle row) and Hargreaves (bottom row) equations during 1961-1990.

5.2.3 Multi-Model PET Projections

The GCM-based projections under SSPs 2-4.5 and 5-8.5 over 2021-2050 and 2071-2100 are bias-corrected with NOAA and CRU/JRA and fed to three evapotranspiration equations to estimate future monthly PET in each grid. Accordingly, the long-term annual PET values in the future are

compared with the bias-corrected GCM-based PET values during the historical period to evaluate the changes in this variable for 2021-2050 (Figure 5.7) and 2071-2100 (Figure 5.8).

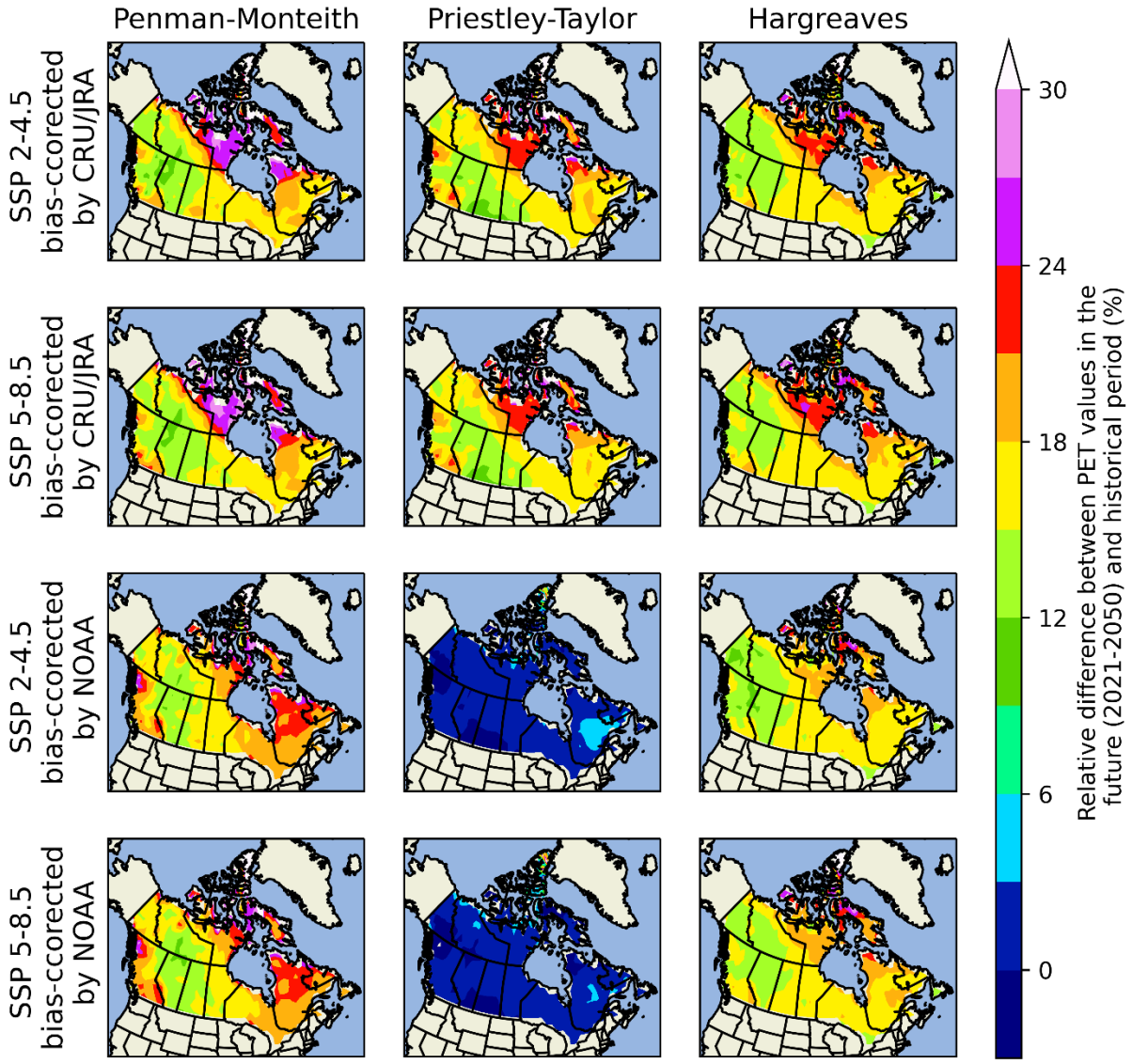

Figure 5.7 Percentage of relative difference between the long-term annual average PET values estimated using three evapotranspiration equations in 2021-2050 under SSP 2-4.5 and SSP 5-8.5 and historical period.

It is clear that PET values would increase considerably in the future when looking at the two figures and on average this increase is about 50 % for all projections over the country but the magnitude of the means is highly dependent on the bias correction and equation used. The largest rise of PET is consistently projected across the Canadian North in particular in the extreme Northern grids with

over 100% increase in both scenarios and horizons. Even though, all three territories are affected by the growth in PET, Nunavut has the highest rate of increase in PET estimates, generally between 20-30% for short- and more than 50% for long-term horizons. Important rises in PET are also estimated for Northern Quebec (up to 24% and over 50% in short- and long-term). On the opposite, central western Canada shows less expansion in PET over both horizons. Nevertheless, the magnitude and spatial distribution of increases depend on the utilized PET equations, bias-correction benchmarks as well as future scenarios and horizons.

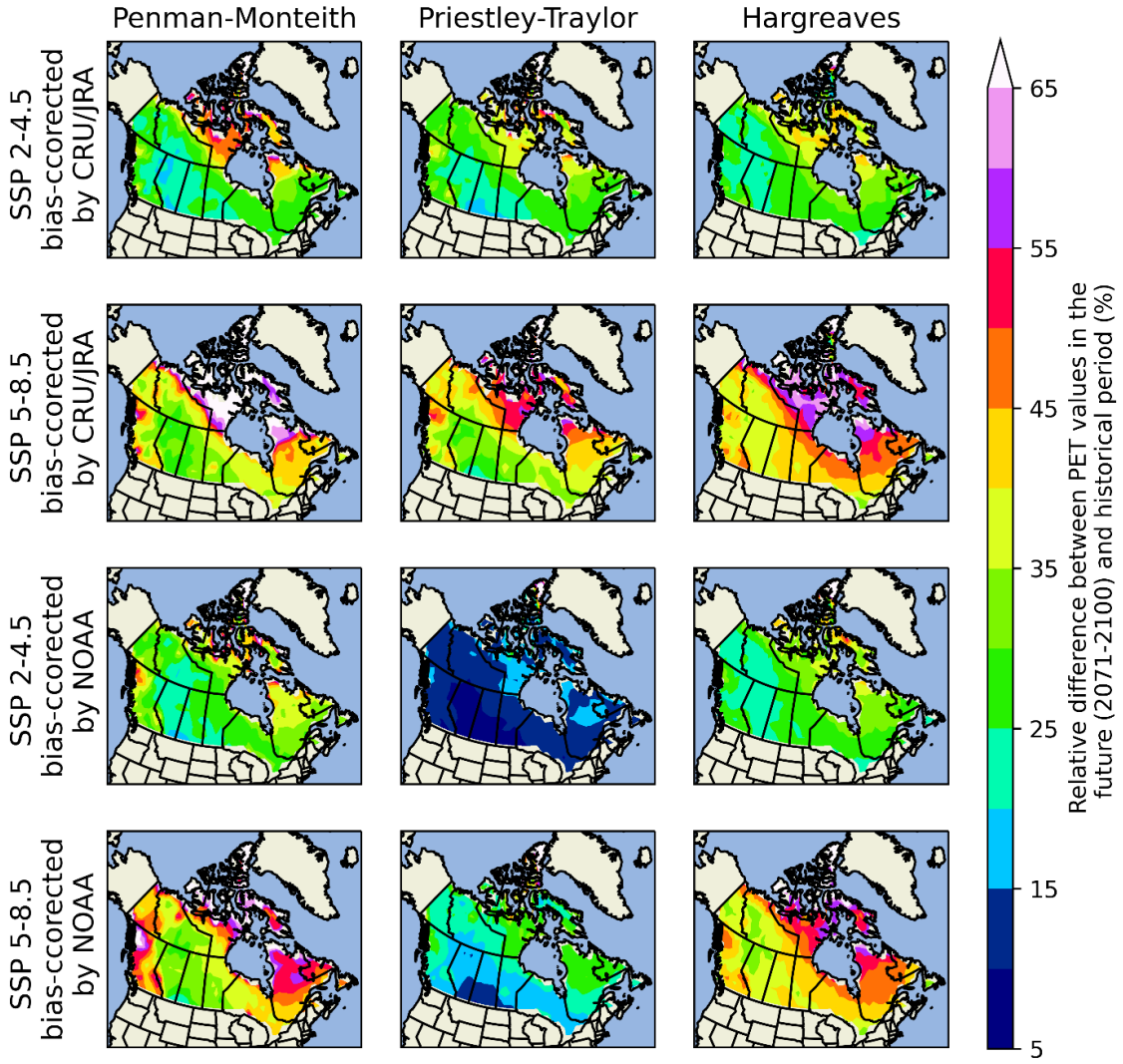

Figure 5.8 Percentage of relative difference between long-term annual average PET values estimated using three evapotranspiration equations in 2071-2100 and historical period under SSP 2-4.5 and SSP 5-8.5.

Obviously, the rate of increase in PET is higher in long-term than short-term horizon due to the more important increases in climatic variables values for this period as shown by Figure B31 and Figure B32. For instance, in 2071-2100, the increase in PET is around 40% and the largest increase can be seen in Northern Canada (over 100%). It is also clear that higher PET values are projected under SSP 5.8.5 particularly for 2071-2100, which is due to 8.5 W/m^2 being the worst-case scenario in terms of global warming and that this scenario presents important augmentation in climatic variables past 2050 while other future scenarios hit a plateau around the mid century (Cook et al., 2020).

Even if both bias-corrected projections present similar change over southern and central Canada for Hargreaves and Penman-Monteith, the importance of the considered benchmarking is also noticeable in future horizons and scenarios. For example, PET CRU/JRA-based bias-correction change is around 10% higher than NOAA over Nunavut during 2021-2050. This difference is doubled for the long-term horizon. Furthermore, Priestley-Taylor PET estimated with NOAA-based bias correction present much lower relative change in comparison to CRU/JRA-based bias corrected Priestley-Taylor estimates and in comparison, to the change presented by the other two equations. The lower change of Priestley-Taylor estimates with NOAA based bias correction may be caused by CRU/JRA having higher increase of rlds and lower change of rsus compared to NOAA in the future as shown in Figure B31 and Figure B32.

The impact of using different PET equations is also visible by moving from left to right in each panel in short- and long-term horizons and under both SSPs. For example, in the short-term horizon, the projected change for the Penman-Monteith estimates is ~3% higher than the one projected for Hargreaves over Nunavut for both, SSP 2-4.5 and SSP 5-8.5. As mentioned previously, the projected change of Priestley-Taylor PET estimated with bias-corrected NOAA simulations show abnormally low magnitude compared to other projections for the two horizons and scenarios. Hargreaves equation estimates display 5% higher relative difference over the eastern part of Canada (from Manitoba to the Maritimes) in comparison to the other equations for SSP 5-8.5 and long-term horizon. Again, this is probably caused by the important increase in Tmin and Tmax by the end of the century, which are the only two inputs of the Hargreaves equation, but might also be caused by the diminution of Rh and U over Southern Canada resulting in lower estimates of Penman-Monteith PET -see Figure B32.

5.2.4 Monthly PET Projections in Canadian Zones

Further analyses are provided to understand the monthly range of mean PET values (mm/day) in the future as well as the sensitivity of the GCM projections, utilized benchmarking, as well as PET equations over Canadian zones. Figure 5.9 displays the monthly PET during 2021-2050 for SSPs 2-4.5 and 5-8.5 using the bias-corrected simulations of each climate model (rows) based on CRU/JRA and NOAA benchmarks fed into Penman-Monteith (blue), Priestley-Taylor (red) as well as Hargreaves (black) over Yukon. Figure 5.10 presents the same visualization but for the 2071-2100 period. In each panel, the envelopes contain the PET values for 30 years in the considered horizon as well as all simulations per GCMs in all grids in the given climatic zone. The expected values are also shown with solid lines. Figure B33 to Figure B50 shows similar results of PET over the remaining climatic zones during short- and long-term horizons.

Logically, the projected PET values are larger during the summer months (May to August) and smaller, even close to zero, in fall until midwinter (September to February). Comparisons between Figure 5.9 and Figure 5.10 show that the PET values are slightly larger during the hot months in the long-term than short-term horizons and under SSP 5-8.5 than SSP2-4.5 especially over Northern zones. Results for different climatic zones show that the highest PET values are estimated for the Great Lakes and North East Forest (Figure B44 and Figure B46), whereas the smallest values are projected over East Arctic (Figure B43). Overall, the ensemble and expected PET values as well as peak timing based on the three evapotranspiration equations are not always matching and the divergence highly depends on the considered climatic zone. For instance, the shape and peak PET values by Hargreaves are completely different from those projected by the other PET equations in the East Arctic (Figure B43). Another example is over North West Forest, where the range and peak PET values and timing are different given the three PET equations under SSP 5-8.5 (Figure B47). Focusing on each zone, it can be seen that the peak of PET timing and magnitude by climate models can be diverging, e.g., see the values in the right column for Mackenzie Valley (Figure B45). GCMs also have an impact on the spread of monthly PET estimates – see Figure B50 right two columns where CanESM5 presents a range of values twice larger than MRI-ESM2-0 for summer months. Moreover, among the models, MRI-ESM2-0 tends to present higher PET values than the rest of GCMs especially when the Priestley-Taylor equation is used over the Great Lakes,

North East and West Forests (Figure B44, Figure B46 and Figure B47). In contrast, CanESM5 and UKESM1-0-LL present greater PET values for the other zones.

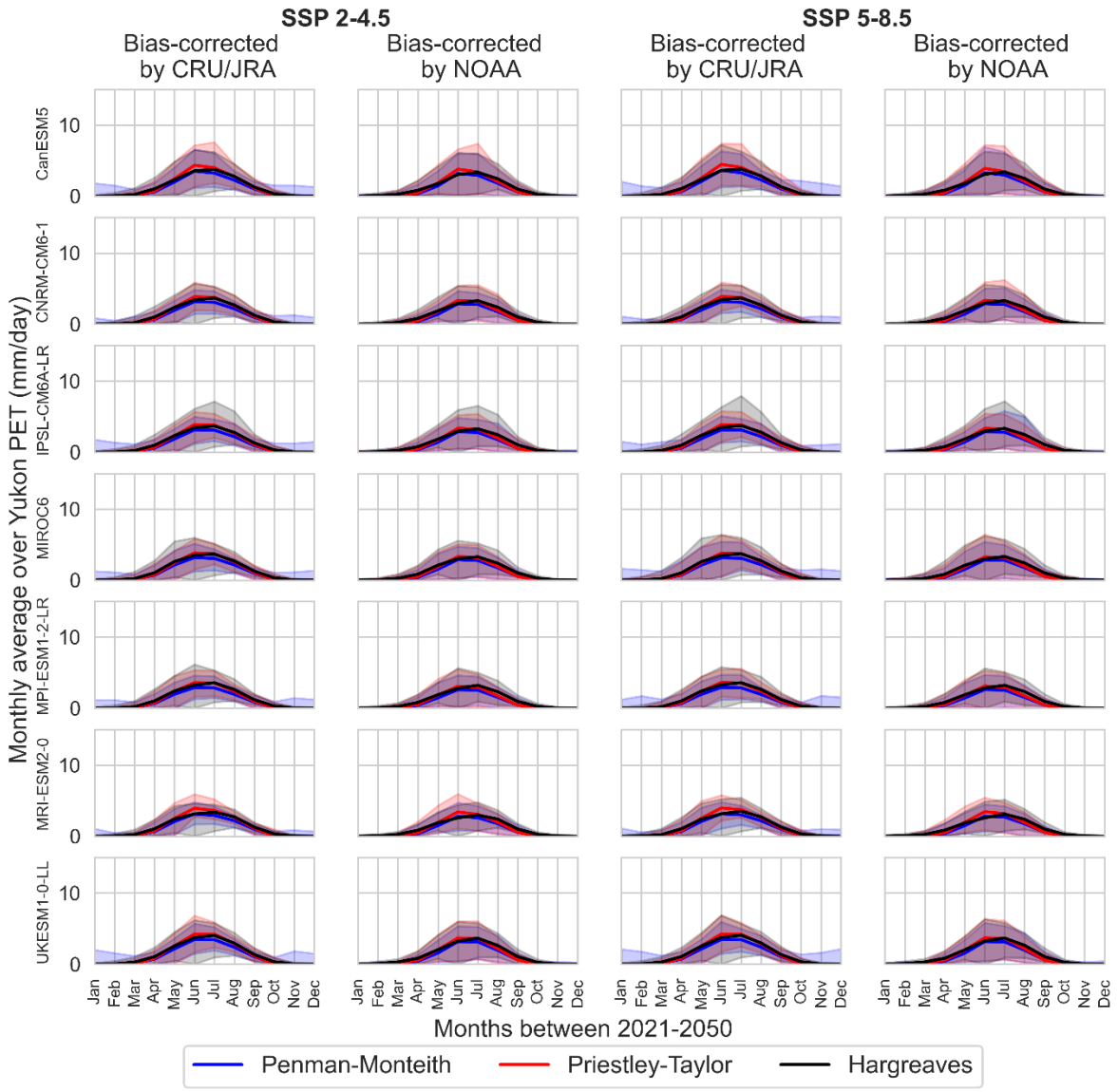

Figure 5.9 Monthly PET values during 2021-2050 and under SSPs 4-4.5 and 5-8.5, estimated using all simulations per climate models (each row) over Yukon.

Moreover, the utilized PET equation plays a key role in estimating future PET values over the year and peak timing. In the Great Lakes and North East Forest (Figure B44 and Figure B46), Priestley-Taylor provides the greatest PET estimates while Penman-Monteith provides the smallest values for all models with a difference of around 1 mm/day for the expected peak values. The Northern

Plains (Figure B48) is the only zone, where Hargreaves equation provides the greatest PET simulations as well as larger expected values. On the opposite, using this equation, the smallest values for PET can be estimated in the East Arctic in comparison to the other two equations (Figure B43).

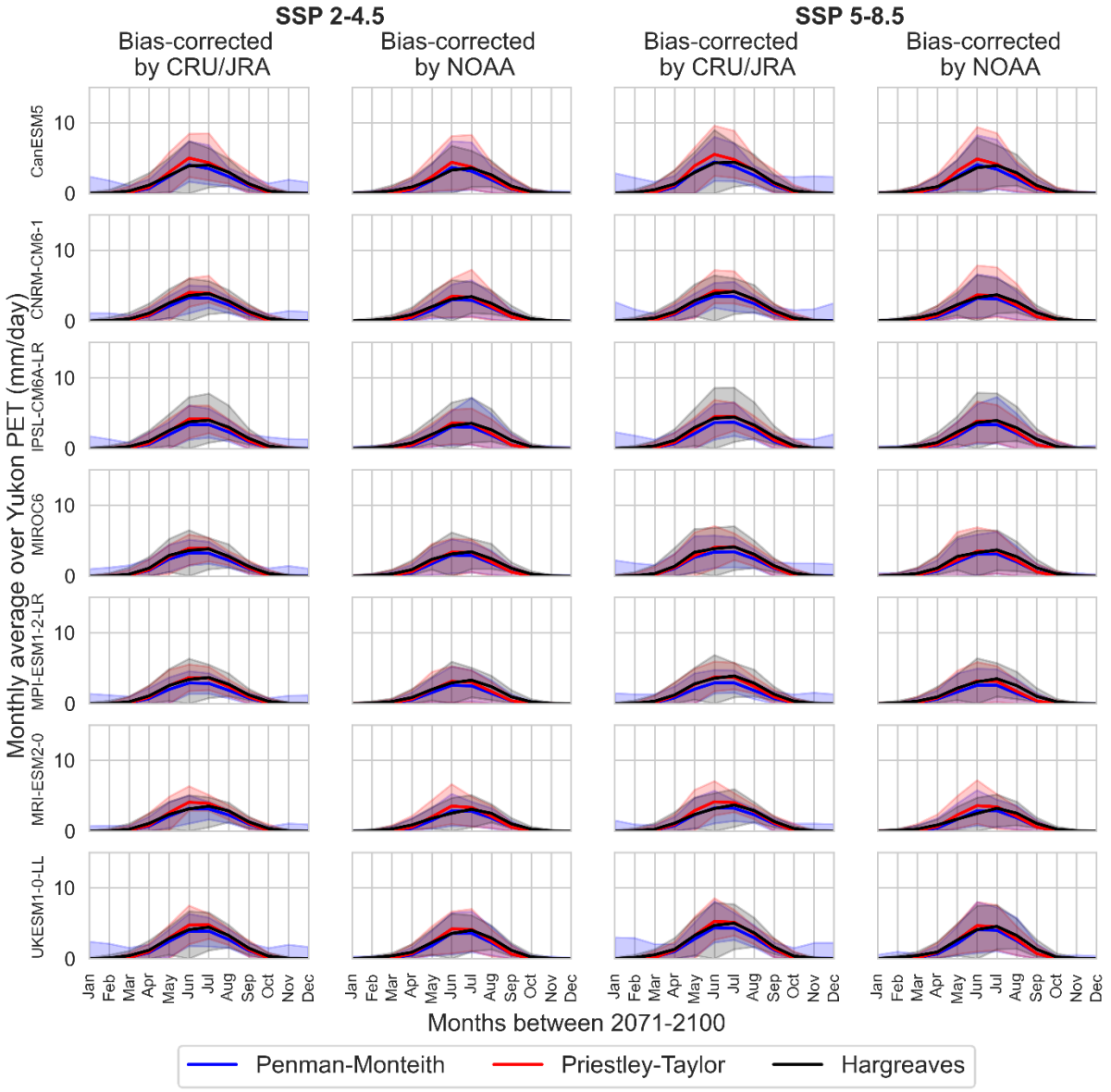

Figure 5.10 Monthly PET values during 2071-2100 and under SSPs 4-4.5 and 5-8.5, estimated using all simulations per climate models (each row) over Yukon.

In addition, the bias-corrected simulations with NOAA present larger spread for PET values over the West Coast than the ones corrected with CRU/JRA –see Figure B49. On the other hand, the

simulations that are bias-corrected with CRU/JRA display higher ranges of PET values in the winter over East Arctic, Yukon, and Northern Plains using Penman-Monteith equation (Figure B43, Figure 5.10 and Figure B48). Therefore, the key factors in terms of their influence on estimating future PET are the location, time (month and season), the utilized PET empirical equation, the benchmarking dataset and finally the GCMs.

CHAPTER 6 GENERAL DISCUSSION

An increase in agriculture-related indices over Canada is observed for both 4.5 and 8.5 W/m^2 forcing in the future. In fact, the maximum increase in GDD is quite spectacular by the end of the century as seen in Figure 4.6. Increases in GDD, or heat accumulation, can potentially affect the yield production (Bootsma et al., 2005; Qian et al., 2013) and affect the country's food security. This is critical over the Northern Plains and Great Lakes regions, where most grain farming activities currently take place. Combination of increases in heat accumulation and small changes in the magnitude of rainfall over growing seasons signifies that irrigation would potentially play a key role in supporting agricultural activities in these regions. In contrast, increases in GDD could possibly open new doors for agricultural activities and boost economic production in the northern regions up to the 2050. However, this opportunity seems to be more viable in the short-term horizon as projections of GDD are very high for the end of the century even for these areas. Nevertheless, considering the complex dynamics between soil moisture, crop evapotranspiration and yield more comprehensive research should be done to better investigate the challenges and opportunities to assure food security coast to coast in Canada.

As Canada gets warmer, new challenges are faced with the design and maintenance of infrastructure. In brief, more frequent FAT cycles are projected in higher latitudes such as in the East Arctic, Yukon and Mackenzie Valley zones (*e.g.*, around 5 times more FAT cycles per year by the end of the century). This could potentially make northern communities, mostly indigenous people, highly vulnerable to infrastructure instability such as unreliable houses and ice roads for transportation. Thawing permafrost could also lead to liberation of more CO_2, which would possibly create a loop of warming over these already sensitive areas (Price et al., 2013). Therefore, major adaptations would be needed to fight again climate change in Northern Canada. In contrast, reductions in FAT cycles are projected by climate models in lower latitudes by the end of the century. For instance, a reduction of about 30 days in FAT cycles is projected by the end of the century in the Northern Plains zone, which comes with new challenges and opportunities that the country should be prepared for. In addition to FAT, increases in AMPs are observed across the Canadian zones under both 4.5 and 8.5 W/m^2 forcing. For instance, general increases in AMPs of 25 mm/day are extremely concerning for the Maritimes, West Coast, Great Lakes and Southern North East Forest as these regions are already vulnerable to heavy rainfalls. Moreover, since

flooding caused by rain over snowpacks is also common in Canada (Buttle et al., 2016), increases in precipitation could lead to more devastating floods in these regions too. To better address these possible changes over the country, more profound impact study assessments are required such as the determination of the standardized precipitation index for drought prediction or hydrological modelling to determine peak and low flows. Additionally, these impact assessments studies would require the use of bias-corrected GCMs simulations to better represent future climate change over the country by reducing the GCMs errors.

The changes in indices related to human and environmental health are also extremely concerning. For instance, Great Lakes and Northern Plains host many major cities such as Toronto, Montréal, Winnipeg, Calgary, and Regina, which contain high density housing and old infrastructure making them vulnerable to heatwaves (Smoyer-Tomic et al., 2003). Climate models project an increase of over two months in maximum number of hot days and about one month in maximum number of consecutive hot and dry days in the future for these regions, which is frightening. It should be noted that, when this thesis is written (end of July 2021), a horrible heatwave has hit British Columbia, with temperatures reaching 50°C, creating new records of highest temperature in 40 locations in Canada (Roffel, 2021). The hazard caused more than 700 sudden deaths in the province, three times higher numbers than past events (Lindsay and Dickson, 2021). This type of event reminds us of the urgent need for a better evaluation of number of hot days and consecutive dry days in the future for proper adaptation and mitigation of local communities. From another aspect, longer and frequent heatwaves can increase the influx of patients to hospitals and overload the health systems in short duration. The current COVID-19 pandemic has taught us that more effective surge capacity strategies are needed to better accommodate and handle patients in time of crisis.

Projected increases in number of hot and dry days by climate models are also alarming for the environmental health. As an example, these events can potentially increase the chance and frequency of forest fires, which could lead to death and extinction of various habitats (Smoyer-Tomic et al., 2003; McCoy & Burn, 2005; Bush and Lemmen, 2019). Moreover, Canadian Government is spending between 800 million to 1.5 billion dollars every year to fight forest fires (Government of Canada, 2020b). Most of large Canadian forest fires, *i.e.*, with more than 200 ha burned, occur in the Boreal and Taiga forests during the summer months (Stocks et al., 2002). The climate models project an increase of 15 days in MCD over these regions under 8.5 W/m^2 by 2100,

which can potentially increase the risk of fire with various environmental and socioeconomic impacts. Up to the 27th of July, 987 wildfires had occurred in British Columbia during the summer 2021 with 1540 km^2 of areas burned and 97% of these areas still add active fires causing 3700 homes to be evacuated. Normally, considering past averages observed data, the number of wildfires should have been of 490 with 500 km^2 of areas burned by the end of July (Brown et al., 2021). With that said, more profound investigations, such as estimation of the Canadian Forest Weather Index System indices and usage of downscaled GCMs are needed to better assess the climate change impact on Canadian forest fires (Stocks et al., 2013; Bush and Lemmen, 2019).

Furthermore, the increases in PET across Canadian zones can also be alarming for many reasons. In brief, alteration in PET can potentially affect freshwater availability, e.g., in rivers, lakes and wetlands. Wetlands are extremely important for Canada's environments as they act as buffers for temperature but also as a natural water decontaminant and protect against flooding (Bush and Lemmen, 2019). Alterations in PET can also potentially affect soil moisture, agricultural water demand, crop yield, and irrigation water supply. These changes should be carefully studied in the future as they are critical for agricultural management, especially in the Prairies, which are the breadbaskets of Canada (Faith, 2017).

CHAPTER 7 CONCLUSION AND RECOMMENDATIONS

Due to the importance of climate models in quantifying the impact of climate change in Canada, in this study, the behaviour of recently released CMIP6 models is compared with their precedent counterparts and reanalyses datasets. Moreover, the simulations of both CMIP5 and CMIP6 models are used to understand changes in key climate indices over Canada. These indices include growing degree days, mean seasonal rainfall, annual maximum precipitation, freeze and thaw cycles, maximum number of hot days and maximum number of consecutive dry days. In addition, the change in PET is also investigated as evapotranspiration is preeminent in Canadian zones. For this purpose, PET was first estimated in the historical period using Penman-Monteith, Priestley-Taylor and Hargreaves equations as well as CMIP6 simulations and reference datasets. Due to the existence of errors in GCMs projections, QDM is used for bias correction. The bias-corrected simulations are then fed to the three evapotranspiration equations to estimate PET in the future. Key findings of these analyses are provided below. Moreover, limitations of this study are discussed, and further recommendations are also given.

Overall, it is found that the projections of CMIP5 and CMIP6 models are not necessarily similar under the historical and future scenarios across Canada. Furthermore, there is no evident superiority of CMIP6 models over CMIP5 with respect to NOAA and NCEP. Also, the projections of CMIP6 and CMIP5 do not overlap each other. Even CMIP6 models with a large number of simulations do not necessarily cover other individual CMIP6 models' simulations nor CMIP5 ones (for example CanESM5 whom add 50 simulations). GCMs still present biases for GDD and MSR indices and some models present larger errors such as IPSL-CM6A-LR for MSR. Therefore, it is important, to use a wide range of GCMs and their simulations in future impact assessments for better representation of future hazards. Nevertheless, both CMIP phases reveal significant changes in the considered climatic indices over time and space. For instance, CMIP6 models under 4.5 W/m^2 and 8.5 W/m^2 radiative forcing project an average range of increase for the mean annual Tmax (and Tmin) to be around 3.9-5.0℃ (and 4.4-5.7℃) in short-term and 6.2-11.6℃ (and 7.0-13.1℃) in long-term horizon over Canada in comparison to the historical period. The models project an average change in mean annual precipitation by around 0.31-0.34 mm/day in short-term and 0.54-0.87 mm/day in long-term. The combinations of these changes could be alarming for Canada's

food security, infrastructure sustainability, and human health protection, which are discussed below.

Additionally, the present work showed that PET values based on raw GCMs did not match the benchmark values by NOAA and CRU/JRA and that the use of QDM for bias correction was highly efficient in reducing the error to less than 10%. The formulas used to estimate PET have an important impact on the calculated magnitude of PET using both benchmarks and CMIP6 GCMs. Furthermore, all future projections display an increase in PET values by the end of the century. This growth in PET values highly depends on the location and season of the year, but also on the employed PET formula, benchmark considered for bias correction as well as climate models. Therefore, estimating PET with a diverse set of formulas is the path to follow for better understanding of climate change impacts. Indeed, the three PET equations estimated with CMIP6 simulations showcased different results which had not been investigated before for Canada in other studies. For similar reasons, the use of multi GCMs, multi benchmarks as well as multi simulations is highly recommended to present more future possibilities of PET projections.

It should also be noted that there are some limitations in this study and uncertainties in our results stem from various sources. Most importantly, usage of reanalyses for bias correction of GCMs can be problematic. Indeed, reanalyses are well known to have their own biases due to flaws in data assimilation schemes, data availability and quality, as well as model errors, among others (Fujiwara et al., 2017; Donat et al., 2014). Nevertheless, high quality station data are also not available in all regions in Canada particularly in the North; therefore, the interpolated observed data are also not reliable (Harris, 2020). A better coverage of meteorological stations in Northern Canada would help future climate change studies, but also mix datasets containing ground, satellite or drones' observations would also be relevant. Another source of uncertainty in the analyses can be due to regridding, which provides GCMs climate data to the same resolution, but affects the model skills depending on the utilized interpolation method (Accadia et al., 2003; Szolday et al., 2009). Furthermore, in our analyses, only QDM is used for bias correction. However, the performance of different bias-correction methods can be different which may lead to diverging estimates in the future (Cannon et al., 2015). Thus, a range of acceptable bias-correction techniques can be used for future analyses (Cannon et al, 2015; Iizumi et al., 2017; Teutschbein and Seibert, 2012). In addition to considered error measures, profound statistical analysis such as sensitivity analysis or

comparison of trends in variables can also be used to better evaluate the behaviour of raw and bias-corrected simulations (Hempel et al., 2013; Vorobyeva and Volodin, 2021).

Regardless of these limitations, this thesis provides valuable information about the performance of the state-of-the-art CMIP6 models in Canada and sheds light on the possible changes in a set of climate indices and PET across Canada. Further studies for comprehensive assessment of climate change impacts are needed to determine the risks linked to future hazards and thereby produce appropriate adaptation policies for Canada. But, most importantly, communication of climate change with the public must be prioritized to assure a commitment to environmental protection at every level of society.

REFERENCES

Accadia, C., Mariani, S., Casaioli, M., Lavagnini, A., & Speranza, A. (2003). Sensitivity of precipitation forecast skill scores to bilinear inter- polation and a simple nearest-neighbor average method on high-resolution verification grids. Weather and Forecasting, 18, 5, 918–932. https://doi.org/10.1175/1520-0434(2003)018<0918:sopfss>2.0.co;2

Ajjur, S. B., & Al-Ghamdi, S. G. (2021). Evapotranspiration and water availability response to climate change in the Middle East and North Africa. Climatic Change, 166(3–4), 1–18. https://doi.org/10.1007/s10584-021-03122-z

Akinsanola, A. A., Kooperman, G. J., Pendergrass, A. G., Hannah, W. M., & Reed, K. A. (2020). Seasonal representation of ex- treme precipitation indices over the United States in CMIP6 present-day simulations. Environmental Research Letters. https://doi.org/10.1088/1748-9326/ab92c1

Allen, R. G., Pereira, L. S., Raes, D., & Smith, M. (1998). Crop evapotraspiration guidelines for computing crop water requirements. In FAO Irrigation & drainage Paper 56. FAO, Food and Agriculture Organization of the United Nations,Roma.

Almazroui, M., Saeed, S., Saeed, F., Islam, M. N., & Ismail, M. (2020). Projections of precipitation and temperature over the South Asian countries in CMIP6. Earth Systems and Environment, 4(2), 297–320. https://doi.org/10.1007/s41748-020-00157-7

Anctil, F., Rousselle, J., & Lauzon, N. (2012). Hydrologie : Cheminements de l'eau (2e éd.). Québec, QC : Presses internationales Polytechnique

Barnett, N., Madramootoo, C. A., & Perrone, J. (1998). Performance of some evapotranspiration equations at a site in Quebec. Canadian Agricultural Engineering, 40(2), 89–95.

Beck, H. E., Pan, M., Roy, T., Weedon, G. P., Pappenberger, F., van Dijk, A. I. J. M., et al. (2019). Daily evaluation of 26 precipitation da- tasets using Stage-IV gauge-radar data for the CONUS. Hydrology and Earth System Sciences, 23(1), 207–224. https://doi.org/10.5194/hess-23-207-2019

Beck, H. E., Vergopolan, N., Pan, M., Levizzani, V., van Dijk, A. I. J. M., Weedon, G. P., et al. (2017). Global-scale evaluation of 22 precipi- tation datasets using gauge observations and hydrological modelling. Hydrology and Earth System Sciences, 21(12), 6201–6217. https://doi.org/10.5194/hess-21-6201-2017

Beck, H. E., Wood, E. F., Pan, M., Fisher, C. K., Miralles, D. G., Van Dijk, A. I. J. M., et al. (2019). MSWEP V2 global 3-hourly 0.1° precipitation: Methodology and quantitative assessment. Bulletin of the American Meteorological Society, 100(3), 473–500. https://doi.org/10.1175/bams-d-17-0138.1

Berg, A., & Sheffield, J. (2019). Historic and Projected Changes in Coupling Between Soil Moisture and Evapotranspiration (ET) in CMIP5 Models Confounded by the Role of Different ET Components. Journal of Geophysical Research: Atmospheres, 5791–5806. https://doi.org/10.1029/2018JD029807

Bernhardt, T. (2010). *Canada's Ecozones.* Retrieved from http://canadianbiodiversity.mcgill.ca/english/ecozones/ecozones.htm

Bock, M., Gasser, P. Y., Pettapiece, W. W., Brierley, A. J., Bootsma, A., Schut, P., et al. (2018). The land suitability rating system is a spatial planning tool to assess crop suitability in Canada. Frontiers in Environmental Science, 6, 77. https://doi.org/10.3389/fenvs.2018.00077

Bootsma, A., Gameda, S., & McKenney, D. W. (2005). Potential impacts of climate change on corn, soybeans and barley yields in Atlantic Canada. Canadian Journal of Soil Science, 85(2), 345–357. https://doi.org/10.4141/S04-025

Bourdeau-Goulet, S. C., & Hassanzadeh, E. (2021). Comparisons Between CMIP5 and CMIP6 Models: Simulations of Climate Indices Influencing Food Security, Infrastructure Resilience, and Human Health in Canada. Earth's Future, 9(5), 1–17. https://doi.org/10.1029/2021EF001995

Brown S., Crawford T., Chan C., Carrigg D., & Raptis M. (2021, July 27*). B.C. wildfires update for July 27: Wildfire flares west of Kamloops overnight | Firefighters from Australia arrive today | 250 wildfires, with 3,700 homes evacuated.* Retrieved from https://vancouversun.com/news/local-news/bc-wildfires-update-heres-the-latest-on-wildfire-situation-in-british-columbia

Bush, E., & Lemmen, D. S. (Eds.), (2019). Canada's changing climate report. Ottawa, ON. Retrieved from http://www.changingclimate.ca/CCCR2019

Bustinza, R., Lebel, G., Gosselin, P., Bélanger, D., & Chebana, F. (2013). Health impacts of the July 2010 heat wave in Quebec, Canada. BMC Public Health, 13(1), 56. https://doi.org/10.1186/1471-2458-13-56

Buttle, J. M., Allen, D. M., Caissie, D., Davison, B., Hayashi, M., Peters, D. L., … Whitfield, P. H. (2016). Flood processes in Canada: Regional and special aspects. Canadian Water Resources Journal, 41(1–2), 7–30. https://doi.org/10.1080/07011784.2015.1131629

Cannon, A. J. (2020). Reductions in daily continental-scale atmospheric circulation biases between generations of global climate models: CMIP5 to CMIP6. Environmental Research Letters, 15(6), 064006. https://doi.org/10.1088/1748-9326/ab7e4f

Cannon, A. J., Sobie, S. R., & Murdock, T. Q. (2015). Bias correction of GCM precipitation by quantile mapping: How well do methods preserve changes in quantiles and extremes? Journal of Climate, 28(17), 6938–6959. https://doi.org/10.1175/jcli-d-14-00754.1

Chen, H., Sun, J., Lin, W., & Xu, H. (2020). Comparison of CMIP6 and CMIP5 models in simulating climate extremes. Science Bulletin. https://doi.org/10.1016/j.scib.2020.05.015

Chen, Z., Zhou, T., Zhang, L., Chen, X., Zhang, W., & Jiang, J. (2020). Global land monsoon precipitation changes in CMIP6 projections. Geophysical Research Letters, 47(14), e2019GL086902. https://doi.org/10.1029/2019gl086902

Compo, G. P., Whitaker, J. S., Sardeshmukh, P. D., Matsui, N., Allan, R. J., Yin, X., et al. (2011). The twentieth century reanalysis project. Quarterly Journal of the Royal Meteorological Society, 137(654), 1–28. https://doi.org/10.1002/qj.776

Cook, B. I., Mankin, J. S., Marvel, K., Williams, A. P., Smerdon, J. E., & Anchukaitis, K. J. (2020). Twenty-first century drought projections in the CMIP6 forcing scenarios. Earth's Future, 8(6). https://doi.org/10.1029/2019ef001461

Council of Canadian Academies. (2019). Canada’s top climate change risks: The expert panel on climate change risks and adaptation potential. Ottawa, ON: Council of Canadian Academies. Retrieved from Report-Canada-top-climate-change-risks.pdf

Dallaire, G., Poulin, A., Arsenault, R., & Brissette, F. (2021). Uncertainty of potential evapotranspiration modelling in climate change impact studies on low flows in North America. Hydrological Sciences Journal, 66(4), 689–702. https://doi.org/10.1080/02626667.2021.1888955

Decker, M., Brunke, M. A., Wang, Z., Sakaguchi, K., Zeng, X., & Bosilovich, M. G. (2012). Evaluation of the reanalysis products from GSFC, NCEP, and ECMWF using flux tower observations. Journal of Climate, 25(6), 1916-1944. https://doi.org/10.1175/JCLI-D-11-00004.1

Di Luca, A., Pitman, A. J., & de Elía, R. (2020). Decomposing temperature extremes errors in CMIP5 and CMIP6 models. Geophysical Research Letters, 47(14), 1–10. https://doi.org/10.1029/2020gl088031

Direction régionale de santé publique du CIUSSS du Centre-Sud-de-l'Île-de-Montréal. (2019). Enquête épidémiologique – Vague de chaleur à l'été 2018 à Montréal. Montréal, QC: Gouvernement du Québec. https://santemontreal.qc.ca/fileadmin/user_upload/Uploads/tx_asssmpublications/pdf/publications/Enquete_epidemiologique_-_Vague_de_chaleur_a_l_ete_2018_a_Montreal_version-15mai_EUSHV_finale.pdf

Djaman, K., O'Neill, M., Diop, L., Bodian, A., Allen, S., Koudahe, K., & Lombard, K. (2019). Evaluation of the Penman-Monteith and other 34 reference evapotranspiration equations under limited data in a semiarid dry climate. Theoretical and Applied Climatology, 137(1–2), 729–743. https://doi.org/10.1007/s00704-018-2624-0

Donat, M. G., Sillmann, J., Wild, S., Alexander, L. V., Lippmann, T., & Zwiers, F. W. (2014). Consistency of temperature and precipitation extremes across various global gridded in situ and reanalysis datasets. Journal of Climate, 27(13), 5019–5035. https://doi.org/10.1175/jcli-d-13-00405.1

Dong, B., & Dai, A. (2017). The uncertainties and causes of the recent changes in global evapotranspiration from 1982 to 2010. Climate Dynamics, 49(1), 279–296. https://doi.org/10.1007/s00382-016-3342-x

Droogers, P., & Allen, R. G. (2002). Estimating reference evapotranspiration under inaccurate data conditions. Irrigation and drainage systems, 16(1), 33-45. https://doi.org/10.1023/A:1015508322413

ECMWF. (2020, November 9). *Fact Sheet: Reanalysis*. Retrieved from https://www.ecmwf.int/en/about/media-centre/focus/2020/fact-sheet-reanalysis

Edwards, P. N. (2011). History of climate modelling. Wiley Interdisciplinary Reviews: Climate Change, 2(1), 128–139. https://doi.org/10.1002/wcc.95

Eyring, V., Bony, S., Meehl, G. A., Senior, C. A., Stevens, B., Stouffer, R. J., & Taylor, K. E. (2016). Overview of the coupled model intercom- parison project phase 6 (CMIP6) experimental design and organization. Geoscientific Model Development, 9(5), 1937–1958. https://doi.org/10.5194/gmd-9-1937-2016

Faith, C. (2017, August 1). *The Breadbaskets Of The World*. Retrieved from https://www.worldatlas.com/articles/the-breadbaskets-of-the-world.html

Fan, X., Duan, Q., Shen, C., Wu, Y., & Xing, C. (2020). Global surface air temperatures in CMIP6: Historical performance and future chang- es. Environmental Research Letters, 15(10), 104056. https://doi.org/10.1088/1748-9326/abb051

Fan, X., Duan, Q., Shen, C., Wu, Y., & Xing, C. (2020). Global surface air temperatures in CMIP6: historical performance and future changes. Environmental Research Letters, 15(10), 104056. https://doi.org/10.1088/1748-9326/abb051

Faramarzi, M., Srinivasan, R., Iravani, M., Bladon, K. D., Abbaspour, K. C., Zehnder, A. J. B., & Goss, G. G. (2015). Setting up a hydrolog- ical model of Alberta: Data discrimination analyses prior to calibration. Environmental Modelling & Software, 74, 48–65. https://doi.org/10.1016/j.envsoft.2015.09.006

Fernandes, R., Korolevych, V., & Wang, S. (2007). Trends in land evapotranspiration over Canada for the period 1960-2000 based on in situ climate observations and a land surface model. Journal of Hydrometeorology, 8(5), 1016–1030. https://doi.org/10.1175/JHM619.1

Fu, G., Liu, Z., Charles, S. P., Xu, Z., & Yao, Z. (2013). A score-based method for assessing the performance of GCMs: A case study of southeastern Australia. Journal of Geophysical Research: Atmospheres, 118(10), 4154-4167. https://doi.org/10.1002/jgrd.50269

Fujiwara, M., Wright, J. S., Manney, G. L., Gray, L. J., Anstey, J., Birner, T., … Zou, C. Z. (2017). Introduction to the SPARC Reanalysis Intercomparison Project (S-RIP) and overview of the reanalysis systems. Atmospheric Chemistry and Physics, 17(2), 1417–1452. https://doi.org/10.5194/acp-17-1417-2017

Gaur, A., Gaur, A., & Simonovic, S. (2018). Future changes in flood hazards across Canada under a changing climate. Water, 10(10), 1441. https://doi.org/10.3390/w10101441

Government of Canada (2020a). Extreme heat: Heat waves. Last modified July 14, 2020. Retrieved from https://www.canada.ca/en/health-canada/services/sun-safety/extreme-heat-heat-waves.html

Government of Canda. (2020b, September 22). Forest Fires. Retrieved from https://www.nrcan.gc.ca/our-natural-resources/forests-forestry/wildland-fires-insects-disturban/forest-fires/13143?_ga=2.179218788.156612418.1608962043-2117275676.1608962043

Grenier, P., Firlej, A., Blondlot, A., Logan, T., & Ricard, M.-P. (2019). The issue of properly ordering climate indices calculation and bias correction before identifying spatial analogs for agricultural applications. Climate Services, 16, 100122. https://doi.org/10.1016/j.cliser.2019.100122

Grose, M. R., Narsey, S., Delage, F. P., Dowdy, A. J., Bador, M., Boschat, G., & Power, S. (2020). Insights from CMIP6 for Australia's future climate. Earth's Future, 8(5), e2019EF001469. https://doi.org/10.1029/2019ef001469

Guest, G., Zhang, J., Maadani, O., & Shirkhani, H. (2020). Incorporating the impacts of climate change into infrastructure life cycle as- sessments: A case study of pavement service life performance. Journal of Industrial Ecology, 24(2), 356–368. https://doi.org/10.1111/jiec.12915

Gusain, A., Ghosh, S., & Karmakar, S. (2020). Added value of CMIP6 over CMIP5 models in simulating Indian summer monsoon rainfall. Atmospheric Research, 232, 104680. https://doi.org/10.1016/j.atmosres.2019.104680

Ha, K. J., Moon, S., Timmermann, A., & Kim, D. (2020). Future changes of summer monsoon characteristics and evaporative demand over Asia in CMIP6 simulations. Geophysical Research Letters, 47(8), e2020GL087492. https://doi.org/10.1029/2020gl087492

Hao, Z., Singh, V. P., & Xia, Y. (2018). Seasonal drought prediction: advances, challenges, and future prospects. Reviews of Geophysics, 56(1), 108-141. https://doi.org/10.1002/2016RG000549

Hargreaves, G. H., & Allen, R. G. (2003). History and Evaluation of Hargreaves Evapotranspiration Equation. Journal of Irrigation and Drainage Engineering, 129(1), 53–63. https://doi.org/10.1061/(asce)0733-9437(2003)129:1(53)

Harris, I., Osborn, T. J., Jones, P., & Lister, D. (2020). Version 4 of the CRU TS monthly high-resolution gridded multivariate climate dataset. Scientific Data, 7(1), 1–18. https://doi.org/10.1038/s41597-020-0453-3

Hassanzadeh, E. (2019). Trade-offs between human and environment: Challenges for regional water management under changing condi- tions. Water, 11(9), 1773. https://doi.org/10.3390/w11091773

Hassanzadeh, E., Nazemi, A., & Elshorbagy, A. (2014). Quantile-based downscaling of precipitation using genetic programming: Applica- tion to IDF curves in Saskatoon. Journal of Hydrologic Engineering, 19(5), 943–955. https://doi.org/10.1061/(asce)he.1943-5584.0000854

Hausfather, Z. (2019). CMIP6: The next generation of climate models explained. Carbon Brief, December 2. Retrieved from https://www.carbonbrief.org/cmip6-the-next-generation-of-climate-models-explained

Hempel, S., Frieler, K., Warszawski, L., Schewe, J., & Piontek, F. (2013). A trend-preserving bias correction – The ISI-MIP approach. Earth System Dynamics, 4(2), 219–236. https://doi.org/10.5194/esd-4-219-2013

Henstra, D., & Thistlethwaite, J. (2017). Climate change, floods, and municipal risk sharing in Canada. Institute on Municipal Finance and Governance. Retrieved from http://hdl.handle.net/1807/81204

Herring, D. & Lindsey, R. (2020, October 29). *Hasn't Earth warmed and cooled naturally throughout history?* Retrieved from https://www.climate.gov/news-features/climate-qa/hasnt-earth-warmed-and-cooled-naturally-throughout-history

Huber, L., & Gillespie, T. J. (1992). Modeling leaf wetness in relation to plant disease epidemiology. Annual Review of Phytopathology, 30(1), 553–577. https://doi.org/10.1146/annurev.py.30.090192.003005

IBC (Insurance Bureau of Canada). (2015). The financial management of flood risk. Retrieved from http://assets.ibc.ca/Documents/Natural%20Disasters/The_Financial_Management_of_Flood_Risk.pdf

Iizumi, T., Takikawa, H., Hirabayashi, Y., Hanasaki, N., & Nishimori, M. (2017). Contributions of different bias-correction methods and reference meteorological forcing data sets to uncertainty in projected temperature and precipitation extremes. Journal of Geophysical Research: Atmospheres, 122(15), 7800-7819. https://doi.org/10.1002/2017JD026613

IPCC, (2007): Climate Change 2007: Synthesis Report. Contribution of Working Groups I, II and III to the Fourth Assessment Report of the Intergovernmental Panel on Climate Change [Core Writing Team, Pachauri, R.K and Reisinger, A. (eds.)]. IPCC, Geneva, Switzerland, 104 pp. Retrieved from https://www.ipcc.ch/site/assets/uploads/2018/02/ar4_syr_full_report.pdf

IPCC, (2014): Climate Change 2014: Synthesis Report. Contribution of Working Groups I, II and III to the Fifth Assessment Report of the Intergovernmental Panel on Climate Change [Core Writing Team, R.K. Pachauri and L.A. Meyer (eds.)]. IPCC, Geneva, Switzerland, 151 pp. Retrieved from https://ar5-syr.ipcc.ch/ipcc/ipcc/resources/pdf/IPCC_SynthesisReport.pdf

IPCC-TGICA, (2007): General Guidelines on the Use of Scenario Data for Climate Impact and Adaptation Assessment. Version 2. Prepared by T.R. Carter on behalf of the Intergovernmental Panel on Climate Change, Task Group on Data and Scenario Support for Impact and Climate Assessment, 66 pp. Retrieved from https://www.ipcc-data.org/guidelines/index.html

Jaramillo, P., & Nazemi, A. (2018). Assessing urban water security under changing climate: Challenges and ways forward. Sustainable Cities and Society, 41, 907–918. https://doi.org/10.1016/j.scs.2017.04.005

Jeong, D. I., Sushama, L., Diro, G. T., & Khaliq, M. N. (2016). Projected changes to winter temperature characteristics over Canada based on an RCM ensemble. Climate Dynamics, 47(5–6), 1351–1366. https://doi.org/10.1007/s00382-015-2906-5

Jiang, J., Zhou, T., Chen, X., & Zhang, L. (2020). Future changes in precipitation over Central Asia based on CMIP6 projections. Environ- mental Research Letters, 15(5), 054009. https://doi.org/10.1088/1748-9326/ab7d03

Jones, J. W., Hoogenboom, G., Porter, C. H., Boote, K. J., Batchelor, W. D., Hunt, L. A., et al. (2003). The DSSAT cropping system model. European Journal of Agronomy, 18(3–4), 235–265. https://doi.org/10.1016/s1161-0301(02)00107-7

Jones, P. W. (1999). First- and second-order conservative remapping schemes for grids in spherical coordinates. Monthly Weather Review, 127(9), 2204–2210. https://doi.org/10.1175/1520-0493(1999)127<2204:fasocr>2.0.co;2

Kalnay, E., Kanamitsu, M., Kistler, R., Collins, W., Deaven, D., Gandin, L., et al. (1996). The NCEP/NCAR 40-year reanalysis project. Bulle- tin of American Meteorological Society, 77(3), 437–471. https://doi.org/10.1175/1520-0477(1996)077<0437:tnyrp>2.0.co;2

Keuler, K., Block, A., Ahrens, W., Heimann, D., Zemsch, A., Dittmann, E., ... & Hauffe, D. (2006). Quantifizierung von Ungenauigkeiten regionaler Klima-und Klimaänderungssimulationen (QUIRCS). Abschlussbericht, BTU Cottbus.

Kim, Y.-H., Min, S.-K., Zhang, X., Sillmann, J., & Sandstad, M. (2020). Evaluation of the CMIP6 multi-model ensemble for climate extreme indices. Weather and Climate Extremes, 29, 100269. https://doi.org/10.1016/j.wace.2020.100269

Kobayashi, S., Ota, Y., Harada, Y., Ebita, A., Moriya, M., Onoda, H., … Kiyotoshi, T. (2015). The JRA-55 reanalysis: General specifications and basic characteristics. Journal of the Meteorological Society of Japan, 93(1), 5–48. https://doi.org/10.2151/jmsj.2015-001

Kumar, R., Jat, M. K., & Shankar, V. (2012). Methods to estimate irrigated reference crop evapotranspiration - A review. Water Science and Technology, 66(3), 525–535. https://doi.org/10.2166/wst.2012.191

Lehner, F., Deser, C., Maher, N., Marotzke, J., Fischer, E. M., Brunner, L., et al. (2020). Partitioning climate projection uncertainty with multiple large ensembles and CMIP5/6. Earth System Dynamics, 11(2), 491–508. https://doi.org/10.5194/esd-11-491-2020. https://doi.org/10.5194/esd-2019-93

Lemmen, D. S., Warren, F. J., Lacroix, J., & Bush, E. (Eds.), (2008). From impacts to adaptation: Canada in a changing climate 2007. Ottawa, ON: Government of Canada. Retrieved from https://www.nrcan.gc.ca/impacts-adaptation-canada-changing-climate/10253

Lindsay B. & Dickson C. (2021, June 30). *Village of Lytton, B.C., evacuated as mayor says 'the whole town is on fire'*. Retrieved from https://www.cbc.ca/news/canada/british-columbia/bc-wildfires-june-30-2021-1.6085919

Lindsey, R. (2020, August 2014). *Climate Change: Atmospheric Carbon Dioxide*. Retrieved from https://www.climate.gov/news-features/understanding-climate/climate-change-atmospheric-carbon-dioxide

Liu, X., Li, C., Zhai, T., & Han, L. (2020). Future changes of global potential evapotranspiration simulated from CMIP5 to CMIP6 models. Atmospheric and Oceanic Science Letters, 13(6), 568-575. https://doi.org/10.1080/16742834.2020.1824983

Maher, N., Milinski, S., Suarez-Gutierrez, L., Botzet, M., Dobrynin, M., Kornblueh, L., et al. (2019). The Max Planck institute grand ensem- ble: Enabling the exploration of climate system variability. Journal of Advances in Modeling Earth Systems, 11(7), 2050–2069. https://doi.org/10.1029/2019ms001639

Mailhot, A., & Duchesne, S. (2010). Design criteria of urban drainage infrastructures under climate change. Journal of Water Resources Planning and Management, 136(2), 201–208. https://doi.org/10.1061/(asce)wr.1943-5452.0000023

Maraun, D., & Widmann, M. (2018). Statistical downscaling and bias correction for climate research. Cambridge University Press. https://doi.org/10.1017/9781107588783

Martel, J.-L., Mailhot, A., Brissette, F., & Caya, D. (2018). Role of natural climate variability in the detection of anthropogenic climate change signal for mean and extreme precipitation at local and regional scales. Journal of Climate, 31(11), 4241–4263. https://doi.org/10.1175/jcli-d-17-0282.1

Masud, B., Cui, Q., Ammar, M. E., Bonsal, B. R., Islam, Z., & Faramarzi, M. (2021). Means and extremes: Evaluation of a CMIP6 mul- ti-model ensemble in reproducing historical climate characteristics across Alberta, Canada. Water, 13(5), 737. https://doi.org/10.3390/w13050737

Maulé, C., Helgason, W., McGinn, S., & Cutforth, H. (2006). Estimation of standardized reference evapotranspiration on the Canadian Prairies using simple models with limited weather data. Canadian Biosystems Engineering, 48, 1.

Mccoy, V. M., & Burn, C. R. (2005). Potential Alteration by Climate Change of the Forest-Fire Regime in the Boreal Forest of Central Yukon Territory. 58(3), 276–285.

Merrifield, A. L., Brunner, L., Lorenz, R., Medhaug, I., & Knutti, R. (2020). An investigation of weighting schemes suitable for incorpo- rating large ensembles into multi-model ensembles. Earth System Dynamics, 11(3), 807–834. https://doi.org/10.5194/esd-11-807-2020

Mladjic, B., Sushama, L., Khaliq, M. N., Laprise, R., Caya, D., & Roy, R. (2011). Canadian RCM projected changes to extreme precipitation characteristics over Canada. Journal of Climate, 24(10), 2565–2584. https://doi.org/10.1175/2010jcli3937.1

Mohammed, A., Abu Samra, S., Zayed, T., Bagchi, A., & Nasiri, F. (2020). A resilience-based optimization model for maintenance and rehabilitation of pavement networks in a freeze-thaw environment. Canadian Journal of Civil Engineering. https://doi.org/10.1139/cjce-2019-0559

Na, Y., Fu, Q., & Kodama, C. (2020). Precipitation probability and its future changes from a global cloud-resolving model and CMIP6 sim- ulations. Journal of Geophysical Research: Atmospheres, 125(5), e2019JD031926. https://doi.org/10.1029/2019jd031926

National Round Table on the Environment and the Economy. (2010). Degrees of change: Climate warming and the stakes for Canada. Otta- wa, ON: NRTEE. http://nrt-trn.ca/climate/climate-prosperity/degrees-of-change

NOAA. (2020). *Did you know? Potential Evapotranspiration.* Retrieved from https://www.ncdc.noaa.gov/monitoring-references/dyk/potential-evapotranspiration

O'Neill, B. C., Tebaldi, C., Van Vuuren, D. P., Eyring, V., Friedlingstein, P., Hurtt, G., et al. (2016). The scenario model intercomparison project (ScenarioMIP) for CMIP6. Geoscientific Model Development (Vol. 9, pp. 3461–3482). Geoscientific Model Development. https://doi.org/10.5194/gmd-9-3461-2016

Oudin, L., Michel, C., & Anctil, F. (2005). Which potential evapotranspiration input for a lumped rainfall-runoff model? Part 1 - Can rainfall-runoff models effectively handle detailed potential

evapotranspiration inputs? Journal of Hydrology, 303(1–4), 275–289. https://doi.org/10.1016/j.jhydrol.2004.08.025

Palko, K. (2017). Synthesis. In K. Palko, & D. S. Lemmen (Eds.), Climate risks and adaptation practices for the Canadian transportation sector 2016 (pp. 12–25). Ottawa, ON: Government of Canada. Retrieved from https://www.nrcan.gc.ca/climate-change/impacts-adaptations/climate-risks-adaptation-practices-canadian-transportation-sector-2016/19623

Papalexiou, S. M., Rajulapati, C. R., Clark, M. P., & Lehner, F. (2020). Robustness of CMIP6 historical global mean temperature simu- lations: Trends, long-term persistence, autocorrelation, and distributional shape. Earth's Future, 8(10), e2020EF001667. https://doi.org/10.1029/2020ef001667

Pascoe, C., Lawrence, B. N., Guilyardi, E., Juckes, M., & Taylor, K. E. (June 2019). Designing and Documenting experiments in CMIP6. Geo- scientific model Development discussions (pp. 1–27). https://doi.org/10.5194/gmd-2019-98

PCDMI. (2013). *CMIP5 - Coupled Model Intercomparison Project Phase 5 – Overview.* Retrieved from https://pcmdi.llnl.gov/CMIP6/

PCDMI. (2019, February 13). *CMIP6 - Coupled Model Intercomparison Project Phase 6 – Overview.* Retrieved from https://pcmdi.llnl.gov/mips/cmip5/

Plummer, D. A., Caya, D., Frigon, A., Côté, H., Giguère, M., Paquin, D., et al. (2006). Climate and climate change over North America as simulated by the Canadian RCM. Journal of Climate, 19(13), 3112–3132. https://doi.org/10.1175/jcli3769.1

Prairie Climate Center. (2019). The climate atlas of Canada (Map version 2). Winnipeg: University of Winnipeg. Retrieved from https://climateatlas.ca

Price, D. T., Alfaro, R. I., Brown, K. J., Flannigan, M. D., Fleming, R. A., Hogg, E. H., … Venier, L. A. (2013). Anticipating the consequences of climate change for Canada ' s. 365(December), 322–365.

Priestley, C. H. B., & Taylor, R. J. (1972). On the assessment of surface heat flux and evaporation using large-scale parameters. Monthly weather review, 100(2), 81-92.

Prudhomme, C., & Williamson, J. (2013). Derivation of RCM-driven potential evapotranspiration for hydrological climate change impact analysis in Great Britain: A comparison of methods and associated uncertainty in future projections. Hydrology and Earth System Sciences, 17(4), 1365–1377. https://doi.org/10.5194/hess-17-1365-2013

Prudhomme, Christel. (2006). GCM and downscaling uncertainty in modelling of current river flow: Why is it important for future impacts? IAHS-AISH Publication, (308), 375–381.

Qian, B., De Jong, R., Gameda, S., Huffman, T., Neilsen, D., Desjardins, R., et al. (2013). Impact of climate change scenarios on Canadian agroclimatic indices. Canadian Journal of Soil Science, 93(2), 243–259. https://doi.org/10.4141/cjss2012-053

Qian, B., Jing, Q., Smith, W., Grant, B., Cannon, A. J., & Zhang, X. (2020). Quantifying the uncertainty introduced by internal climate var- iability in projections of Canadian crop production. Environmental Research Letters, 15(7), 074032. https://doi.org/10.1088/1748-9326/ab88fc

Randall, D. A., Wood, R. A., Bony, S., Colman, R., Fichefet, T., Fyfe, J., et al. (2007). Climate models and their evaluation. In Climate change 2007: The physical science basis. Contribution of working group I to the fourth assessment report of the IPCC (FAR) (pp. 589–662). Cambridge University Press.

Riahi, K., Van Vuuren, D. P., Kriegler, E., Edmonds, J., O'Neill, B. C., Fujimori, S., et al. (2017). The shared socioeconomic pathways and their energy, land use, and greenhouse gas emissions implications: an overview. Global Environmental Change, 42, 153–168. https://doi.org/10.1016/j.gloenvcha.2016.05.009

Roffel, B. (2021, July 2). *B.C.'s heat wave likely contributed to 719 sudden deaths in a week, coroner says — triple the usual number*. Retrieved from https://www.cbc.ca/news/canada/british-columbia/heat-wave-719-deaths-1.6088793

Scheff, J., & Frierson, D. M. W. (2015). Terrestrial aridity and its response to greenhouse warming across CMIP5 climate models. Journal of Climate, 28(14), 5583–5600. https://doi.org/10.1175/JCLI-D-14-00480.1

Schoetter, R., Hoffmann, P., Rechid, D., & Schlünzen, K. H. (2012). Evaluation and bias correction of regional climate model results using model evaluation measures. Journal of Applied Meteorology and Climatology, 51(9), 1670-1684. https://doi.org/10.1175/JAMC-D-11-0161.1

Schulzweida, U., Kornblueh, L., & Quast, R. (2006). CDO user's guide. Climate Data Operators, Version, 1(6), 205–209.Last modified Octo- ber 2020. Retrieved from https://code.mpimet.mpg.de/projects/cdo/embedded/cdo.pdf

Schurer, A., Ballinger, A. P., Friedman, A. R., & Hegerl, G. (2020). Human influence strengthens the contrast between tropical wet and dry regions. Environmental Research Letters. https://doi.org/10.1088/1748-9326/ab83ab

Seiller, G., & Anctil, F. (2016). How do potential evapotranspiration formulas influence hydrological projections? Hydrological Sciences Journal, 61(12), 2249–2266. https://doi.org/10.1080/02626667.2015.1100302

Seneviratne, S. I., & Hauser, M. (2020). Regional climate sensitivity of climate extremes in CMIP6 versus CMIP5 multimodel ensembles. Earth's Future, 8(9), e2019EF001474. https://doi.org/10.1029/2019ef001474

Sentelhas, P. C., Gillespie, T. J., & Santos, E. A. (2010). Evaluation of FAO Penman-Monteith and alternative methods for estimating reference evapotranspiration with missing data in Southern Ontario, Canada. Agricultural Water Management, 97(5), 635–644. https://doi.org/10.1016/j.agwat.2009.12.001

Shea, D. (2014). The climate data guide: Regridding Overview – National Center for Atmospheric Research. Last modified January 13, 2014. Retrieved from https://climatedataguide.ucar.edu/climate-data-tools-and-analysis/regridding-overview

Sheffield, J., Barrett, A. P., Colle, B., Nelun Fernando, D., Fu, R., Geil, K. L., et al. (2013). North American climate in CMIP5 experiments. Part I: Evaluation of historical simulations of continental and regional climatology. Journal of Climate, 26(23), 9209–9245. https://doi.org/10.1175/jcli-d-12-00592.1

Shrestha, A., Rahaman, M. M., Kalra, A., Jogineedi, R., & Maheshwari, P. (2020). Climatological drought forecasting using bias corrected CMIP6 climate data: A case study for India. Forecasting, 2(2), 59–84. https://doi.org/10.3390/forecast2020004

Sillmann, J., Kharin, V. V., Zhang, X., Zwiers, F. W., & Bronaugh, D. (2013). Climate extremes indices in the CMIP5 multimodel ensem- ble: Part 1. Model evaluation in the present climate. Journal of Geophysical Research - D: Atmospheres, 118(4), 1716–1733. https://doi.org/10.1002/jgrd.50203

Slivinski, L. C., Compo, G. P., Sardeshmukh, P. D., Whitaker, J. S., McColl, C., Allan, R. J., et al. (2020). An evaluation of the performance of the twentieth century reanalysis version 3. Journal of Climate, 34(4), 1417–1438. https://doi.org/10.1175/jcli-d-20-0505.1

Slivinski, L. C., Compo, G. P., Whitaker, J. S., Sardeshmukh, P. D., Giese, B. S., McColl, C., et al. (2019). Towards a more reliable historical reanalysis: Improvements for version 3 of the twentieth century reanalysis system. Quarterly Journal of the Royal Meteorological Society, 145(724), 2876–2908. https://doi.org/10.1002/qj.3598

Smith, W. N., Grant, B. B., Desjardins, R. L., Kroebel, R., Li, C., Qian, B., et al. (2013). Assessing the effects of climate change on crop produc- tion and GHG emissions in Canada. Agriculture, Ecosystems & Environment, 179, 139–150. https://doi.org/10.1016/j.agee.2013.08.015

Smoyer-Tomic, K. E., Kuhn, R., & Hudson, A. (2003). Heat wave hazards: An overview of heat wave impacts in Canada. Natural Hazards, 28(2–3), 463–485. https://doi.org/10.1023/A:1022946528157

Stocks, B. J., Mason, J. A., Todd, J. B., Bosch, E. M., Wotton, B. M., Amiro, B. D., et al. (2002). Large forest fires in Canada, 1959–1997. Journal of Geophysical Research: Atmospheres, 107(D1), FFR-5. https://doi.org/10.1029/2001JD000484

Stouffer, R. J., Eyring, V., Meehl, G. A., Bony, S., Senior, C., Stevens, B., & Taylor, K. E. (2017). CMIP5 scientific gaps and recommendations for CMIP6. Bulletin of the American Meteorological Society, 98(1), 95–105. https://doi.org/10.1175/bams-d-15-00013.1

Su, B., Huang, J., Mondal, S. K., Zhai, J., Wang, Y., Wen, S., ... & Li, A. (2021). Insight from CMIP6 SSP-RCP scenarios for future drought characteristics in China. Atmospheric Research, 250, 105375. https://doi.org/10.1016/j.atmosres.2020.105375

Szolgay, J., Parajka, J., Kohnová, S., & Hlavčová, K. (2009). Comparison of mapping approaches of design annual maximum daily precipitation. Atmospheric Research, 92(3), 289–307. https://doi.org/10.1016/j.atmosres.2009.01.009

Tam, B. Y., Szeto, K., Bonsal, B., Flato, G., Cannon, A. J., & Rong, R. (2019). CMIP5 drought projections in Canada based on the standardized precipitation evapotranspiration index. Canadian Water Resources Journal/Revue canadienne des ressources hydriques, 44(1), 90–107. https://doi.org/10.1080/07011784.2018.1537812

Taylor, K. E., Stouffer, R. J., & Meehl, G. A. (2012). An overview of CMIP5 and the experiment design. Bulletin of the American Meteorolog- ical Society, 93(4), 485–498. https://doi.org/10.1175/bams-d-11-00094.1

Teutschbein, C., & Seibert, J. (2012). Bias correction of regional climate model simulations for hydrological climate-change impact studies: Review and evaluation of different methods. Journal of Hydrology, 456–457(457), 12–29. https://doi.org/10.1016/j.jhydrol.2012.05.052

Touzé-Peiffer, L., Barberousse, A., & Le Treut, H. (2020). The Coupled Model Intercomparison Project: History, uses, and structural effects on climate research. Wiley Interdisciplinary Reviews: Climate Change, 11(4), 1–15. https://doi.org/10.1002/wcc.648

Turcotte, N. (2013). We grow a lot more than you may think. Government of Canada. Retrieved from https://publicentrale-ext.agr.gc.ca/pub_view-pub_affichage-eng.cfm?&publication_id=11996E

Van Vuuren, D. P., Edmonds, J., Kainuma, M., Riahi, K., Thomson, A., Hibbard, K., et al. (2011). The representative concentration path- ways: An overview. Climatic Change, 109(1), 5–31. https://doi.org/10.1007/s10584-011-0148-z

Vorobyeva, V., & Volodin, E. (2021). Evaluation of the INM RAS climate model skill in climate indices and stratospheric anomalies on seasonal timescale. Tellus, Series A: Dynamic Meteorology and Oceanography, 73(1), 1–12. https://doi.org/10.1080/16000870.2021.1892435

Wang, B., Jin, C., & Liu, J. (2020). Understanding future change of global monsoons projected by CMIP6 models. Journal of Climate, 33(15), 6471–6489. https://doi.org/10.1175/jcli-d-19-0993.1

Wazneh, H., Arain, M. A., & Coulibaly, P. (2020). Climate indices to characterize climatic changes across southern Canada. Meteorological Applications, 27(1), e1861. https://doi.org/10.1002/met.1861

Weiß, M., & Menzel, L. (2008). A global comparison of four potential evapotranspiration equations and heir relevance to stream flow modelling in semi-arid environments. Advances in Geosciences, 18, 15–23. https://doi.org/10.5194/adgeo-18-15-2008

Xing, Z., Chow, L., Meng, F. R., Rees, H. W., Monteith, J., & Lionel, S. (2008). Testing reference evapotranspiration estimation methods using evaporation pan and modelling in maritime region of Canada. Journal of Irrigation and Drainage Engineering, 134(4), 417–424. https://doi.org/10.1061/(ASCE)0733-9437(2008)134:4(417)

Xu, C. Y., & Singh, V. P. (1998). Dependence of evaporation on meteorological variables at different time-scales and intercomparison of estimation methods. Hydrological Processes, 12(3), 429–442. https://doi.org/10.1002/(sici)1099-1085(19980315)12:3<429::aid-hyp581>3.0.co;2-a

Xu, C. Y., & Singh, V. P. (2002). Cross comparison of empirical equations for calculating potential evapotranspiration with data from Switzerland. Water Resources Management, 16(3), 197-219. https://doi.org/10.1023/A:1020282515975

Yan, X., & Mohammadian, A. (2020). Estimating future daily pan evaporation for Qatar using the Hargreaves model and statistically downscaled global climate model projections under RCP climate change scenarios. Arabian Journal of Geosciences, 13(18). https://doi.org/10.1007/s12517-020-05944-0

Yazdandoost, F., Moradian, S., Izadi, A., & Aghakouchak, A. (2020). Evaluation of CMIP6 precipitation simulations across different cli- matic zones: Uncertainty and model intercomparison. Atmospheric Research, 105369. https://doi.org/10.1016/j.atmosres.2020.105369

Yigzaw, W., Hossain, F., & Kalyanapu, A. (2013). Impact of artificial reservoir size and land use/land cover patterns on probable maximum precipitation and flood: Case of Folsom Dam on the

American River. Journal of Hydrologic Engineering, 18(9), 1180–1190. https://doi.org/10.1061/(asce)he.1943-5584.0000722

Yu, H., Wei, Y., Zhang, Q., Liu, X., Huang, J., Feng, T., & Zhang, M. (2020). Multi-model assessment of global temperature variability on different time scales. International Journal of Climatology, 40(1), 273-291. https://doi.org/10.1002/joc.6209

Zhai, J., Mondal, S. K., Fischer, T., Wang, Y., Su, B., Huang, J., … Uddin, M. J. (2020). Future drought characteristics through a multi-model ensemble from CMIP6 over South Asia. Atmospheric Research, 246(April), 105111. https://doi.org/10.1016/j.atmosres.2020.105111

Zhang, Y., Qian, B., & Hong, G. (2020). A Long-Term, 1-km Resolution Daily Meteorological Dataset for Modeling and Mapping Permafrost in Canada. Atmosphere, 11(12), 1363. https://doi.org/10.3390/atmos11121363

Zhu, E., Yuan, X., & Wu, P. (2020). Skillful decadal prediction of droughts over large-scale river basins across the globe. Geophysical Re- search Letters, 47(17), e2020GL089738. https://doi.org/10.1029/2020gl089738

Zhu, H., Jiang, Z., Li, J., Li, W., Sun, C., & Li, L. (2020). Does CMIP6 inspire more confidence in simulating climate extremes over China? Advances in Atmospheric Sciences, 37(10), 1119–1132. https://doi.org/10.1007/s00376-020-9289-1

APPENDIX A SUPPLEMENTARY MATERIAL OF CHAPTER 4

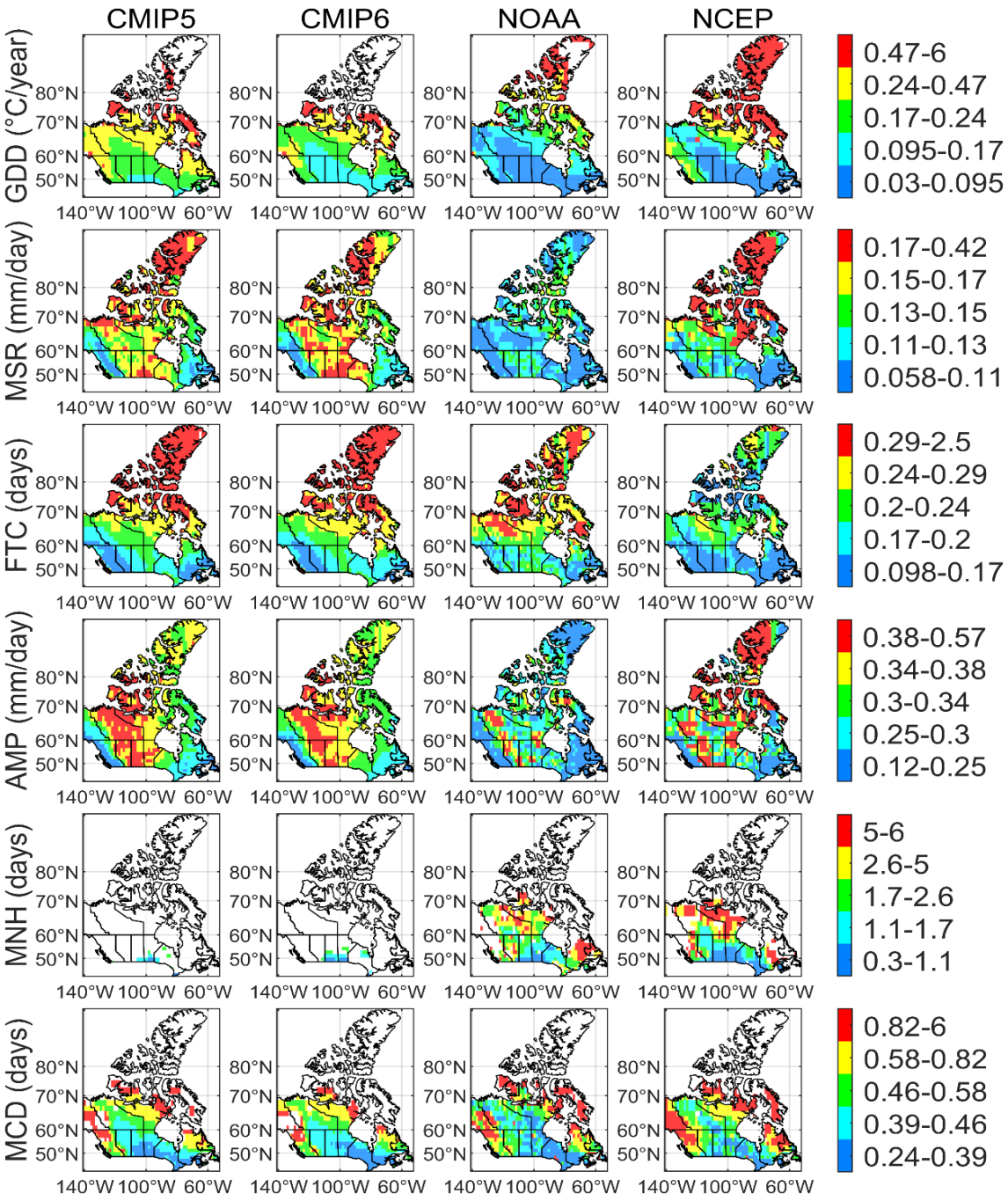

Figure A1 GDD, MSR, FTC, AMP, MNH, and MCD multi-model ensemble CV values, estimated by CMIP5 and CMIP6 in comparison to NOAA and NCEP estimates during the historical period. The white grids represent a null CV, where the mean is equal to 0.

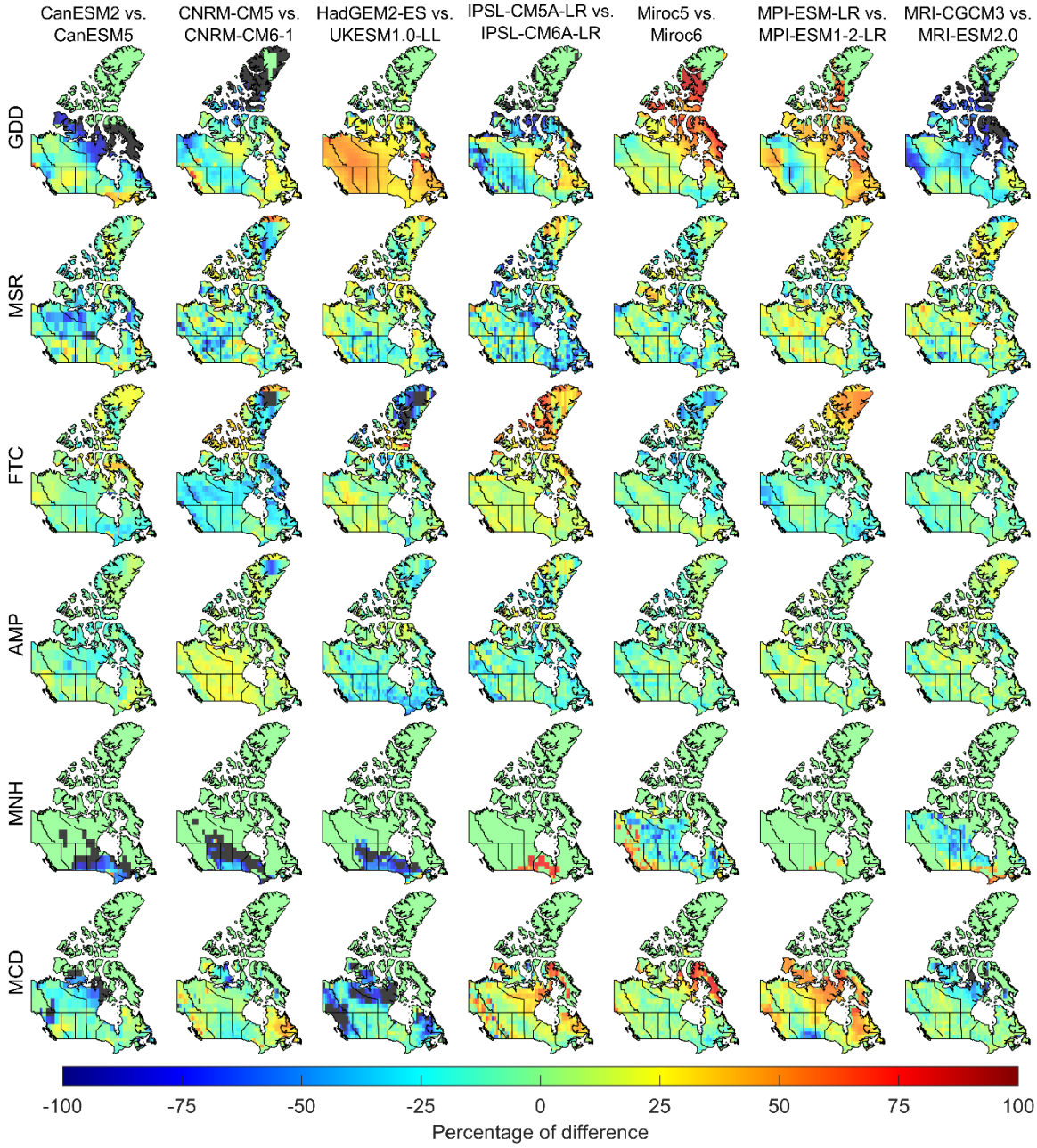

Figure A2 Percentage of relative difference between the multi-simulation ensemble CV values, estimated by CMIP5 models and their CMIP6 counterparts during the historical period.

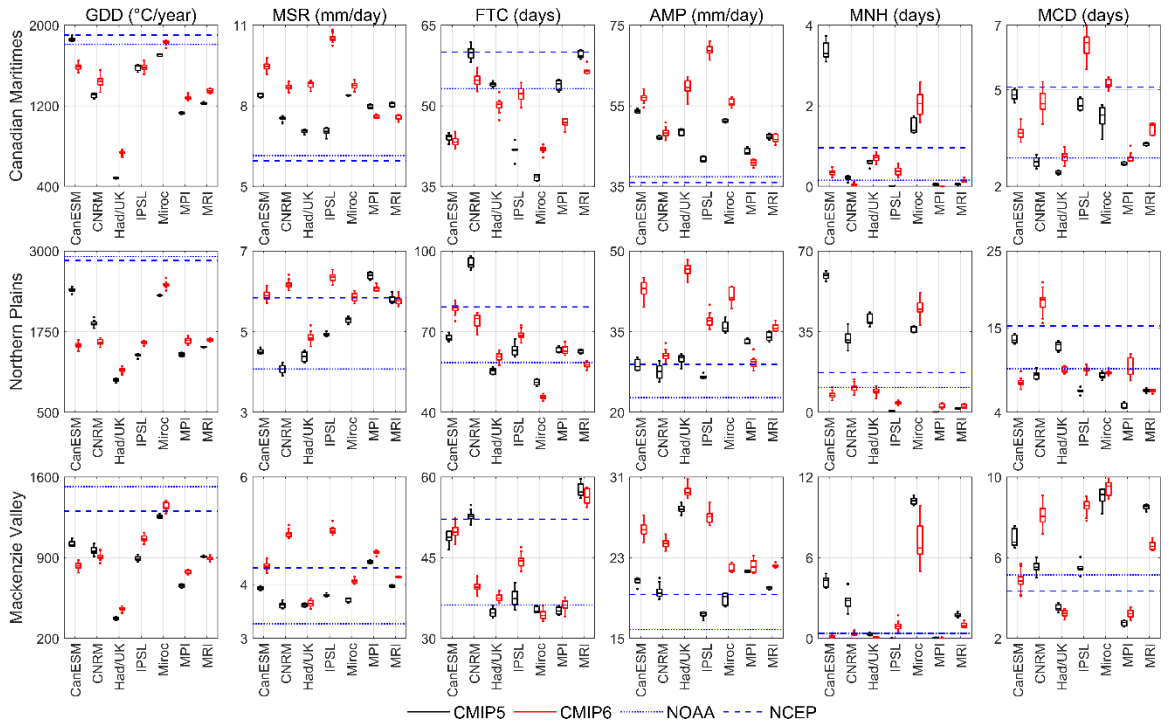

Figure A3 Long-term annual average values for six climate indices, estimated by simulations of CMIP5 (black boxplot) and CMIP6 (red boxplots), as well as NOAA (dotted line), and NCEP (dashed line) in the Canadian Maritimes, Northern Plains and Mackenzie Valley.

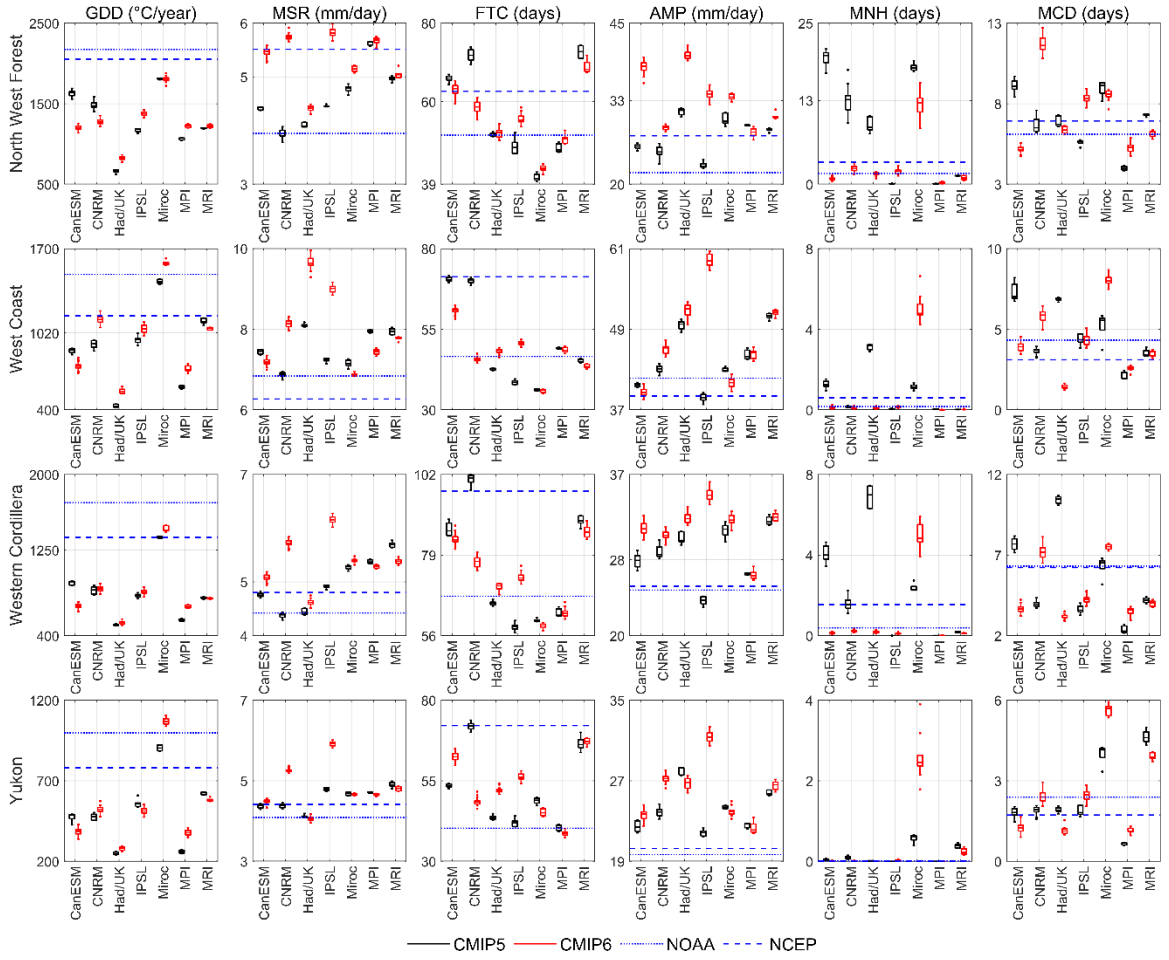

Figure A4 Long-term annual average values for six climate indices, estimated by simulations of CMIP5 (black boxplot) and CMIP6 (red boxplots), as well as NOAA (dotted line), and NCEP (dashed line) in the North West Forest, West Coast, Western Cordillera and Yukon.

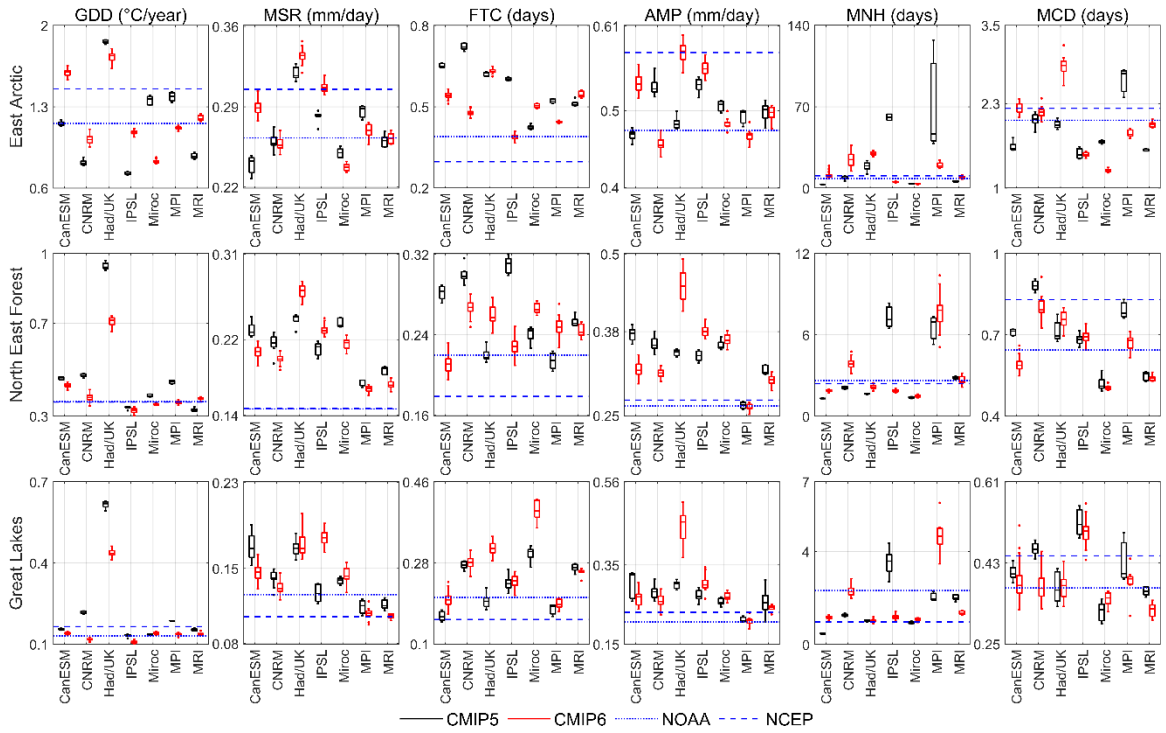

Figure A5 Long-term annual CV values for six climate indices, estimated by simulations of CMIP5 (black boxplots) and CMIP6 (red boxplots), as well as NOAA (dotted line), and NCEP (dashed line) in the East Arctic, North East Forest and Great Lakes.

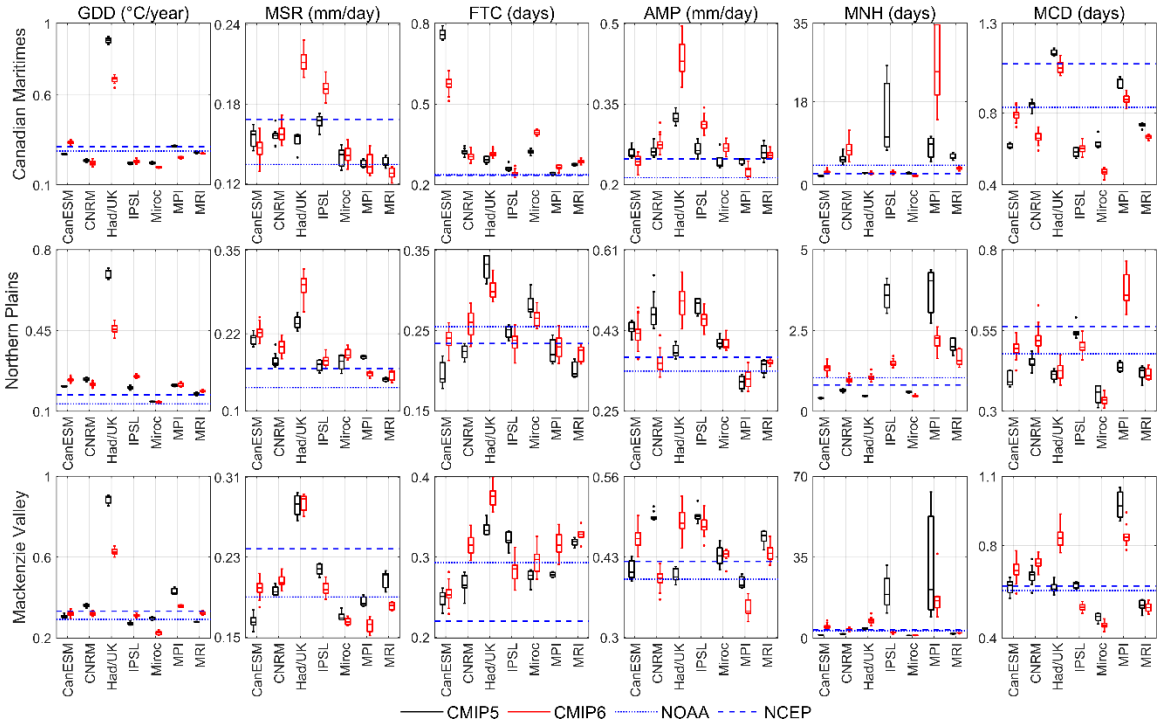

Figure A6 Long-term annual CV values for six climate indices, estimated by simulations of CMIP5 (black boxplots) and CMIP6 (red boxplots), as well as NOAA (dotted line), and NCEP (dashed line) in the Canadian Maritimes, Northern Plains and Mackenzie Valley.

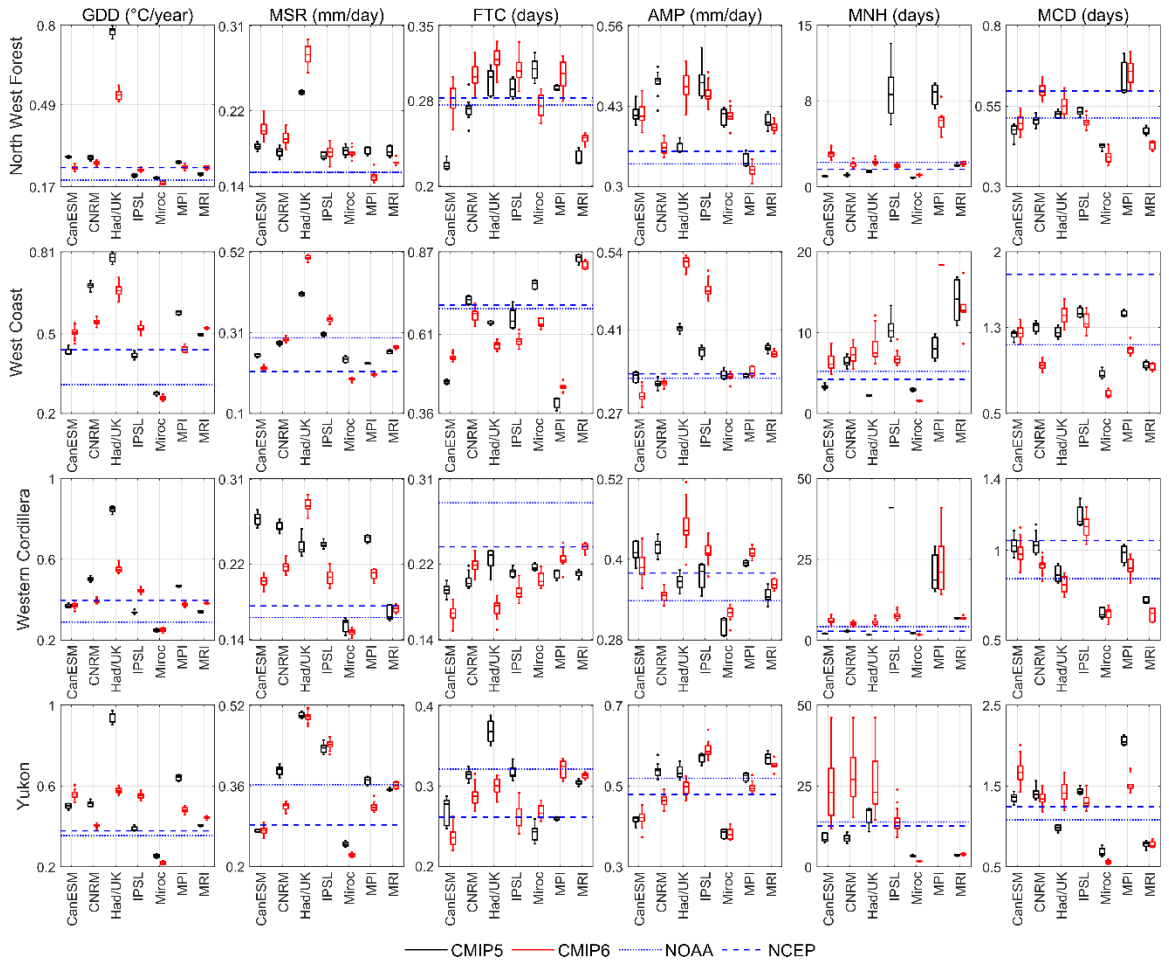

Figure A7 Long-term annual CV values for six climate indices, estimated by simulations of CMIP5 (black boxplot) and CMIP6 (red boxplots), as well as NOAA (dotted line), and NCEP (dashed line) in the North West Forest, West Coast, Western Cordillera and Yukon.

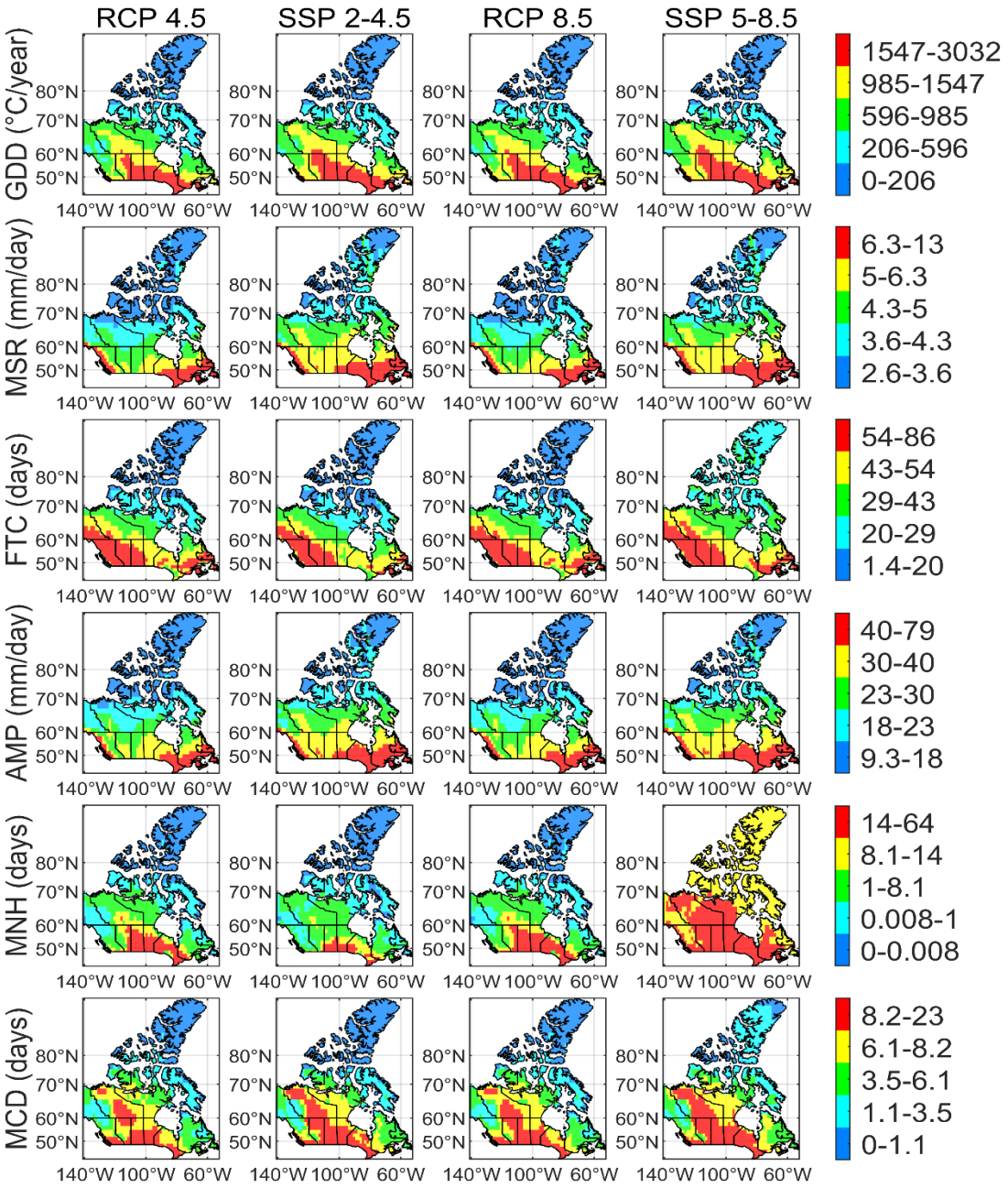

Figure A8 GDD, MSR, FTC, AMP, MNH, and MCD multi-model ensemble mean values, estimated by CMIP5 (RCPs 4.5 and 8.5) and CMIP6 (SSPs 2-4.5 and 5-8.5) scenarios during 2021-2050.

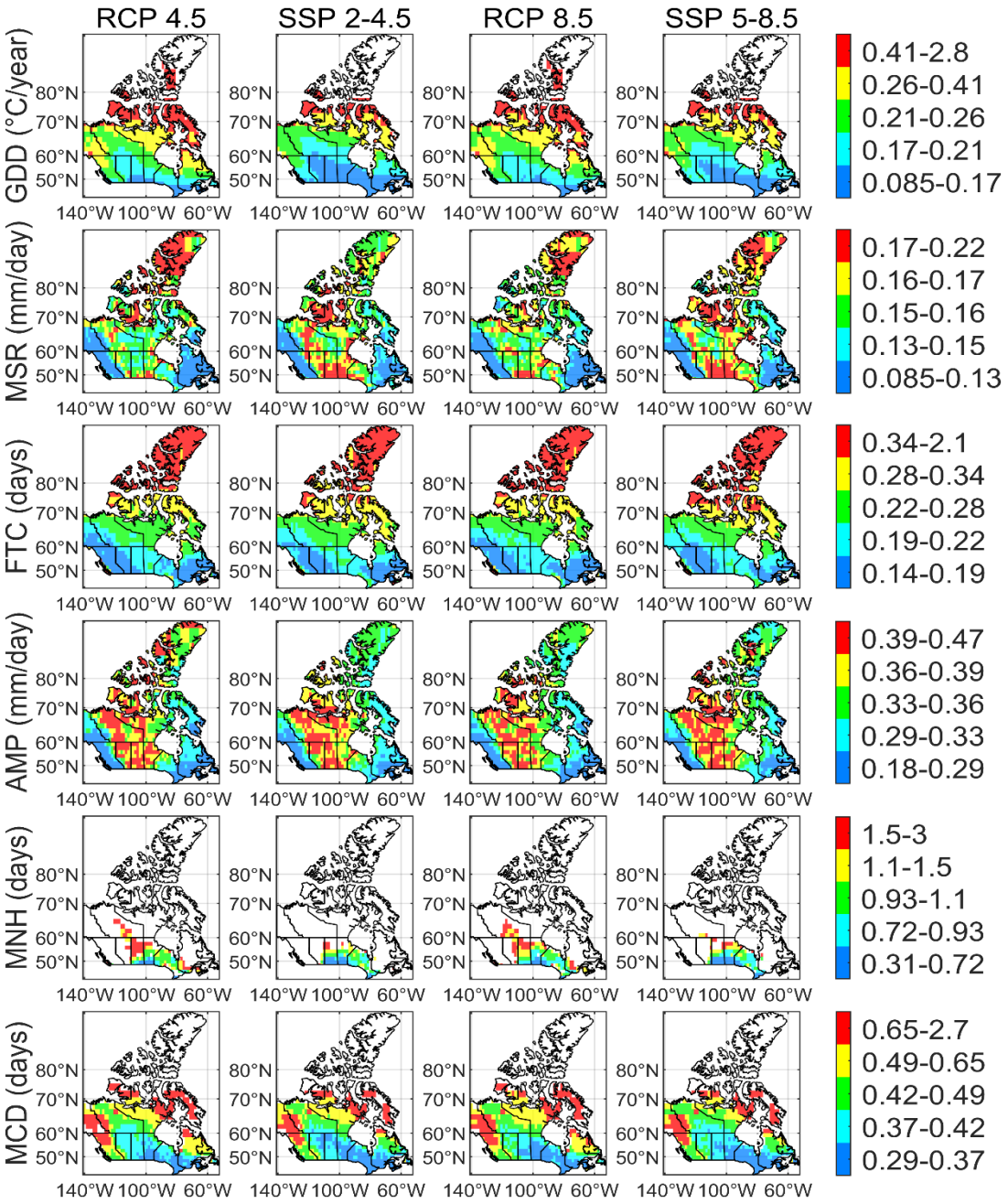

Figure A9 GDD, MSR, FTC, AMP, MNH, and MCD multi-model ensemble CV values, estimated by CMIP5 (RCPs 4.5 and 8.5) and CMIP6 (SSPs 2-4.5 and 5-8.5) scenarios during 2021-2050. The white grids represent a null CV, where the mean is equal to 0.

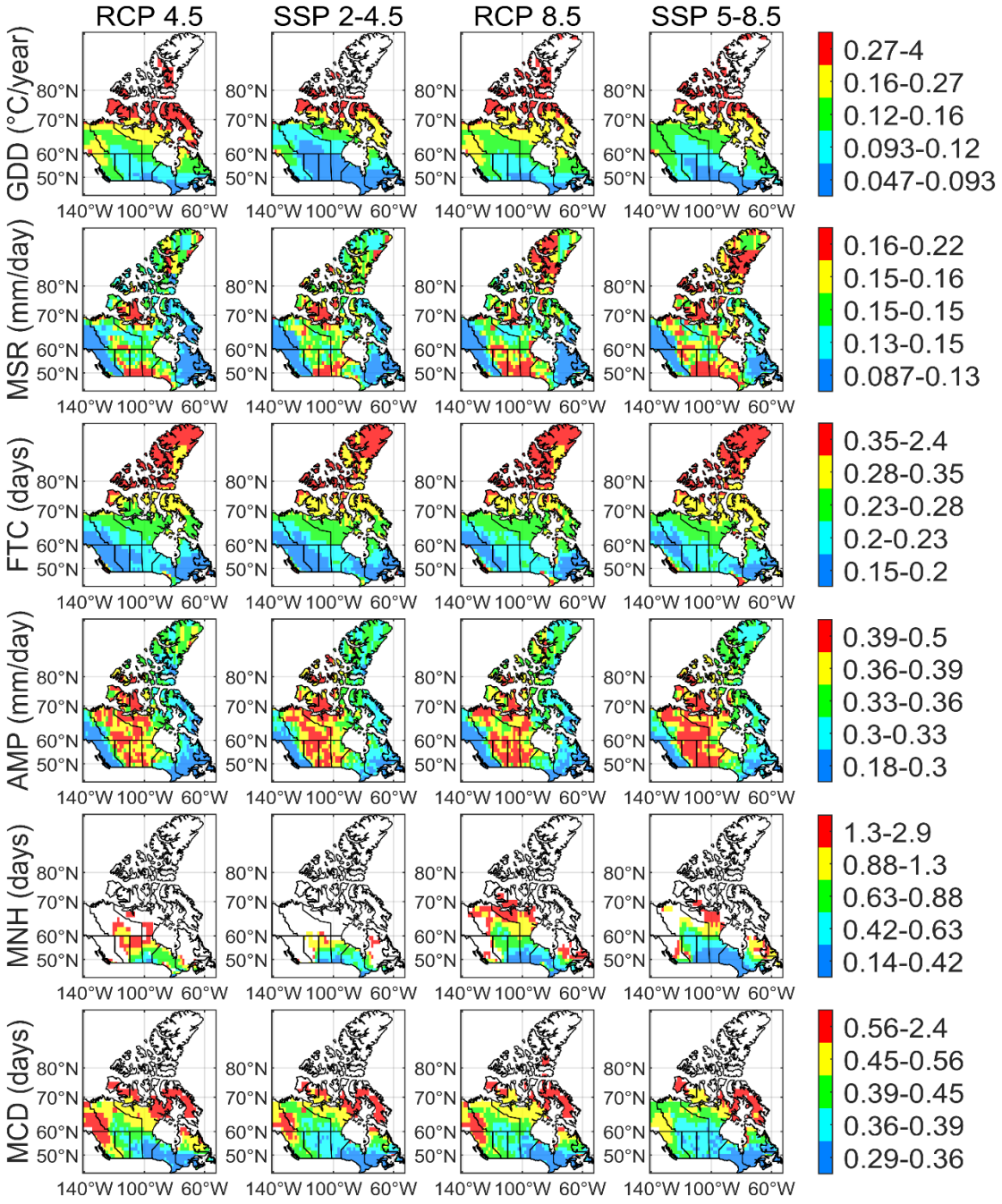

Figure A10 GDD, MSR, FTC, AMP, MNH, and MCD multi-model ensemble CV values, estimated by CMIP5 (RCP 4.5 and 8.5) and CMIP6 (SSP 2-4.5 and 5-8.5) scenarios during 2071-2100. The white grids represent a null CV, where the mean is equal to 0.

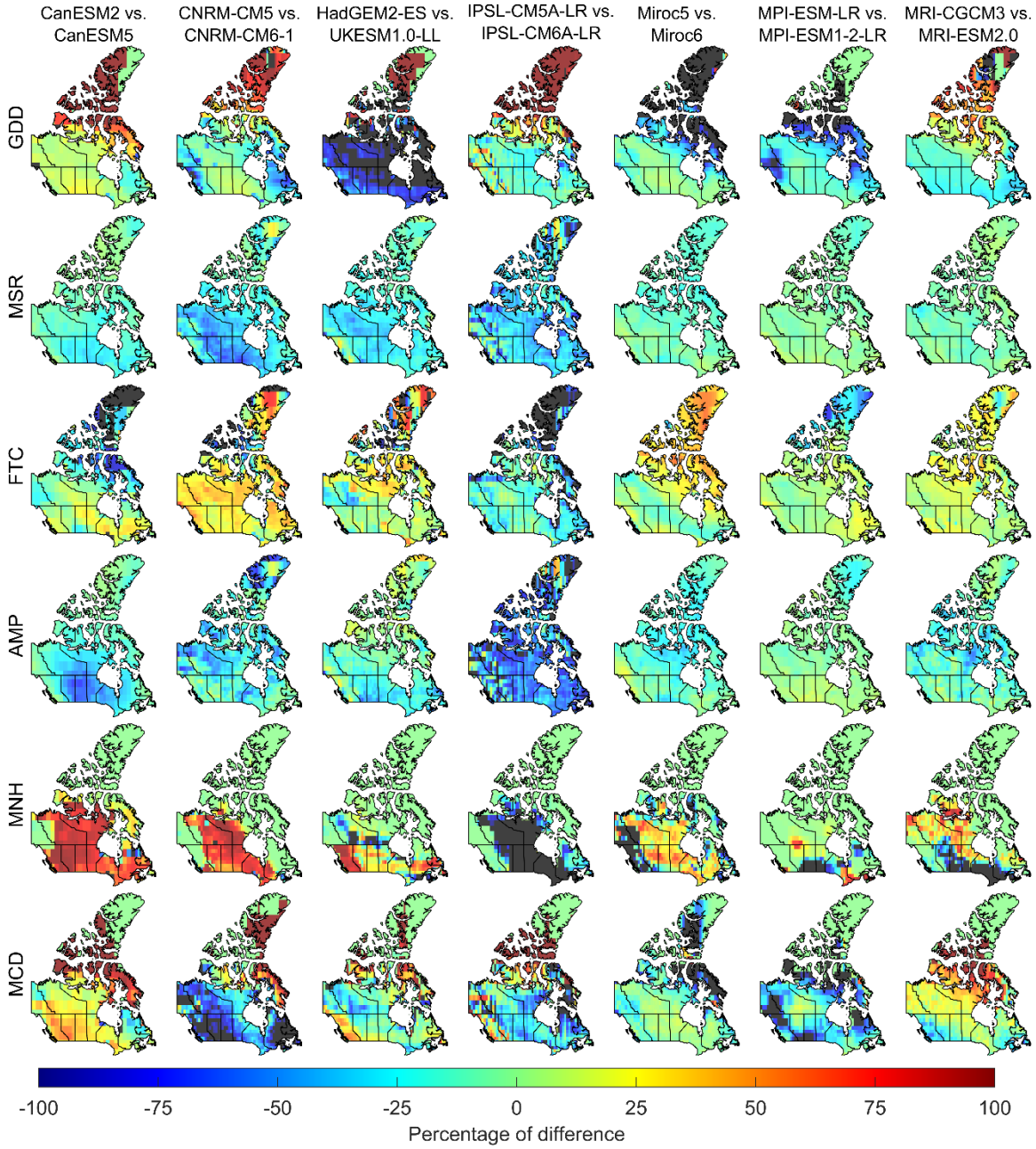

Figure A11 Percentage of relative difference between the multi-simulation ensemble mean values, estimated by CMIP5 models and their CMIP6 counterparts under 4.5 W/m2 forcing during 2021-2050.

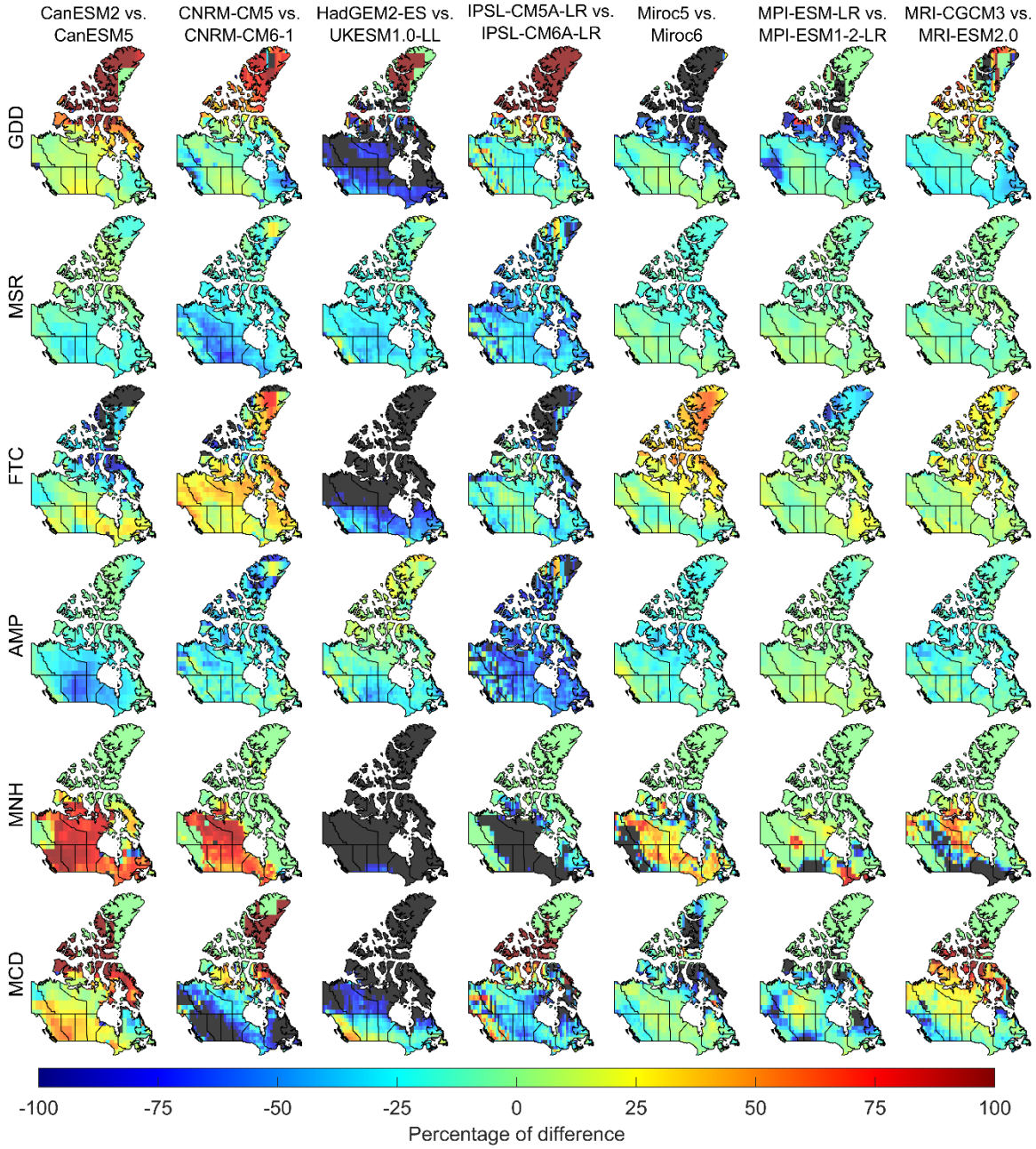

Figure A12 Percentage of relative difference between the multi-simulation ensemble mean values, estimated by CMIP5 models and their CMIP6 counterparts under 8.5 W/m2 forcing during 2021-2050.

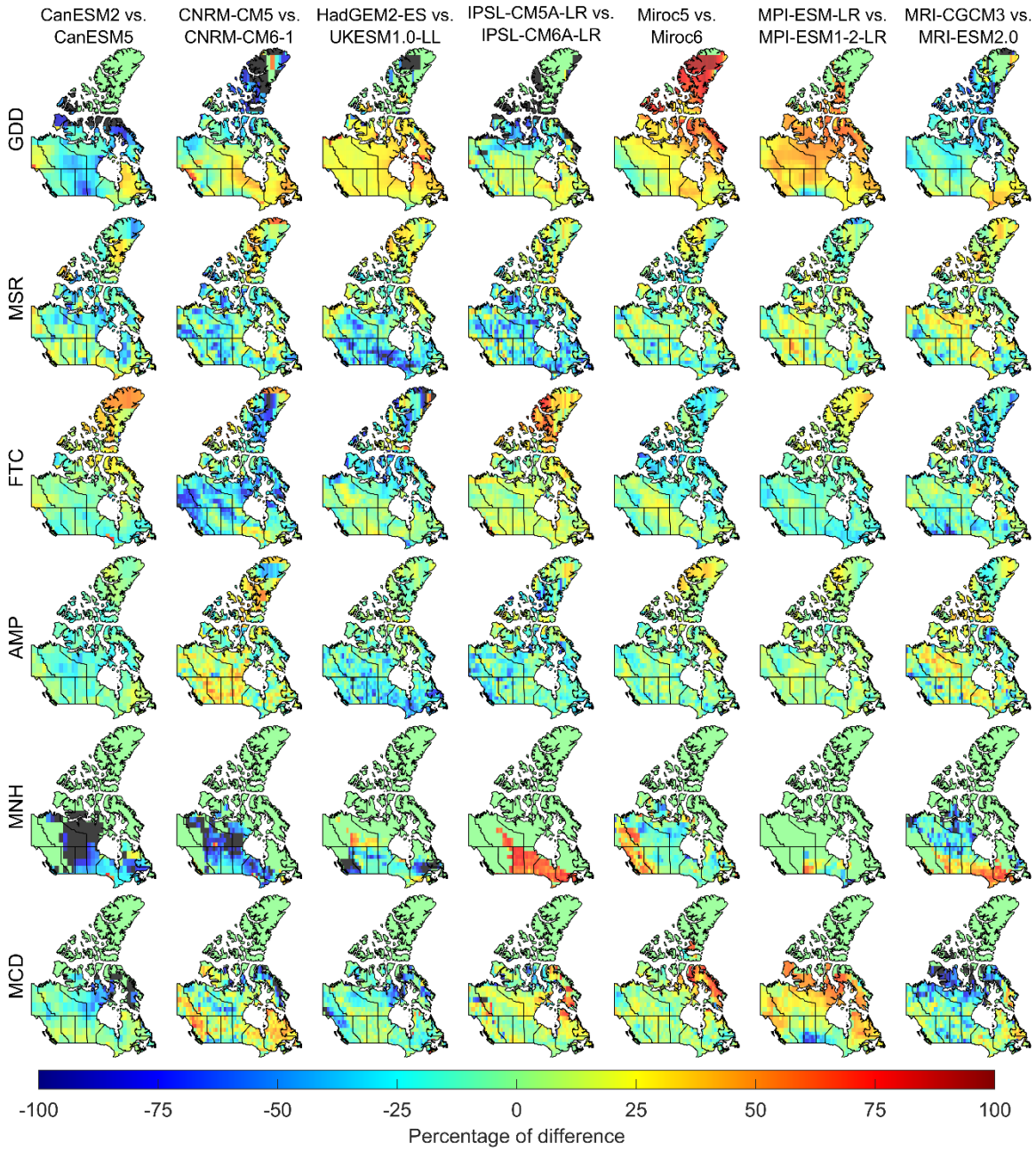

Figure A13 Percentage of relative difference between the multi-simulation ensemble CV values, estimated by CMIP5 models and their CMIP6 counterparts under 4.5 W/m2 forcing during 2021-2050.

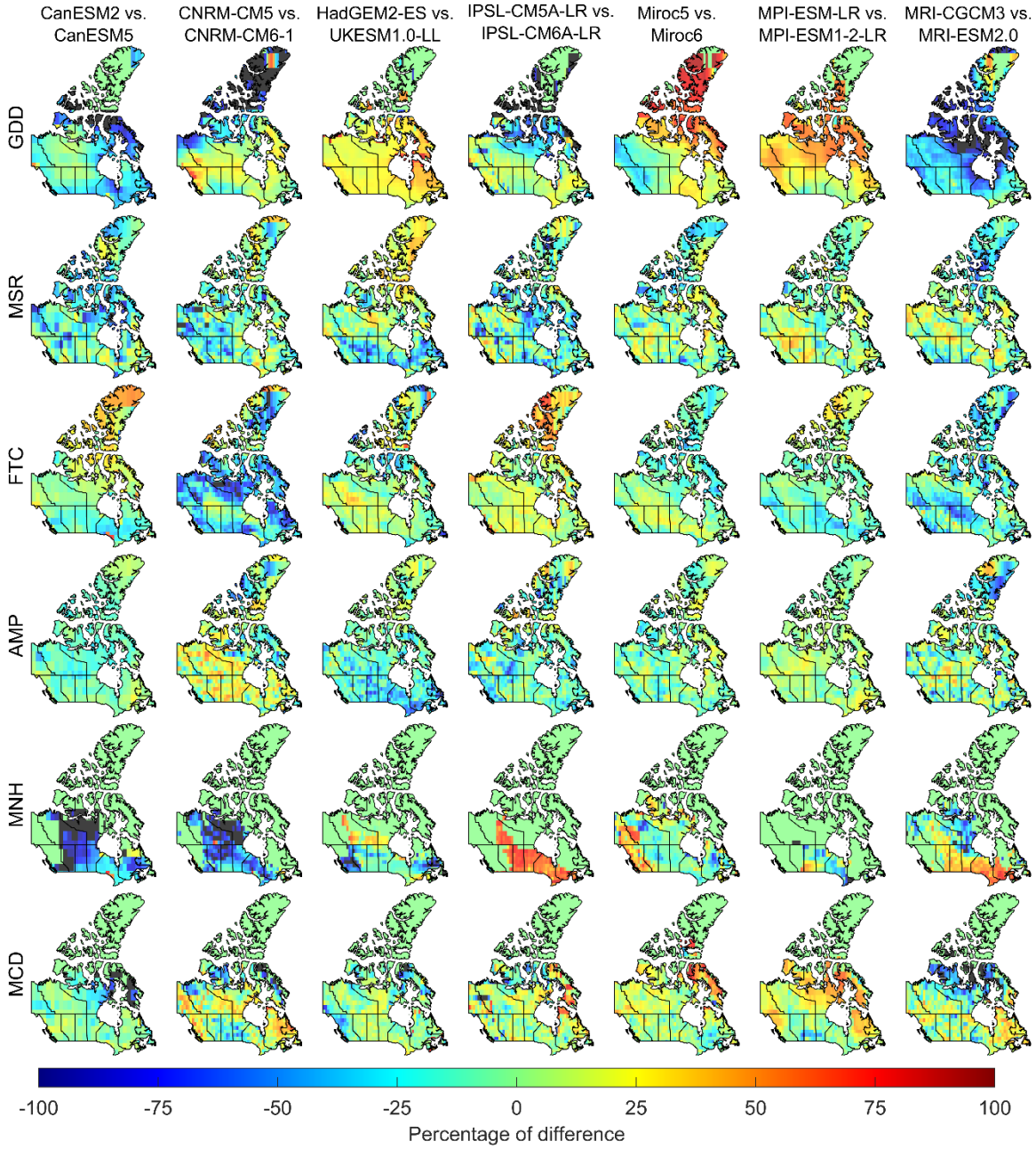

Figure A14 Percentage of relative difference between the multi-simulation ensemble CV values, estimated by CMIP5 models and their CMIP6 counterparts under 8.5 W/m2 forcing during 2021-2050.

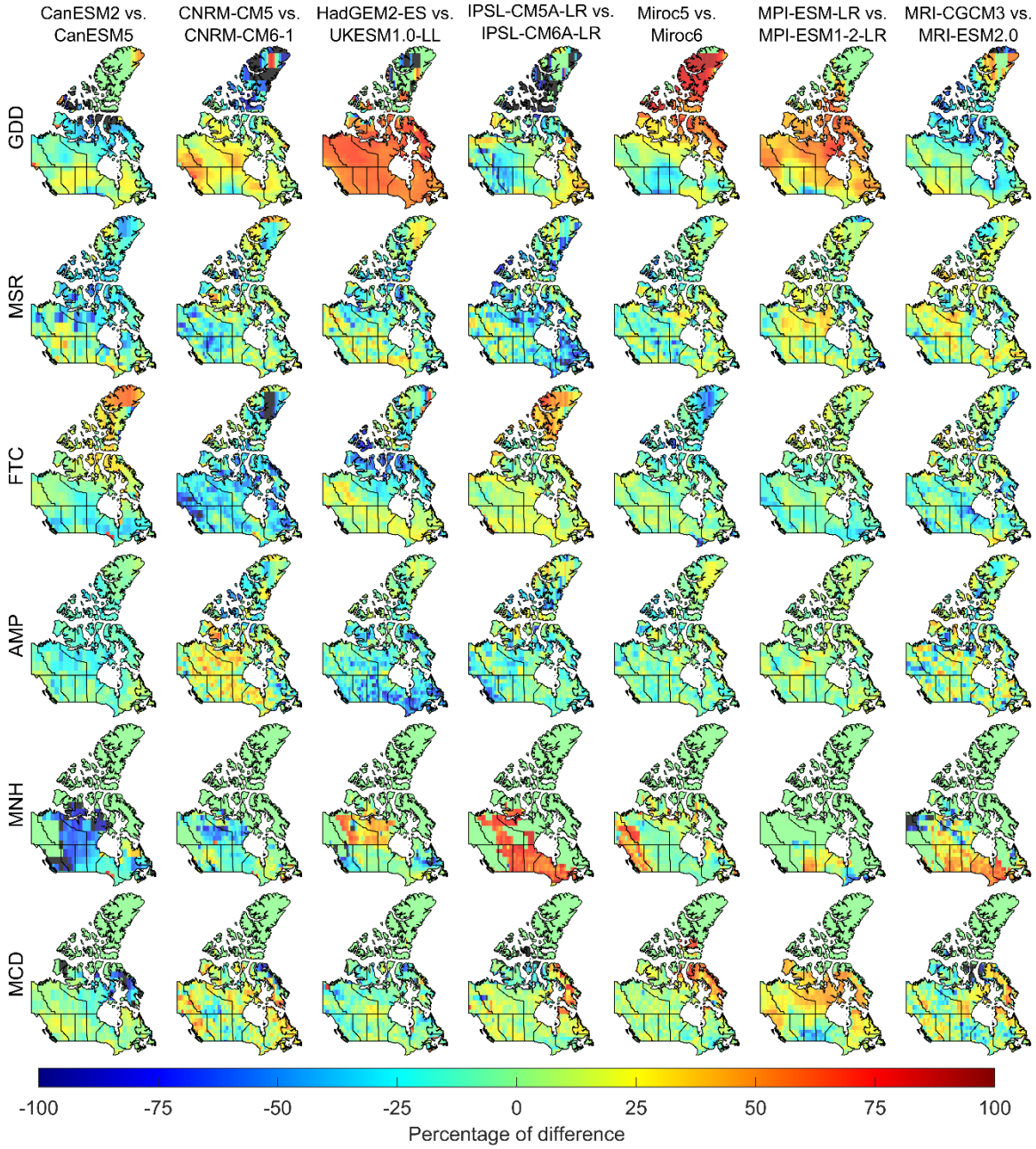

Figure A15 Percentage of relative difference between the multi-simulation ensemble CV values, estimated by CMIP5 models and their CMIP6 counterparts under 4.5 W/m2 forcing during 2071-2100.

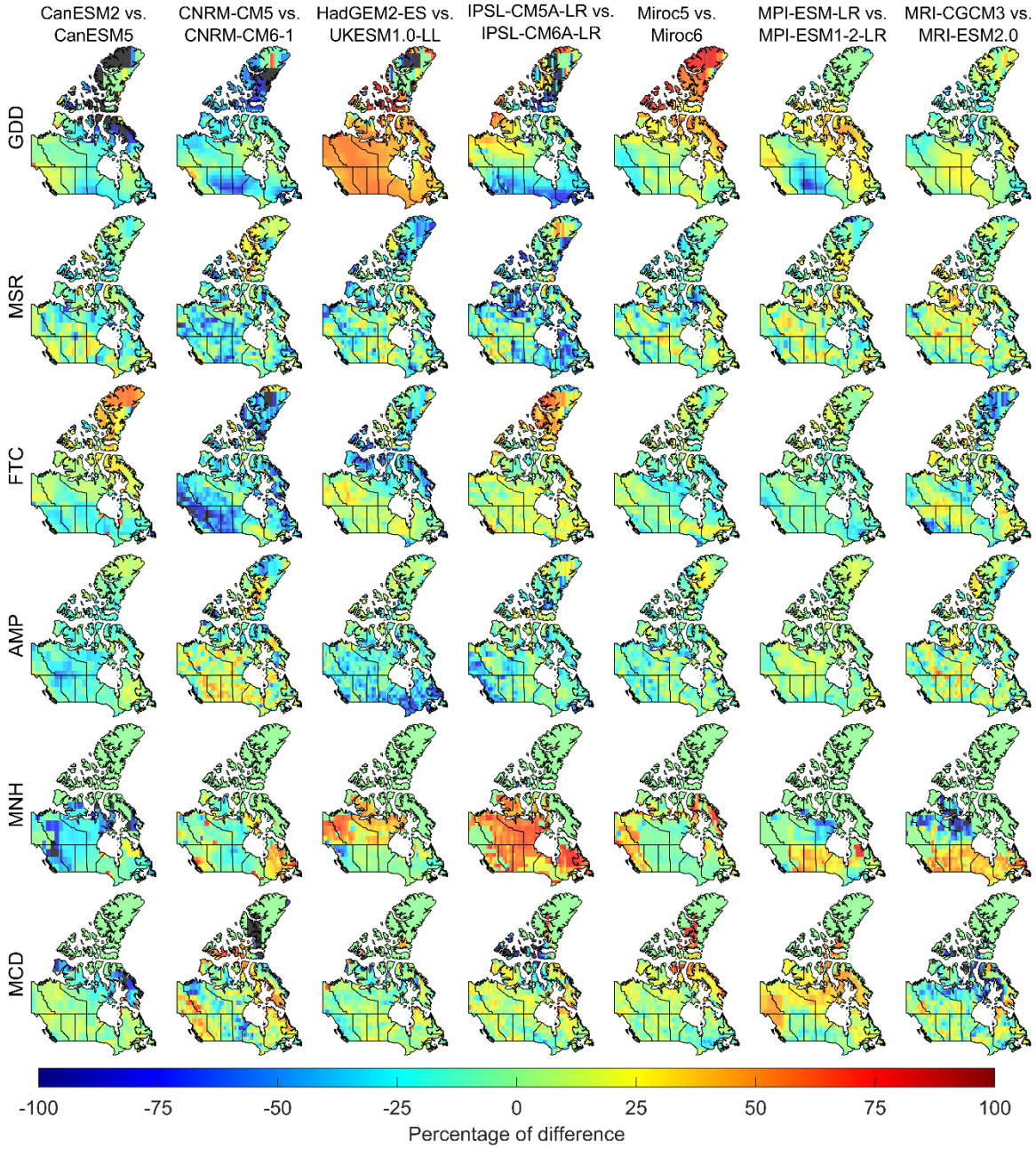

Figure A16 Percentage of relative difference between the multi-simulation ensemble CV values, estimated by CMIP5 models and their CMIP6 counterparts under 8.5 W/m2 forcing during 2071-2100.

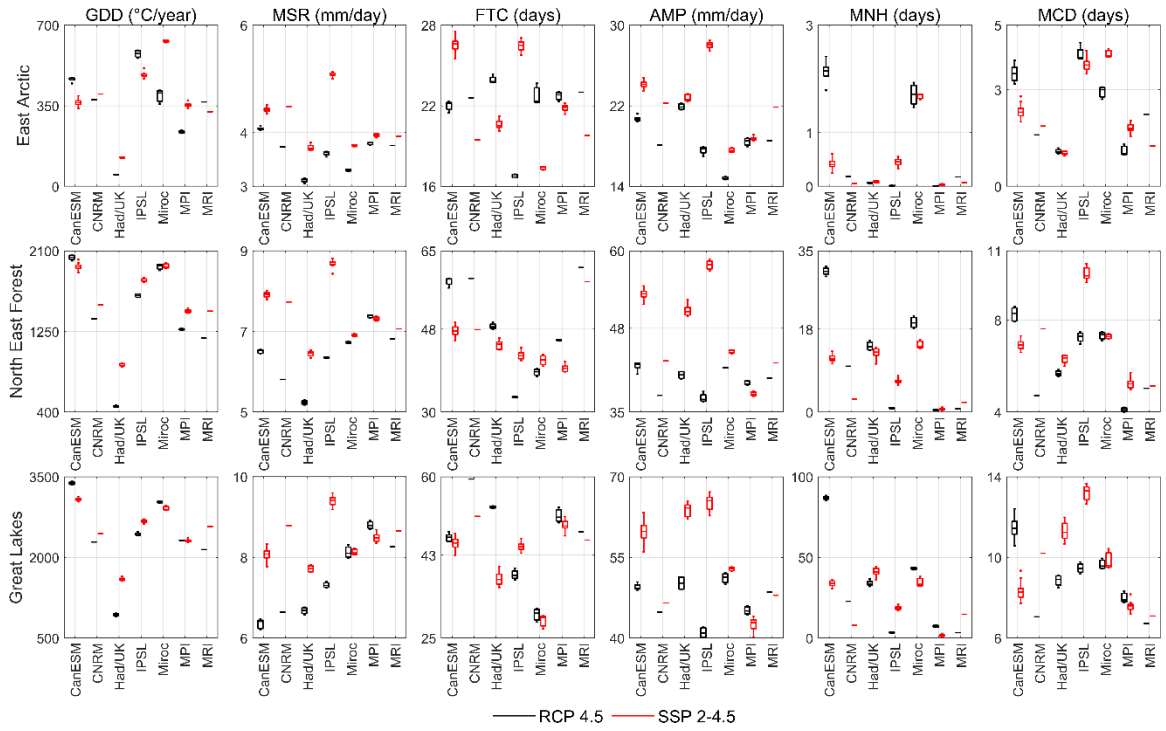

Figure A17 Long-term annual average values of six climate indices, estimated by simulations of CMIP5 under RCP 4.5 (black boxplots), and CMIP6 under SSP 2-4.5 (red boxplots), in the East Arctic, North East Forest and Great Lakes during 2021-2050.

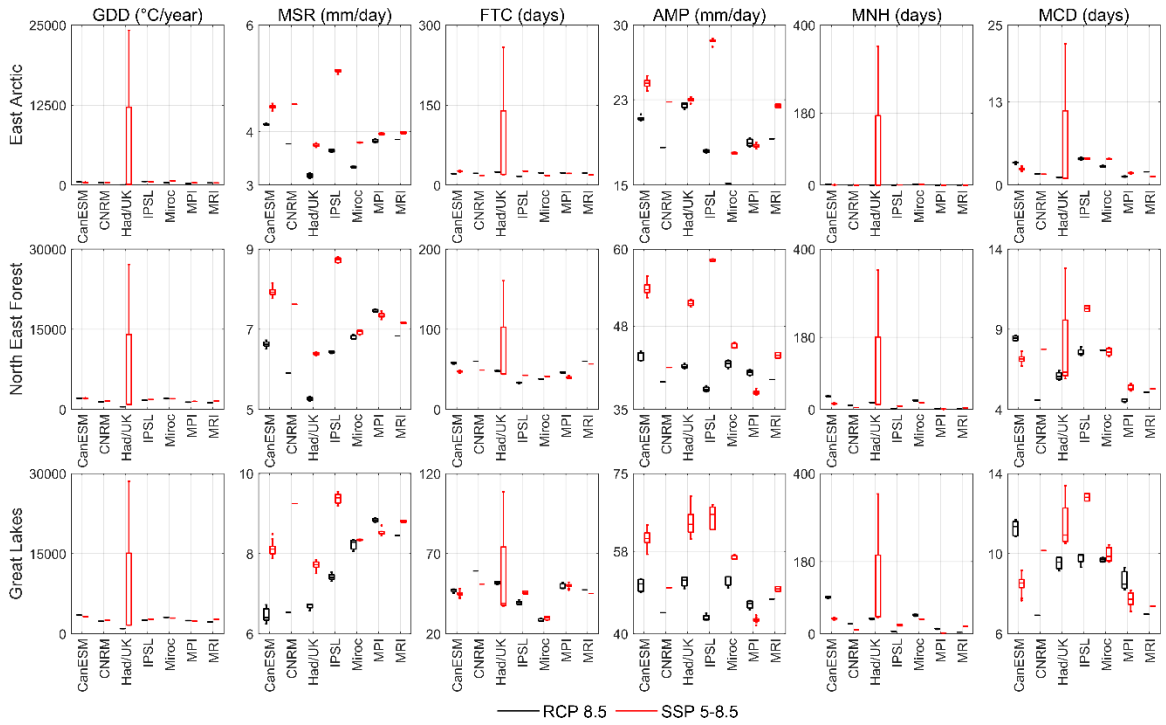

Figure A18 Long-term annual average values of six climate indices, estimated by simulations of CMIP5 under RCP 8.5 (black boxplots), and CMIP6 under SSP 5-8.5 (red boxplots), in the East Arctic, North East Forest and Great Lakes during 2021-2050.

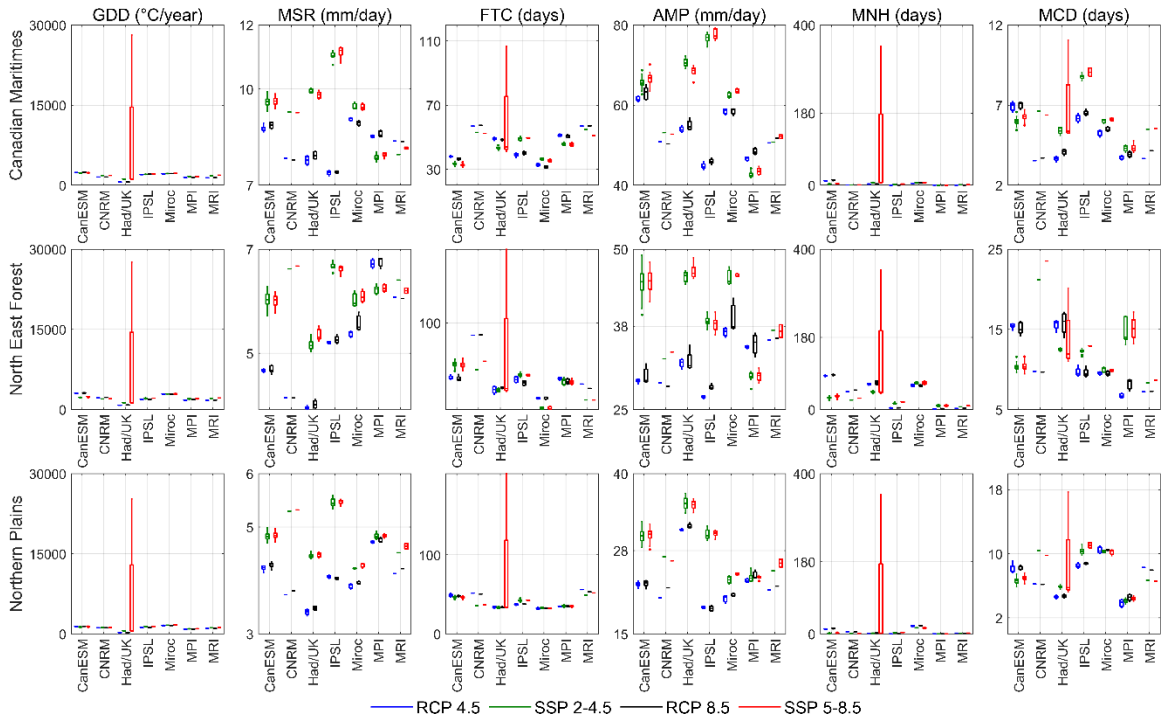

Figure A19 Long-term annual average values of six climate indices, estimated by simulations of CMIP5 under RCPs 4.5 (blue boxplots) & 8.5 (black boxplots), and CMIP6 under SSPs 2-4.5 (green boxplots) & 5-8.5 (red boxplots), in the Canadian Maritimes, Northern Plains and Mackenzie Valley during 2021-2050.

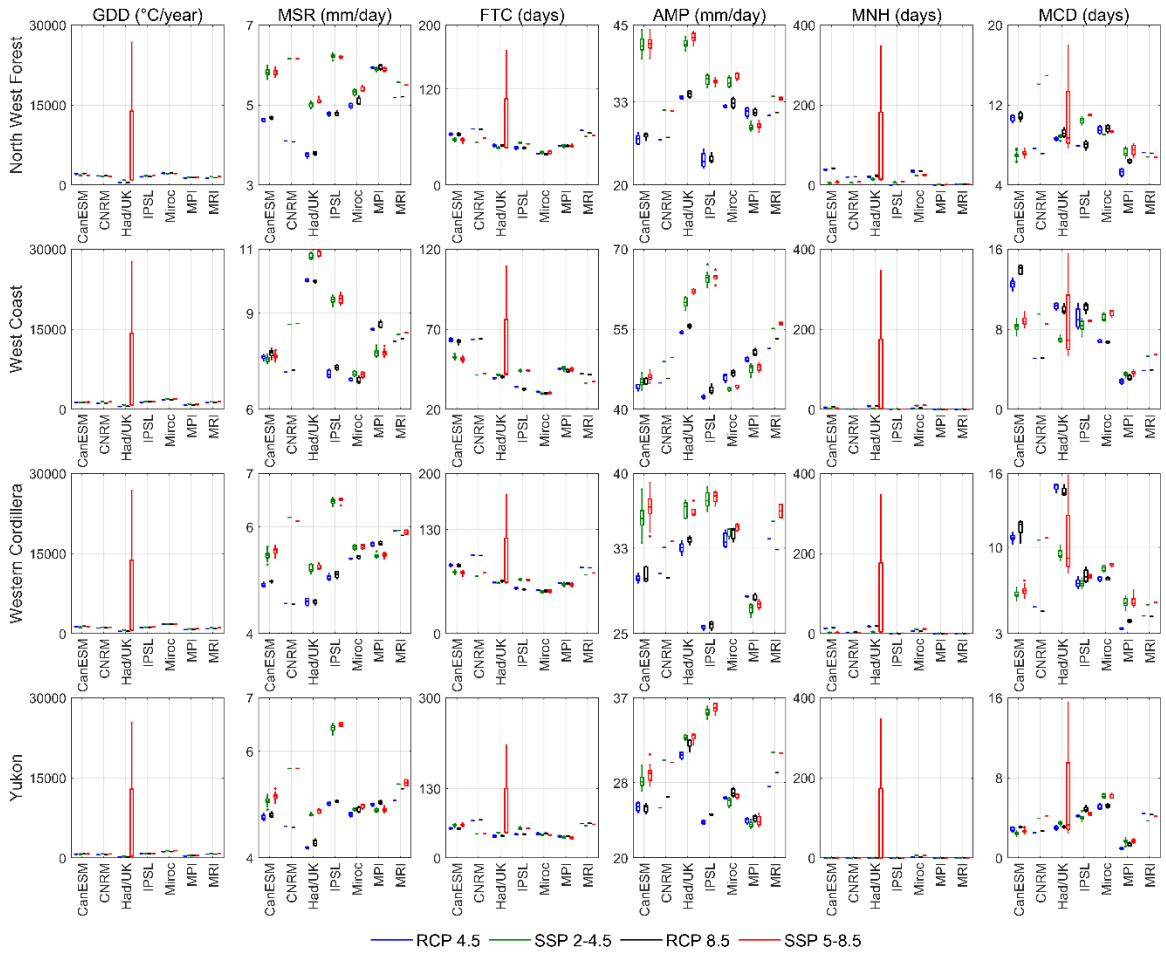

Figure A20 Long-term annual average values of six climate indices, estimated by simulations of CMIP5 under RCPs 4.5 (blue boxplots) & 8.5 (black boxplots), and CMIP6 under SSPs 2-4.5 (green boxplots) & 5-8.5 (red boxplots), in the North West Forest, West Coast, Western Cordillera and Yukon during 2021-2050.

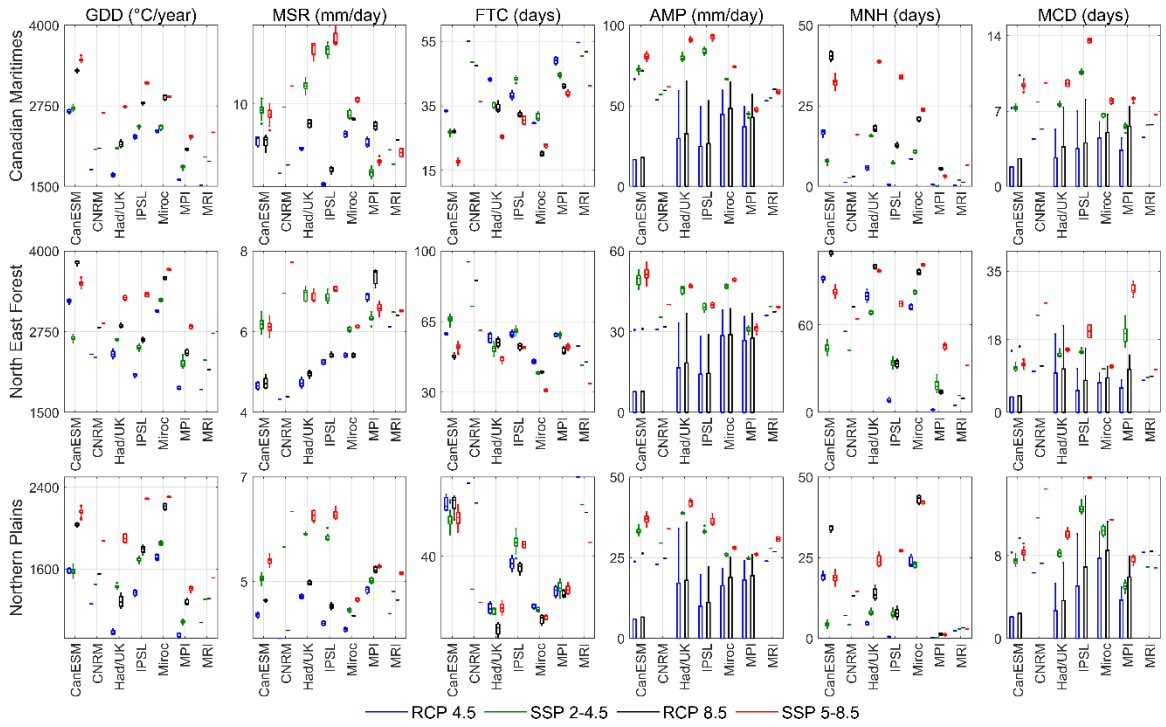

Figure A21 Long-term annual average values of six climate indices, estimated by simulations of CMIP5 under RCPs 4.5 (blue boxplots) & 8.5 (black boxplots), and CMIP6 under SSPs 2-4.5 (green boxplots) & 5-8.5 (red boxplots), in the Canadian Maritimes, Northern Plains and Mackenzie Valley during 2071-2100.

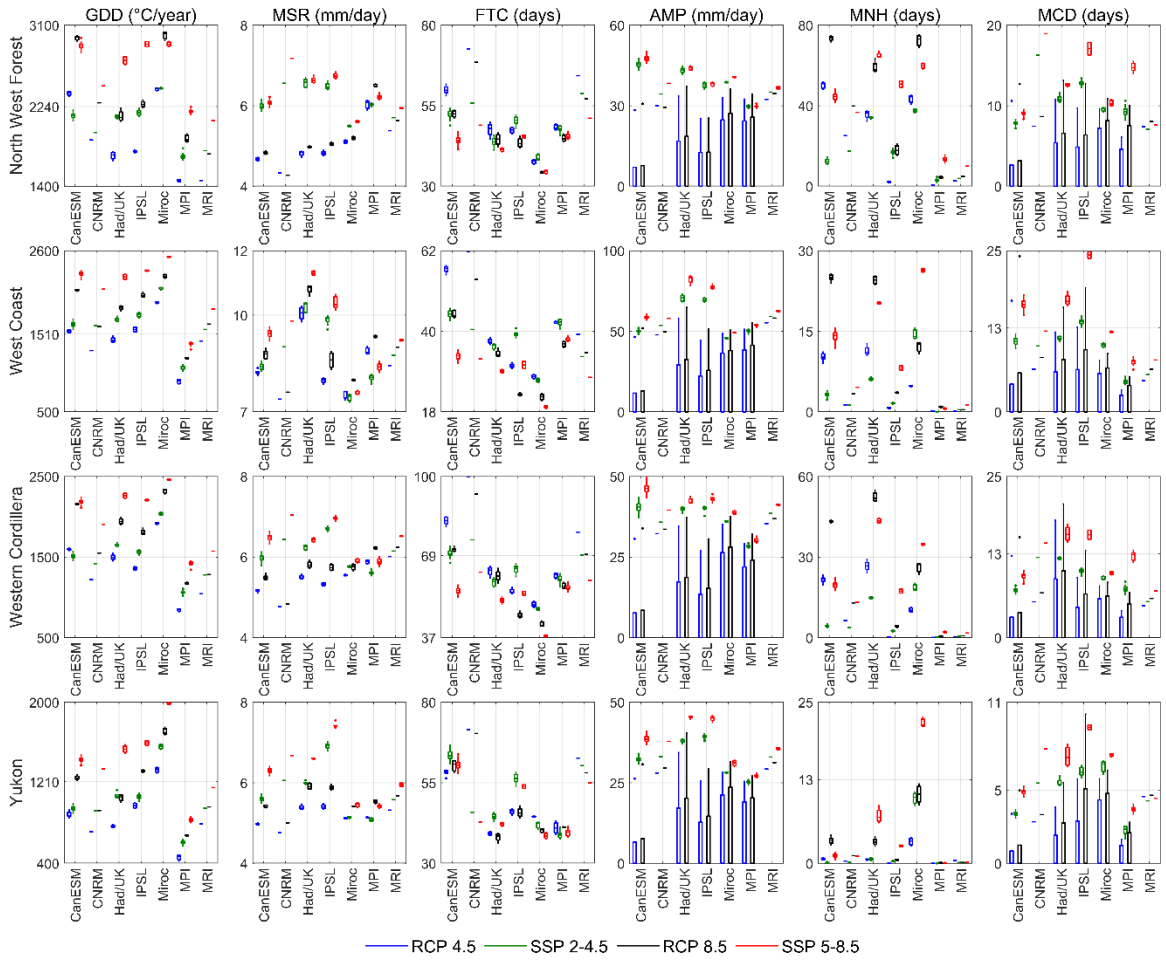

Figure A22 Long-term annual average values of six climate indices, estimated by simulations of CMIP5 under RCPs 4.5 (blue boxplots) & 8.5 (black boxplots), and CMIP6 under SSPs 2-4.5 (green boxplots) & 5-8.5 (red boxplots), in the North West Forest, West Coast, Western Cordillera and Yukon during 2071-2100.

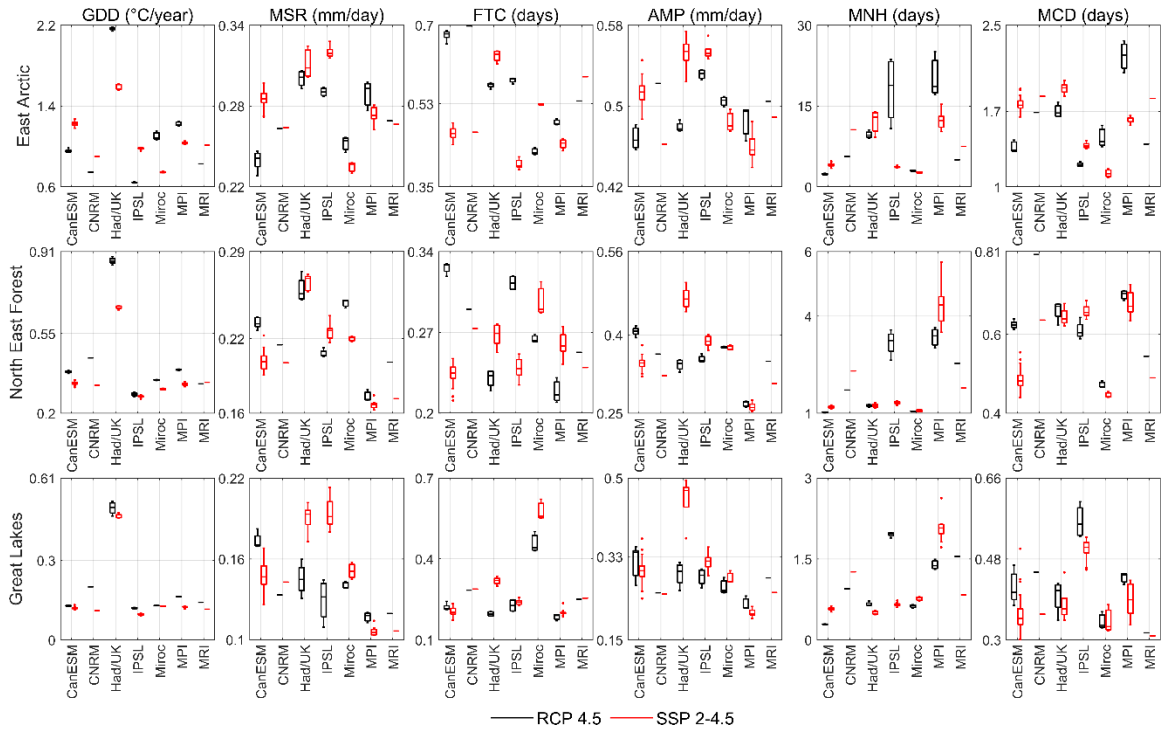

Figure A23 Long-term annual CV values of six climate indices, estimated by simulations of CMIP5 under RCP 4.5 (black boxplots), and CMIP6 under SSP 2-4.5 (red boxplots), in the East Arctic, North East Forest and Great Lakes during 2021-2050.

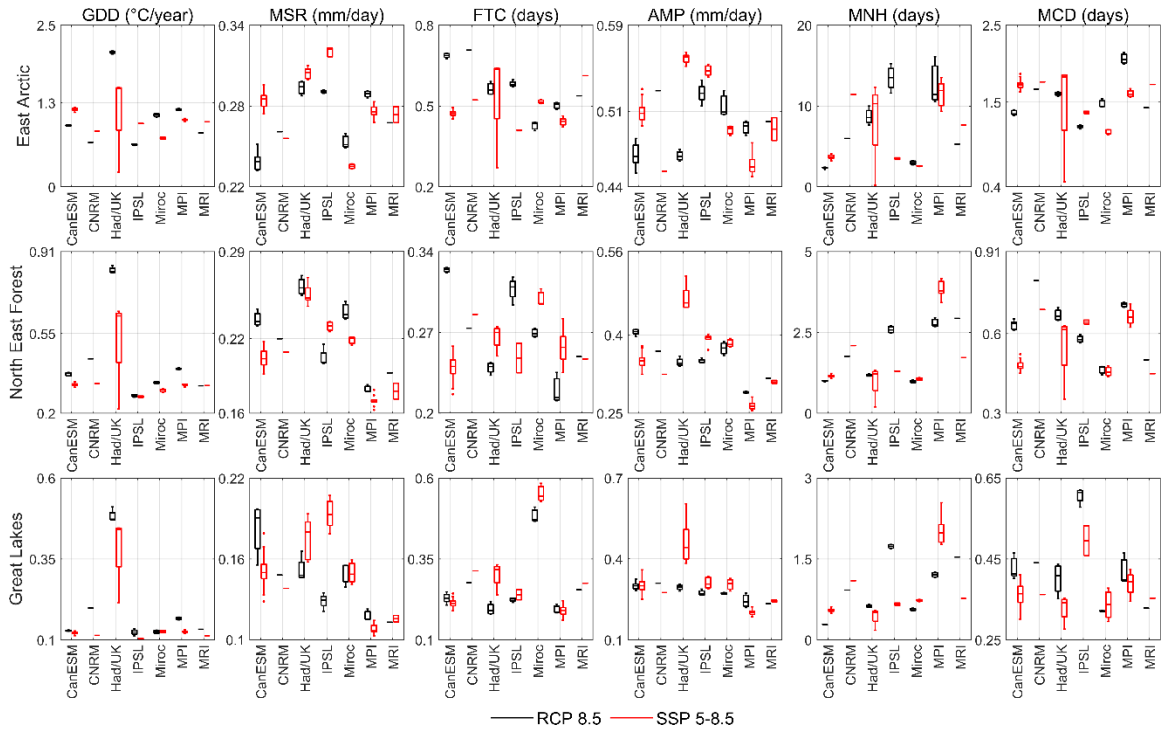

Figure A24 Long-term annual CV values of six climate indices, estimated by simulations of CMIP5 under RCP 8.5 (black boxplots), and CMIP6 under SSP 5-8.5 (red boxplots), in the East Arctic, North East Forest and Great Lakes during 2021-2050.

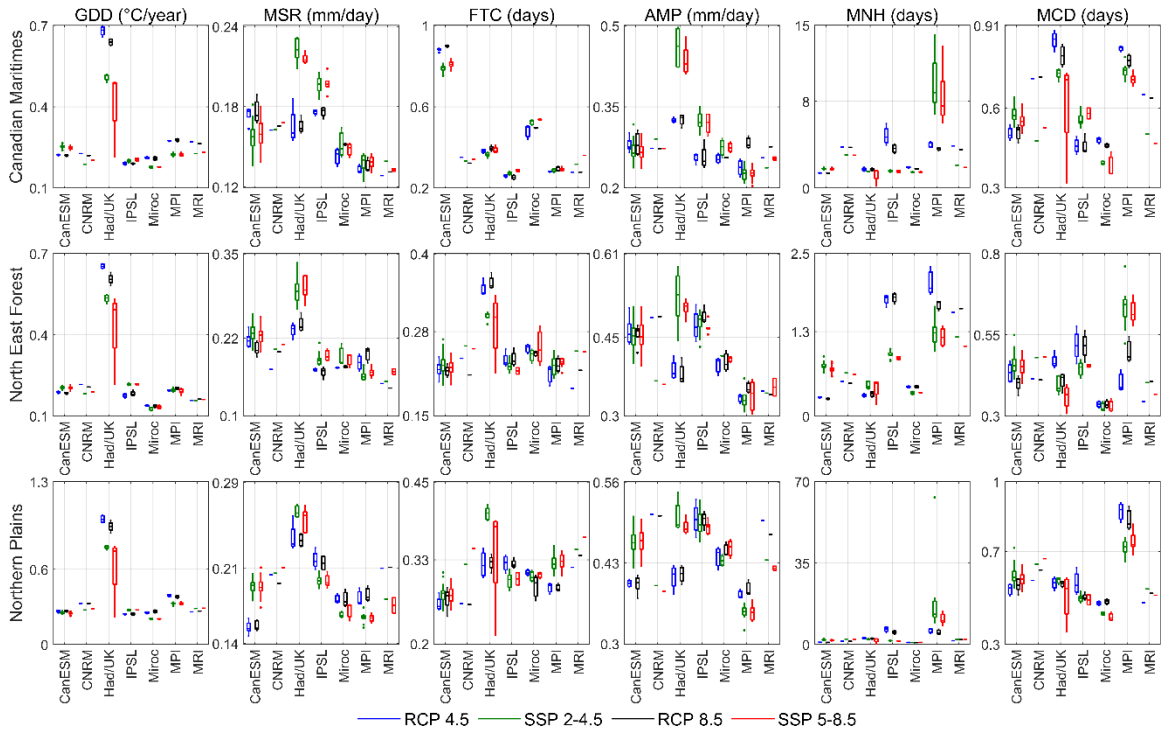

Figure A25 Long-term annual CV values of six climate indices, estimated by simulations of CMIP5 under RCPs 4.5 (blue boxplots) & 8.5 (black boxplots), and CMIP6 under SSPs 2-4.5 (green boxplots) & 5-8.5 (red boxplots), in the Canadian Maritimes, Northern Plains and Mackenzie Valley during 2021-2050.

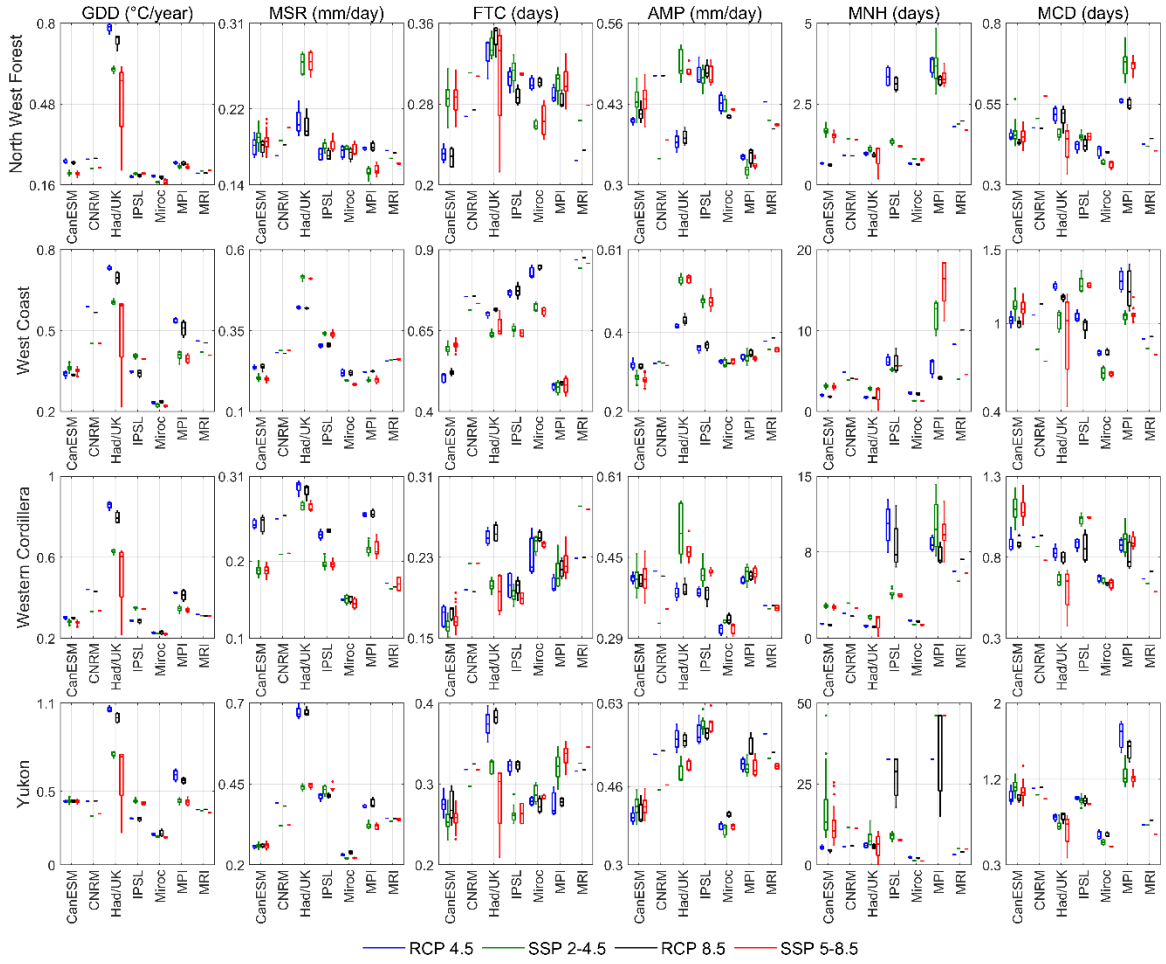

Figure A26 Long-term annual CV values of six climate indices, estimated by simulations of CMIP5 under RCPs 4.5 (blue boxplots) & 8.5 (black boxplots), and CMIP6 under SSPs 2-4.5 (green boxplots) & 5-8.5 (red boxplots), in the North West Forest, West Coast, Western Cordillera and Yukon during 2021-2050.

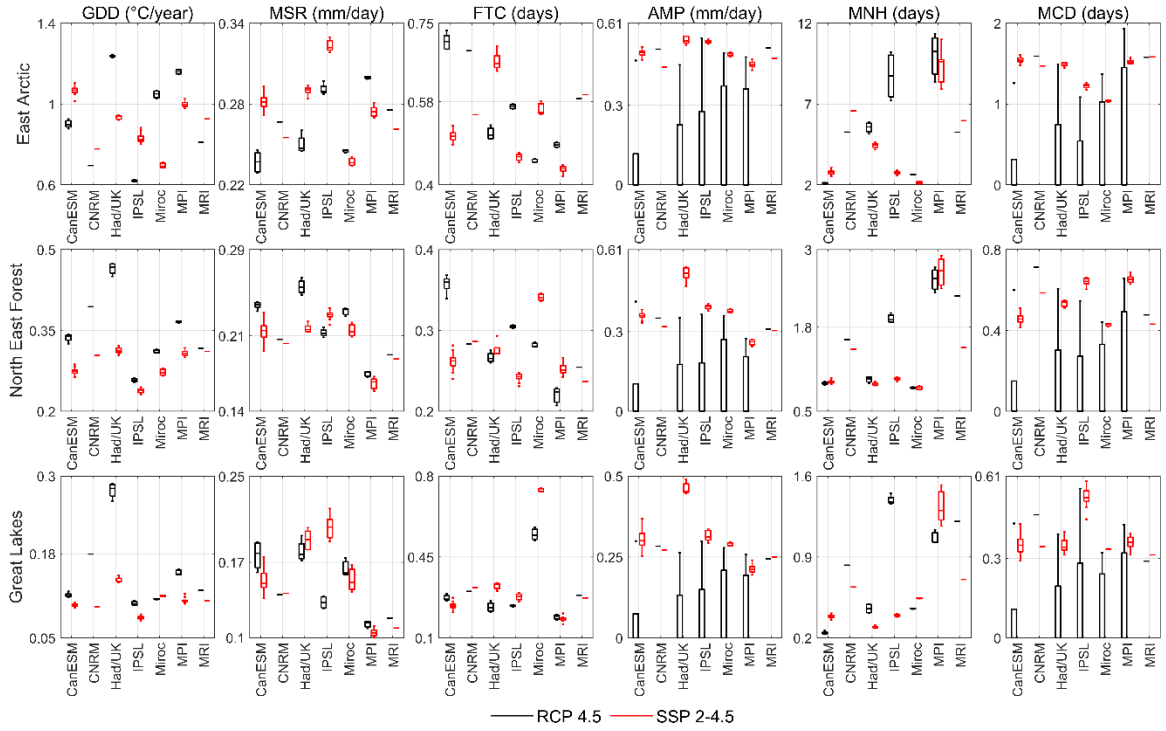

Figure A27 Long-term annual CV values of six climate indices, estimated by simulations of CMIP5 under RCP 4.5 (black boxplots), and CMIP6 under SSP 2-4.5 (red boxplots), in the East Arctic, North East Forest and Great Lakes during 2071-2100.

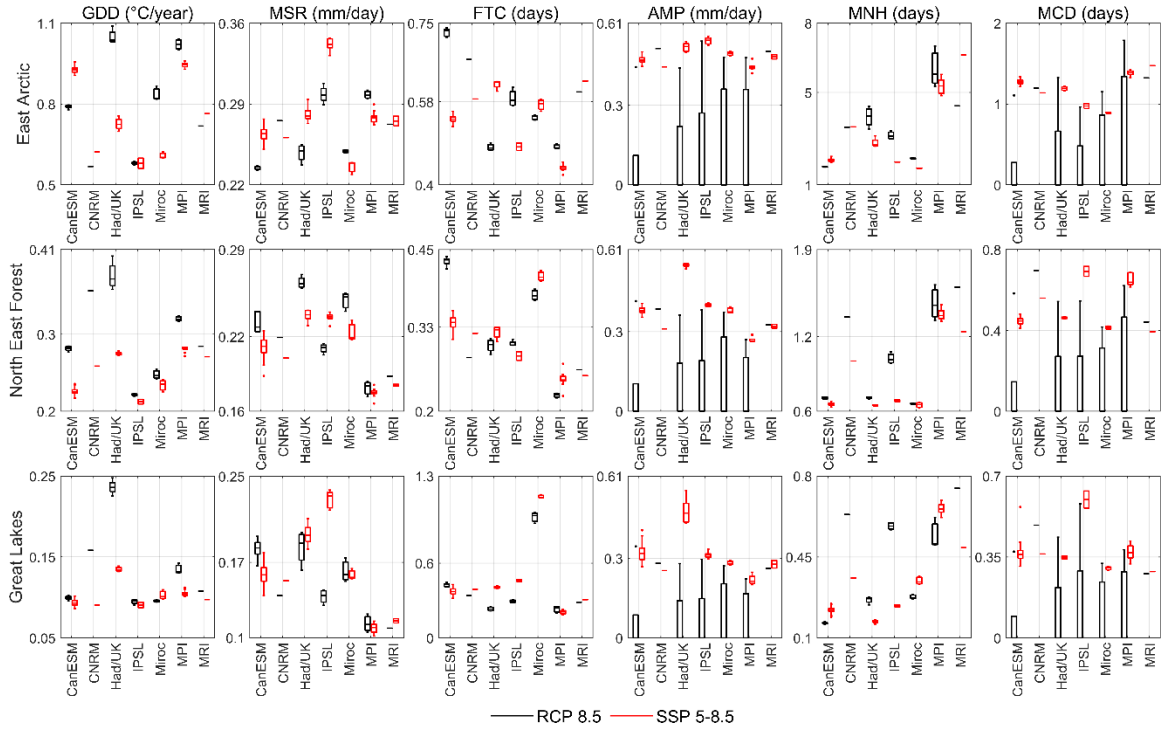

Figure A28 Long-term annual CV values of six climate indices, estimated by simulations of CMIP5 under RCP 8.5 (black boxplots), and CMIP6 models under SSP 5-8.5 (red boxplots), in the East Arctic, North East Forest and Great Lakes during 2071-2100.

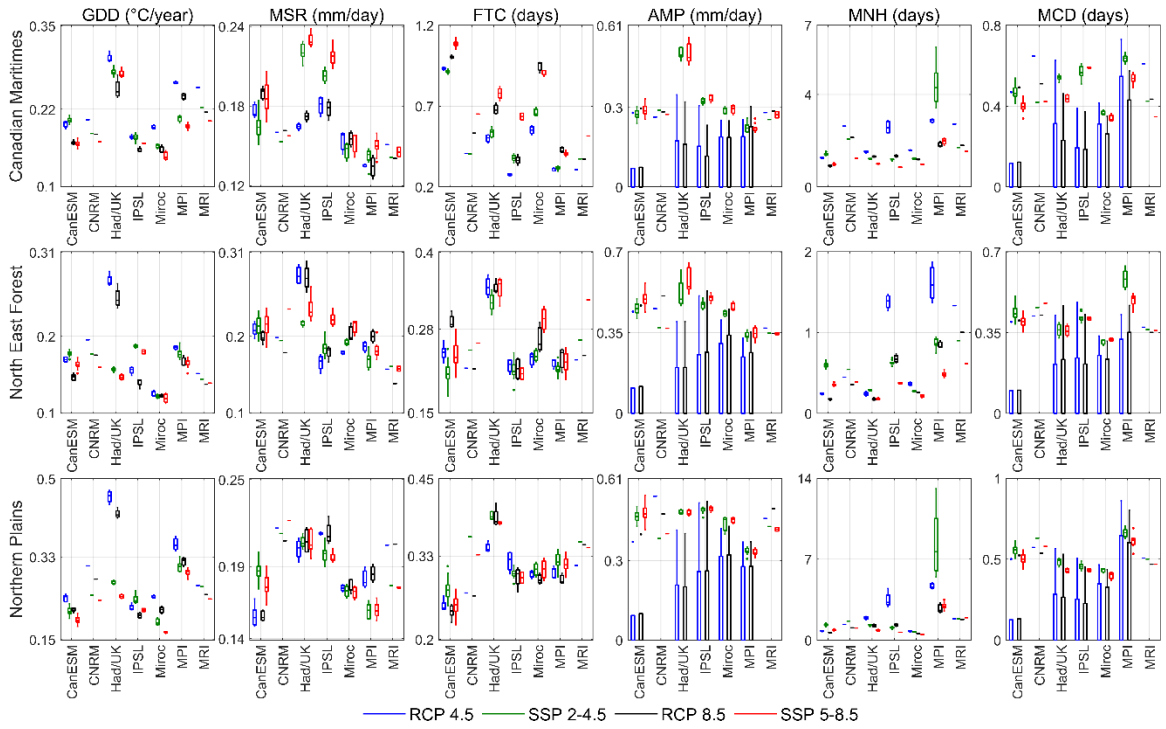

Figure A29 Long-term annual CV values of six climate indices, estimated by simulations of CMIP5 under RCPs 4.5 (blue boxplots) & 8.5 (black boxplots), and CMIP6 under SSPs 2-4.5 (green boxplots) & 5-8.5 (red boxplots), in the Canadian Maritimes and Northern Plains and Mackenzie Valley during 2071-2100.

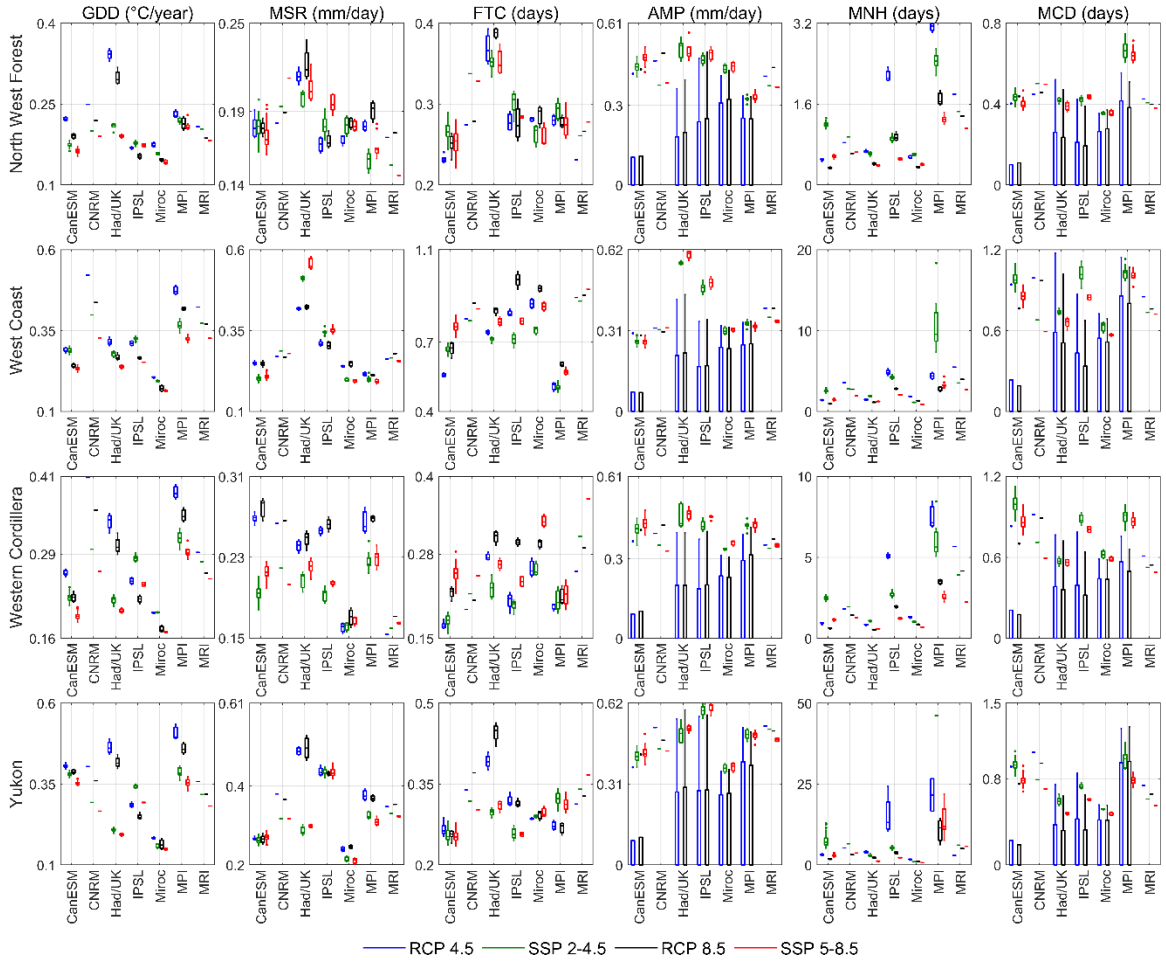

Figure A30 Long-term annual CV values of six climate indices, estimated by simulations of CMIP5 under RCPs 4.5 (blue boxplots) & 8.5 (black boxplots), and CMIP6 under SSP 2-4.5 (green boxplots) & 5-8.5 (red boxplots), in the North West Forest, West Coast, Western Cordillera and Yukon during 2071-2100.

APPENDIX B SUPPLEMENTARY MATERIAL OF CHAPTER 5

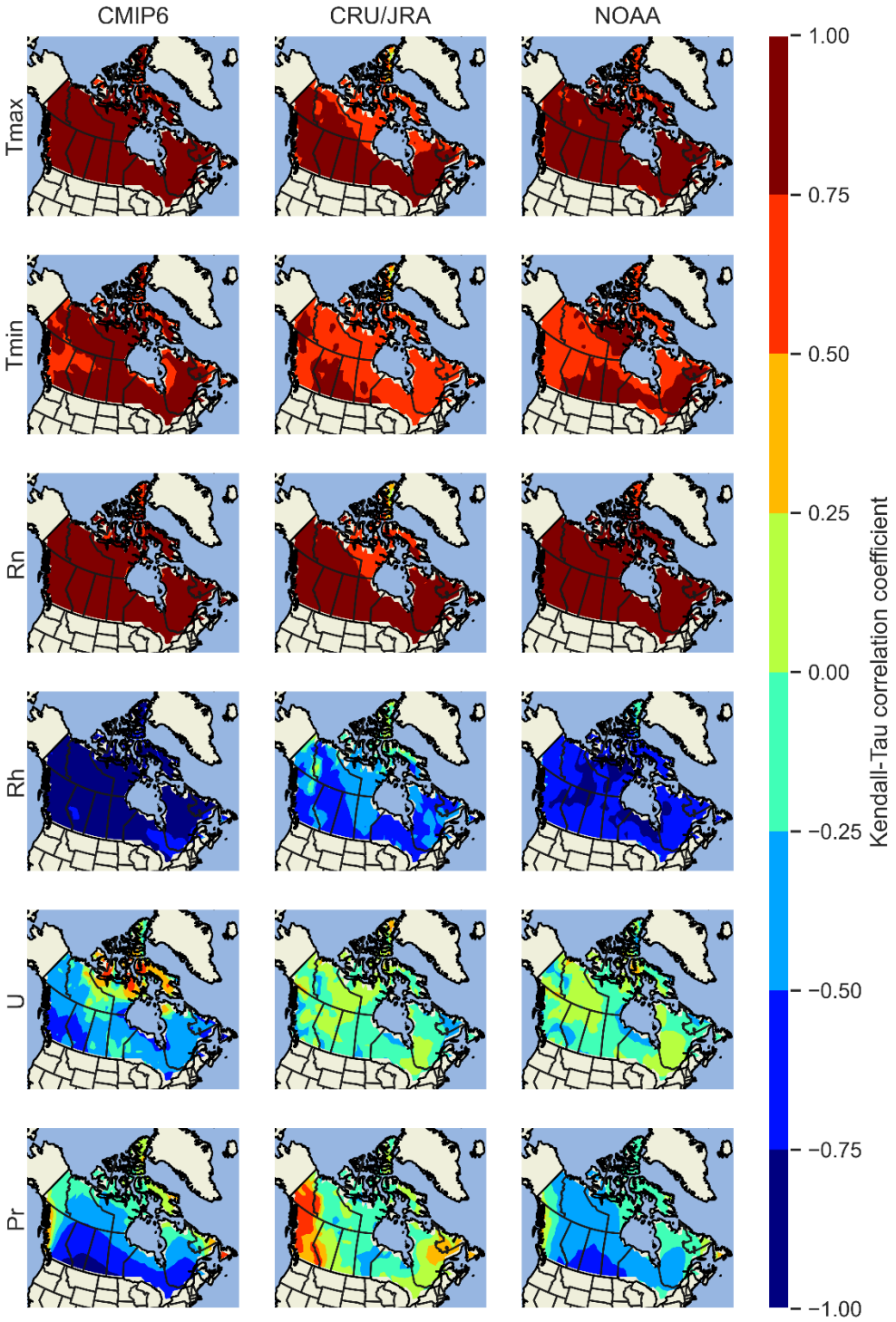

Figure B1 Kendall-Tau coefficient evaluating correlation between climatic variables and Penman-Monteith PET estimates with raw CMIP6, CRU/JRA and NOAA.

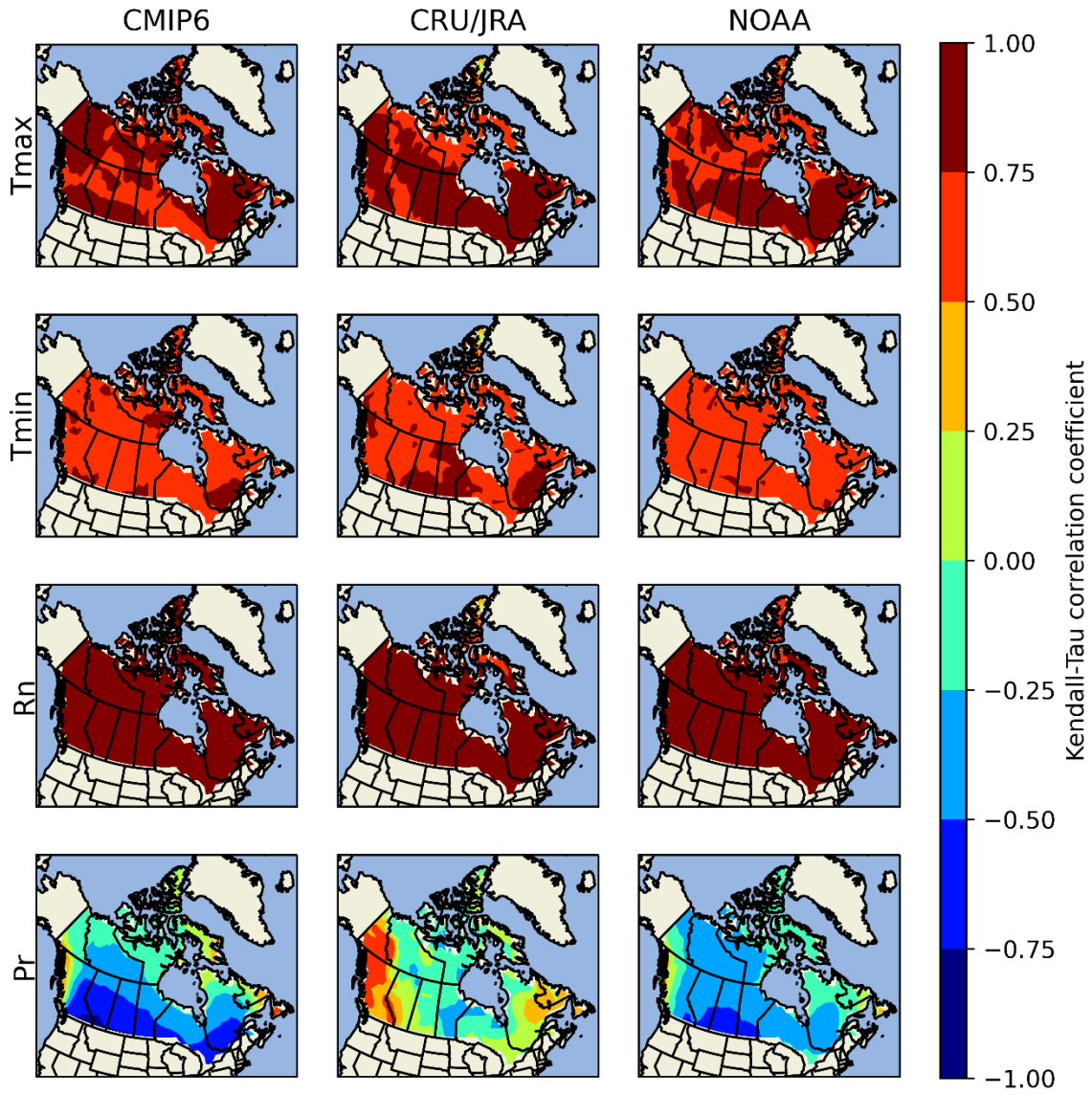

Figure B2 Kendall-Tau coefficient evaluating correlation between climatic variables and Priestley-Taylor PET estimates with raw CMIP6, CRU/JRA and NOAA.

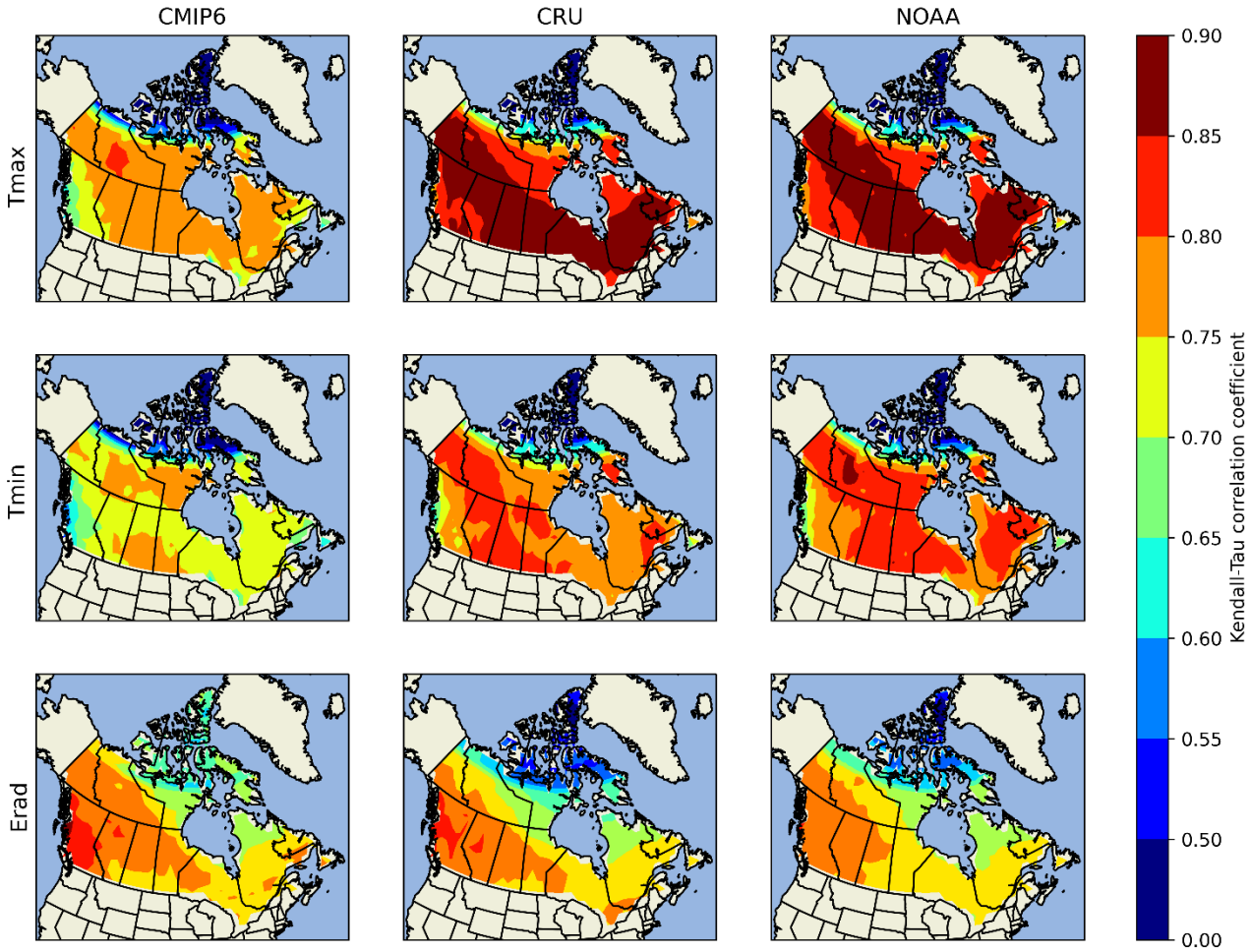

Figure B3 Kendall-Tau coefficient evaluating correlation between climatic variables and Hargreaves PET estimates with raw CMIP6, CRU/JRA and NOAA.

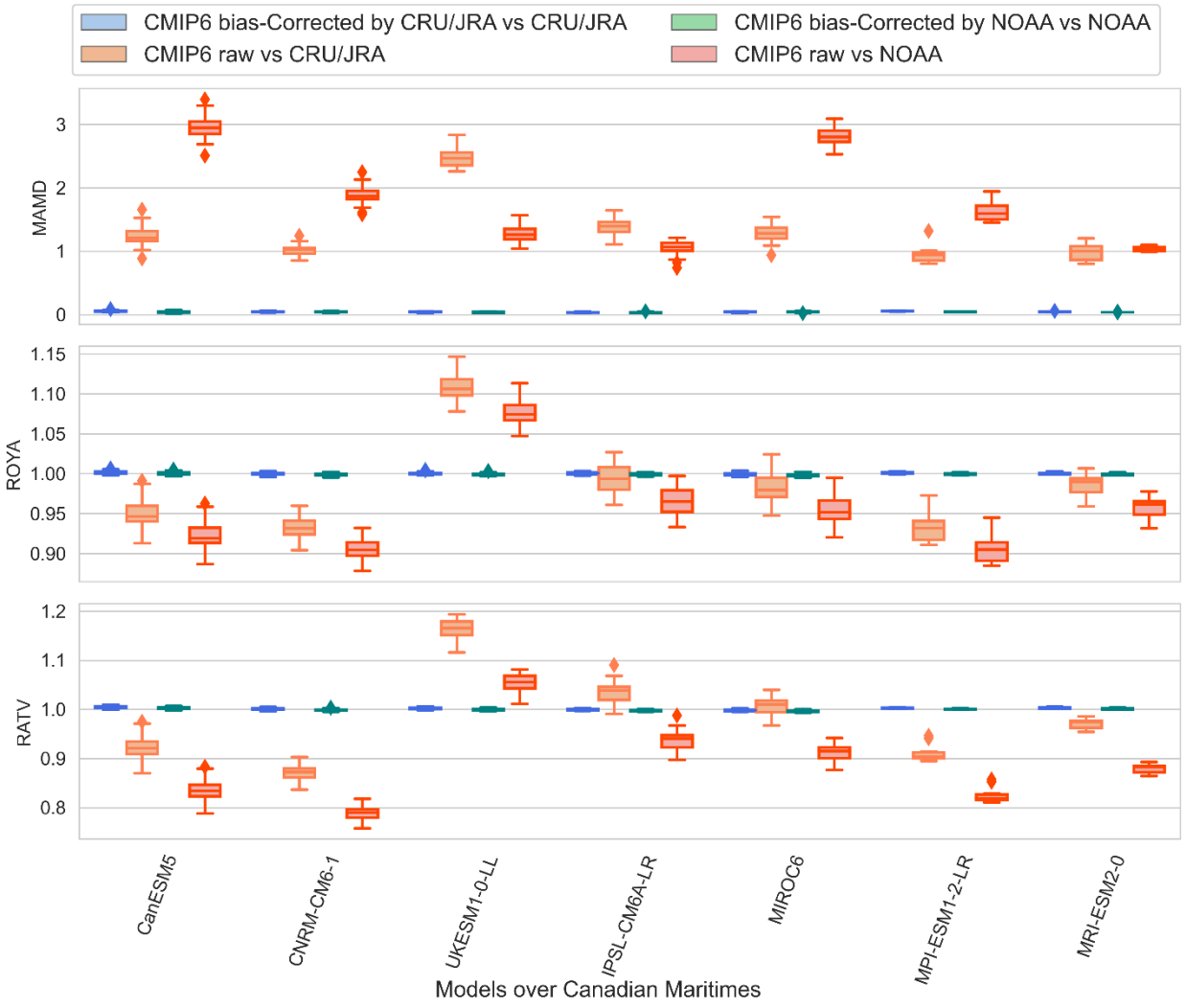

Figure B4 Monthly performance measures of Tmax bias-corrected and raw CMIP6 simulations compared to their respective benchmark (CRU/JRA and NOAA) over Canadian Maritimes during 1961-1990.

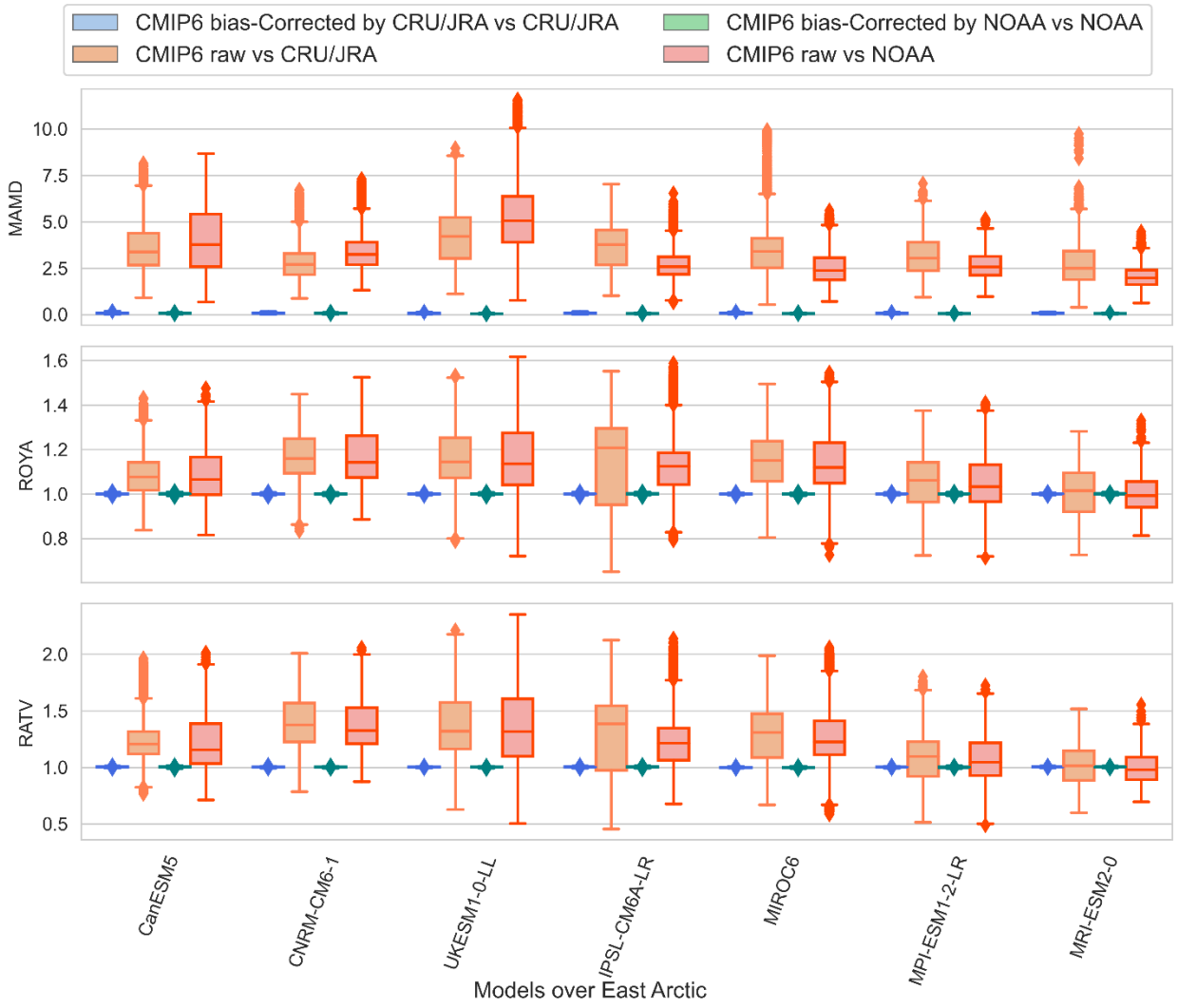

Figure B5 Monthly performance measures of Tmax bias-corrected and raw CMIP6 simulations compared to their respective benchmark (CRU/JRA and NOAA) over East Arctic during 1961-1990.

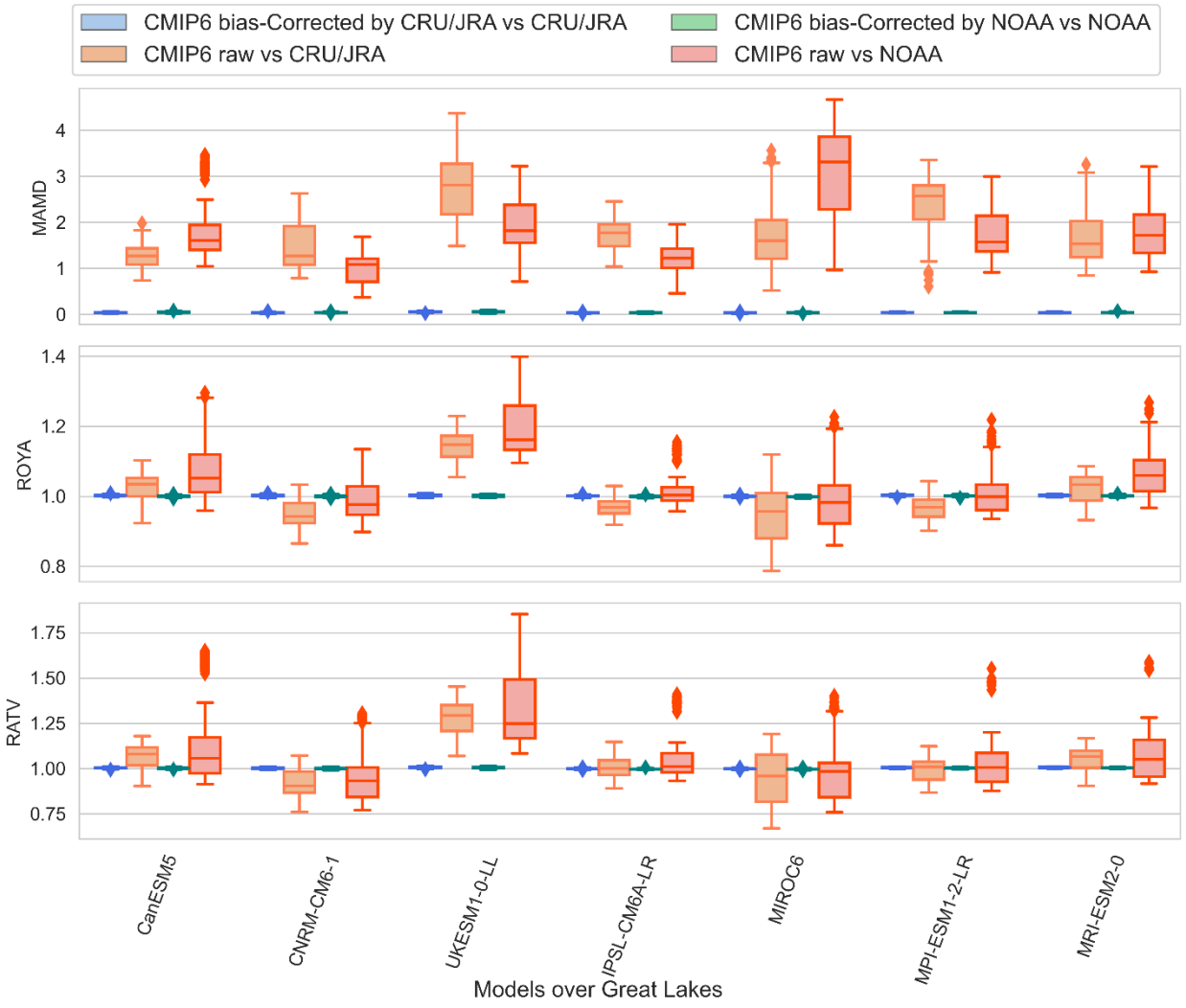

Figure B6 Monthly performance measures of Tmax bias-corrected and raw CMIP6 simulations compared to their respective benchmark (CRU/JRA and NOAA) over Great Lakes during 1961-1990.

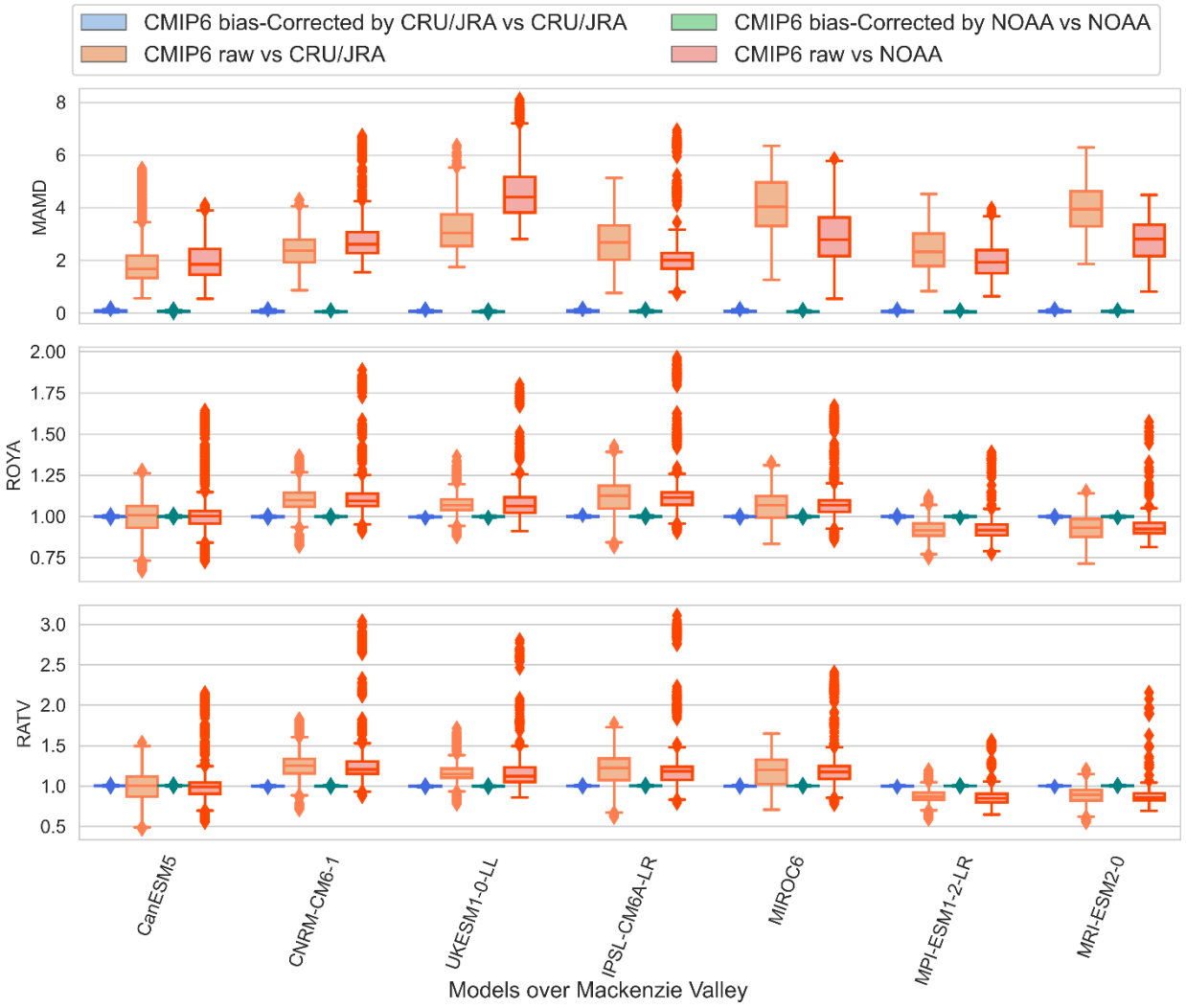

Figure B7 Monthly performance measures of Tmax bias-corrected and raw CMIP6 simulations compared to their respective benchmark (CRU/JRA and NOAA) over Mackenzie Valley during 1961-1990.

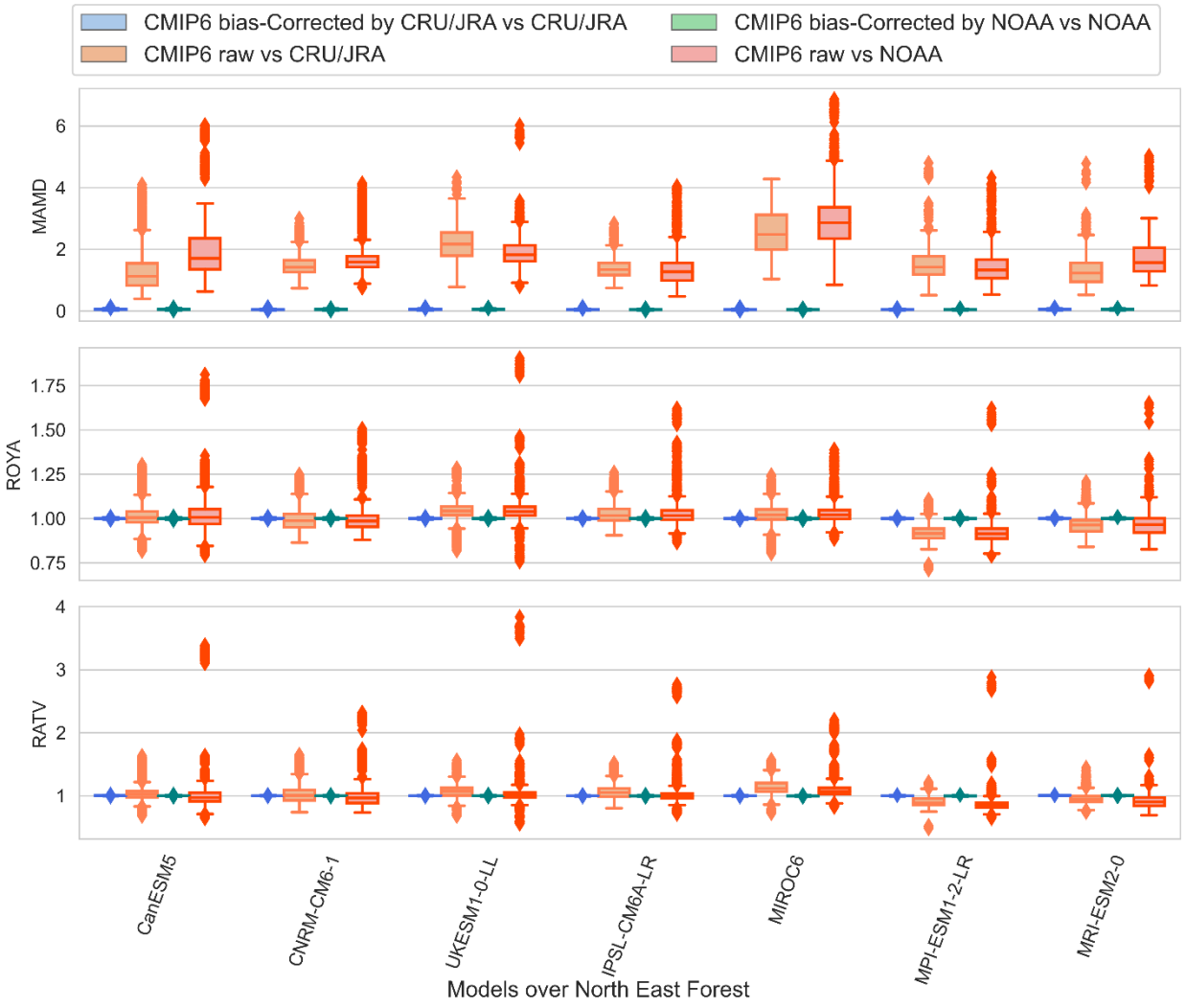

Figure B8 Monthly performance measures of Tmax bias-corrected and raw CMIP6 simulations compared to their respective benchmark (CRU/JRA and NOAA) over North East Forest during 1961-1990.

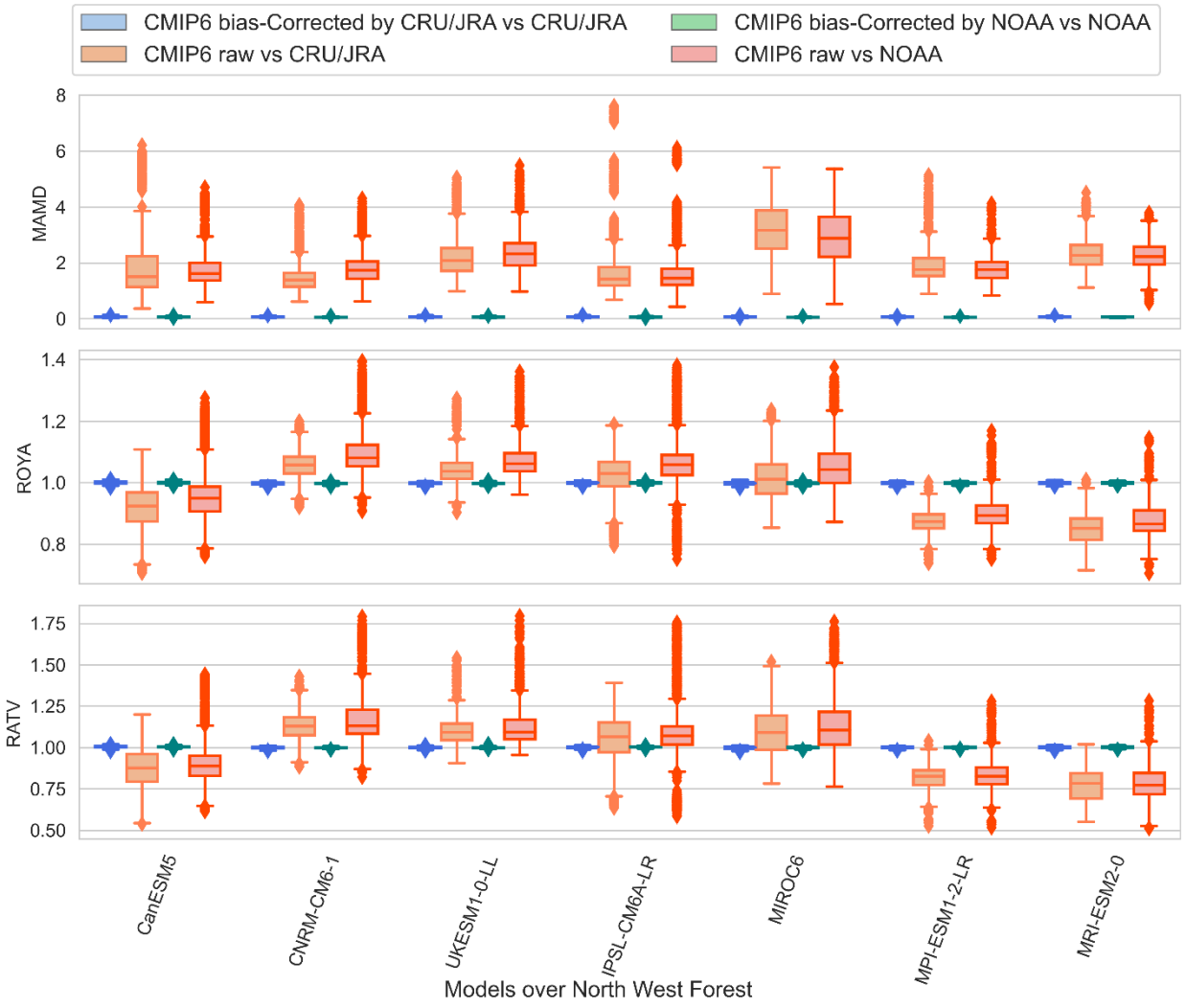

Figure B9 Monthly performance measures of Tmax bias-corrected and raw CMIP6 simulations compared to their respective benchmark (CRU/JRA and NOAA) over North West Forest during 1961-1990.

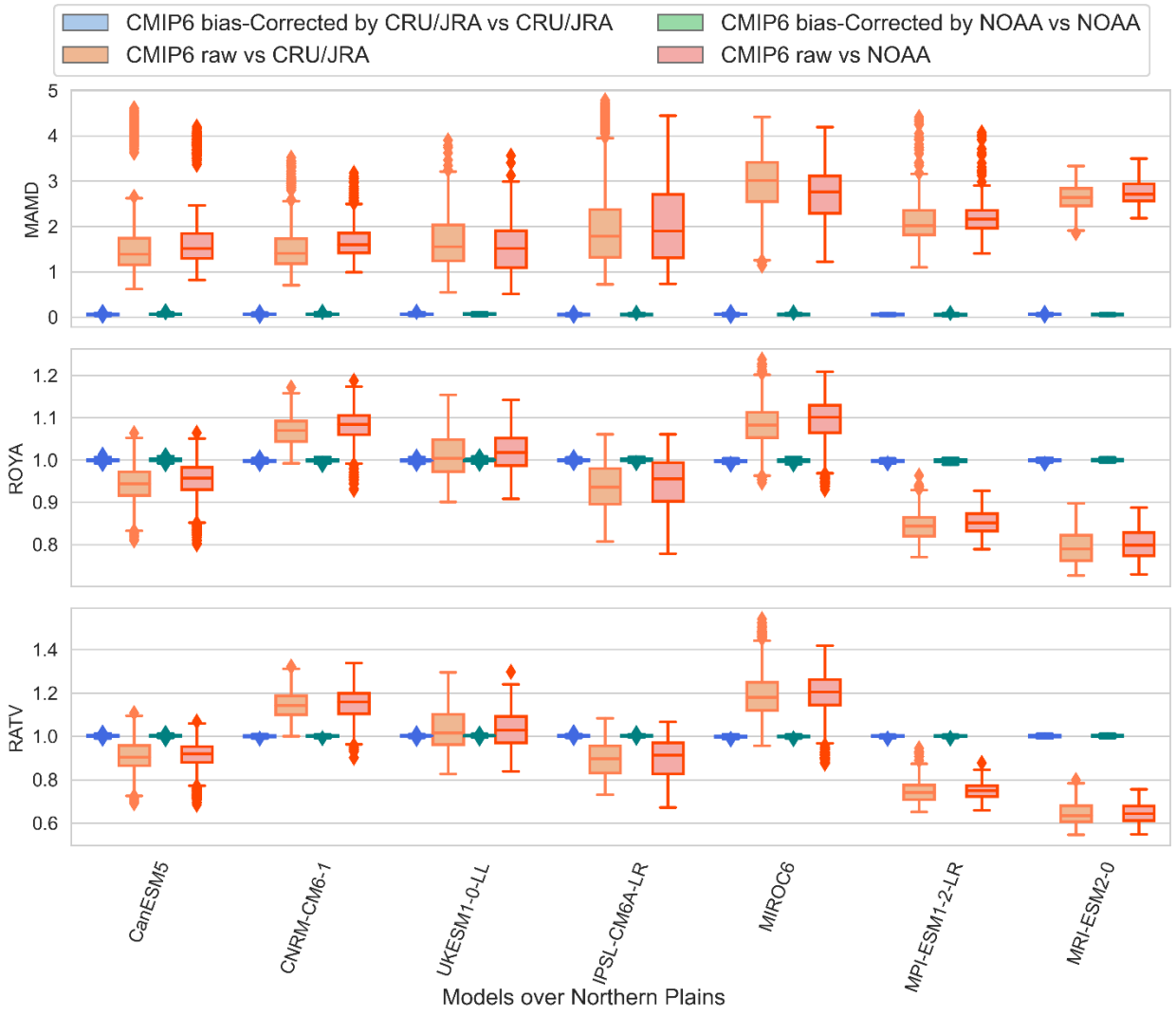

Figure B10 Monthly performance measures of Tmax bias-corrected and raw CMIP6 simulations compared to their respective benchmark (CRU/JRA and NOAA) over North West Forest during 1961-1990.

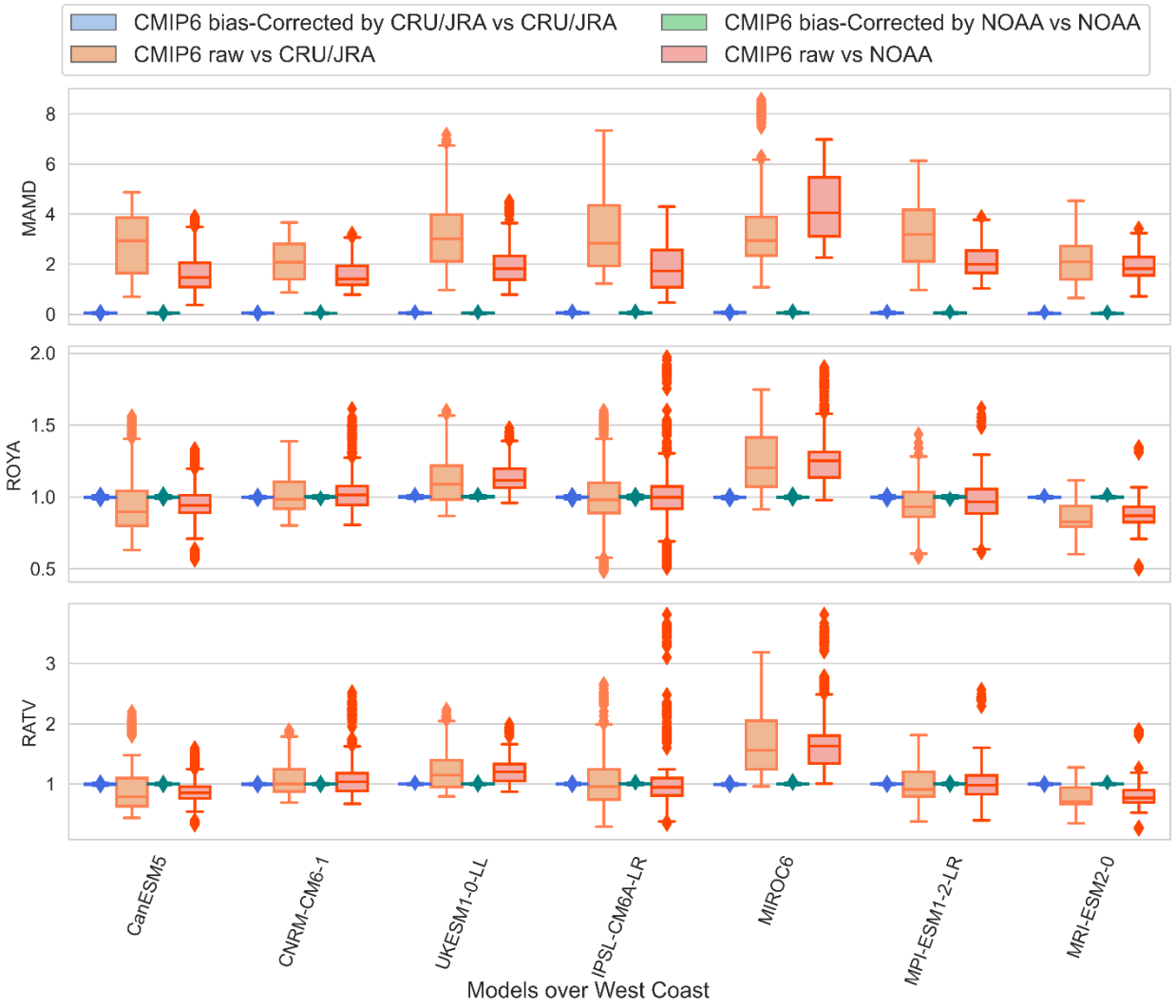

Figure B11 Monthly performance measures of Tmax bias-corrected and raw CMIP6 simulations compared to their respective benchmark (CRU/JRA and NOAA) over West Coast during 1961-1990.

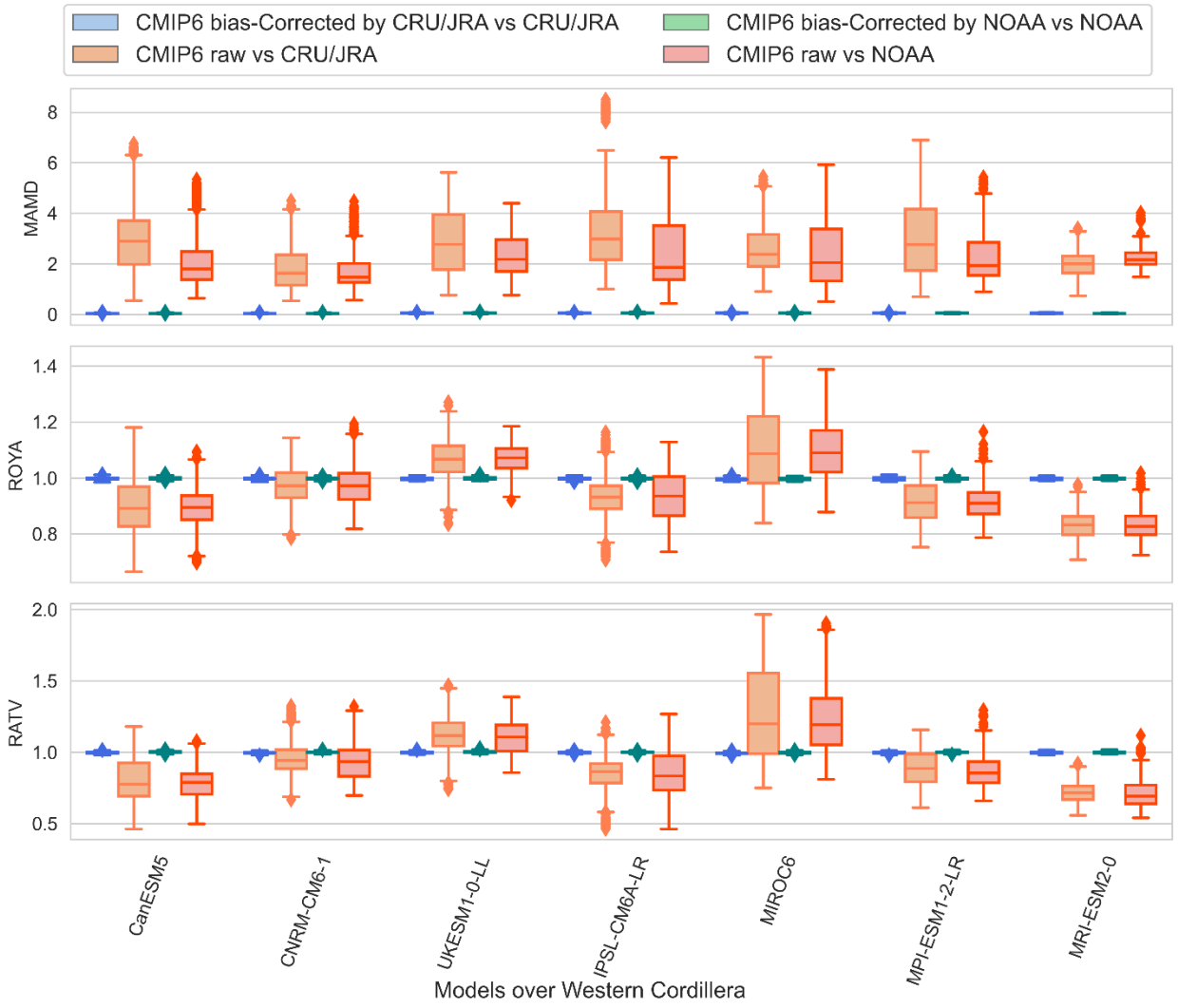

Figure B12 Monthly performance measures of Tmax bias-corrected and raw CMIP6 simulations compared to their respective benchmark (CRU/JRA and NOAA) over Western Cordillera during 1961-1990.

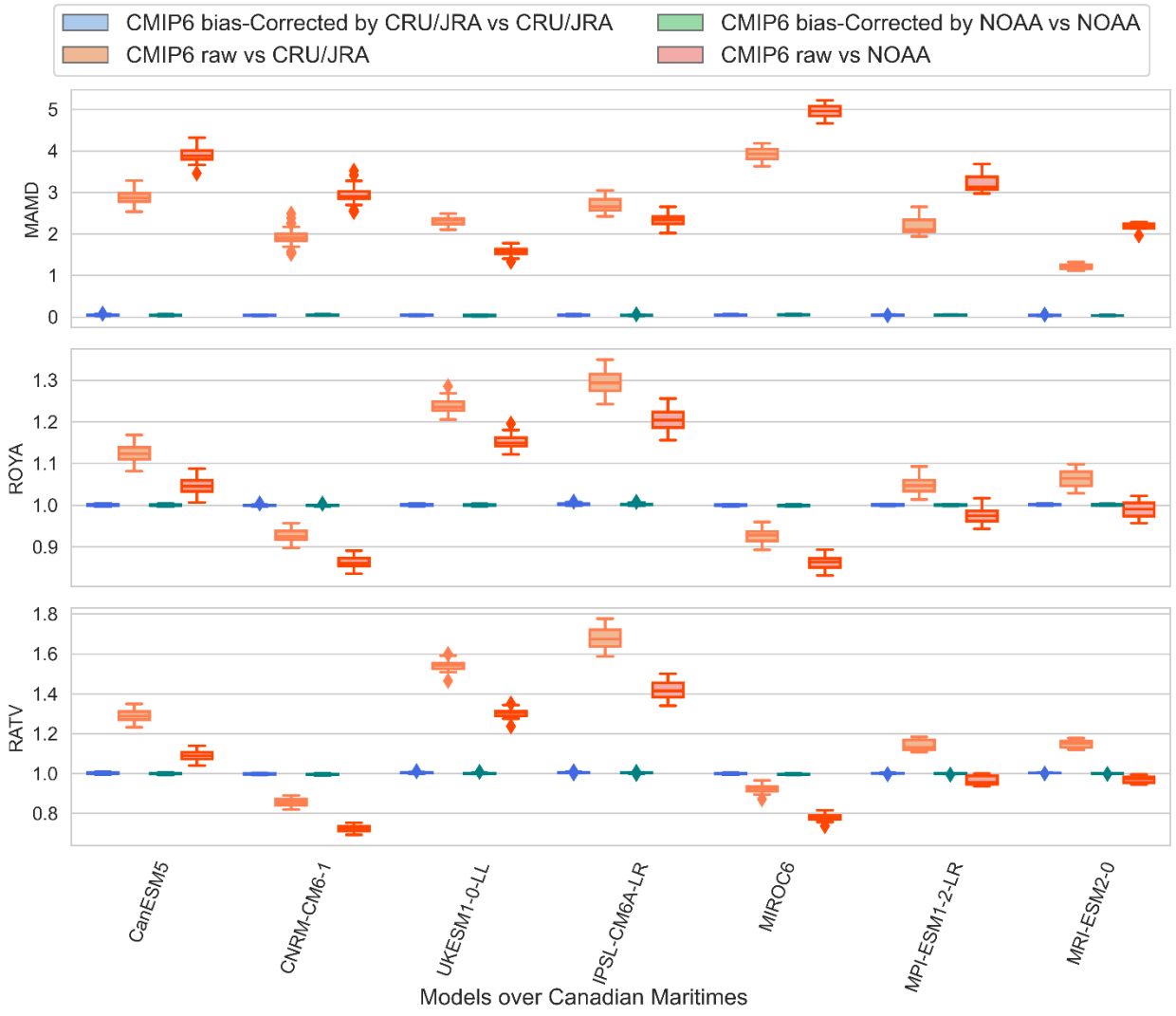

Figure B13 Monthly performance measures of Tmin bias-corrected and raw CMIP6 simulations compared to their respective benchmark (CRU/JRA and NOAA) over Canadian Maritimes during 1961-1990.

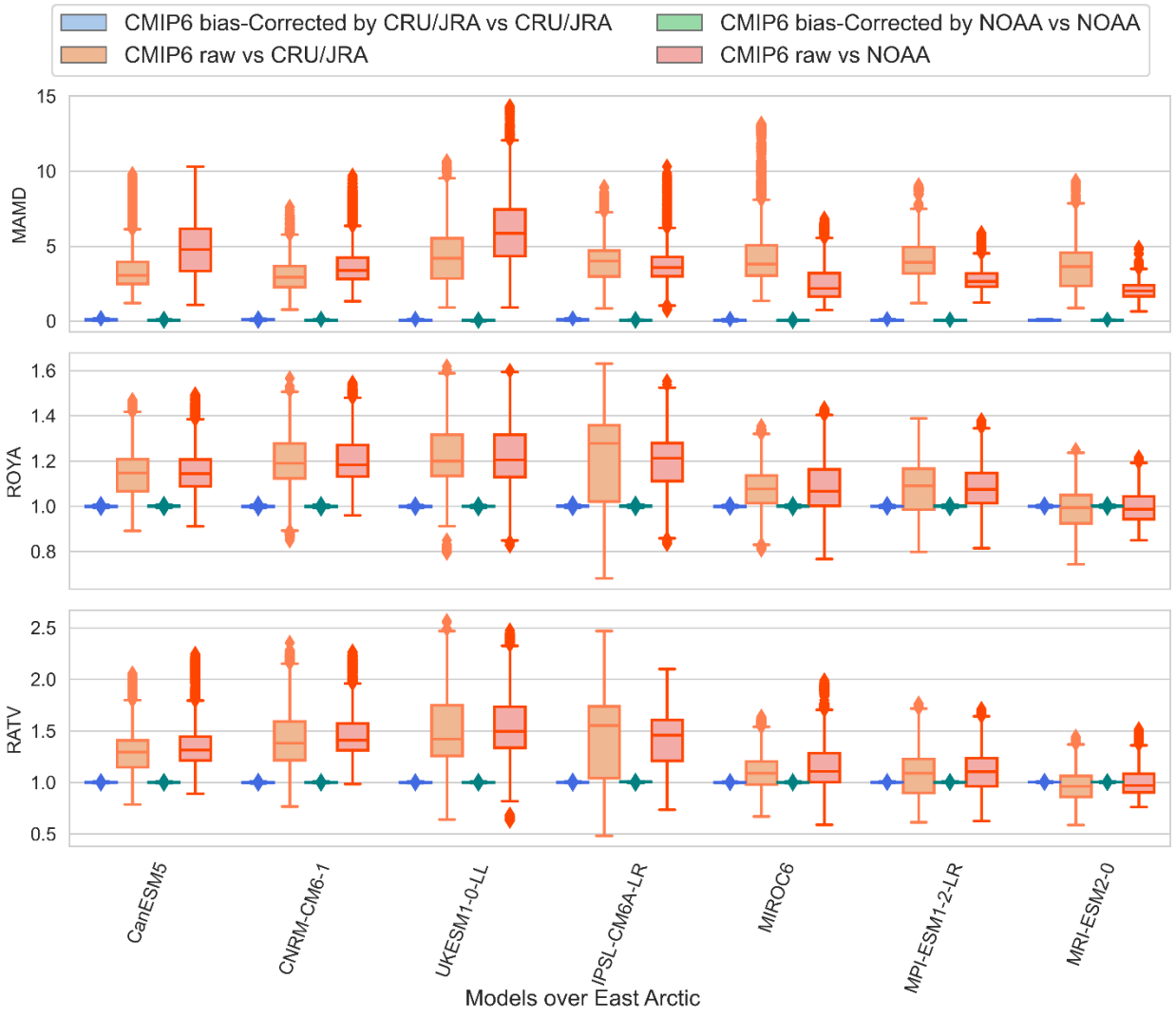

Figure B14 Monthly performance measures of Tmin bias-corrected and raw CMIP6 simulations compared to their respective benchmark (CRU/JRA and NOAA) over East Arctic during 1961-1990.

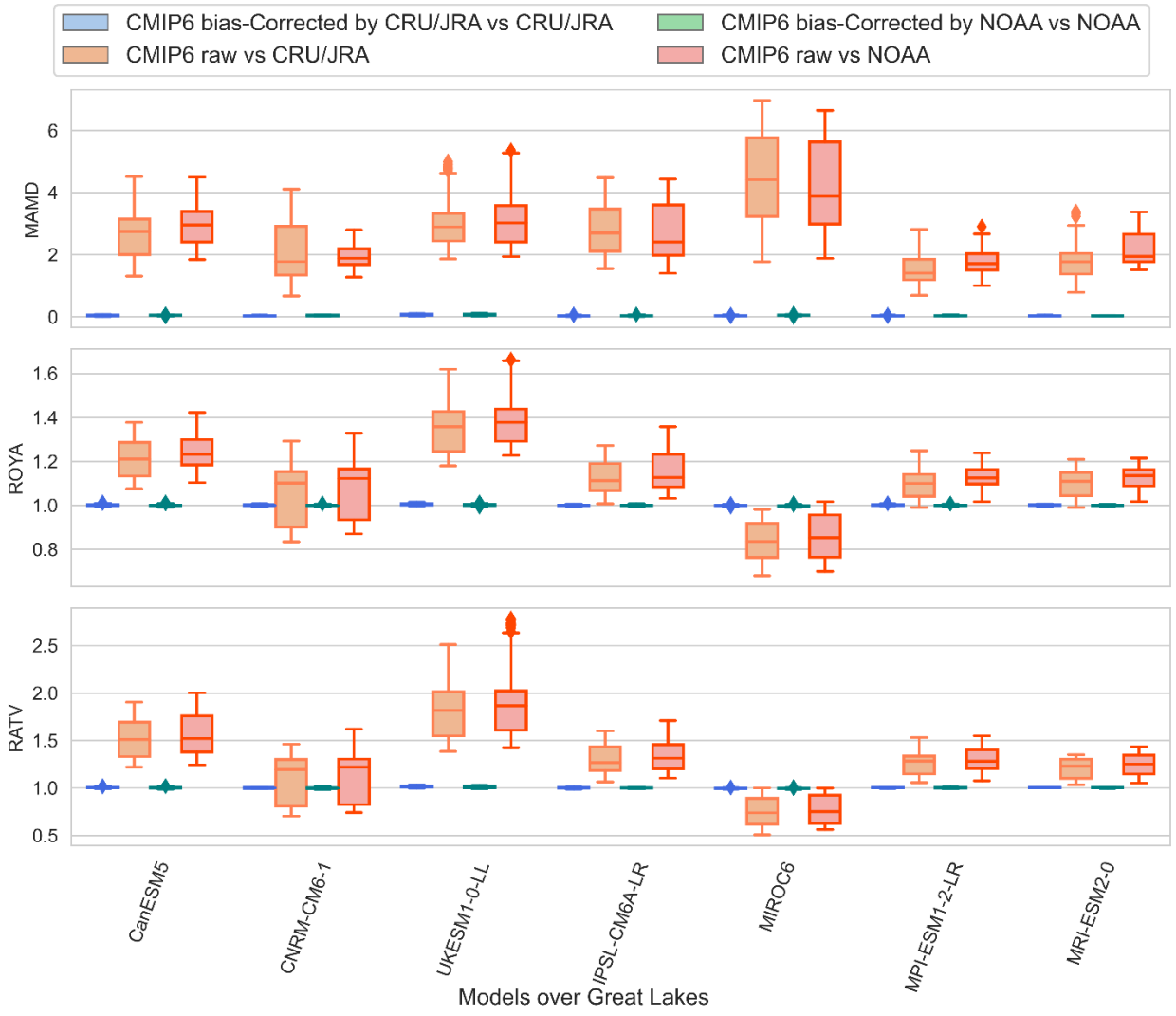

Figure B15 Monthly performance measures of Tmin bias-corrected and raw CMIP6 simulations compared to their respective benchmark (CRU/JRA and NOAA) over Great Lakes during 1961-1990.

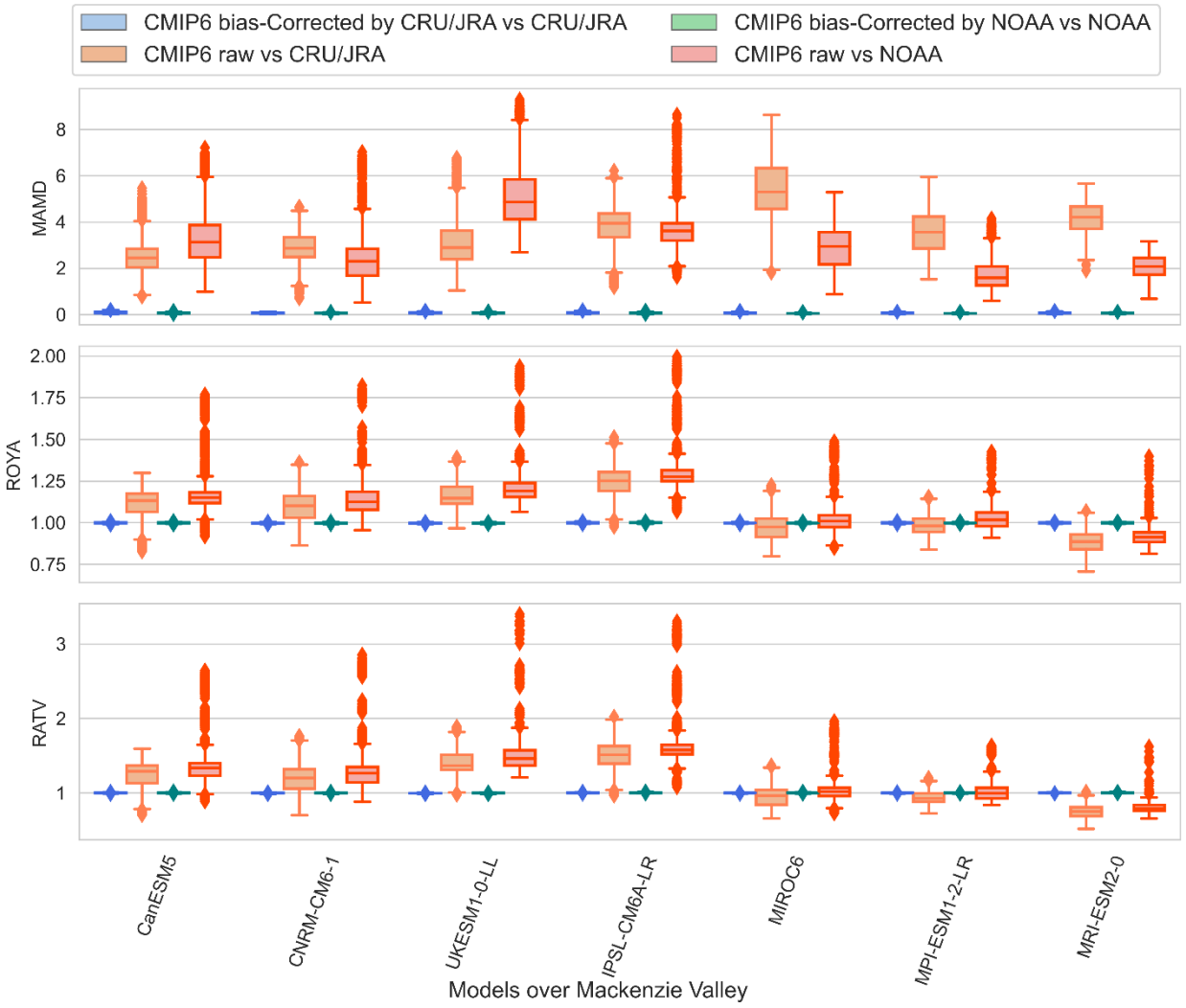

Figure B16 Monthly performance measures of Tmin bias-corrected and raw CMIP6 simulations compared to their respective benchmark (CRU/JRA and NOAA) over Mackenzie Valley during 1961-1990.

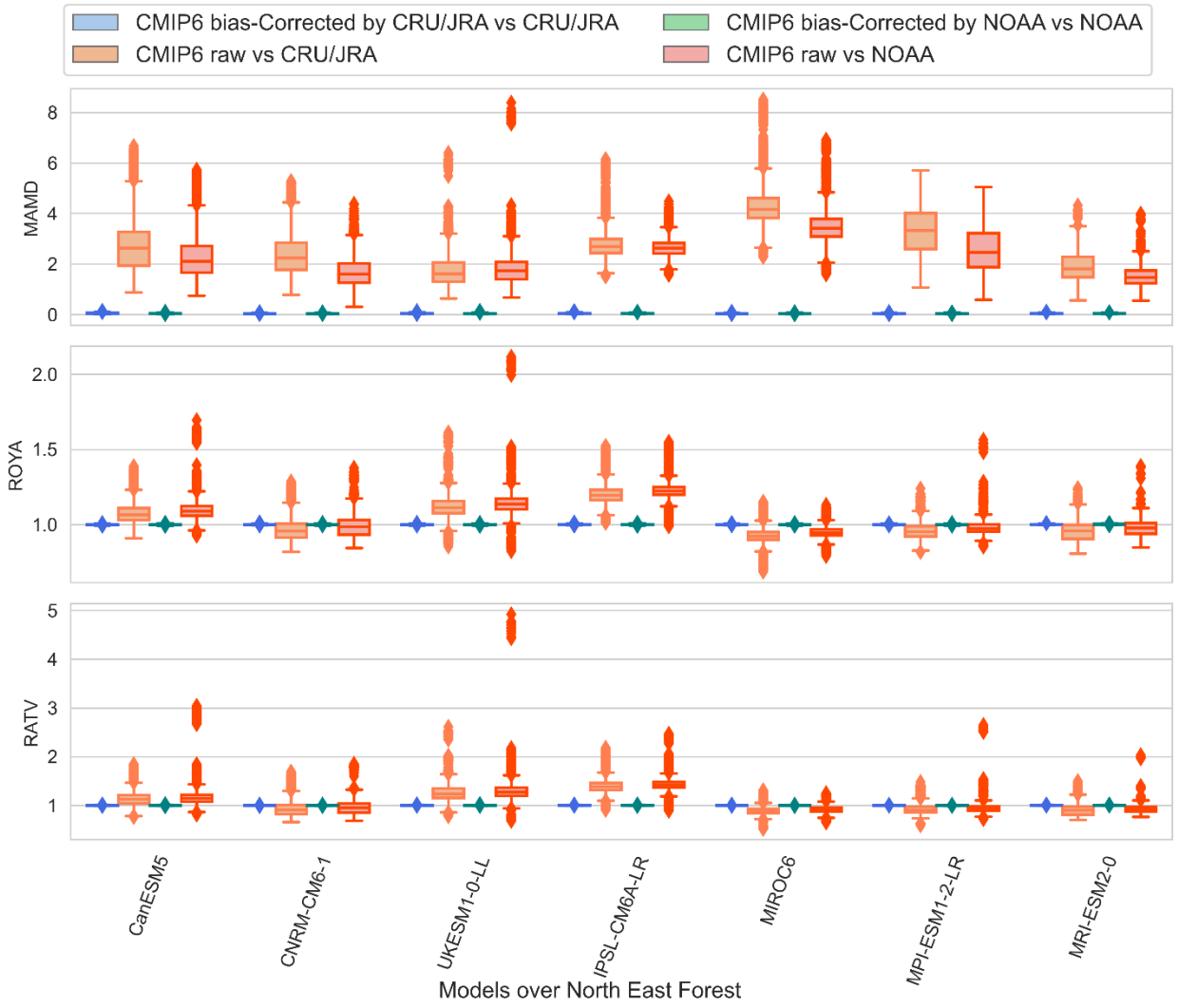

Figure B17 Monthly performance measures of Tmin bias-corrected and raw CMIP6 simulations compared to their respective benchmark (CRU/JRA and NOAA) over North East Forest during 1961-1990.

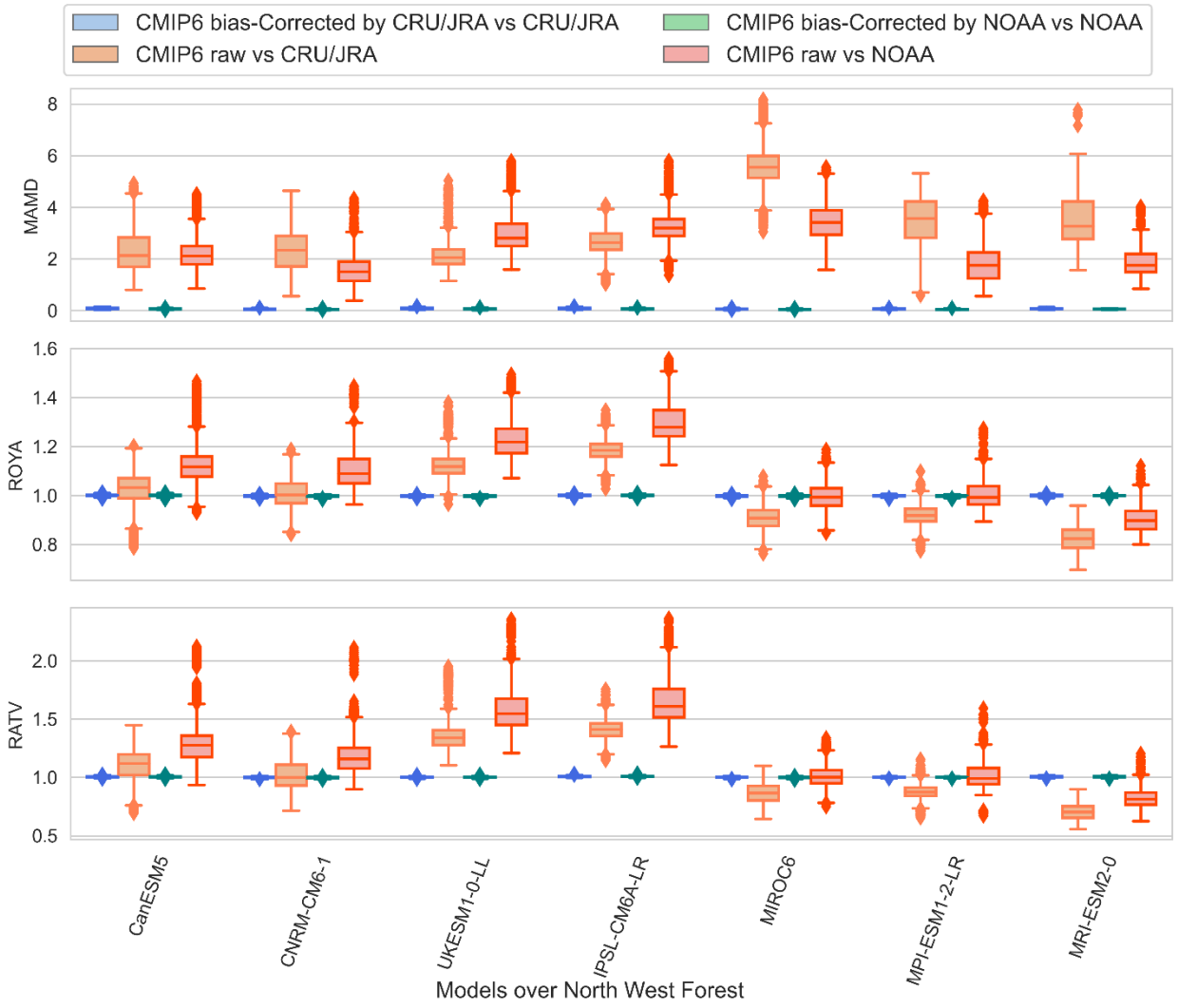

Figure B18 Monthly performance measures of Tmin bias-corrected and raw CMIP6 simulations compared to their respective benchmark (CRU/JRA and NOAA) over North West Forest during 1961-1990.

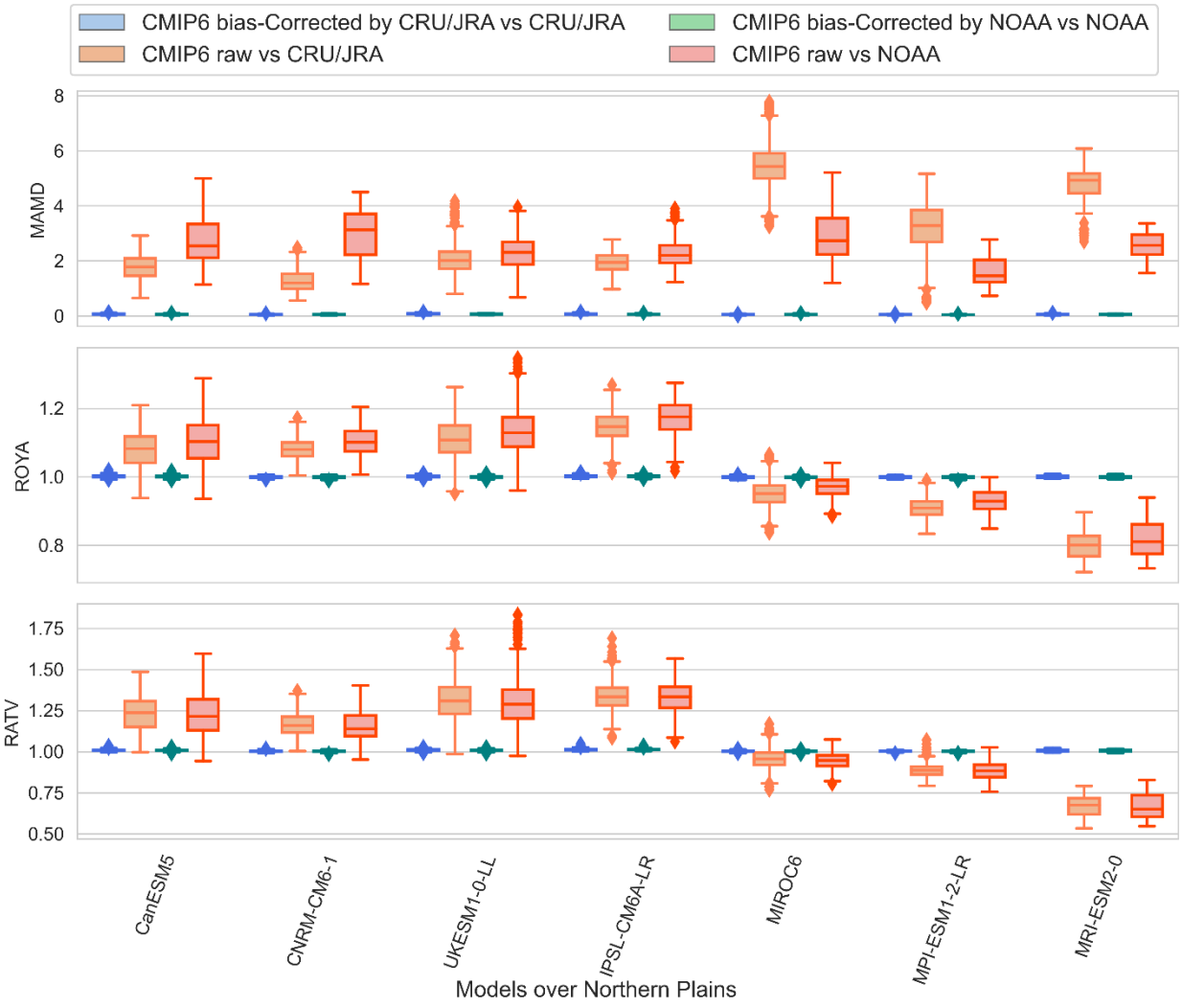

Figure B19 Monthly performance measures of Tmin bias-corrected and raw CMIP6 simulations compared to their respective benchmark (CRU/JRA and NOAA) over Northern Plains during 1961-1990.

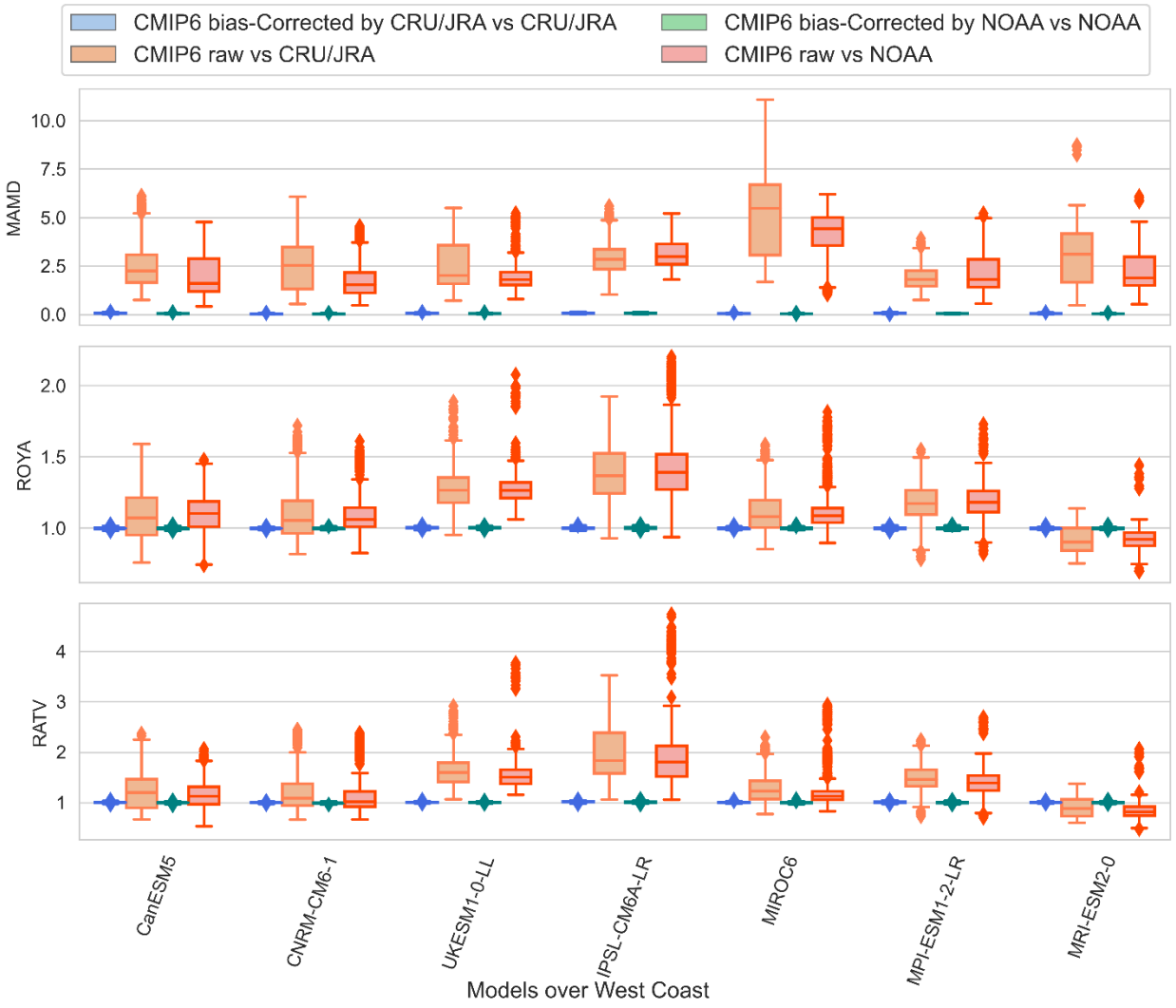

Figure B20 Monthly performance measures of Tmin bias-corrected and raw CMIP6 simulations compared to their respective benchmark (CRU/JRA and NOAA) over West Coast during 1961-1990.

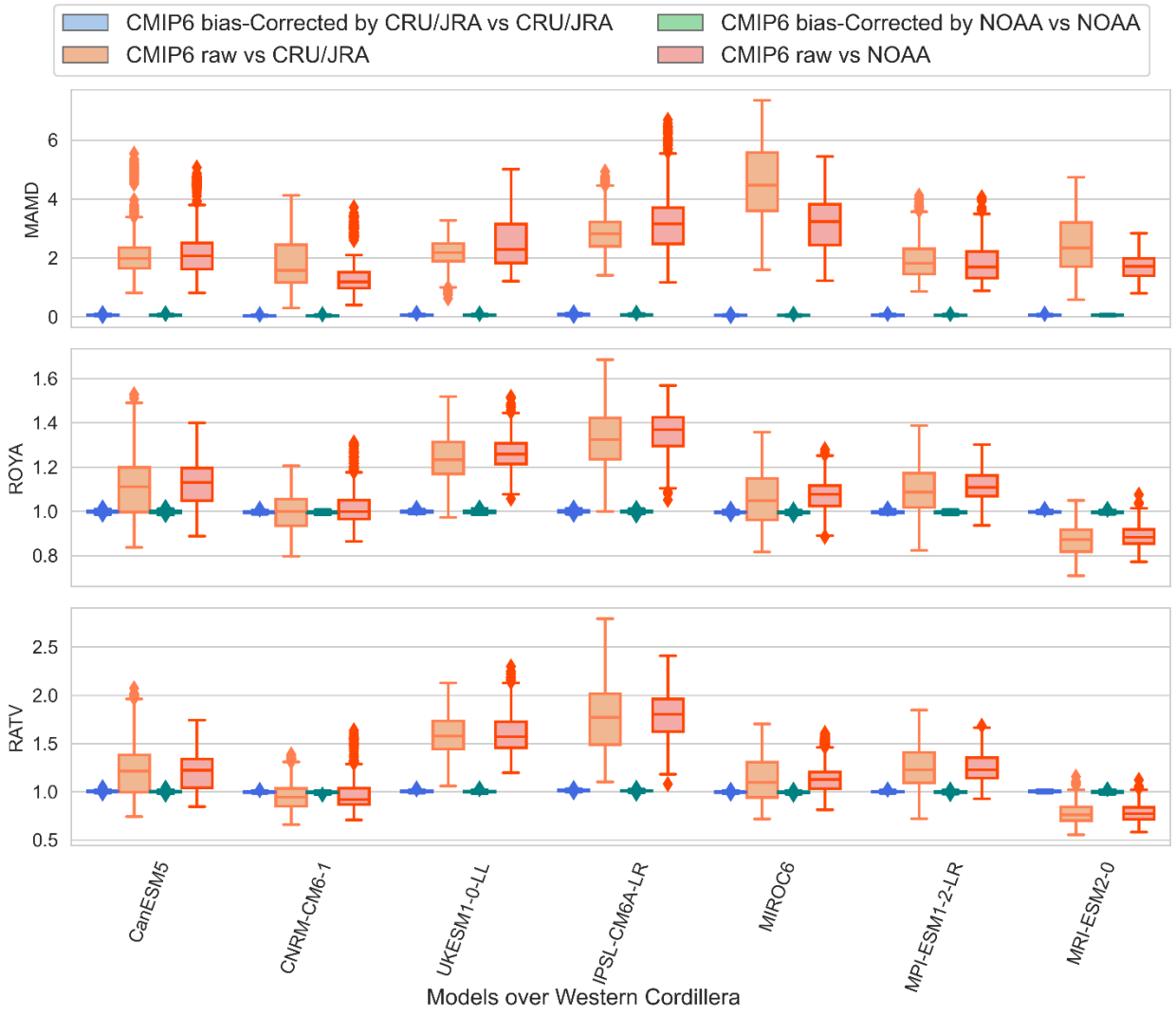

Figure B21 Monthly performance measures of Tmin bias-corrected and raw CMIP6 simulations compared to their respective benchmark (CRU/JRA and NOAA) over Western Cordillera during 1961-1990.

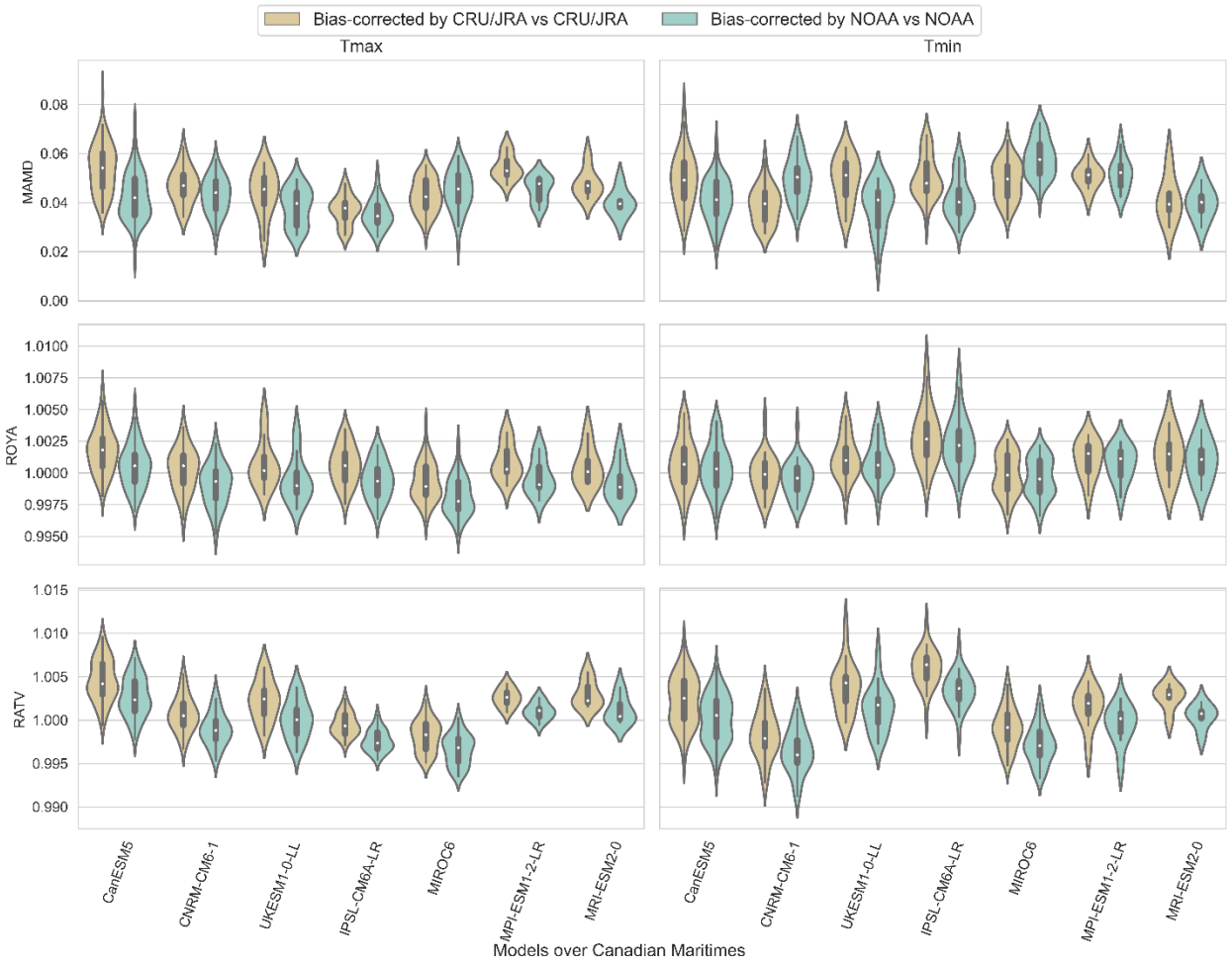

Figure B22 Monthly performance measures of Tmax and Tmin bias-corrected CMIP6 simulations compared to their respective benchmark (CRU/JRA and NOAA) over Canadian Maritimes during 1961-1990.

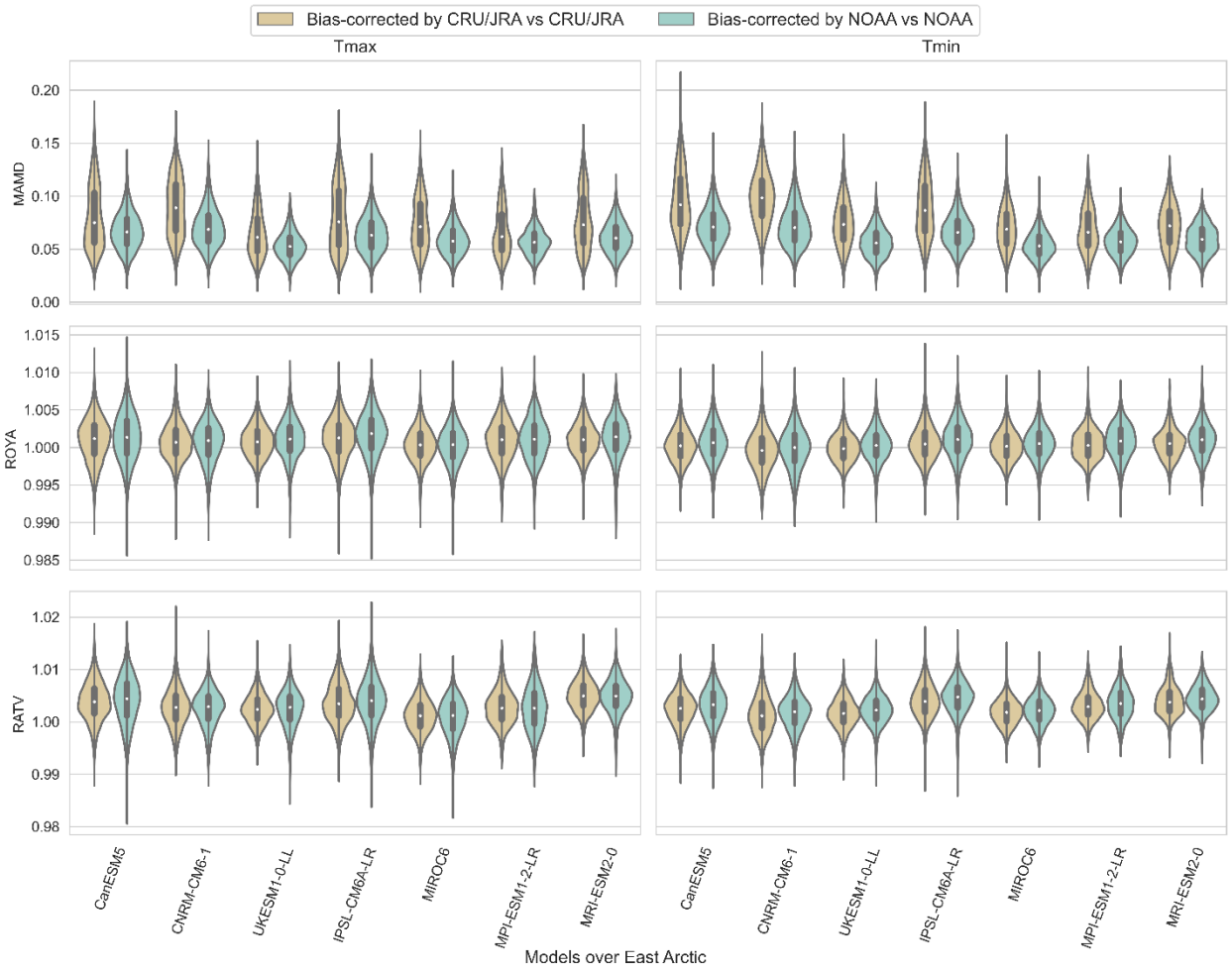

Figure B23 Monthly performance measures of Tmax and Tmin bias-corrected CMIP6 simulations compared to their respective benchmark (CRU/JRA and NOAA) over East Arctic during 1961-1990.

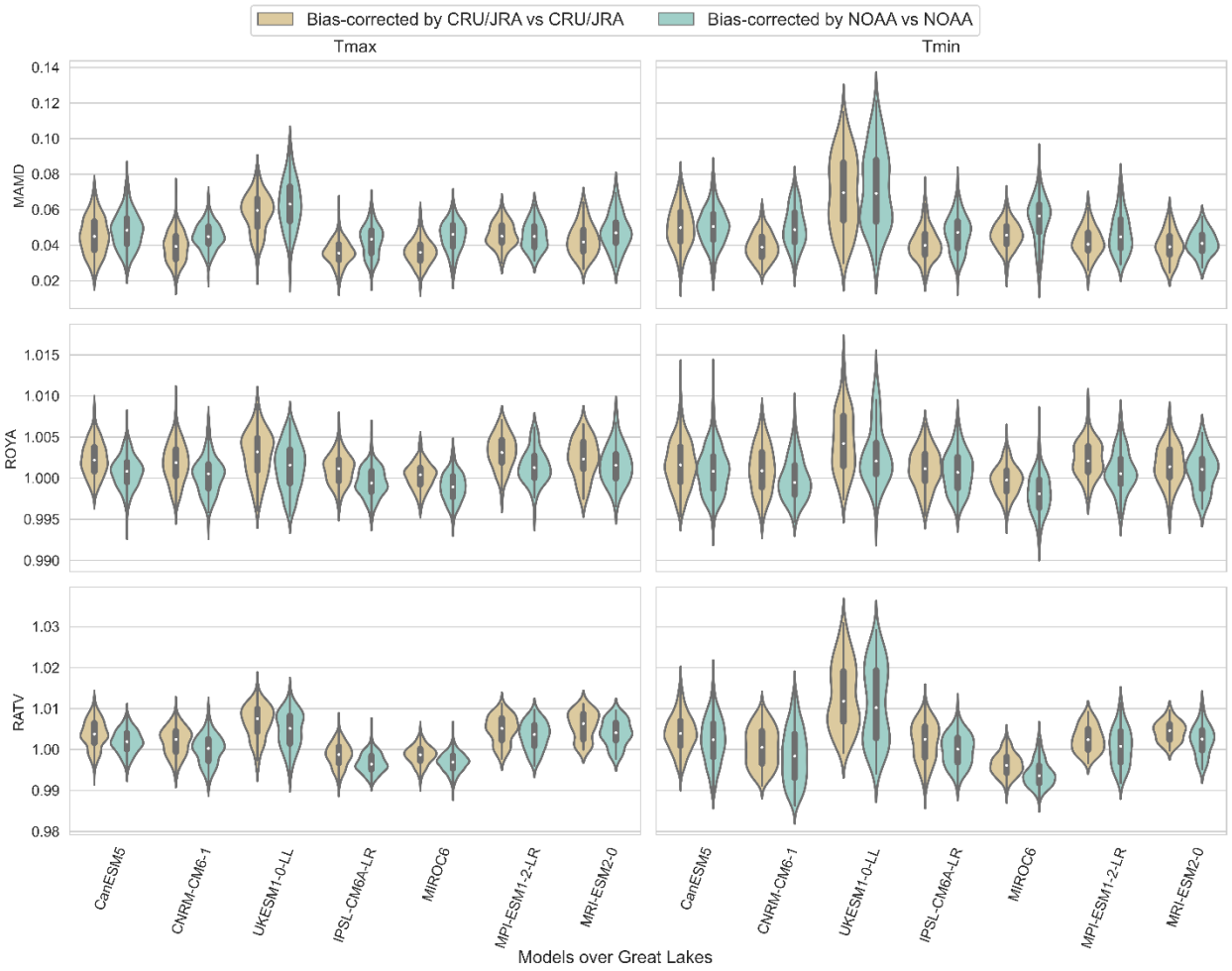

Figure B24 Monthly performance measures of Tmax and Tmin bias-corrected CMIP6 simulations compared to their respective benchmark (CRU/JRA and NOAA) over Great Lakes during 1961-1990.

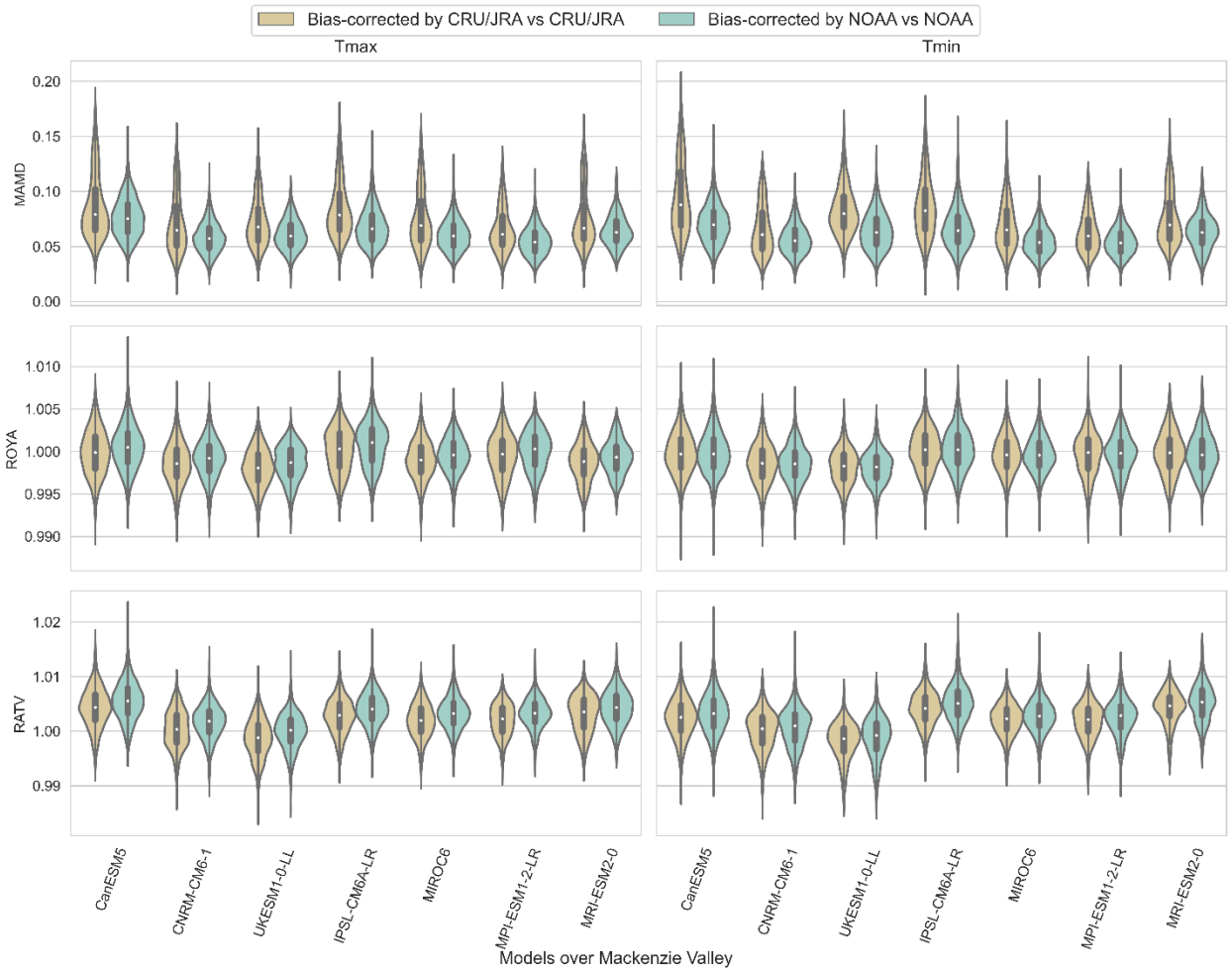

Figure B25 Monthly performance measures of Tmax and Tmin bias-corrected CMIP6 simulations compared to their respective benchmark (CRU/JRA and NOAA) over Mackenzie Valley during 1961-1990.

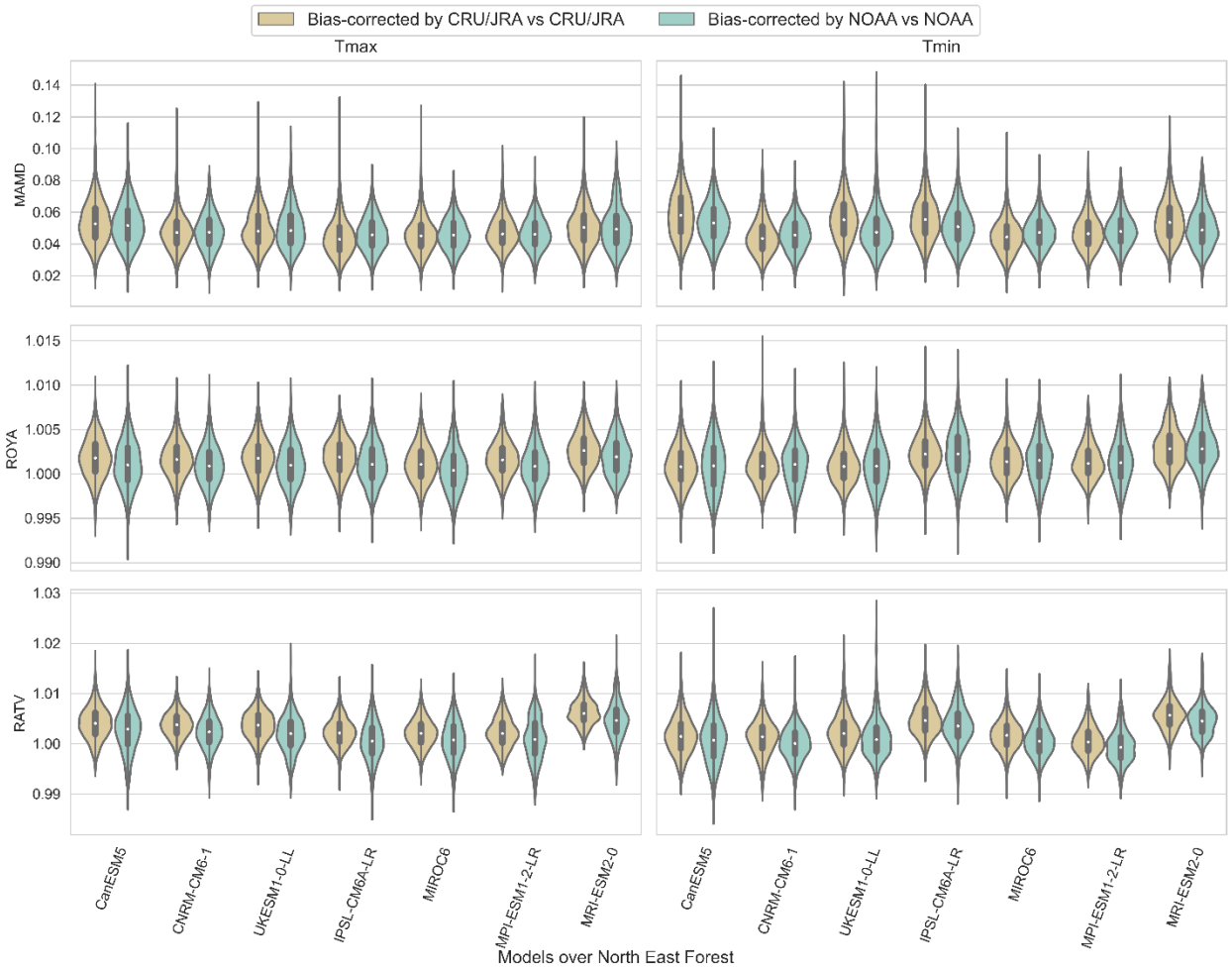

Figure B26 Monthly performance measures of Tmax and Tmin bias-corrected CMIP6 simulations compared to their respective benchmark (CRU/JRA and NOAA) over North East Forest during 1961-1990.

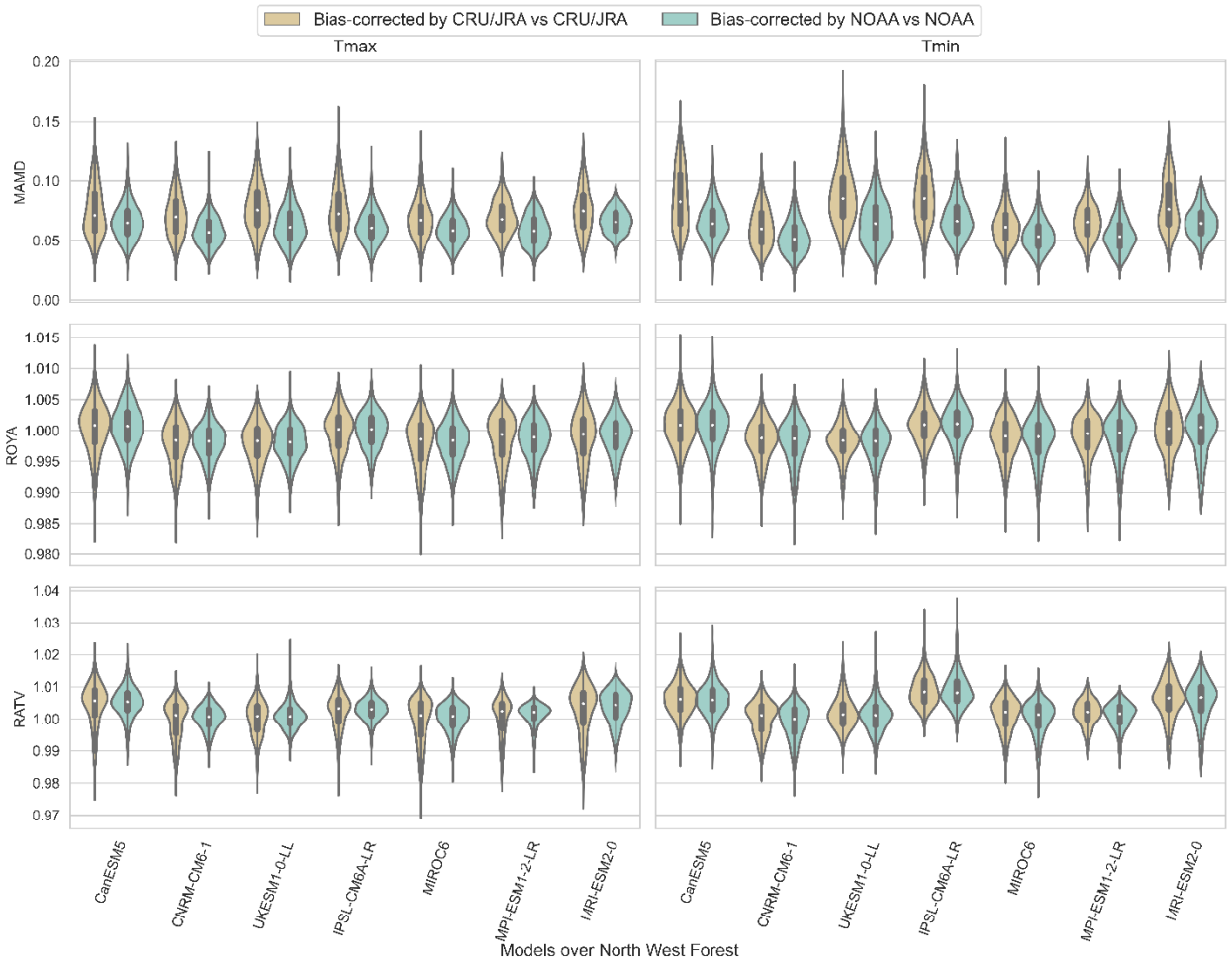

Figure B27 Monthly performance measures of Tmax and Tmin bias-corrected CMIP6 simulations compared to their respective benchmark (CRU/JRA and NOAA) over North West Forest during 1961-1990.

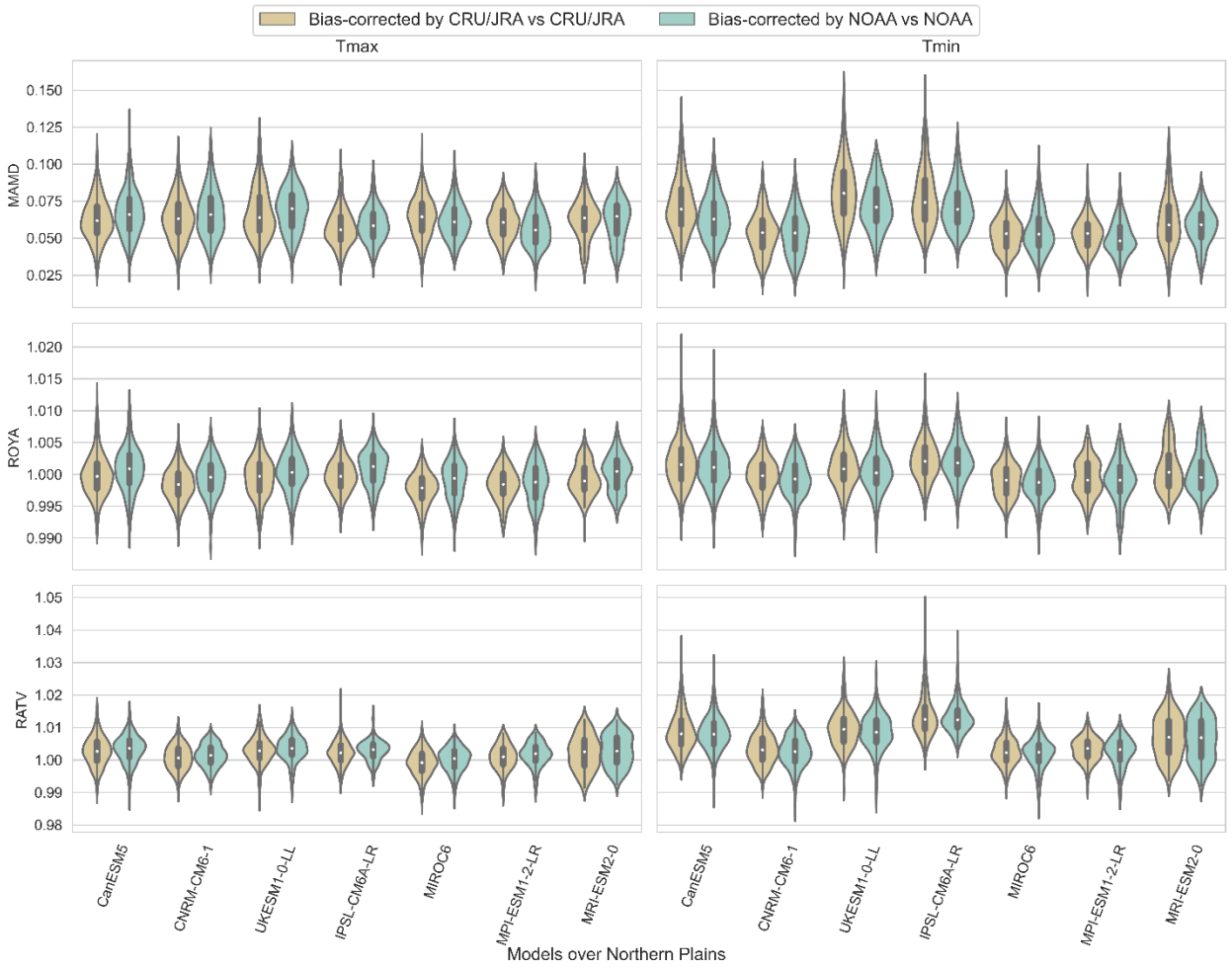

Figure B28 Monthly performance measures of Tmax and Tmin bias-corrected CMIP6 simulations compared to their respective benchmark (CRU/JRA and NOAA) over Northern Plains during 1961-1990.

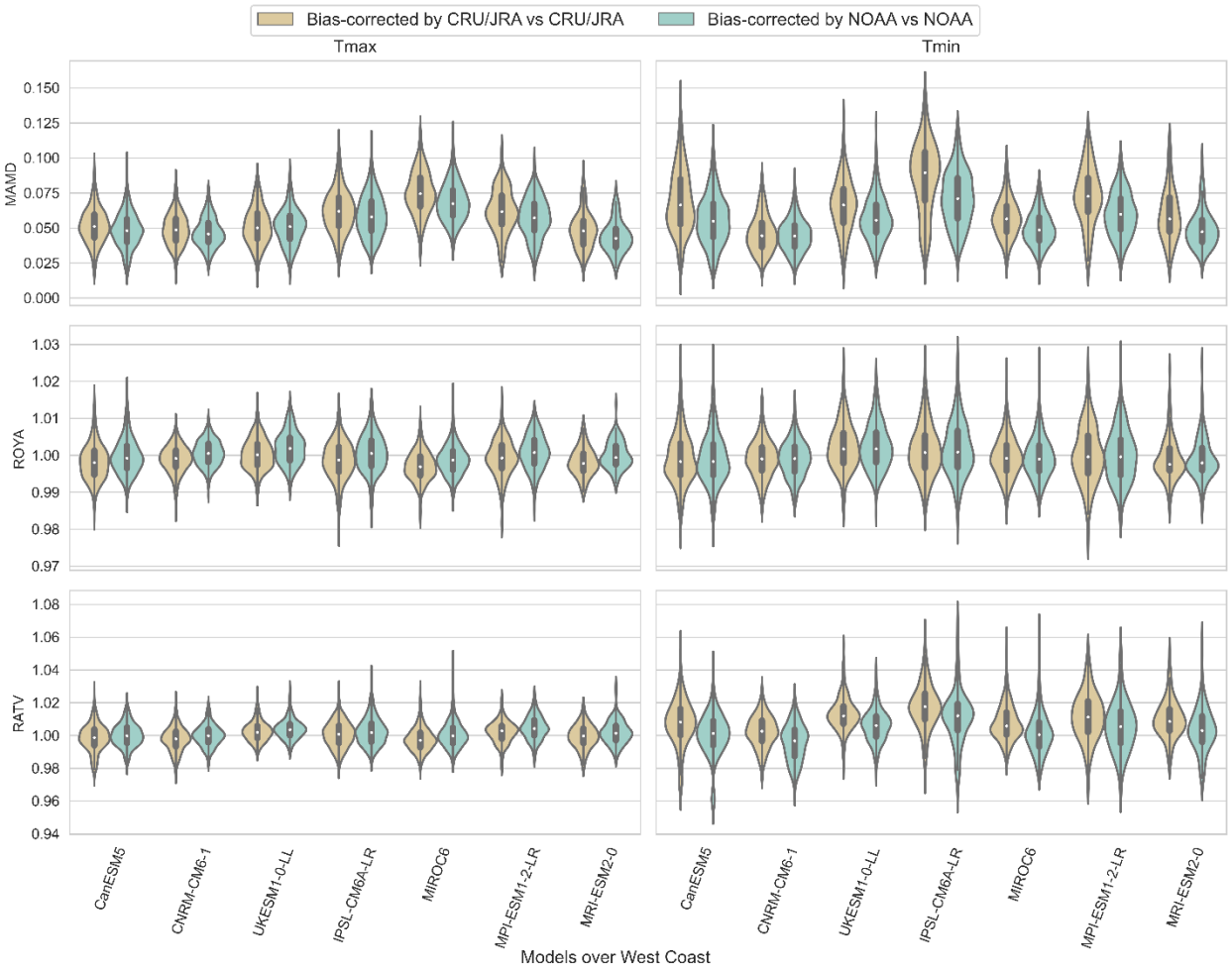

Figure B29 Monthly performance measures of Tmax and Tmin bias-corrected CMIP6 simulations compared to their respective benchmark (CRU/JRA and NOAA) over West Coast during 1961-1990.

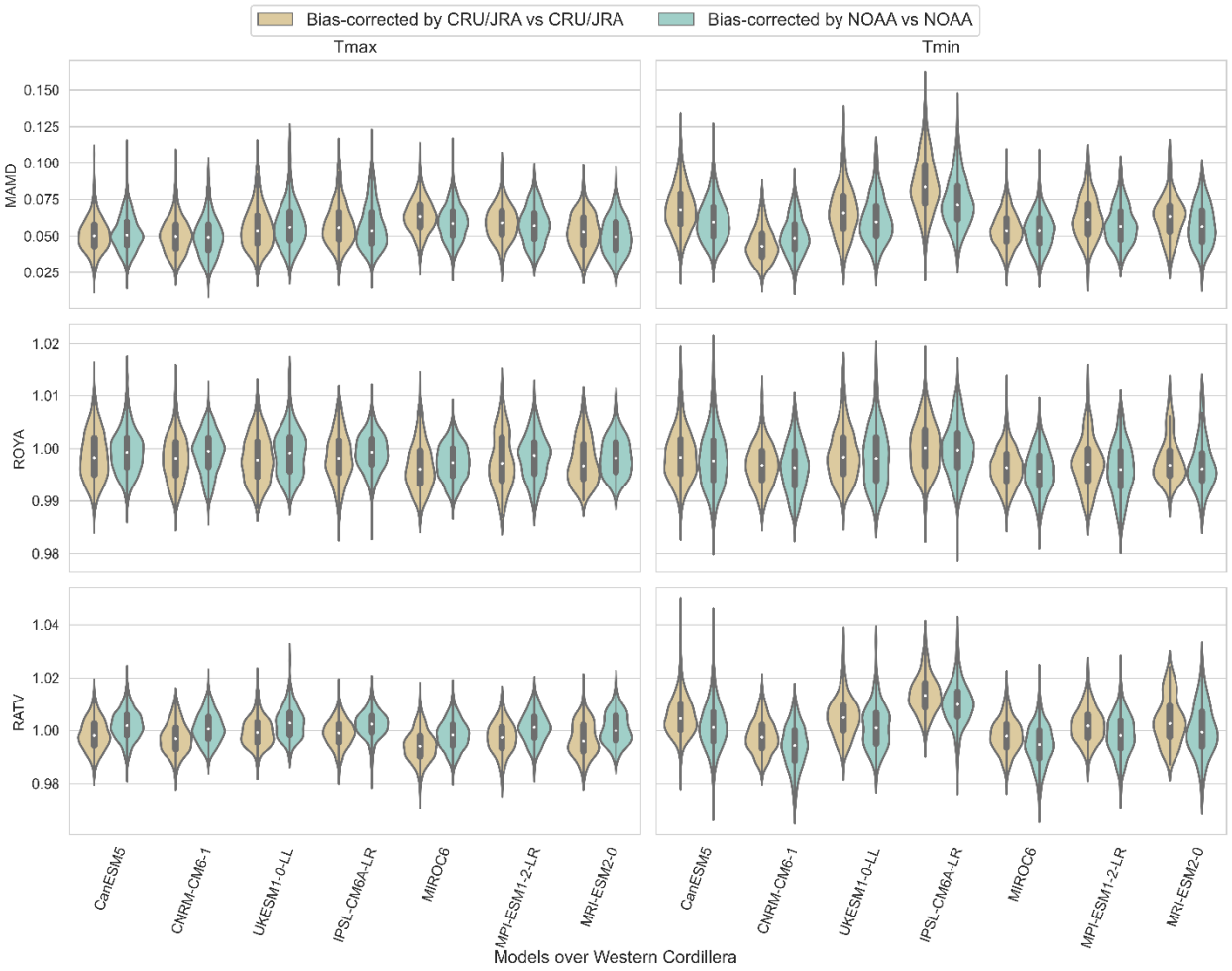

Figure B30 Monthly performance measures of Tmax and Tmin bias-corrected CMIP6 simulations compared to their respective benchmark (CRU/JRA and NOAA) over Western Cordillera during 1961-1990.

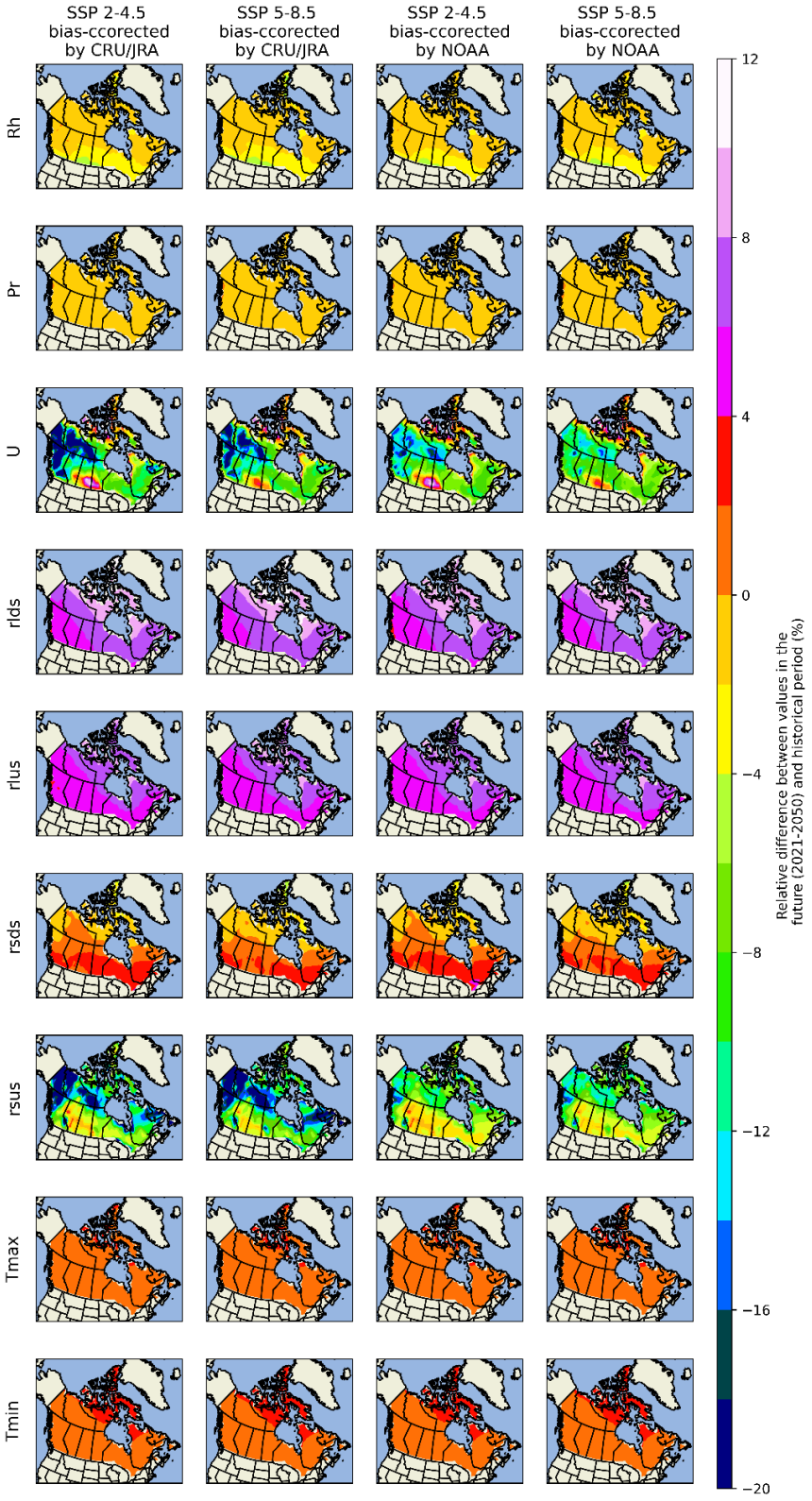

Figure B31 Percentage of relative difference between the long-term annual average climatic indices values estimated in 2021-2050 under SSP 2-4.5 and SSP 5-8.5 and historical period.

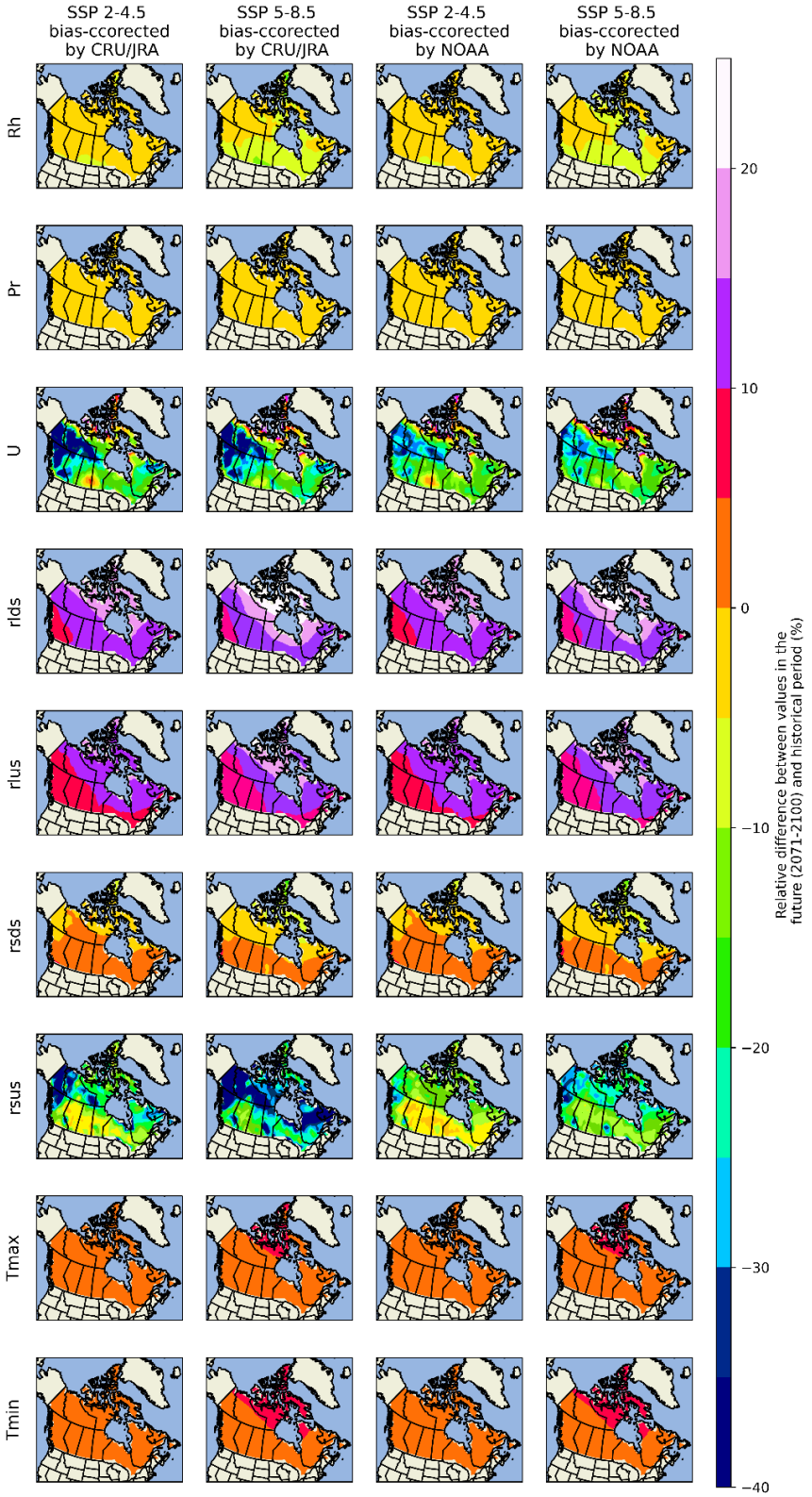

Figure B32 Percentage of relative difference between the long-term annual average climatic indices values estimated in 2071-2100 under SSP 2-4.5 and SSP 5-8.5 and historical period.

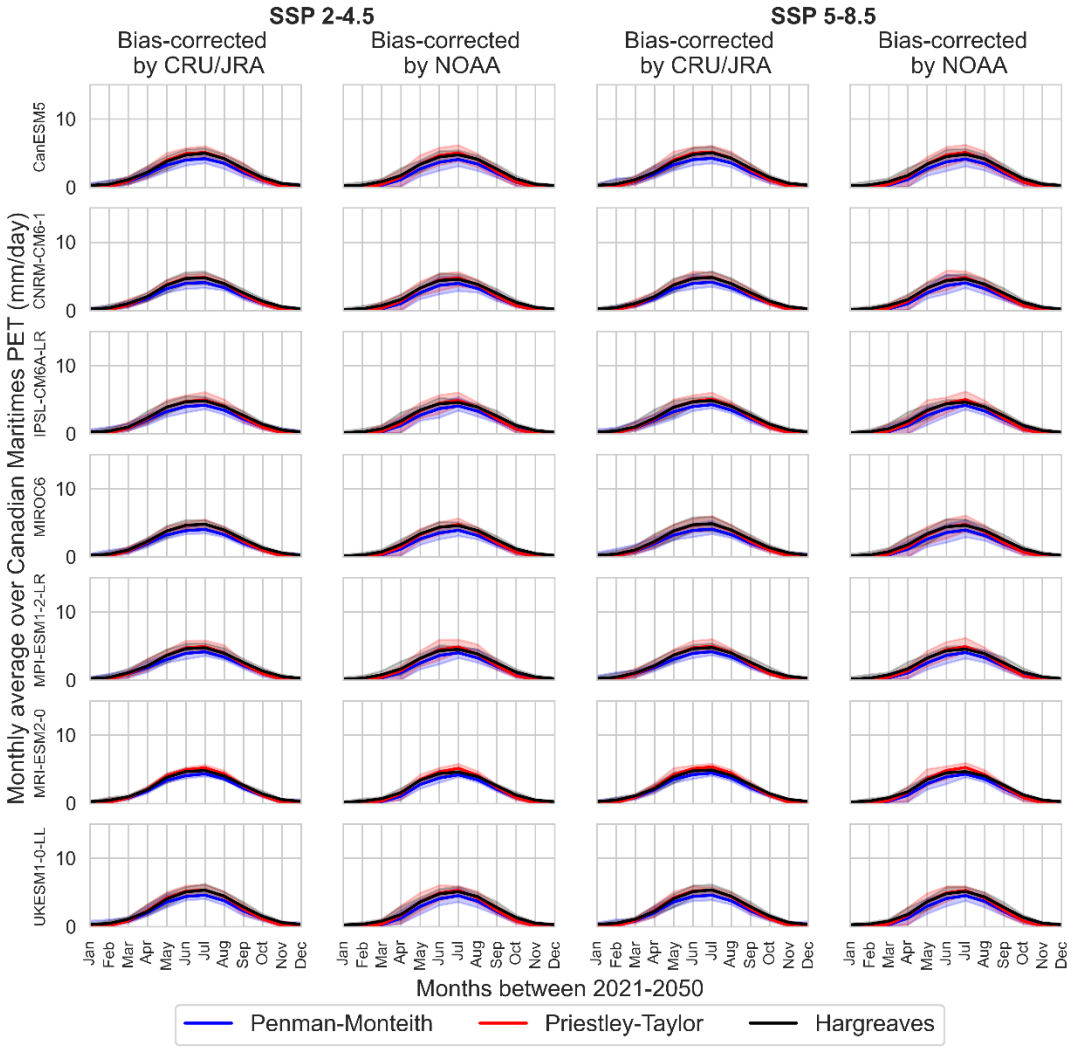

Figure B33 Monthly PET values during 2021-2050 and under SSPs 4-4.5 and 5-8.5, estimated using all simulations per climate models (each row) over Canadian Maritimes.

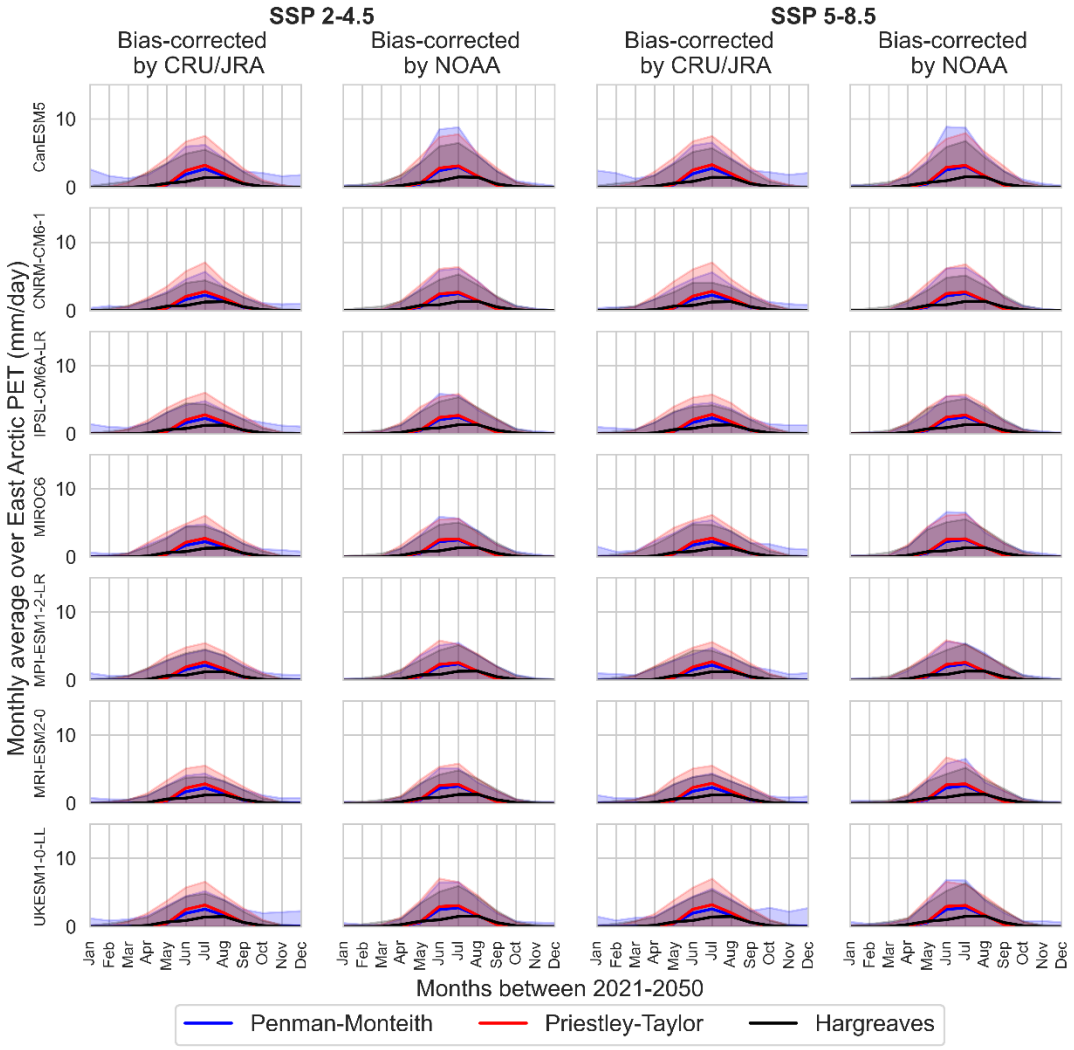

Figure B34 Monthly PET values during 2021-2050 and under SSPs 4-4.5 and 5-8.5, estimated using all simulations per climate models (each row) over East Arctic.

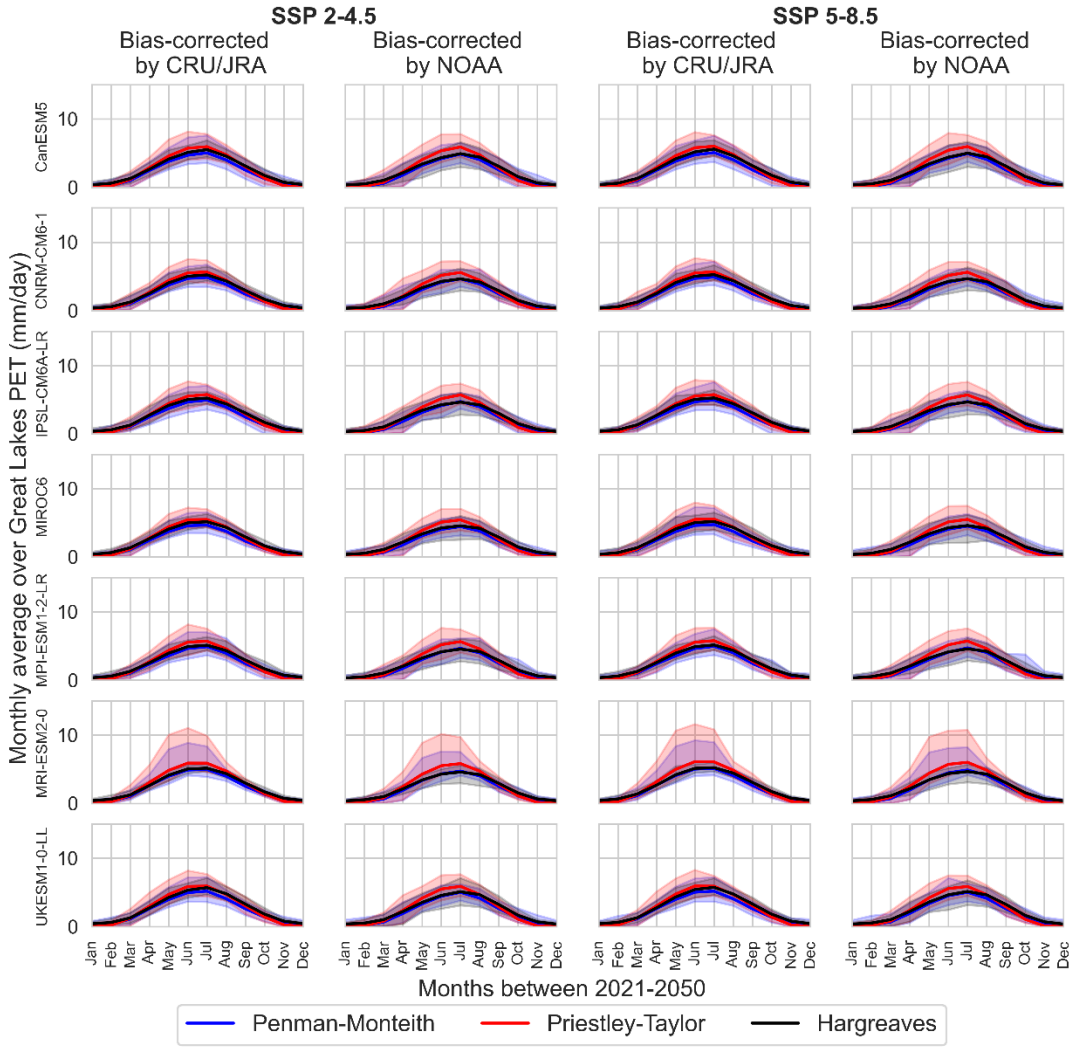

Figure B35 Monthly PET values during 2021-2050 and under SSPs 4-4.5 and 5-8.5, estimated using all simulations per climate models (each row) over Great Lakes.

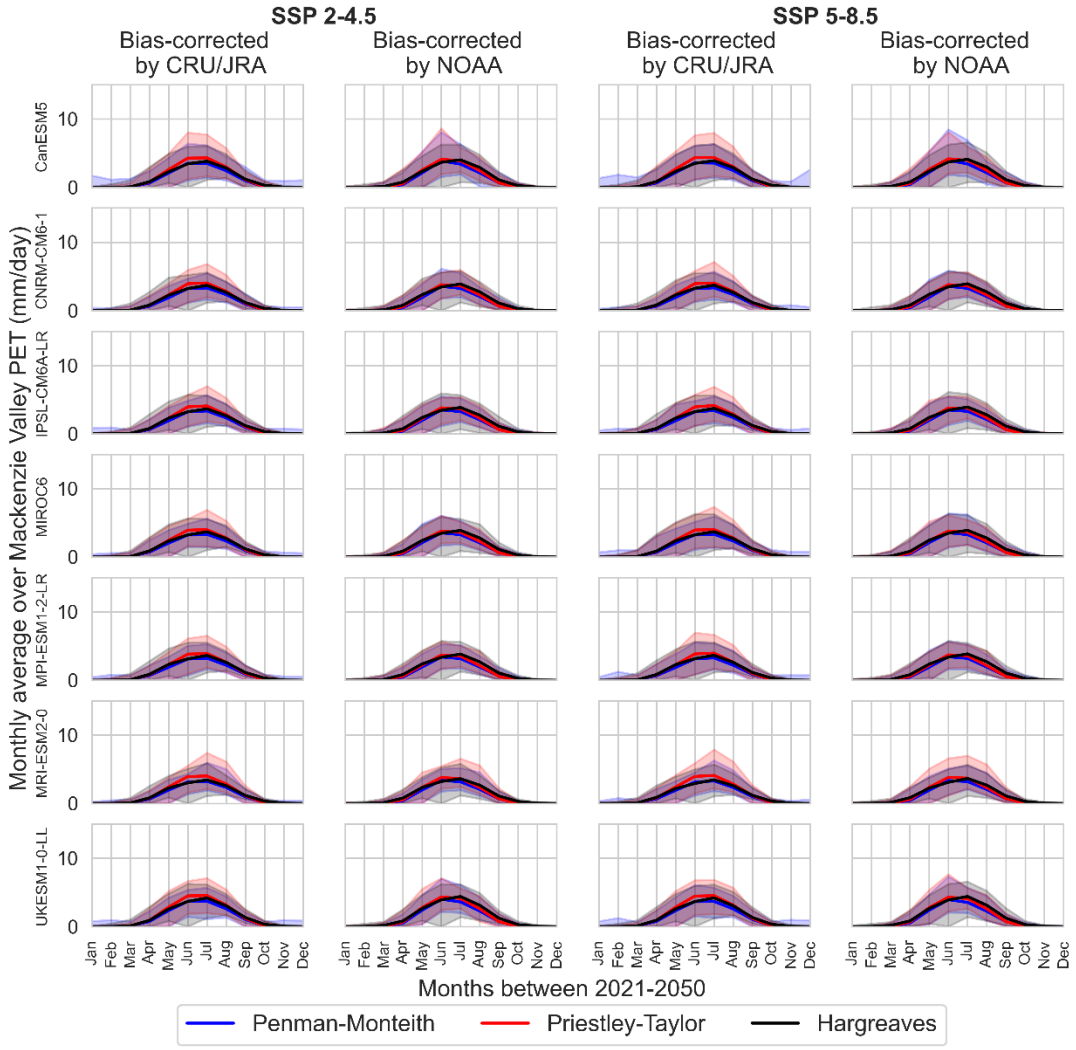

Figure B36 Monthly PET values during 2021-2050 and under SSPs 4-4.5 and 5-8.5, estimated using all simulations per climate models (each row) over Mackenzie Valley.

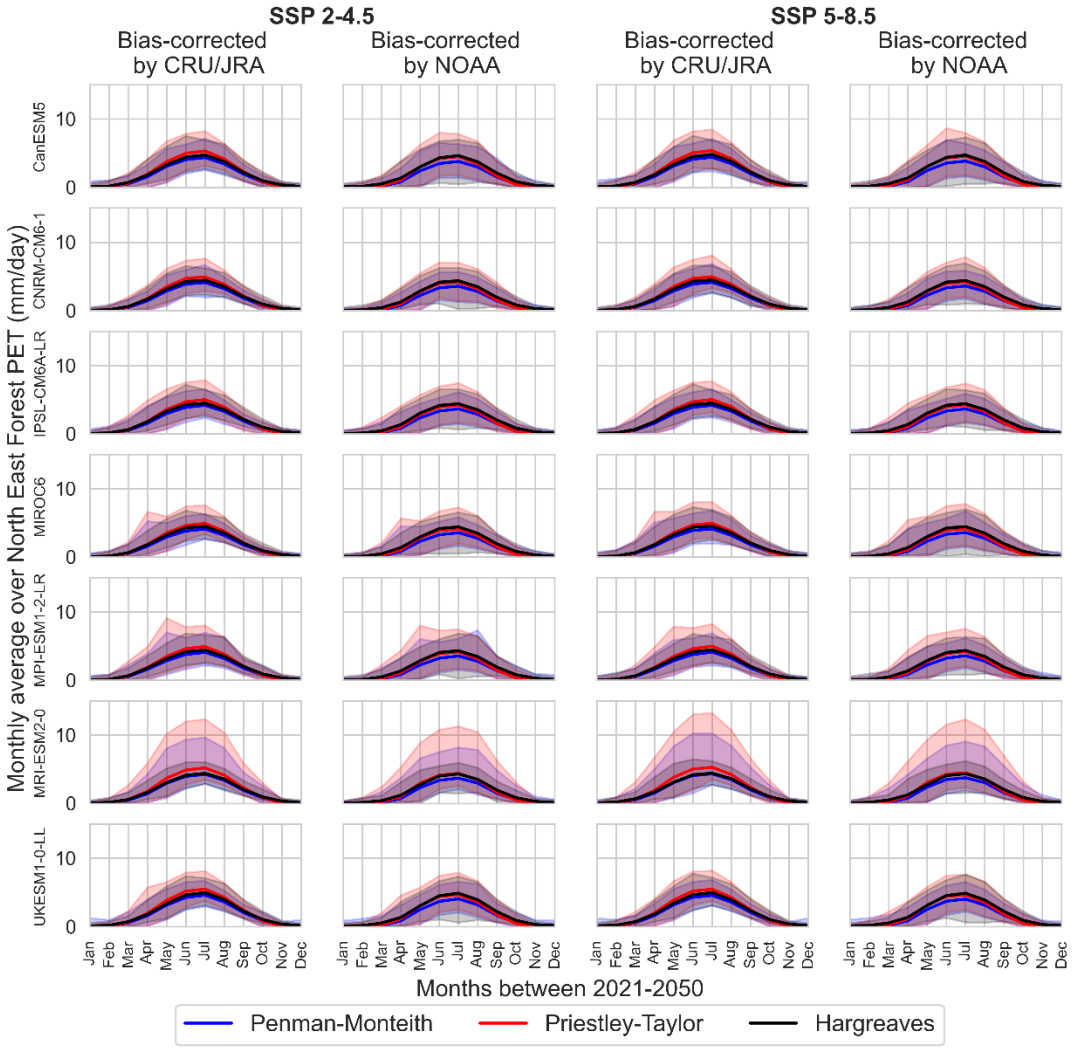

Figure B37 Monthly PET values during 2021-2050 and under SSPs 4-4.5 and 5-8.5, estimated using all simulations per climate models (each row) over North East Forest.

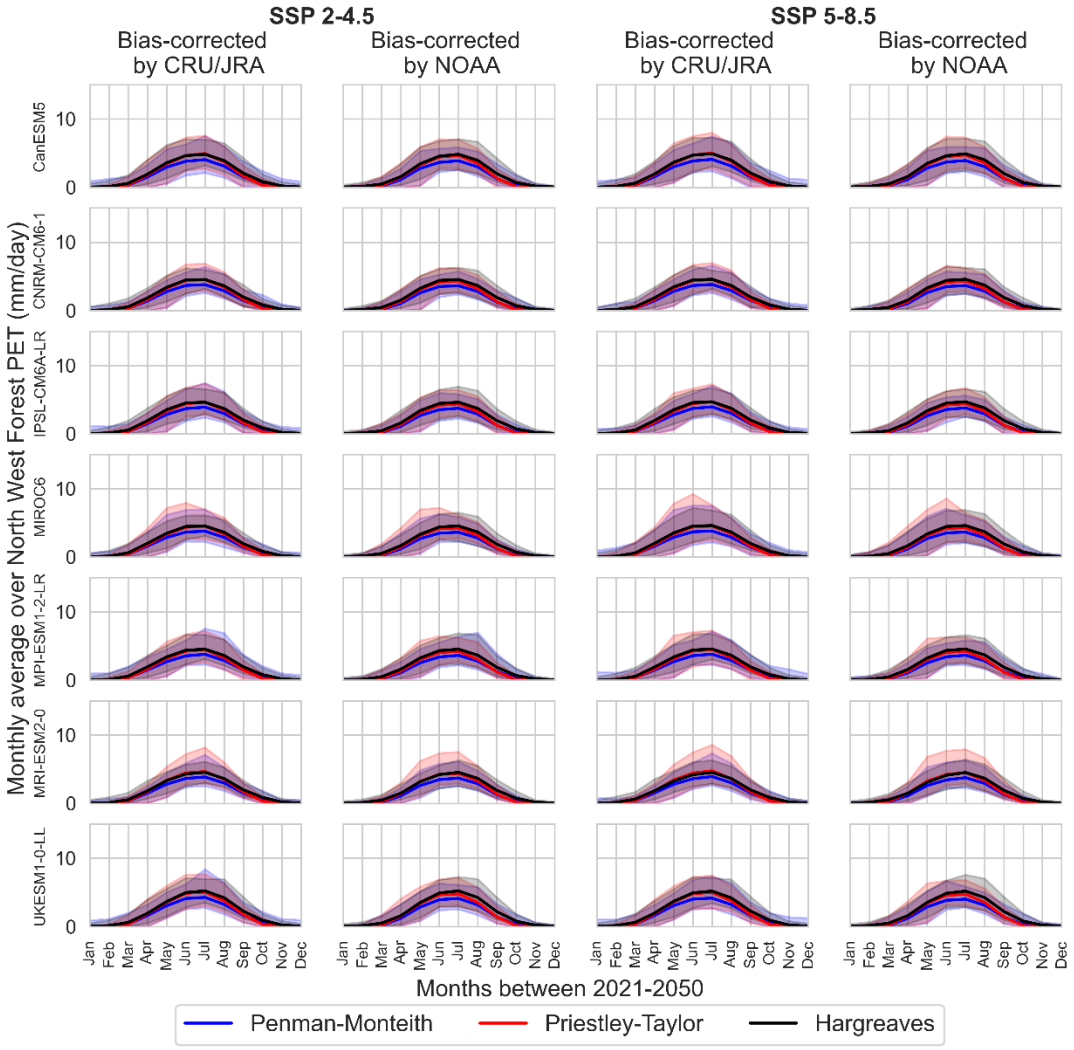

Figure B38 Monthly PET values during 2021-2050 and under SSPs 4-4.5 and 5-8.5, estimated using all simulations per climate models (each row) over North West Forest.

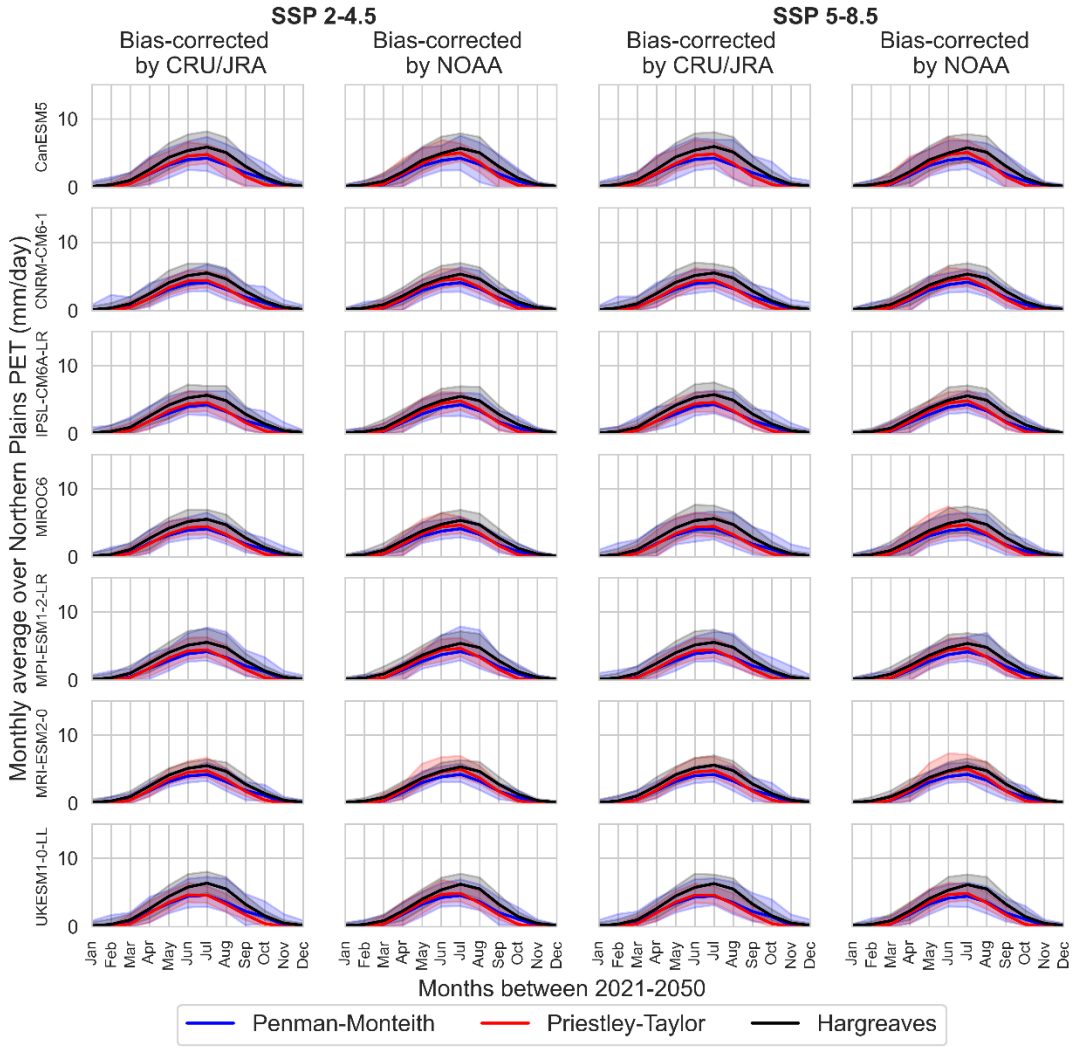

Figure B39 Monthly PET values during 2021-2050 and under SSPs 4-4.5 and 5-8.5, estimated using all simulations per climate models (each row) over Northern Plains.

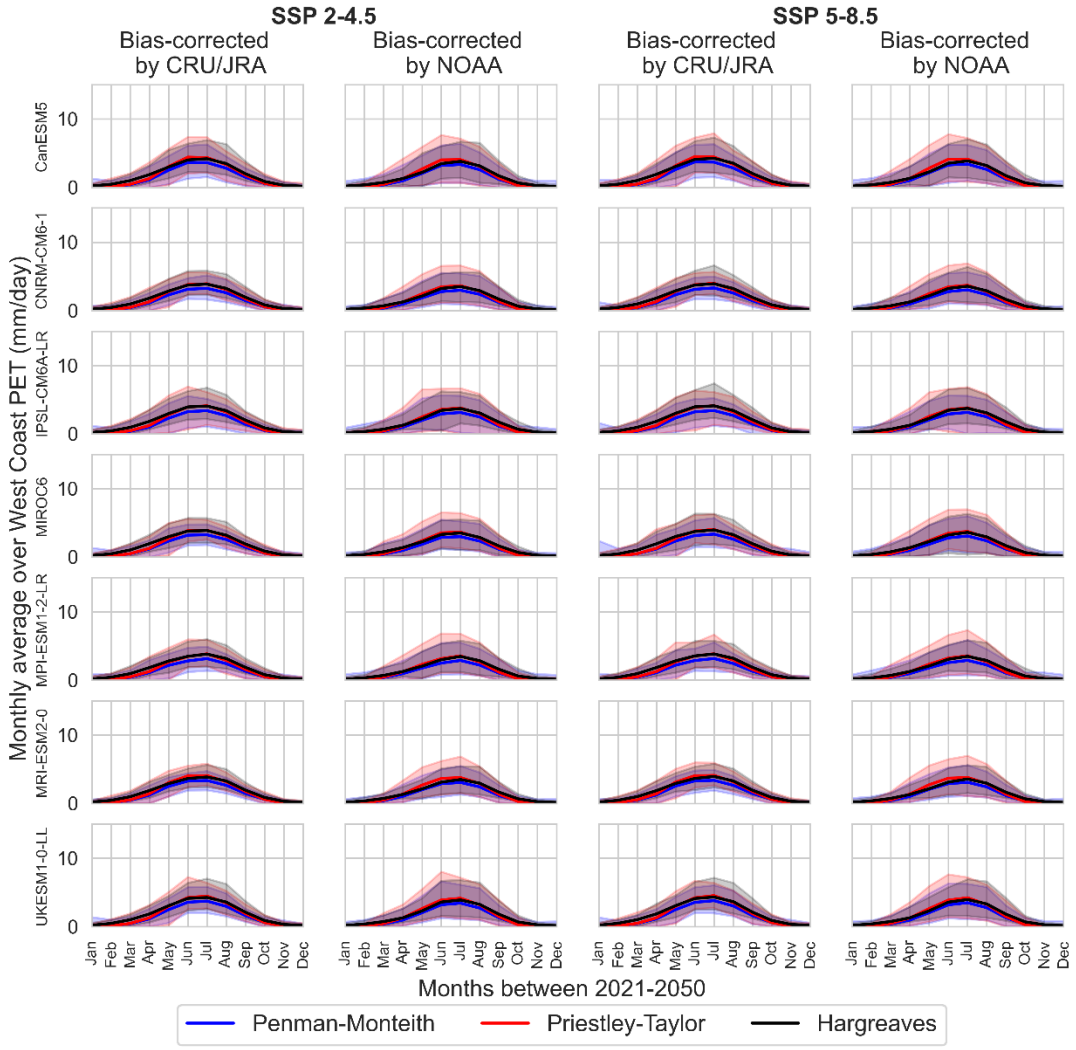

Figure B40 Monthly PET values during 2021-2050 and under SSPs 4-4.5 and 5-8.5, estimated using all simulations per climate models (each row) over West Coast.

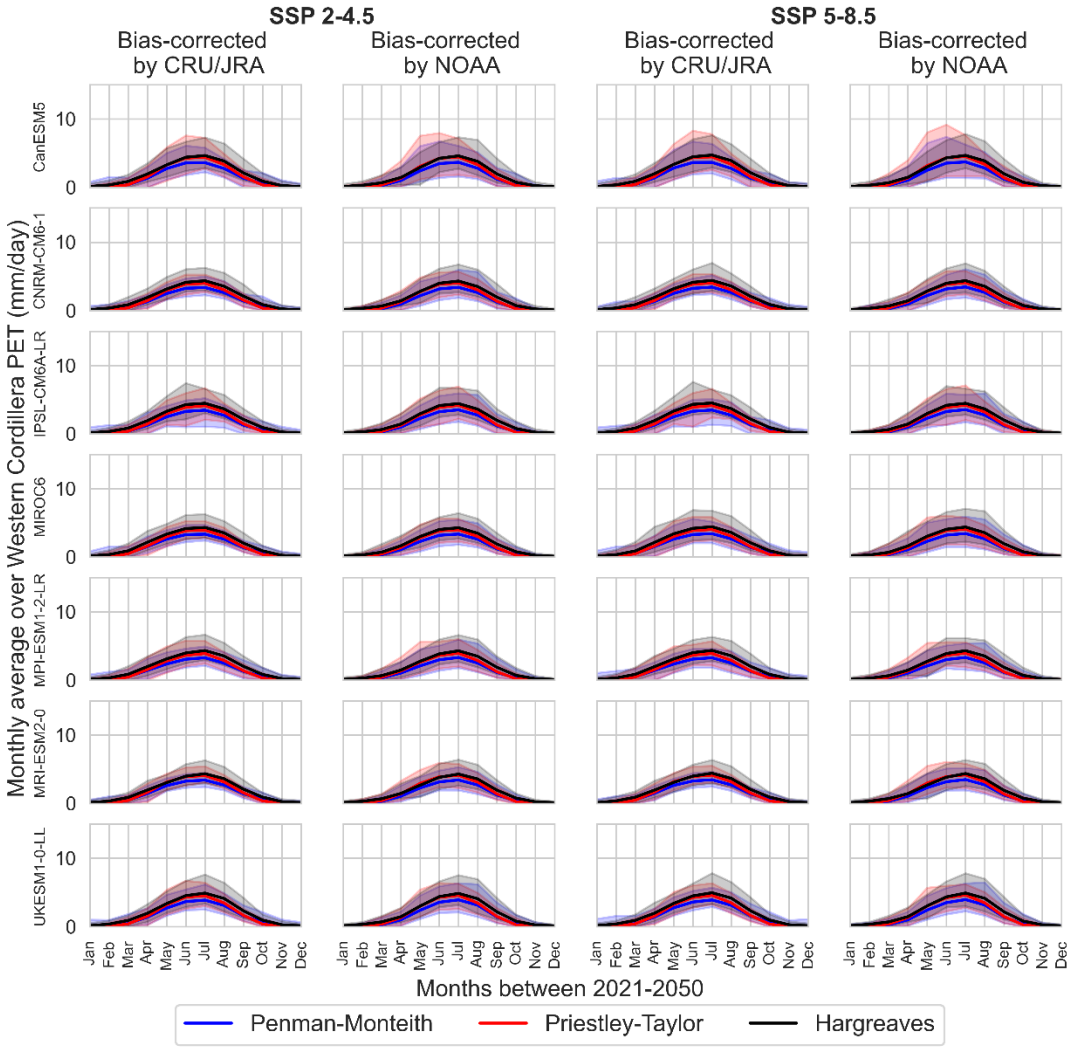

Figure B41 Monthly PET values during 2021-2050 and under SSPs 4-4.5 and 5-8.5, estimated using all simulations per climate models (each row) over Western Cordillera.

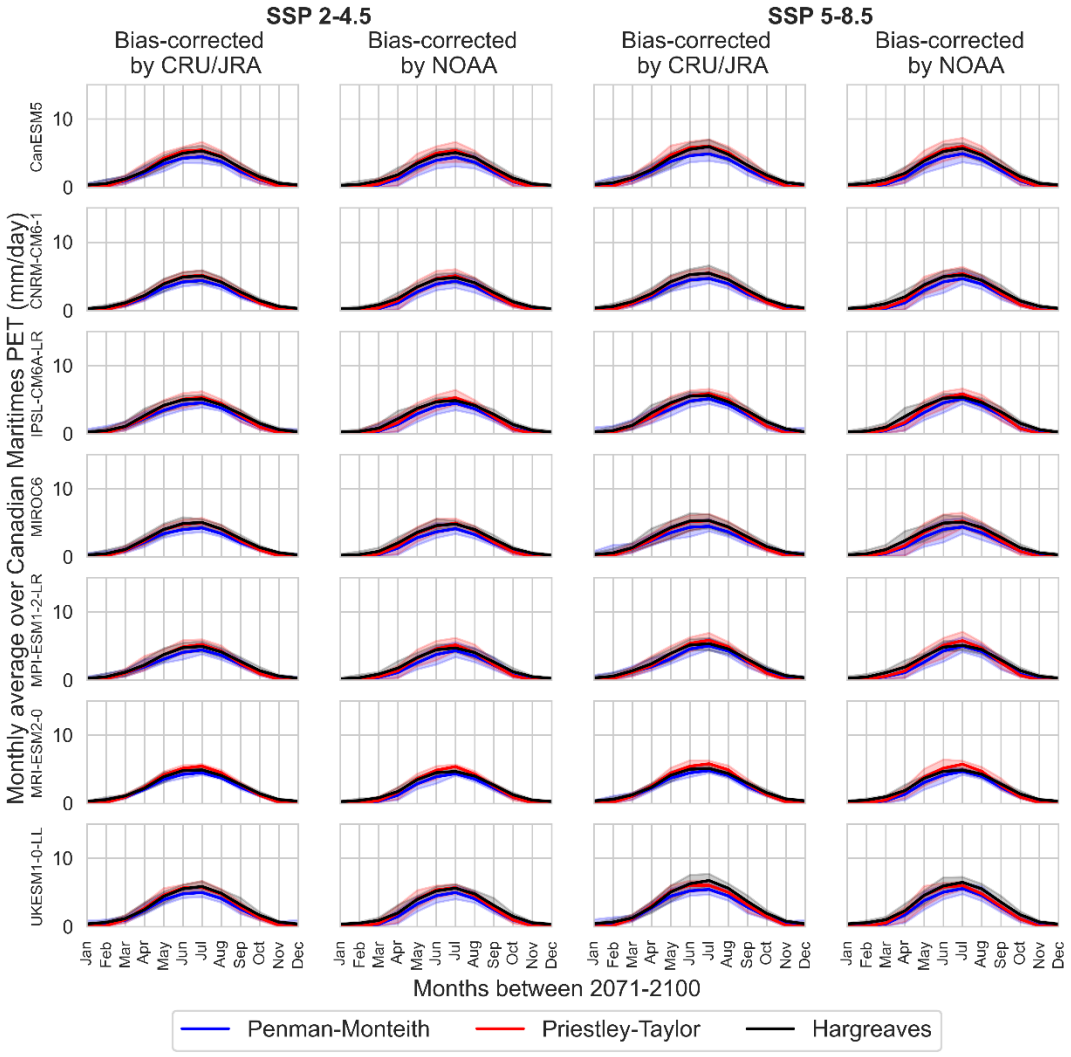

Figure B42 Monthly PET values during 2071-2100 and under SSPs 4-4.5 and 5-8.5, estimated using all simulations per climate models (each row) over Canadian Maritimes.

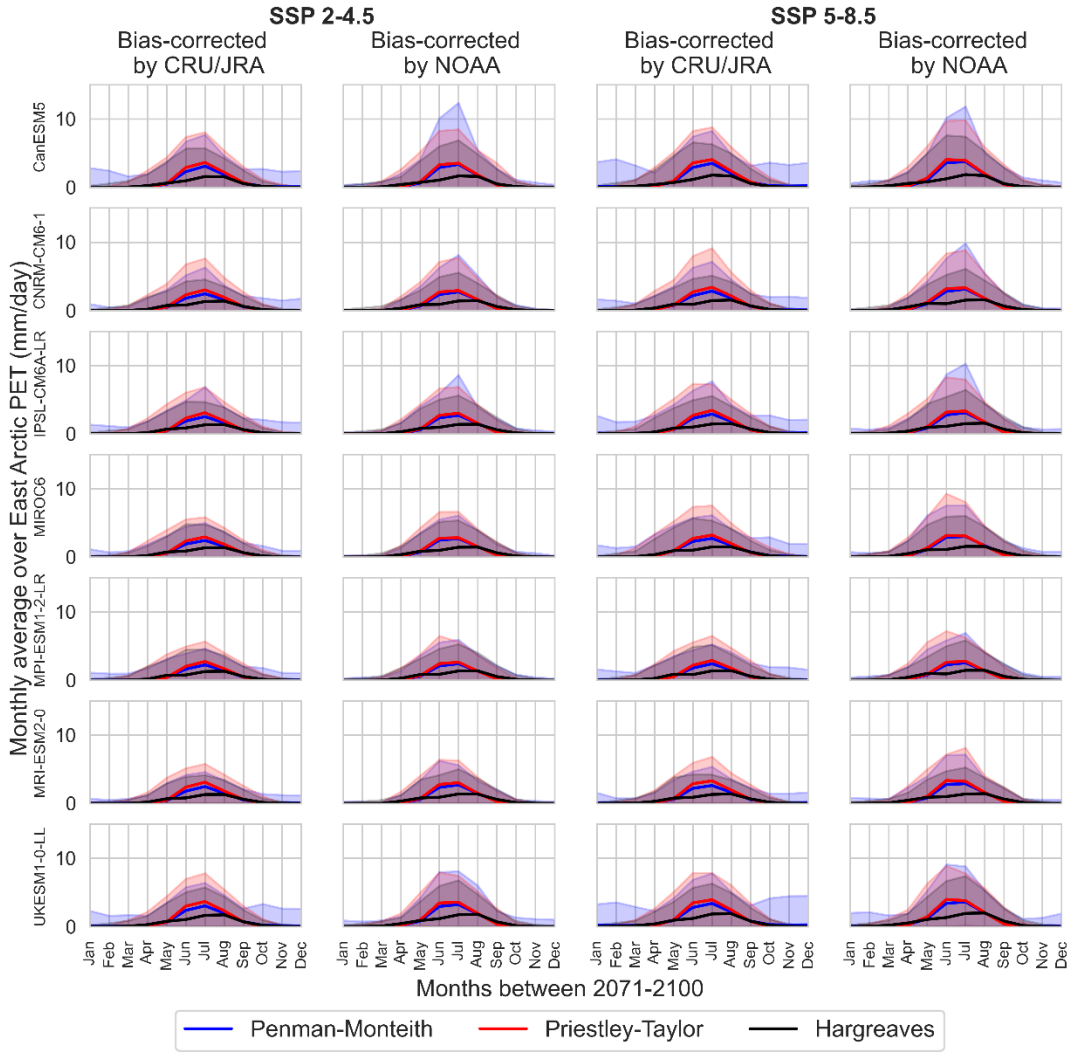

Figure B43 Monthly PET values during 2071-2100 and under SSPs 4-4.5 and 5-8.5, estimated using all simulations per climate models (each row) over East Arctic.

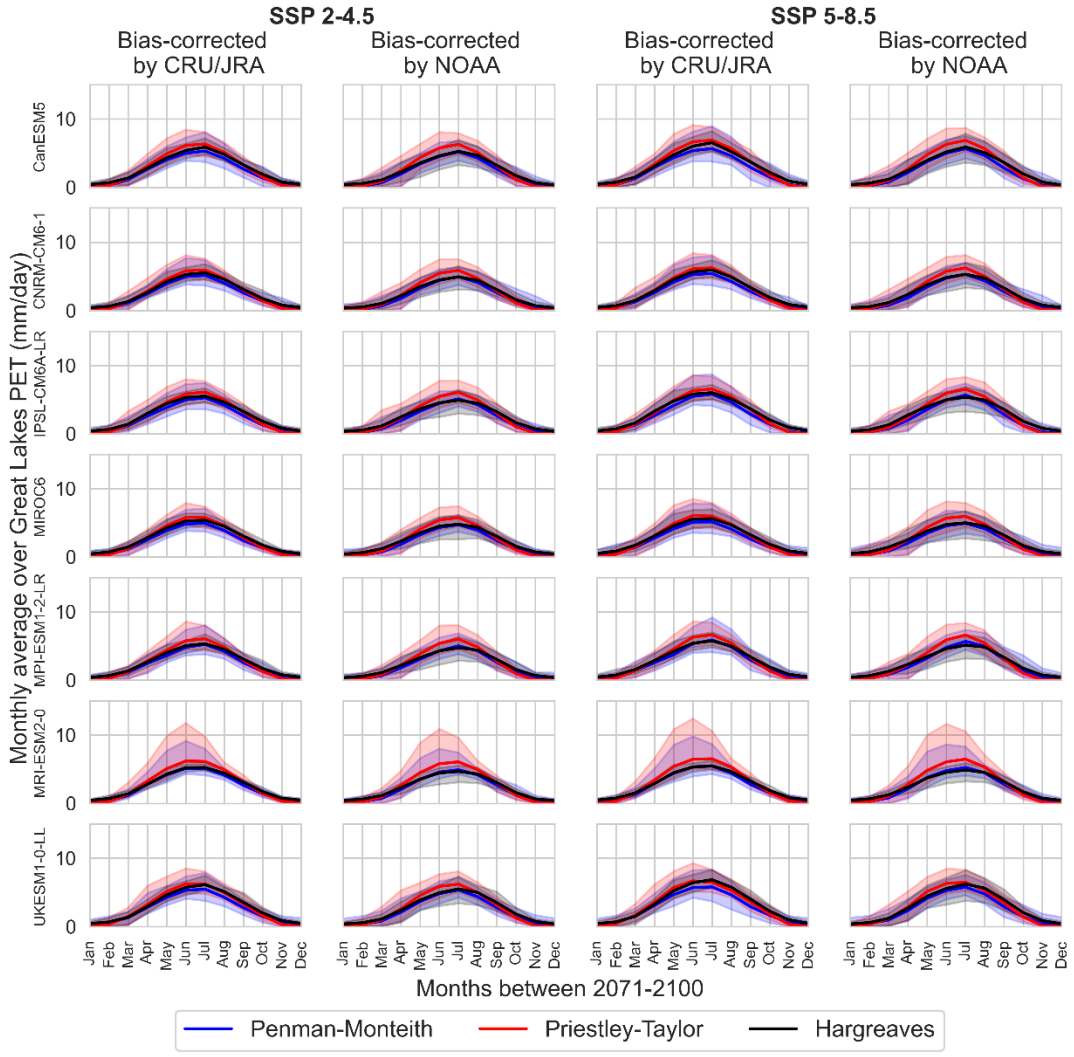

Figure B44 Monthly PET values during 2071-2100 and under SSPs 4-4.5 and 5-8.5, estimated using all simulations per climate models (each row) over Great Lakes.

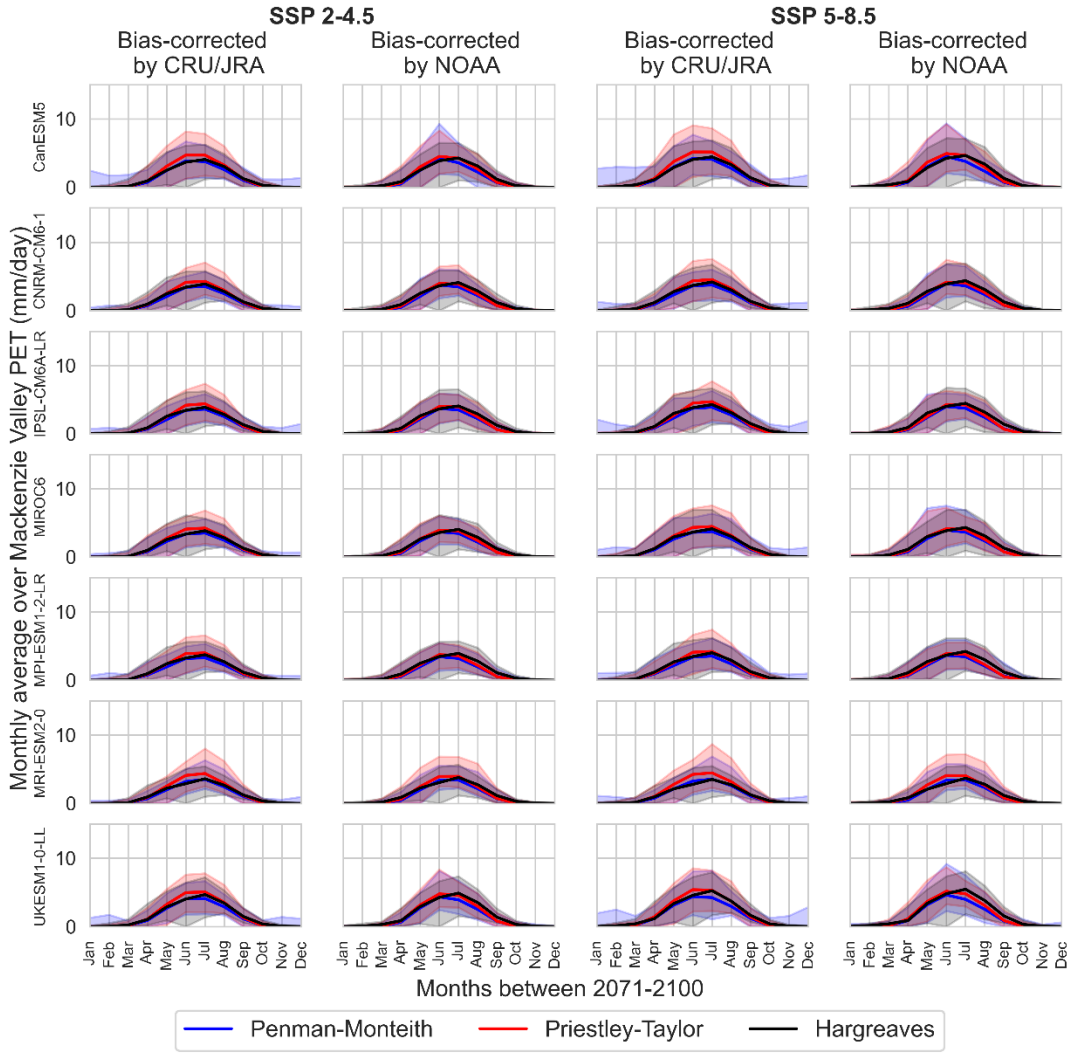

Figure B45 Monthly PET values during 2071-2100 and under SSPs 4-4.5 and 5-8.5, estimated using all simulations per climate models (each row) over Mackenzie Valley.

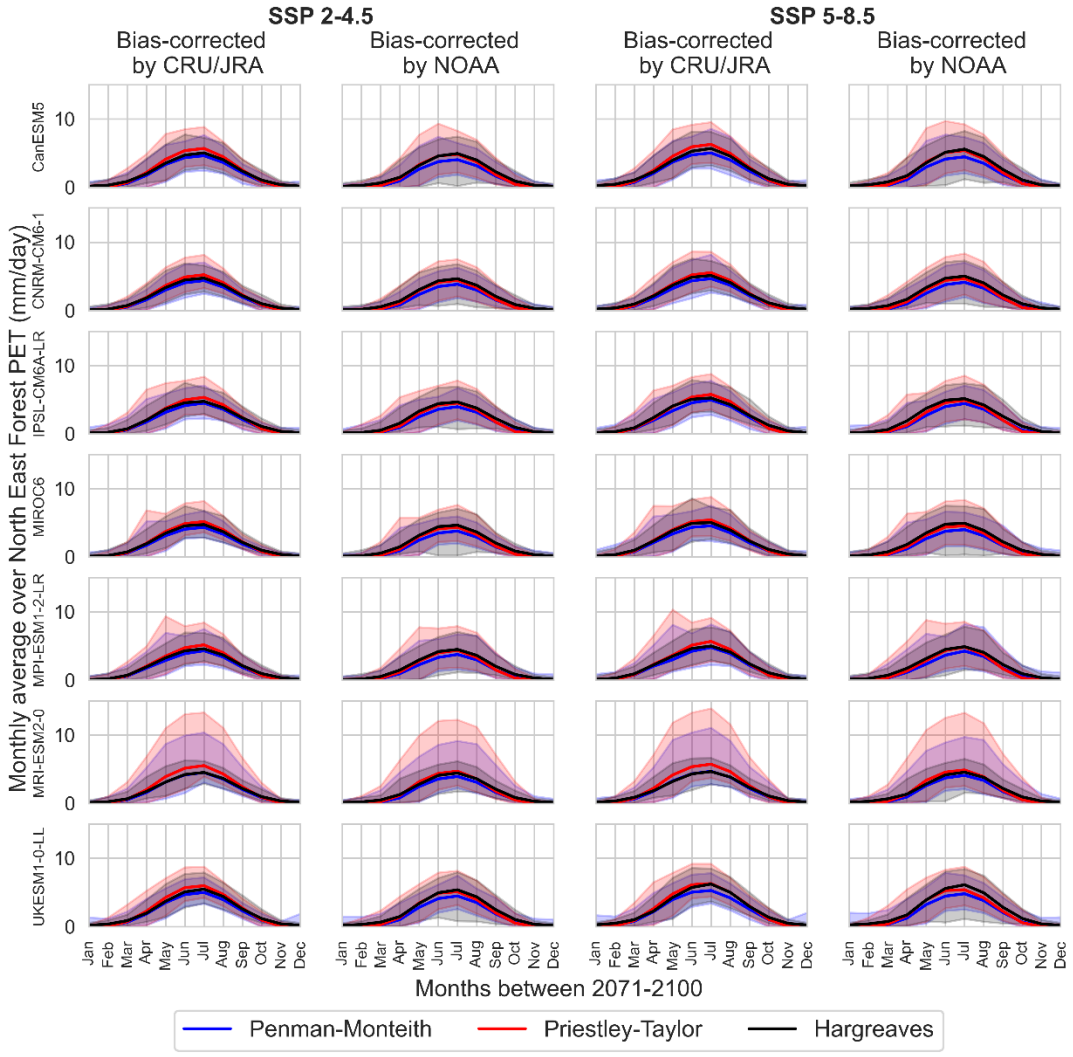

Figure B46 Monthly PET values during 2071-2100 and under SSPs 4-4.5 and 5-8.5, estimated using all simulations per climate models (each row) over North East Forest.

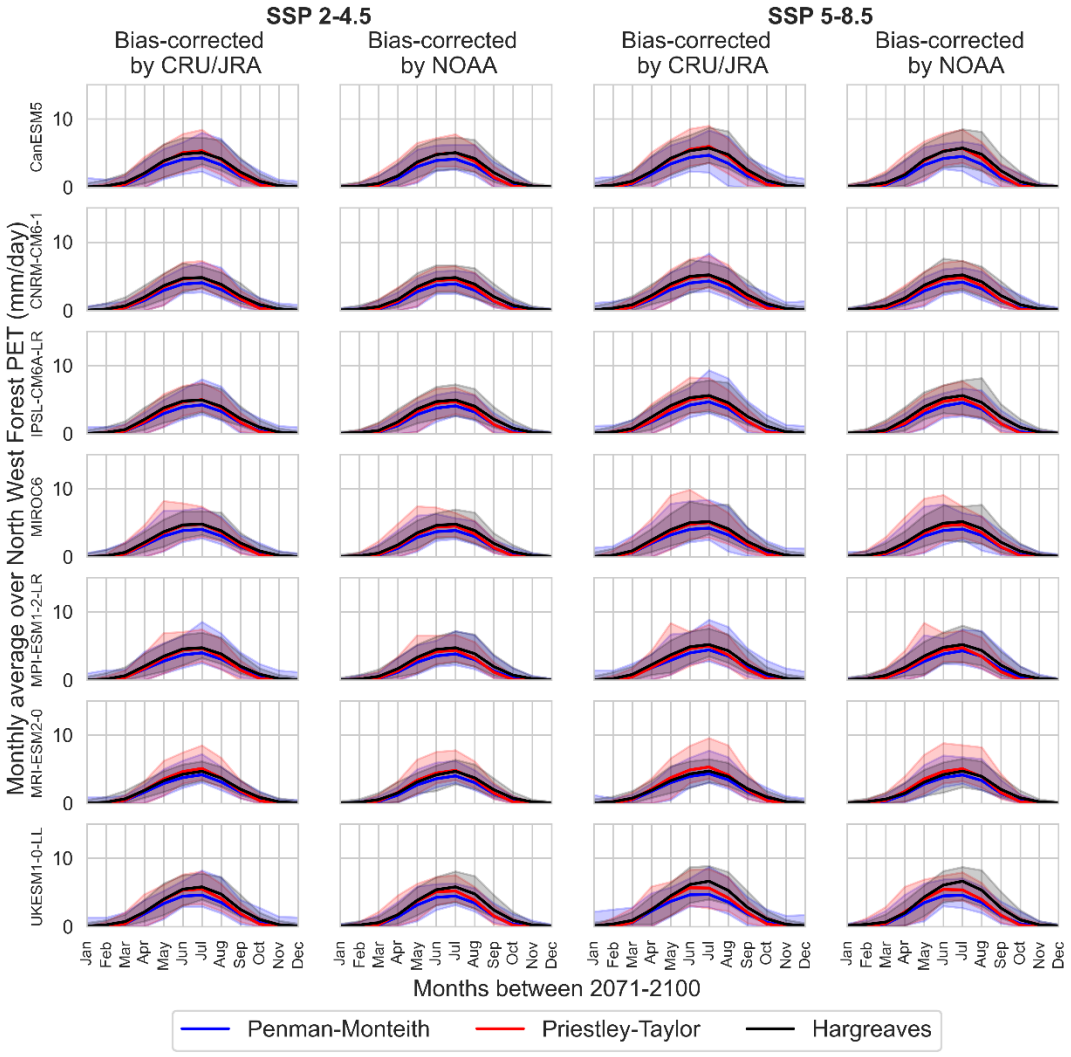

Figure B47 Monthly PET values during 2071-2100 and under SSPs 4-4.5 and 5-8.5, estimated using all simulations per climate models (each row) over North West Forest.

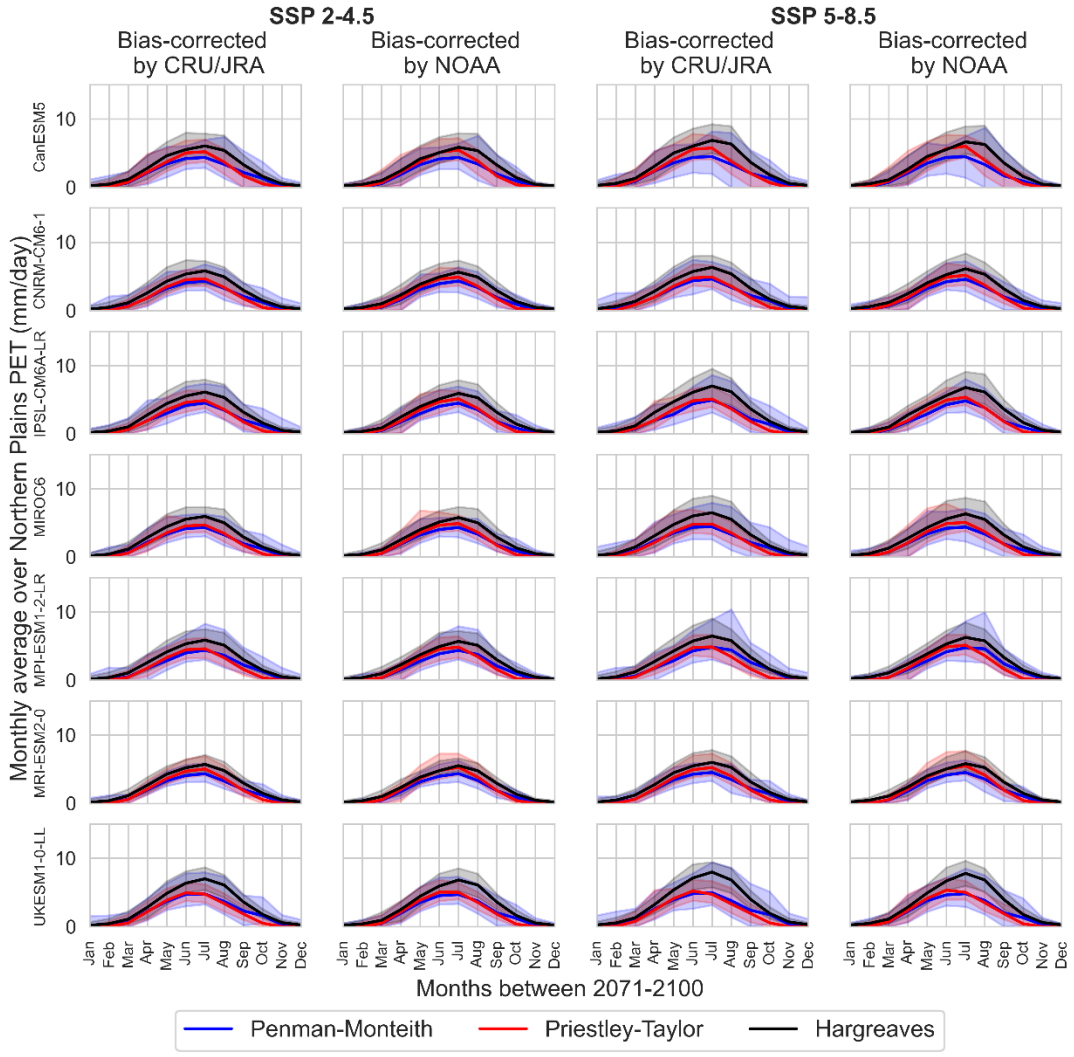

Figure B48 Monthly PET values during 2071-2100 and under SSPs 4-4.5 and 5-8.5, estimated using all simulations per climate models (each row) over Northern Plains.

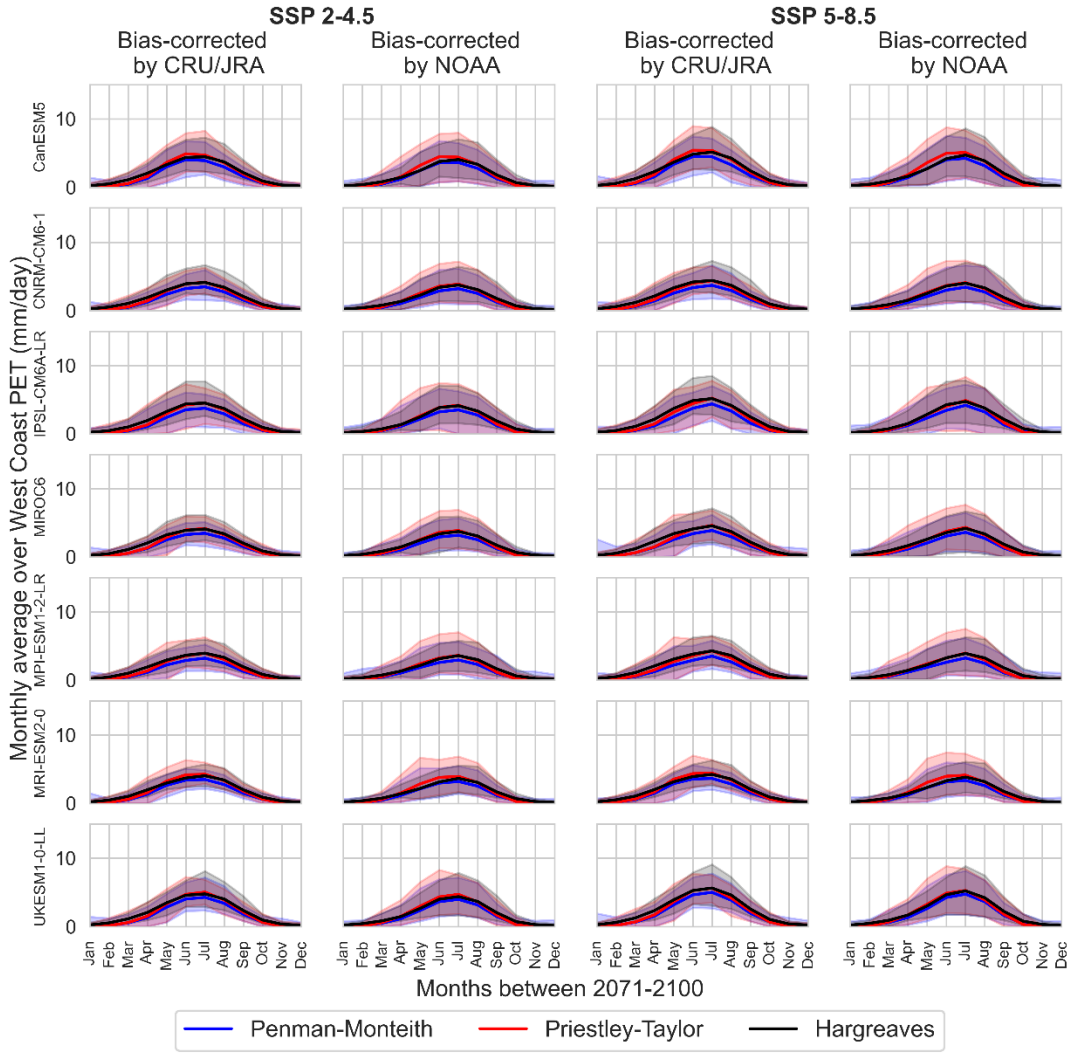

Figure B49 Monthly PET values during 2071-2100 and under SSPs 4-4.5 and 5-8.5, estimated using all simulations per climate models (each row) over West Coast.

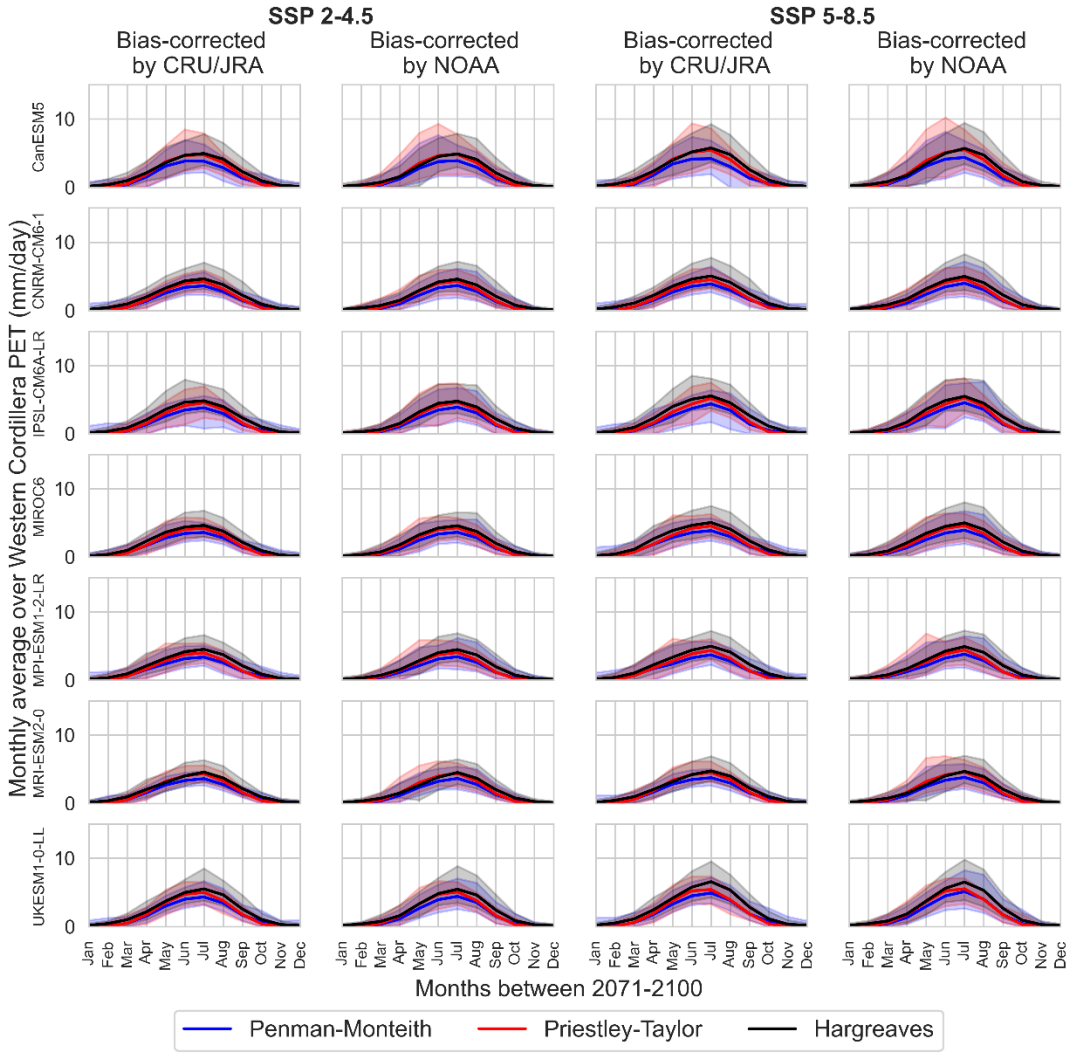

Figure B50 Monthly PET values during 2071-2100 and under SSPs 4-4.5 and 5-8.5, estimated using all simulations per climate models (each row) over Western Cordillera.